STRUCTURE-ACTIVITY STUDIES ON MOLECULAR PROCESSES IN SYNAPTIC TRANSMISSION

by

Gordon R. Clarke

Department of Physics, The City University, London

Submitted for the degree of Ph.D.

March, 1976

CONTENTS

LIST OF TABLES

LIST OF TABLES (continued)

In Appendices

LIST OF ILLUSTRATIONS

ACKNOWLEDGEMENTS

I would like to thank Dr. E.G. Steward for helpful advice, criticism and support throughout this project. I am also indebted to my colleagues [redacted] for many fruitful discussions.

[redacted] prepared the photographs for this volume. The manuscript was interpreted and expertly typed by my wife, [redacted], with much effort and little complaint.

I am also grateful to the SRC for the award of a Research Studentship for the duration of the work.

ABSTRACT

In this study, two amino-acid transmitter systems have been investigated - the GABA system and the glutamate system. Pharmacological information on each has been collated from the literature, providing a basis for structure-activity studies.

To obtain structural information on the transmitters, which are nearly all flexible molecules, conformational investigations have been carried out using a variety of methods. Crystal structure data has been gathered, both from the literature and from two X-ray crystal structure determinations carried out in the course of the work. One of these employs a novel method for least-squares refinement of charged moieties. Conformational congruences are apparent among the solid-state conformations of agonists in each transmitter system.

Information on conformation in solution has also been obtained, two methods having been applied. The first, more sophisticated, method is a continuum model treatment based on molecular orbital calculations. The second technique is a simple potential energy method, applicable to a wider range of compounds. A tendency towards partially folded molecules in solution is apparent in both sets of results for GABA agonists. The second method has also been applied to some transmitters in the glutamate system.

Following the conformational investigations, structure-activity schemes have been developed which draw together pharmacological and conformational results in the GABA system. Crystal structure results indicate possible congruent receptor-active conformations, and solution conformations correlate quantitatively with transmitter potency. The results for the glutamate system also indicate possible receptor-active congruent conformations.

In conclusion, the structure-activity results lead on to discussion of possible receptor structure and the mode of action of GABA agonists. The inferences of the present work are compatible with suggestions on GABA receptor-structure derived by other techniques.

LIST OF ABBREVIATIONS, SYMBOLS AND CONVENTIONS

a,b,c,	crystallographic unit cell axial lengths
α, β, γ	crystallographic unit cell inter-axial angles
βA	β alanine
βABA	β aminobutyric acid (β methyl β alanine)
cis ACA	cis-4-aminocrotonic acid
trans ACA	trans-4-aminocrotonic acid
7 ACA	7-aminocaprylic acid
εACA	ε aminocaproic acid
ACCA	aminocyclohexane carboxylic acid
arg	arginine in protein structures
ATA	4-aminotetrolic acid
δAVA	δ aminovaleric acid
BIC	bicuculline
C_i	relative concentration of drug i over reference compound to produce a standard tissue response
CNDO	Complete Neglect of Differential Overlap (MO method)
CNS	Central Nervous System
D	in α amino-acids the D form is: 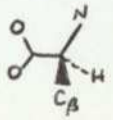
DLH	DL homocysteic acid
e	the electronic charge
e_i	efficacy of drug i
Ecav	cavity energy in solvent effect calculations
Edis	dispersion energy in solvent effect calculations
Ees	electrostatic energy in solvent effect calculations
Eisol	isolated molecule energy
Esolv	solvent effect energy
Etot	total molecular energy including solvent effects
EHT	Extended Hückel Theory (MO method)
EPSP	Excitatory Post-Synaptic Potential
Fc	calculated crystallographic structure factor
Fo	observed crystallographic structure factor
Fm,n	statistical significance parameter for regression lines
αFG	α fluoro GABA

αGA	α guanidinoacetic acid
GABA	γ aminobutyric acid
γGB	γ guanidinobutyric acid
gly	glycine
glu	L-glutamic acid in protein structures
glutamate	L-glutamic acid
βGP	β guanidinopropionic acid
δGP	δ guanidinopentanoic acid
HA966	1 hydroxy-3-aminopyrolid-2-one
HBIC	protonated bicuculline
βHG	β hydroxy GABA
h, k, l	Miller indices
ImAc	imidazoleacetic acid
ImLa	imidazolelactic acid
ImPr	imidazolepropionic acid
IPSP	Inhibitory Post-Synaptic Potential
K	drug-receptor affinity constant
k_1	" " association rate constant
k_2	" " dissociation rate constant
K_E	" " equilibrium constant
L	opposite stereochemical configuration to D (see above)
MO	Molecular Orbital
MeImAc	1 methyl imidazole-4-acetic acid
βMBA	β methyl β alanine (β aminobutyric acid)
musc	muscimol
NMeBIC	N methyl bicuculline
NMR	Nuclear Magnetic Resonance
$P(x_R)$	x_R (see below) probability function
$P(x_T)$	x_T (see below) " "
PAR	Physicochemical-Activity Relationships

PCILO	Perturbative Configuration Interaction of Localised Orbitals (MO method)
PE	Potential Energy
P(uvw)	Patterson function
R	Crystallographic residual factor
(R)	stereochemical arrangement around an asymmetric atom such that the attached groups occur in order of increasing molecular weight clockwise, when viewed with the group of lowest molecular weight below the asymmetric atom
(S)	opposite configuration to (R)
SAR	Structure-Activity Relationships
SOLVEFF	solvent effect calculation program
SS	sum of squares about mean of a group of values
T_i	total interaction probability for a transmitter molecule i
T_n	torsion angle for bond n. The convention employed throughout for torsion angle ABCD is: looking along BC, T_n is the clockwise angle by which AB must be rotated to eclipse CD.
x_R	receptor charge separation
x_T	transmitter-charge separation (see Figs 2.1 and 2.2)
U	crystal structure temperature factors
ULCC	University of London Computer Centre

1.1 PREAMBLE

The design of drugs for therapeutic purposes is hampered by the lack of a theoretical basis linking the structure and the biological activity of endogenous and exogenous 'drug' molecules. This is particularly important for series of drugs, such as neurotransmitters, which act at specific receptors rather than those with more generalised actions such as anaesthetics. The latter group have often proved amenable to correlations between measureable physicochemical properties and biological activities (Hansch, 1973) but, for the former, it is often necessary to synthesise vast numbers of transmitter analogues before a sufficiently active drug, without undesirable side effects, can be identified.

It is sometimes therapeutically desirable to enhance or block the action of natural neurotransmitters in the mammalian central nervous system (CNS). The β adrenergic blocking agents employed in the treatment of heart disease are a case in point. Here, although correlations between biological activities and physicochemical properties can be made, an understanding of the nature of the drug-receptor interaction awaits a precise description of the molecular geometry of the receptor. The present work concerns a similar problem, namely the action of the natural neurotransmitters γ amino butyric acid (GABA) ($HOOC(CH_2)_3NH_2$) and L-glutamic acid (glutamate) ($HOOC.CH(NH_2).(CH_2)_2.COOH$) and their analogues.

There is now good evidence for the inhibitory transmitter role of GABA (Curtis & Johnston, 1974) and the excitatory transmitter role of glutamate (Johnson, 1972) in various regions of the mammalian CNS and in the peripheral nervous system of invertebrates (see 1.3). The balance and straightforward enzymatic interconversion of these similar molecules may be a key to the functional plasticity of the nervous system (Curtis & Johnston, 1970). Disturbance of the levels of these amino acids

in the brain, particularly GABA, seems to be involved in various neurological disorders. These include Huntington's chorea (Crow, 1974; Roberts 1975), various types of convulsion, including epilepsy (Kier, George & Höltje, 1974), schizophrenia (Swagel, Ikeda & Roberts, 1973) and psychosomatic disorders (Roberts, 1975). The action of barbiturates may also involve interference with GABA-sensitive synapses (Nicoll, 1975). Hence elucidation of the mode of action and the relationship between the structure and activity of GABA is desirable.

The design of therapeutic GABA-mimetic drugs is a complicated process. It is not only necessary for them to possess the appropriate stereochemical features for GABA-like transmitter activity, they must also be able to cross the blood-brain barrier - the system which normally prevents the invasion of the CNS by substances which may disturb it. Thus, although therapeutic substances must not be so closely similar to the natural transmitter that they will be rejected by the blood-brain barrier, they must possess the appropriate disposition of atoms, or ultimately, of electron density, to be recognised by the receptor. The present work has been concerned with the latter problem; that is the identification of appropriate stereochemical dispositions, in both the GABA and glutamate transmitter systems.

In common with all the natural transmitter substances so far discovered, GABA and glutamate are flexible molecules. Indeed, flexibility may be essential to neurotransmitter activity (Conti, Damiani, Pietronero & Russo, 1971; Warner, Player & Steward, 1973; Richards, Aschman & Hammond, 1975). Thus, the determination of atomic arrangements necessary for transmitter action is not merely a matter of inspection of chemical formulae; conformational studies on the transmitter molecule are required. In a number of neurotransmitter systems such investigations have led to reliable predictions of pharmacological activity based on the structural complementarity of transmitter and receptor (Gill, 1959; Kier, 1970; Richards, 1974). In the present work, therefore,

conformational studies have been carried out in order to establish qualitative and quantitative structure-activity correlations in the GABA and glutamate systems.

Before the results are described, it is necessary to present some pertinent background information concerning the nature of the transmitter-receptor interaction, and also to assemble the pharmacological information which is available concerning GABA and glutamate and their respective analogues. Hence, the nature of chemical transmission at synapses and approaches to the study of receptors are described in 1.2.1; the mathematics of the drug receptor interaction and a discussion of the processes which may be involved in the generation of biological response are presented in 1.2.2; and the techniques employed by pharmacologists in obtaining the results used in the present study are detailed in 1.2.3. Structural and electronic features of GABA and glutamate agonists are described in 1.3.1, and a brief resume of the relevant pharmacological data is presented in 1.3.2. A survey of receptor theories for the inhibitory and excitatory amino acids is presented in 1.3.3.

The ultimate aim of the present work is to obtain a picture of the structural features of the GABA receptor and, secondarily, of the glutamate receptor. Knowledge of the molecular geometry of receptors should provide the most unambiguous theoretical basis for the design of drugs and reveal much about the molecular processes involved in amino-acid transmission.

Within this framework, the aims have been to extend the information available on the conformational preferences of amino-acid transmitters (chapter 2) and to use this information to establish structure-activity correlations (chapter 3). These, in turn, have provided material for the further elucidation of receptor geometry (chapter 4). A detailed description of the scope of the work may be found in 1.4, after the summary of background information and contemporary ideas on amino-acid transmitters and receptors.

1.2 Drug-receptor interactions at synapses

1.2.1 Investigation of the transmitter-receptor interaction

(a) Chemical transmission at synapses

Since the pioneering work of Elliott (1904, 1905), Dixon (1906, 1907), Dale (1914) and Loewi (1922), chemical transmission at synapses has been described in progressively greater detail Evidence has been gathered about the role of several substances as synaptic transmitters, the first being acetylcholine (Engelhart & Loewi, 1930). It is much more recently, however, that the transmitter roles of serotonin, the catecholomines and histamine have been demonstrated and only over the last few years that the endogenous nature of amino acid transmitters has been confirmed (Curtis & Johnston, 1974).

The general principles of chemical transmission have been reviewed by many authors (see e.g. Katz, 1966; McLennan, 1970a) but the detailed mechanisms are not yet well understood. In principle when a nerve impulse arrives at a synapse (fig. 1.1) transmitter molecules are released from vesicles in the presynaptic nerve terminal (Gray, 1975), diffuse across the synaptic cleft and interact with a 'receptive substance' (Langley 1905) in the post-synaptic membrane, triggering a transient local membrane permeability change to certain ions. The essence of a transmitter-receptor interaction is transience. There is neither time nor energy available for covalent binding (Mittag, 1970), so the interactions which occur invole mainly ionic, dipolar, dispersive, hydrophobic or hydrogen bonding (Gill, 1965). These forces (excepting hydrophobic bonding) are weaker in aqueous solution than in the gas phase, due to the involvement of water molecules, and stronger chelate like complexes may also be formed (Burgen, 1970).

In the case of inhibitory transmission by GABA, the permeability change resulting from transmitter action is an

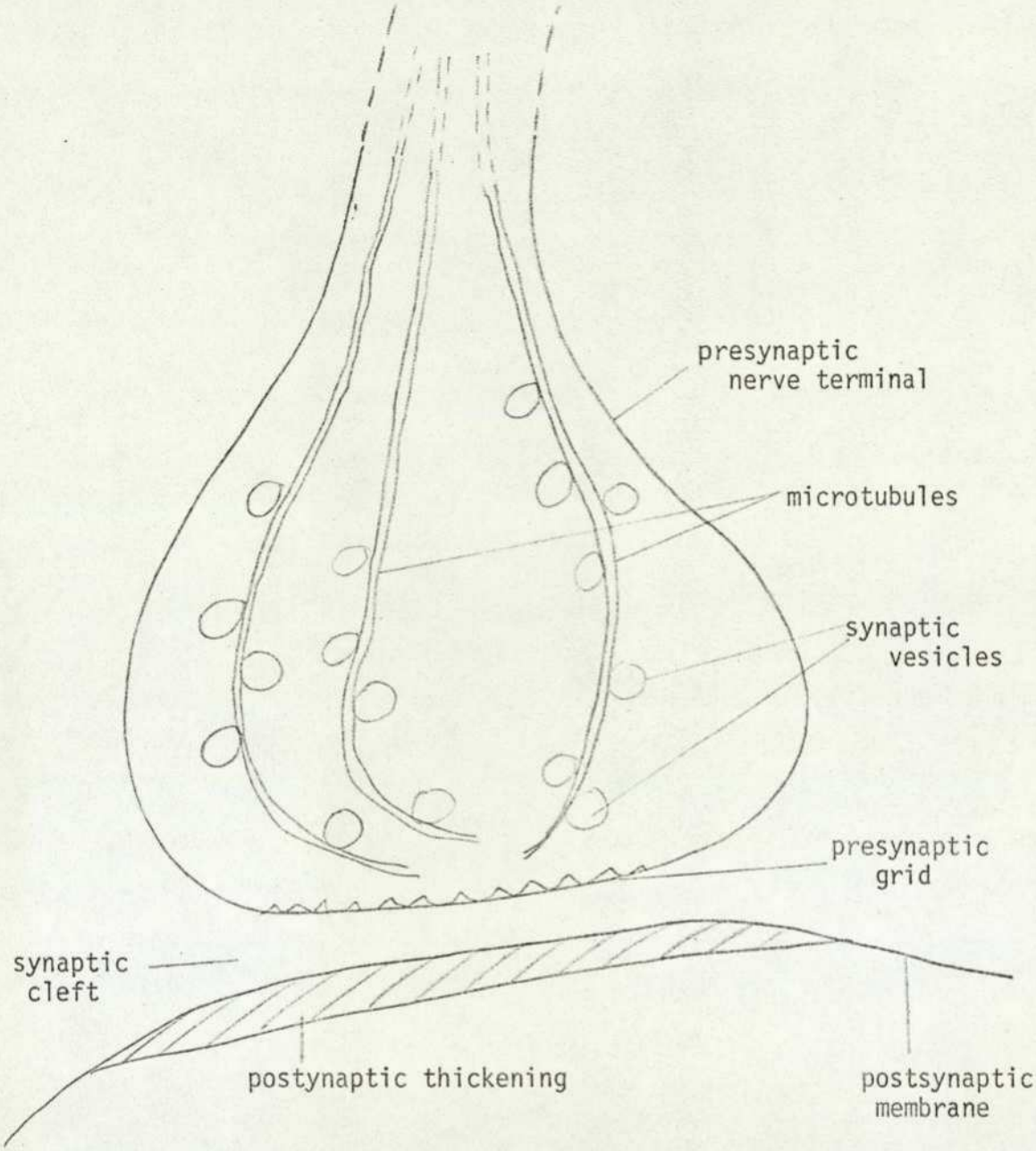

Fig. 1.1 Morphology of a synapse (after Gray, 1975). Vesicles move along microtubules (which may be involved in their genesis) to "vesicle attachment sites" on the presynaptic grid - a triangular array of protein units. Thence, they release the transmitter substance they contain into the synaptic cleft via pores in the presynaptic grid.

increase in the membrance conductance for Cl^- ions. The outcome of this is a transient hyperpolarisation of the postsynaptic membrane; the trans-membrane potential becomes more negative, departing from its resting value of $\sim$ -70mV. The localised hyperpolarisation so produced is termed an 'inhibitory post-synaptic potential" (IPSP). When an excitatory transmitter, such as glutamate, is bound, a more generalised conductance increase ensues, particularly to Na^+ ions, and the post-synaptic membrane becomes locally depolarised. The local depolarisation is known as an "excitatory post-synaptic potential" (EPSP). The mechanism of conductance change is discussed in 1.2.2.

Most nerve cells possess a high density of synapses on their cell bodies and dendrites (fig. 1.2). Hence, at any instant, there may be a large number of EPSP's and IPSP's in existence. In regions where they overlap, EPSP's and IPSP's sum together, so the cell body acts as an integrating device for a large number of incoming signals. If the sum of the EPSP's and IPSP's in the region of the "axon hillock", the area of the cell body closest to the axon, leaves the membrane in a sufficiently depolarised state ($\sim$ -35mV) the cell will "fire", i.e. an impulse (the action potential) will be propagated along the axon. The mechanism of propagation of the impulse is similar to that of its initiation. Each successive segment of the axon is caused to fire by the ion exchange processes occuring in the preceding segment, which result in depolarisation spreading from the centre of the impulse at any instant.

The mechanism by which conductance changes occur at synapses and along axons may be similar. There is evidence (Denburg, Eldefrawi & O'Brien, 1972) that the neurotransmitter acetylcholine can cause axon depolarisation as well as synaptic depolarisation. This implies that receptive substances or 'receptors' for neurotransmitters may exist in the axon membrane as well as the postsynaptic membrane.

Receptors are now generally thought to be protein macromolecules with chemo-recognition properties for the appropriate

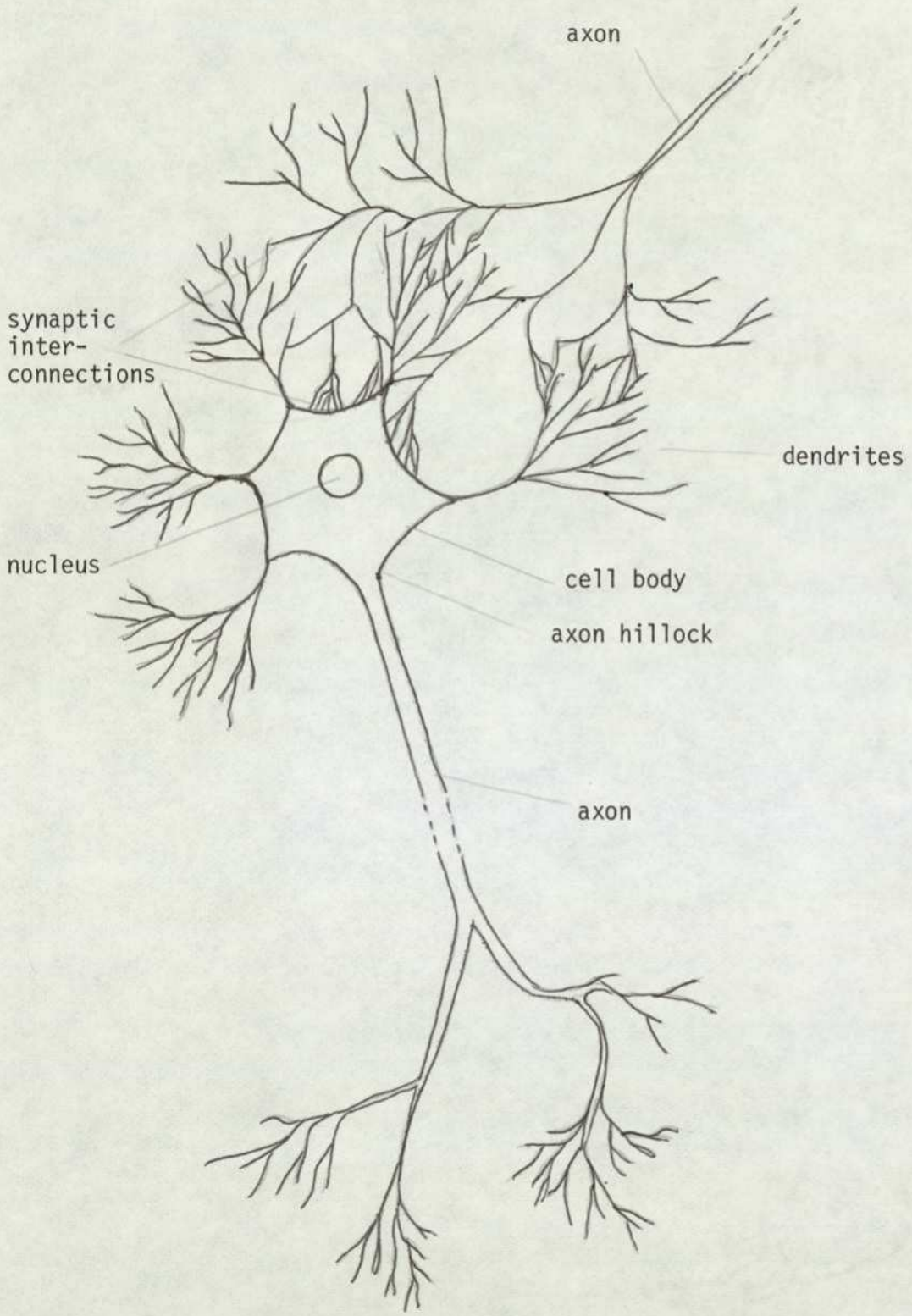

Fig. 1.2 Diagram of nerve cells and interconnections

small transmitter molecules (Gill, 1965; Mittag, 1970). Contemporary opinion on membrane structure (see Appendix 1) would indicate the macromolecules to be embedded in the post-synaptic membrane, the nature of which is a lipid bilayer of fluid consistency (Singer & Nicolson, 1972). Thus receptor proteins and their associated structures would have a degree of freedom of movement, in keeping with the hypotheses of Changeux et al (1970) who postulate the likely role of major conformational changes in membrane-bound macromolecules in the mediation of transmitter-activated membrane permeability changes (1.2.2b).

A brief feasibility study on the investigation of neuronal membrane by low-angle X-ray diffraction is reported in Appendix 1.

(b) Direct investigation of receptors

The study of transmitter-receptor interactions can be approached either from the transmitter or receptor viewpoint, but at present the former is by far the simpler. Little is yet known about the molecular architecture of receptor macromolecules (Mittag, 1970).

Fluorescent probe studies (Changeux, Blumenthal, Kasa & Podleski, 1970) on *in vivo* synaptic material may provide a means of investigating conformational changes occurring during membrane excitation, but, ultimately, the elucidation of the structure of receptors may well come about via the isolation of receptor material itself (Moran & Triggle, 1970; Rang, 1971; Keynes, 1972 and refs. therein). This could be reconstituted in *in vitro* membrane models such as those recently developed for the acetyl-choline receptor (Parisi, Reader & de Robertis, 1972). The reconstituted receptor would be amenable to biochemical and pharmacological investigation, without the complications of *in vivo* systems, where enzymes, for example may degrade applied chemical substances before they reach the receptor. It is interesting and a little surprising that reconstituted systems

have been shown to exhibit transmitter-binding and ionic-permeability properties very similar to the in vivo material (Jain, 1974). X-ray crystallographic studies such as those carried out to investigate the active site of lysozyme (Beddell, Moult & Phillips, 1970) could similarly reveal the transmitter binding sites of isolated receptors.

Recent attempts to isolate GABA and glutamate receptor material (de Robertis & de Plazas, 1974; de Plazas & de Robertis, 1974) have proved successful, but, as yet, sufficient quantities for crystallisation are not available. The GABA and glutamate receptors from shrimp muscle have thus both been shown to be proteolipids (hydrophobic proteins), although receptors for the two substances appear to be independent of one another, confirming similar pharmacological evidence (Takeuchi & Takeuchi, 1967).

(c) Investigating receptors via transmitters

In view of the difficulty of direct receptor investigation, the present work has concentrated on the study of transmitter-receptor interactions via transmitters.

The high potency and specificity of transmitter molecules (often active at concentrations of less than 10^{-8}M) implies some particular mechanism for recognition by synaptic receptors, so receptor models have been developed on the basis of complementarity between structural and electronic features of transmitter and receptor (Paton, 1970).

Structural analogues of natural transmitter molecules are often found to act as agonists, that is, mimicking the action of the natural transmitter at synaptic receptors. The structural analogy needs to be a close one with respect to charge distribution and the presence of essential functional and hydrophobic groups. Conversely certain molecules, sometimes again structural analogues of the transmitters, can act as antagonists, blocking the action of agonist drugs. Increasing hydrophobicity and rigidity of

transmitter analogues tends to favour antagonistic activity (Paton & Rang, 1965; Beers & Reich, 1970). Antagonism can occur in a variety of forms; direct competition with the transmitter for the receptor, chemical inactivation of the transmitter, interaction with another region of the receptor-permeability mechanism in the postsynaptic membrane, or the mediation of an opposite pharmacological effect. It follows that the derivation of information about the molecular geometry of receptor sites from blocking studies is only possible in the case of competitive antagonists. Moreover, it is usually difficult to prove that an antagonist acts at precisely the same site as the transmitter it blocks. The investigation of structure-activity relationships (SAR) among structurally related agonists, however, can provide indications of the geometry of particular receptors, although the potency of agonists does not depend on their binding properties alone (see 1.2.3 for further discussion).

SAR studies concern (i) the correlation, using linear free energy relationships of physicochemical properties of drug molecules with their biological activities (Hansch, 1973) sometimes known as physicochemical-activity relationships (PAR) (Goodford, 1973)), or (ii) the 'mapping' of receptor sites using conformational studies of agonist molecules and the principle of drug-receptor complementarity (Gill, 1959; Kier, 1970; Beers & Reich, 1970). Throughout the present work, the term PAR will be attached to the former, and SAR to the latter. It is the SAR approach which has been successfully applied to transmitter-receptor interactions since all the natural transmitters so far discovered are flexible molecules. Conformational preference is therefore important in their synaptic action. The interpretation of SAR is not trival. Much is unknown - both the pertinent conformations of the drug molecules and the nature of the interaction. For example, multiple binding could occur at one site (Burger, 1970). Furthermore, the interaction itself may cause changes in the geometry of the receptor site (Kier, 1970; Richards et al, 1975), although this may not affect the recognition

properties of the receptor. Despite these drawbacks, however, correlations between conformational or physicochemical properties and biological activities have been obtained for many series of drugs, and have shown some predictive value in forecasting efficacious chemicals for therapeutic use (Hansch, 1973; Goodford, 1973 (on PAR); Kier, 1970, 1971; Richards, 1974 (on SAR)).

1.2.2 The mechanism of drug action

(a) The mathematics of drug-receptor binding

It has proved very difficult to provide a comprehensive theoretical basis for the observed dose-response relationships of agonists. The major theoretical approaches have been 'Occupation Theory' (Clark, 1937) in which response is assumed to be proportional to the number of receptors occupied; and 'Rate Theory' (Paton, 1961) in which response is assumed proportional to the rate of association of the drug-receptor complex. Allosteric models (Karlin, 1967; Changeux, Thiery, Tung & Kittel, 1967), similar to those suggested for enzyme-substrate interactions, have also been put forward on an occupation theory basis. This field has recently been reviewed by Rang (1971) and Paton (1970).

The discussion below outlines the main theories, bringing in examples from the pharmacology of amino-acid transmitters. The present work afforded some scope for the application of these theories to the GABA system, in the light of SAR findings. The results are described in 3.2.3.

(i) Occupation theory

A.J. Clark (1937) in a review of early work on drug-receptor interactions showed that a simple Langmuir expression could account for many dose-response observations. Thus, if one

drug molecule interacts with one receptor:

$$y = \frac{C}{C+1/K}$$

where y is the proportion of receptors occupied and thus the fraction of maximal response, C is the concentration of agonist and K is the affinity constant of the drug-receptor equilibrium. It follows that the dose to produce a half maximal response = 1/K, so K can be directly determined. Unfortunately, the results obtained in dose-response studies do not always conform to this simple equation. Results are highly dependent upon the method of measurement employed and no allowance can be made directly for desensitization of the receptor during the experiment. This effect, lowering the individual response of receptors as transmitter action is prolonged, is likely to modify the results (Paton, 1970). Furthermore, there are probably intermediate steps between drug binding and response which may be interrelated in a non-linear fashion, so the ultimate measured response is only dependent on the drug concentration via a complex chain of events. Hence the simple Langmuir binding function can neither be clearly demonstrated nor disproved by current experimental results.

It follows from the equation above, for example, that a plot of log(E/Emax-E) against log C (known as a Hill plot after Hill (1909)) when E is the effect of concentration C of drug and Emax is the maximum effect, should be a straight line of unit slope. This is seldom the case (Rang, 1971). If the Hill plot has a slope n, the corresponding Langmuir expression is:

$$y = \frac{C^n}{C^n+1/K}$$

which for integral n could imply that n molecules of drug combine with one receptor. The Hill plot for the effect of GABA on the membrane conductance of crayfish muscle, (Takeuchi & Takeuchi, 1969) for example, has a slope of 2, suggesting that two GABA molecules may combine with each receptor before a response is elicited. Even here, however, the method of measurement can alter

the result to a value of 3.5-4 (Feltz, 1971). Non-integral slopes are better explained by maintaining the simple Langmuir binding function (n=1) and postulating allosteric mechanisms involving interaction between receptors (Changeux et al, 1967), than by assuming awkward numerical combinations of molecules in the reaction (Rang, 1971; see below).

The effects of competitive antagonists can also be mathematically treated under occupation theory leading to the conclusion that an agonist dose-response curve should be shifted in the positive direction along the dose axis when a competitive antagonist is present, but remain parallel to the original curve (Gaddum, 1937, 1957). This was experimentally demonstrated for the first time by Arunlakshana & Schild (1959) for atropine antagonism of acetylcholine. Since the mathematics deals only with competitition for binding sites, dose-response studies with competitive antagonists have yielded less ambiguous results than those on agonists. The results tend to support the idea of a 1:1 Langmuir binding equation for both agonists and antagonists (Rang, 1971), implying that the inconsistencies of agonist results reflect the unknown chain of events linking binding and response, rather than the existence of a more complex binding function.

Despite the usefulness of studies on competitive antagonists, however, it is necessary to rely more on studies of agonists in the GABA and glutamate systems since very few competititve antagonists have yet been discovered. In any case, it is very difficult to determine unequivocally whether an antagonist is truly competitive (Hill, private communication, 1975) (1.2.3).

(ii) The concept of 'efficacy'

The capacity of a drug to bind to a receptor is distinct from its capacity to mediate a response once bound. Agonists bind and mediate a response; competitive agonists bind but fail to mediate a response; and in between are 'partial agonists' which

bind, mediate a limited response and block the action of stronger agonists. This has led to the development, under occupation theory, of parameters which describe the ability to mediate a response at the receptor as distinct from the ability to bind (which is measured by the affinity constant K). The parameters usually employed are 'efficacy' (Stephenson, 1956) or 'intrinsic activity' (Ariens, 1954). These are defined slightly differently (Bowman, Rand & West, 1968, p462) but both imply a continuous spectrum of drugs with varying ability to mediate responses.

The efficacy parameter, e, is defined in such a way that maximal response may be obtained for strong agonists (high e) without requiring maximal occupancy of the receptors. The Langmuir expression including efficacy is:

$$\text{biological response} = S = \frac{eC^n}{C^n + 1/K}$$

S is defined to equal 1 when response is 50% of the maximum obtainable. A dose-response relationship of this kind precludes the simple measurement of affinity and efficacy from dose-response curves. Since for strong agonists (low C) $S \rightarrow eCK$, so for 50% response, $eCK = 1$ and K and e cannot be separated. Under this formalism, antagonists have very low e, partial agonists (such as some of the guanidino acids at GABA receptors (Dudel, 1965; Constanti & Quilliam, 1974)) have $e \sim 1$ and strong agonists can have any high e. During the present work, the mechanism of partial agonism among GABA analogues was briefly examined in the light of SAR results. The findings are developed in 3.2.3.

(iii) Rate theory

A further development in the mathematical description of drug action is the rate theory of Paton (1961) who postulated that response was proportional to the rate of association of the drug-receptor complex rather than to the receptor occupancy. This afforded a simple explanation of many of the observations, but clear proof or refutation is lacking (Waud, 1968). The important

theoretical point here is that efficacy becomes quantised (Paton, 1970); the drug is either bound or not bound and binding causes a 'quantum of excitation' to be released. The continuous variation now appears in the association and dissociation rate constants of the drug-receptor interaction.

The rate of association of the drug-receptor complex is:

$$Z = \frac{Ck_2}{C+k_2/k_1}$$

where k_1 is the rate constant for association and k_2 is that for dissociation. Response is then assumed proportional to Z. When a high concentration of drug is used, response is directly proportional to k_2, so an efficacious compound is one which dissociates quickly from the receptor. The parallels between the rate theory and occupation theory expressions are noteworthy: since $k_2/k_1 = 1/K$, k_2 is the equivalent of e. Nevertheless, the predicted forms of response with time in the two cases are quite different (see Bowman, Rand & West, 1968 p466). As before, certain types of experiment can produce dose-response curves of the appropriate form, but the method of measurement makes all the difference.

(iv) The allosteric model

A second approach involving a quantal response of the receptor to occupation is the allosteric model proposed by Karlin (1967) and Changeux et al (1967). The basic postulate is that the receptor can exist in two states in equilibrium with each other (R and T in Karlin's terminology), such that:

$$\begin{array}{ccc} D + R & \rightleftharpoons & DR \\ \Updownarrow & & \\ D + T & \rightleftharpoons & DT \end{array}$$

K_{dr} K_{dt}

The biological response is mediated only by complexes DR. Agonists tend to bind to and stabilise the R form of the receptor, and antagonists to bind to the T form. The efficacy of a drug is thus dependent on its relative affinity for R and T. Furthermore the process of binding may be co-operative in that neighbouring receptors may tend to exist in the same state.

Such a co-operative scheme can account for non-integral Hill plot slopes and also for the fact that dose-response curves tend to be sigmoid rather than hyperbolic as occupation theory predicts. The effect of GABA at the crustacean neuromuscular junction has marked sigmoid characteristics (Takeuchi & Takeuchi, 1969), as have response curves for other neurotransmitters at their respective synapses (Rang 1971). These may be taken as evidence of allosteric processes, but it should be noted that a sigmoid effect curve could be observed for a simple Langmuir binding function if an intermediate step is involved (Rang 1971).

(b) The generation of biological response

(i) Conformation changes at the receptor

The chain of events between drug binding and biological response is still obscure, although it would appear that the first step is likely to be a change of state of the receptor. A conformationl transition of some kind, similar to the allosteric transitions of enzymes, would be a possible mechanism.

The experimental investigation of such a possibility via rate theory has revealed some evidence in its favour. From observations on acetylcholine antagonism, Rang & Ritter (1969) argue that binding of a drug molecule causes the receptor to change to a desensitised state. For agonists, transition of the receptor from one state to the other could be associated with efficacy. The reaction scheme is:

$$D + R \longrightarrow DR \longrightarrow DR' \longrightarrow D + R' \longrightarrow D + R$$

Such results may demonstrate experimentally the kind of model which Changeux et al (1970) suggest for transmitter action, involving conformational changes in membrane macromolecules during the mediation of ionic permeability changes. The general hypothesis is that 'ionophores', whether channels or active transport mechanisms of some kind, undergo structural transition when a transmitter molecule binds to a 'macromolecular receptor' in close proximity to the ionophore. The coupling between the macromolecular receptor and the ionophore is indirect and analogous to the allosteric mechanisms of enzymes. On this basis a number of hypotheses are advanced to account for various transmitter-receptor observations. In particular, the receptor ionophore unit (termed the 'agonist protomer') undergoes a conformational change, on agonist binding, to a permeable state, in which the macromolecular receptor has a preferential affinity for agonists. When in the impermeable state, preferential affinity for antagonists is exhibited. Co-operative interactions between neighbouring agonist protomers may promote the formation of clusters (reminiscent of the acetylcholine receptor model of Parisi, Reader and de Robertis (1972) mentioned above (1.2.1b), or cross-linking of receptor macromolecules by acetylcholine suggested by Allison (1972)).

Evidence of this kind of process in amino-acid transmission systems has been obtained by Young and Snyder (1974) for the antagonism of glycine action by strychnine. Strychnine appears to bind to a site close to the glycine receptor but not identical with it, and acts by blocking the ionic permeability mechanism. A similar effect may occur in the antagonism of GABA-mediated inhibition by picrotoxin. The antagonist appears to act (Takeuchi & Takeuchi, 1965) by blocking the conductance change normally mediated by GABA, rather than blocking the receptor site itself. Thus the receptor site and permeability mechanism may be distinct, but closely associated, the latter being activated via the former. Biochemical evidence for such a distinction is presented by de Robertis and de Plazas (1975) in a study of the binding of GABA to isolated receptor material.

Although the agonist protomer as a whole is likely to undergo a conformational change when a transmitter molecule is bound, there is no direct evidence as yet of conformational changes occurring at the receptor site itself. Such processes are common in enzyme-substrate interactions (Blake, Johnson, Mair, North, Phillips & Sarma, 1967) and have been suggested in the case of transmitter-receptor interactions on the grounds that all natural transmitters so far discovered are flexibile molecules (Richards, Aschman & Hammond, 1975; Kier, 1970) (see 2.1). No such change need be necessary if for instance, the permeability mechanism is triggered by a charge transfer process, but flexibility of the receptor site may be a feature of GABA and glutamate receptors (Curtis & Watkins, 1960). The evidence for such a possibility is discussed in 1.3.3 and a detailed scheme is developed in 3.2.

(ii) The permeability mechanism

As regards the permeability mechanism itself, two possibilities are generally recognised. The permeant ions migrate across the cell membrane either by passing through channels in the membrane or by active transport involving a carrier molecule. Separate channels or carriers would be present for different ions. Carrier behaviour of this kind has been observed in model membrane systems where antibiotics such as valinomycin or nonactin are introduced into a lipid bilayer. However, the evidence in the case of intact nerve membrane favours the channel hypothesis, on the basis of greater speed and ability to conduct ions at low temperatures (see Keynes (1972)). Keynes suggests that natural pore-forming molecules may extend across the membrane in a dumb-bell form with hydrophilic ends separated by a central section with a hydrophilic core but lipophilic outer side-chains. Hydrated ions would migrate through channels in the hydrophilic central region. A model system of a similar kind has been demonstrated by Urry (1972) using the pore-forming antibiotic gramicidin in an artificial lipid bilayer. Gramicidin possesses

two energetically similar conformations which exhibit opposite dipole moments perpendicular to the plane of the bilayer. In one of these conformations, the molecule possesses a transmembrane pore. Thus pores could be opened by changes in the transmembrane potential. There is a close connection between permeability change and conformational change in this experimental system, paralleling the hypothesis of Changeux et al (1970). A conformational change in nerve membrane proteins dependent on the transmembrane electric field is also discussed by Tredgold (1973) who points out similarities with the ferroelectric transitions which occur in some inorganic materials. This idea is supported by the dielectric hysteresis properties exhibited by some proteins (Tredgold & Sproule, 1973).

In view of these observations, any receptor model must allow for the possibility of structural changes which could result in the formation of channels in the membrane (cf. Gill, 1965). The molecular units which could be involved in receptor architecture are therefore limited (4.2.2) with the result that suggestions of likely amino-acid arrangements in the vicinity of receptor sites can be formulated (Smythies, 1974).

1.2.3 Measuring the effect of transmitter drugs

The relative potency measurements used in the structure-activity correlations of chapter 3 are mainly derived from two types of pharmacological experiment; firing rate or conductance change measurements.

(a) Firing rate studies

Most of the potency values employed in the present work are observations of the firing rate of individual nerve cells, stimulated chemically, electrically or physiologically. For GABA and its agonists, which reduce firing rate, the amount of drug required to produce a standard reduction is measured; for glutamate

and its agonists, which excite cells, the firing rate itself is the value recorded. The drugs are usually administered electrophoretically via multibarrelled micropipettes, and the firing rate measurements taken from an electrode implanted in a cell nearby (see Curtis & Watkins, 1960). With different substances in the barrels the effect of a number of chemical agents on the same cell can be assessed. Solutions in the barrels are adjusted to the appropriate pH for electrophoretic ejection. The ejection current is a measure of the quantity of drug released, so a comparison of currents necessary to produce a standard change in the cell's firing rate is a measure of the relative potency of the drug under test (Bowery & Brown, 1974). Hence:

$$\text{Relative potency} = 1/C_i$$

where C_i is the concentration of drug i which produces the same response in the cell as 1 unit of the standard drug.

It must be assumed that all the drugs under comparison are acting at the same synapses and do not diffuse away or suffer enzymatic degradation to a different extent. Enzymatic removal is not considered to be of great importance in microiontophoresis, so these assumptions are believe to be reasonable (Curtis & Watkins, 1960; Curtis & Johnston, 1970) as is the assumption that the drugs act at physiological pH despite existing at different pH's in their micropipettes (Curtis & Watkins, 1960).

(b) Conductance measurements

The second method of comparing transmitter drugs is to measure directly by means of electrodes the conductance change produced in the cell membrane by a particular drug. Here the cell is normally removed from the animal (in contrast to the microiontophoretic experiments) and placed in a chamber where it is perfused with a nutrient solution containing the drug under test. The concentration of drug is gradually increased and equilibrium conductance measurements taken. A dose-response curve shows how

membrane conductance changes with concentration of drug. The experiment is repeated on the same cell using different drugs (see e.g. Swagel, Ikeda & Roberts, 1973). Again relative potency is defined as $1/C_i$, where C_i is the relative concentration of drug required to produce a standard response. In the study mentioned above, the standard response was the half-maximal response to GABA.

This type of relative potency measurement tallies very closely with values determined from threshold firing rate reduction experiments (Edwards & Kuffler, 1959, cf. Swagel et al, 1973).

(c) Potency values and SAR studies

When relative potencies of drugs, measured as described, are employed in structure-activity correlations, two points should be borne in mind. Firstly, the values obtained for relative potency are very approximate. Repetition of measurements may give a fairly reliable mean, but the scatter of results about the mean is very large. There may be as much as an order of magnitude difference in the relative potency of a drug calculated from experiments on different individual cells of the same type. This is particularly true for the measurements on excitatory amino-acids (Curtis & Watkins, 1963). As a result of this, different sets of experiments sometimes give very different relative potencies for the same substance (see Table 1.1) even on similar preparations. Structure-activity correlations, then, cannot be expected to yield results more consistent than the precision of the biological measurements from which they are derived.

Secondly, potency as defined above may involve more than one variable. That is, both 'affinity' and 'efficacy' of the drug molecule are involved and furthermore, desensitization of the receptor may occur during the experiment (1.2.2). If efficacy were not considered, relative potency would be equivalent to relative affinity, but once efficacy is considered, the two factors become inextricably linked in the dose-response curve (1.2.2a).

This has led some authors to suggest (e.g. Paton, 1970) that more useful SAR studies can be made by comparing the binding characteristics of competitive antagonists than by comparing the relative potencies of agonists. This is probably fair comment in cases where antagonists are known to be competitive, but, particularly in the GABA system, it is technically difficult to assess whether this is really so (Hill, 1975). In any case, although in the GABA and glutamate systems structural considerations support the idea of competitive action by one or two substances, there are not enough established specific antagonists for a comparative study to be made.

Thus it is necessary to make one of the following assumptions: either i) affinity and efficacy can be treated together, desensitization taken to be equal for different agonists and relative potency measurements employed in SAR work, or ii) a sufficient number of known antagonists must be considered to act competitively.

The former assumption has been made here as in similar work in the histamine system (Richards, 1974), because of the lack of data on competitive antagonists and the success of the many PAR studies which use standard relative potencies (Hansch, 1973). It seems reasonable that, when the main structure dependent variable under consideration is conformation, and the functional groups of a series of agonists are closely similar in electronic properties, the 'concept of optimum stereospecificity maximising efficacy' (Kier, 1970) may be adopted. The major variable involved in the present work is the spatial disposition of binding moieties in the transmitter molecule, which, for maximum effect must match exactly the complementary sites on the receptor. The information derived from SAR results in this context is something of a mixture; features which promote binding and those which promote response remaining unresolved. Nevertheless, the results presented in chapter 3 do reveal a possible mechanism of action in the GABA system which brings affinity and efficacy together.

1.3 BACKGROUND TO THE STRUCTURE AND BIOLOGICAL ACTIVITY OF GABA AND L-GLUTAMATE

1.3.1 Chemical features of GABA and L-glutamate agonists

The important structural elements of amino-acid transmitters are their functional groups and the chains, usually flexible, which link them. With respect to biological activity, the important features are the electronic state of the functional groups and the conformational state of the flexible chains, which determine the charge separation of the molecule. The following discussion describes the conformational flexibility which these molecules possess, and the electronic properties of the functional groups important in transmitter action. Further discussion of the role of conformation may be found in 2.1, while the results of conformational analyses of amino-acid transmitters are reported in 2.2-2.4. The torsion angle convention employed throughout this study may be found in the list of conventions on page xiv.

(a) GABA

GABA is the third homologue of the α-ω amino acid series; $H_2N.(CH_2)_nCOOH$.

The molecule possesses four bonds about which rotations can occur affecting its conformation (Fig 1.3). Rotations T_2 and T_3 control the gross shape of the molecule, particularly the distance between the functional groups. These rotations are not free, however; they are restricted by energy barriers of 4-8 kcal/mole (Taylor, 1948). This means that only certain combinations of torsion angles (T_1, T_2, etc) are energetically accessible to the molecule. For a molecule as small as GABA an energy surface can be prepared by potential-energy (PE) or molecular orbital (MO) calculations with T_2 and T_3 as co-ordinates, showing which regions of conformation space are of low energy. Results of such studies are presented in chapter 2. All the potent GABA agonists so far reported possess some degree of flexibility, except for the rigid analogue 4-aminotetrolic acid (ATA). Other rigid compounds which have been tested as GABA agonists, notably the amino benzoic acids

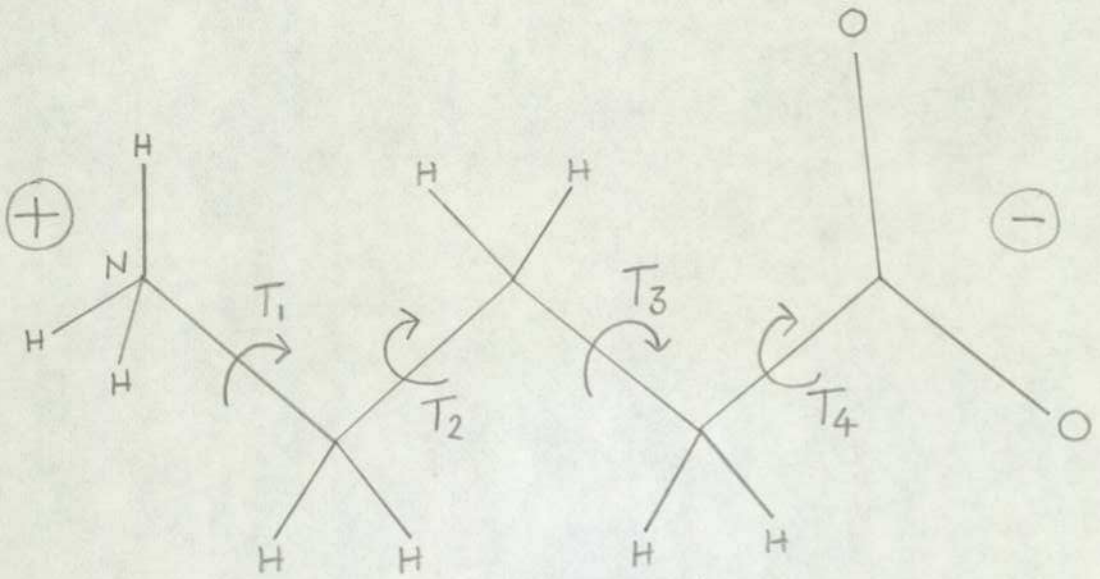

Fig. 1.3 The GABA molecule: illustrating possible rotations

and pyridene 3 carboxylic acid, are inactive (McGeer, McGeer & McLennan, 1961) although this may be an electromeric effect rather than an effect of rigidity.

In neutral aqueous solution, α-ω amino-acids exist predominantly as zwitterions: $^{+}H_3N(CH_2)_nCOO^{-}$, since the pKa for the reaction $^{+}H_3N\text{-} \xrightarrow{H_2O} H_2N\text{-}$ is 9-11 and pKa for $\text{-COOH} \xrightarrow{H_2O} \text{-}\ COO^{-}$ is 2.5 (Conway, 1952). This means, in the former case, that when the pH of the solution is below 9-11, the basic end of the molecule will exist as $^{+}H_3N\text{-}$; and in the latter case, that when the pH of the solution is below 2-5, the acidic end of the molecule will exist as -COOH. Hence in the intervening pH region (including physiological pH, which is ~ 7), the molecules will exist as zwitterions.

This is also the case with most other GABA analogues of the form $X.(CH_2)_n.Y$ (1.3.2) where X can be the guanidino group

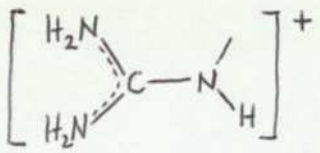

which has a pKa $\sim$12, or the imidazole group

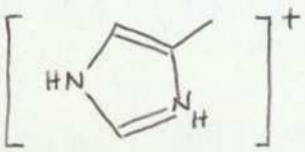

which is likely to be only partially ionised, since it has a pKa $\sim$ 6-7 (Kier, George & Höltje, 1974); and Y can be the sulphonic acid group

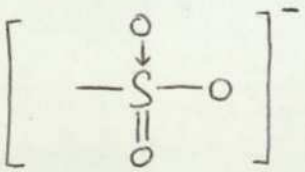

with pKa $\sim$ 1-2, or the isoxazoline ring

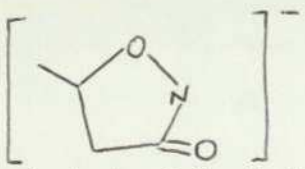

which is also ionised at physiological pH (Kier & Truitt, 1971).

It is possible that a small quantity of the un-ionised compound $X.(CH_2)_n.Y$ exists in neutral solution due to proton transfer, but this will only be a minute amount (Diebel & Swinehart, 1957). Thus it is likely that the species which interacts with the receptor is the zwitterion, so the conformational studies of 2.3 and 2.4 concern the zwitterionic forms of the molecules. (It may be noted, though, that un-ionised molecules are most easily transported through lipid membranes, so if the important receptor sites lie below the membrane surface, un-ionised molecules could take part in the reaction, a supply being kept up by the operation of the neutral $\rightleftharpoons$ zwitterion equilibrium.)

In the case of substituted compounds, fewer pKa values are available but it is likely that the predominant ionic species at physiological pH is the zwitterion in most cases. The form of the active species needs to be known if quantitative comparisons of the potency of different agonists are to be made (3.2, 3.3), since it is necessary to know the concentration of active molecules at the receptor. However, if the equilibrium involved in the formation of the active form is not a rate limiting step in the interaction, a constant supply can be kept up as mentioned above, causing the total concentration of drug to become the important parameter.

The electronic structure of GABA analogues is interesting since if appears to be stable with respect to conformational change (Borthwick & Steward, 1975[a]). Moreover the charge distributions of several GABA-like molecules (GABA, muscimol, ATA, cis and trans amino crotonic acid (ACA), β hydroxy GABA (βHG) and α fluoro GABA (αFG) (Borthwick & Steward, 1975[b]; Warner, 1975)) have been investigated by MO calculations and have been found to be remarkably consistent, particularly with respect to the functional groups. The charge distributions (fig. 1.4) for zwitterions show large negative charges on the oxygen atoms of carboxyl groups, but the positive charges on basic groups such as amino and guanidino are seen to reside mainly on the hydrogen atoms, not the nitrogens.

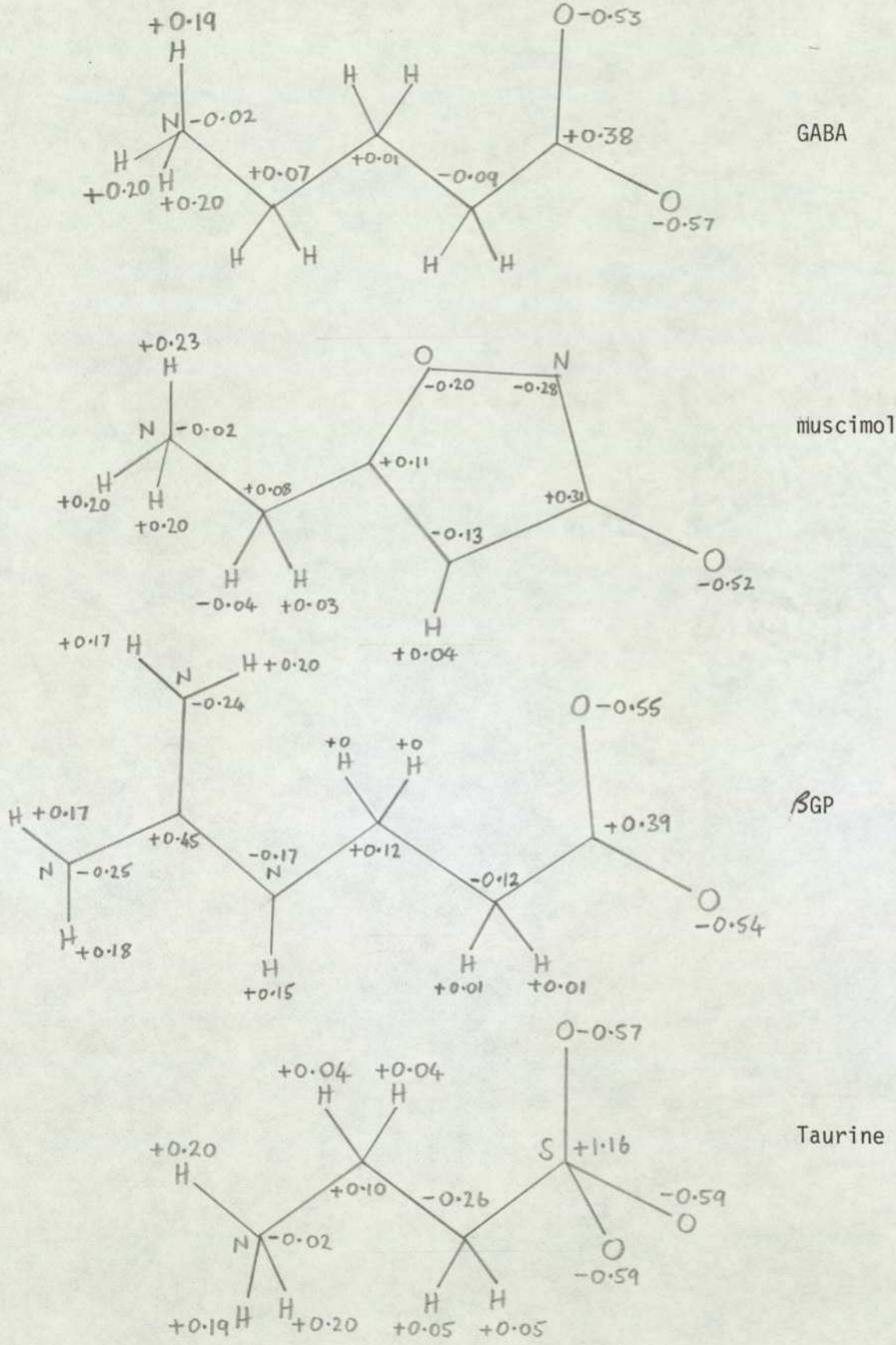

Fig. 1.4 GABA agonists: charge distributions for some zwitterions calculated by the CNDO/2 method (Borthwick & Richards, unpublished.) Units: e

In the isoxazolidone ring (fig 1.4) the negative charge is seen to be shared between the two oxygen atoms and the nitrogen. These observations have important consequences when intercharge distances with respect to rotation about single bonds in the molecule are calculated (2.1), since the positive charge centre is clearly not at the nitrogen atom itself.

(b) L-glutamate

L-glutamate, $HOOC.(CHNH_2)(CH_2)_2COOH$, is structurally a substituted derivative of GABA (fig 1.5). It is a dicarboxylic amino-acid, important in protein structure, as well as possessing a transmitter role and a number of other functions in living organisms. Like GABA, it is a highly flexible molecule with similar opportunities for rotation about single bonds. The structural similarities to GABA suggest the idea that the contrasting transmitter activities of the two compounds may in some way be related (Curtis & Watkins, 1960) but it seems clear on the basis of receptor desensitisation experiments that, in invertebrates at least, the receptors for GABA and L-glutamate are distinct (Takeuchi & Takeuchi, 1965). A number of semi-rigid L-glutamate agonists have been reported recently (Biscoe et al, 1975), but none of them possess the rigidity of ATA.

In neutral aqueous solution, pKa values indicate that glutamic acid, its homologues (e.g. aspartic acid) and structural analogues are likely to exist as monoanions (Curtis & Watkins, 1960) all three ionisable groups being charged. The conformational studies reported in 2.4.4 for glutamate homologues are thus carried out on monoanions. The pKa of the α-carboxyl group is ~ 4 for glutamate.

MO studies (Borthwick & Steward, 1975[a,b]) have revealed the electronic charge distribution of one important glutamate agonist, ibotenic acid, an isoxazolidone glutamate analogue. The results show close similarities to those for GABA-like compounds. In particular, the functional groups appear to possess consistent

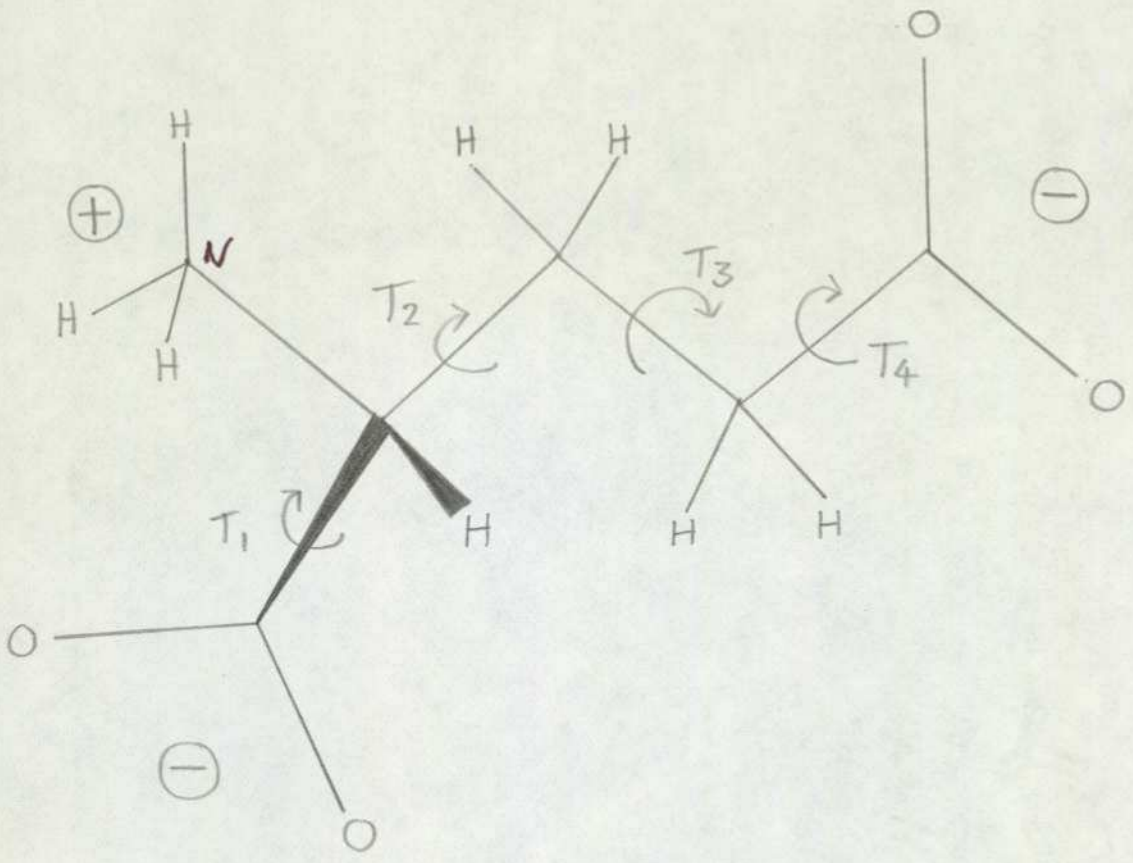

Fig. 1.5 The L-glutamic acid molecule

electronic structure wherever they occur, unless they are involved in very close-approach configurations with other atoms (Borthwick & Steward, 1975[b]). Again the positive charges do not occur on the nitrogen atom itself in the NH_3^+ group so that the positive charge centre is displaced. In the present work this observation is important (as for GABA agonists) when inter-charge distances are considered (2.1).

1.3.2 Pharmacology of GABA and L-glutamate

The pharmacology of GABA and its analogues as inhibitory transmitters and L-glutamate and its analogues as excitatory transmitters has been extensively reviewed, notably by Curtis & Watkins (1960), Curtis & Watkins (1965), Krnjevic (1970), Curtis & Johnston (1970), Johnson (1972), Iversen (1972), Curtis & Johnston (1974).

The two series of pharmacological results are treated in parallel in this section, since parallels between the effects and indeed the molecular structures (1.3.1) of inhibitory and excitatory amino-acids are apparent. In particular, the fundamental finding of the early pharmacological work was that both GABA agonists and L-glutamate agonists show peak activity for a particular chain length in a homologous series. Active molecules all have a positively-charged functional group and a negatively-charged functional group, in the case of inhibitory transmitters, and a positively-charged group and two negatively-charged groups in the case of excitatory transmitters. Hence, Curtis & Watkins (1960, 1965) imply the formula $Y(CH_2)_nX$ for inhibitory amino-acid transmitters, where Y is COO^- or SO_3^- and X is NH_3^+, $NH(CNH_2)NH_2^+$ (the guanidino group) or equivalent. These groups are all ionised at neutral pH and show, respectively similar charge distributions (1.3.1). Maximum inhibitory activity is exhibited by molecules with n=3 (n=2 when X is the guanidino group). The GABA homologue glycine ($^+H_3NCH_2COO^-$) is an important neurotransmitter in its own right in the spinal cord, where there is also some evidence of a transmitter role for taurine ($^+H_3N(CH_2)_2SO_3^-$) (Curtis & Johnston, 1970).

Excitatory transmitters are amino-acids having the formula $Y.(CH_2)_{n-1}.(CHNH_3^+).COO^-$ (Curtis & Watkings, 1960, 1965). Again they exhibit maximum activity for a chain length of 3 (i.e. n=3). L-aspartate (the next lower homologue of L-glutamate) is also a likely neurotransmitter candidate (Curtis & Johnston, 1970).

Inhibitory or excitatory activity is decreased by substitution on the alkyl chain, in most cases, (Tables 1.1 and 1.2) and abolished by substitution on either of the terminal groups, although substitution on the amino group of shorter excitatory amino-acids sometimes enhances activity (Table 1.2).

In tables 1.1 and 1.2 a synopsis of pharmacological results for a range of preparations is presented, for GABA agonists and L-glutamate agonists respectively. The important compounds are illustrated and their activities catalogued. The last column of each table provides a key to structural studies which have been carried out for these molecules. Brief notes on the sites at which GABA or L-glutamate are likely transmitter candidates are set out below, to provide background for the conformational and SAR studies reported in chapters 2 and 3 respectively.

(a) GABA Pharmacology

The results are divided into data from invertebrates and data from vertebrates. Under each heading, information on the transmitter role of GABA, the action of antagonists and the termination of transmission is assembled.

(i) Invertebrate

Invertebrates are useful subjects for the study of inhibitory transmission, since they possess both inhibitory and excitatory synapses in the peripheral nervous system. The

inhibitory processes in vertebrate motor pathways, however, all take place within the brain and spinal cord where experimentation is much more difficult (Iversen, 1972).

The synaptic regions of lobster muscle are sensitive to GABA, which causes a hyperpolarisation by increasing membrane conductance to Cl^-, the typical result of GABA-like action (Curtis & Watkins, 1965). GABA exhibits presynaptic and postsynaptic inhibition (see Fig 1.6) at the crustacean neuro-muscular junction, but there is evidence (Dudel, 1965[a],[b]) that the presynaptic receptors (on the excitatory nerve terminals) and the postsynaptic receptors (on the muscle fibres) may differ. α-ω guanidino acids mimic GABA action at the presynaptic site but (except for α guanidinoacetic acid) not at the postsynaptic site; that is, they fail to produce a change in the conductance of the muscle fibres (Dudel, 1965[a]). β guanidinopropionic acid, in fact, seems to act as a competitive antagonist of GABA at the postsynaptic site (Dudel, 1965[b]). GABA exerts an inhibitory effect on crayfish stretch receptors and giant motor fibres (Curtis & Watkins, 1965) and inhibits some insect muscle fibres (Usherwood & Grundfest, 1965).

Bicuculline (BIC) and picrotoxin block the inhibitory effects of GABA and of the natural transmitter in these preparations but BIC is more effective than picrotoxin on some (McLennan, 1970[b]) and less on others (McLennan, 1973). Picrotoxin appears to act non-competitively, affecting the ionic conductance mechanism rather than the GABA receptor site itself (Takeuchi & Takeuchi, 1969). Some evidence for the competitive action of BIC in invertebrates is provided by the observation (de Robertis & de Plazas, 1974) that the antagonist binds to GABA receptor proteolipids isolated from shrimp muscle.

(ii) Vertebrate

In the spinal cord GABA does not exactly mimic the natural transmitter, which is believed to be glycine (Aprison, Davidoff & Werman, 1970; Curtis et al, 1968). For instance,

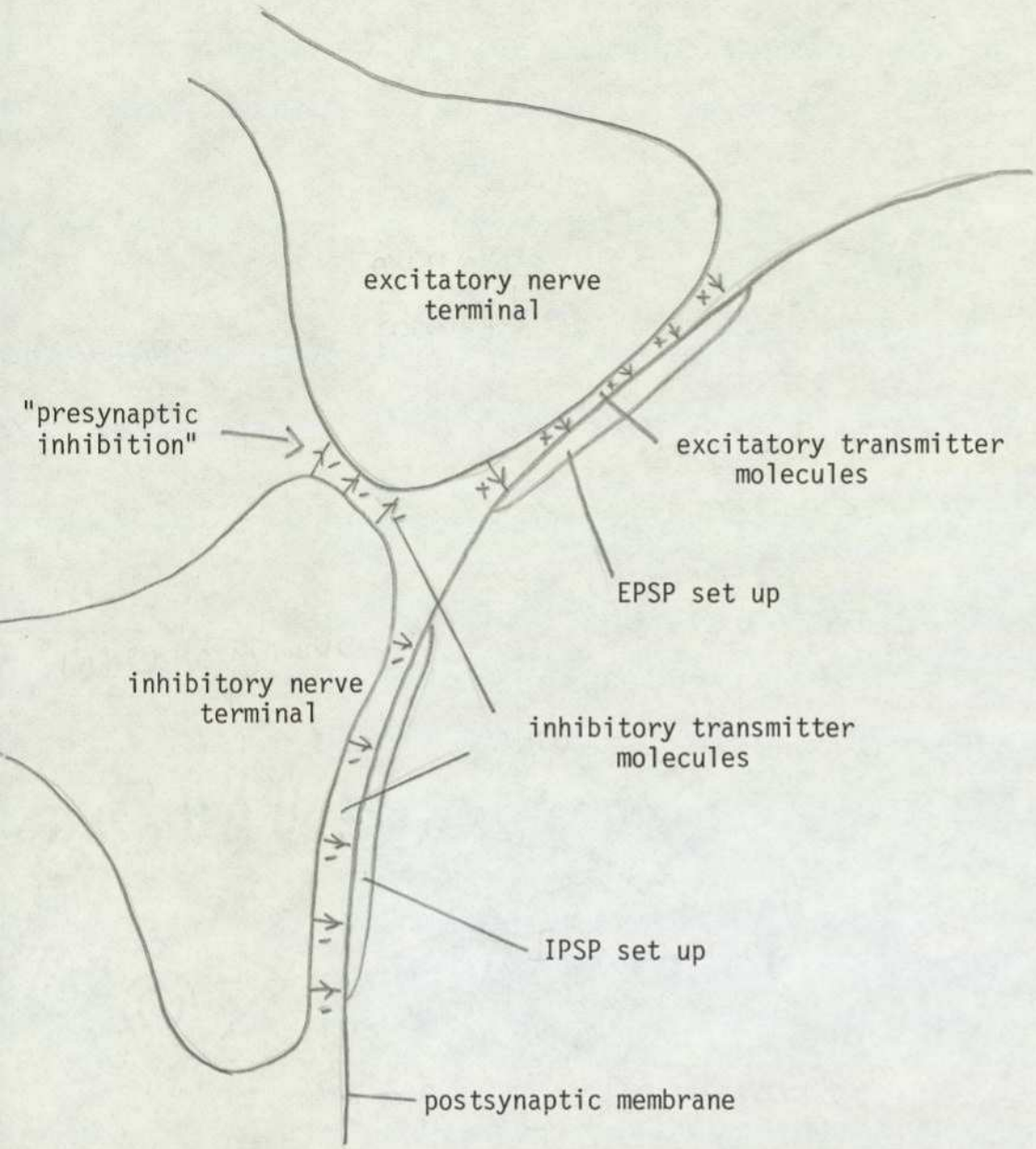

Fig. 1.6 Schematic diagram of a possible anatomical arrangement for presynaptic inhibition

GABA action is not antagonised by strychnine, which blocks glycine action. However, at strychnine insensitive synapses in the cord, particularly the spinal motoneurones in the dorsal horn, GABA is implicated as a transmitter (Curtis & Johnston, 1970). GABA is likely to have an important transmitter role in the brain (Krnjevic & Phillis, 1963), notably in the cerebral cortex and the Purkinje cells of the cerebellum, where strychnine insensitive inhibition predominates (Krnjevic, 1970; Obata, Ito, Ochi & Sato, 1967). Hyperpolarisation by GABA is again due to an increase in membrane conductance to Cl^- (Krnjevic & Schwartz, 1967). GABA is also implicated as a transmitter in cells of the retina (Kuriyama, Sisken, Haber & Roberts, 1968), the visual cortex and the hippocampus (Fonnum & Storm-Mathison, 1971), and has been shown to be released in the cerebral cortex during sleep, when inhibitory processes predominate (Jasper, Khan & Elliott, 1965). In mid-brain regions such as the substantia nigra (Crossman, Walker & Woodruff, 1974) and medulla pons (Dray & Straughan, 1974) there is also evidence for a transmitter role for GABA.

Both pre- and postsynaptic inhibition occur in the cuneate nucleus. GABA is a likely transmitter candidate at both receptors, which would appear to be different (Davidson & Southwick, 1971).

BIC (Curtis, Duggan, Felix & Johnston, 1970[a]) and its more soluble derivative, N-methyl bicuculline (NMeBIC) (Johnston, Beart, Curtis, Game, McCulloch & McLachlan, 1972), picrotoxin and benzyl penicillin (Curtis, Game, Johnston, McCulloch & McLachlan, 1972) all antagonise GABA action in the mammalian CNS. In the case of BIC, stereochemical considerations support the idea that the antagonism exhibited may be competitive (Curtis et al, 1970[a]; Steward, Player, Quilliam, Brown & Pringle, 1971), but there has been some dispute about the pharmacological evidence for competitive action (Godfraind, Krnjevic & Pumain, 1970; Curtis, Duggan, Felix & Johnston 1970[b]; Svenneby & Roberts 1973; Curtis, Johnston, Game & McCulloch, 1974; Straughan, 1974). Only one stereoisomer,

TABLE 1.1 GABA AGONIST RELATIVE POTENCIES

SUBSTANCE	STRUCTURE	Crayfish stretch Receptor a	b	c	Crayfish neuromuscular junction d	e	Mammalian spinal neurones f	Feline cortical inhibition g	Rat hippo-campal neurones h	Rat superior cervical ganglia 1	Structural data available
∝-ω amino acids											
glycine	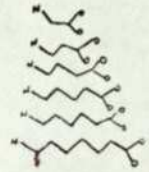	.77	0	.83	.14	0	- -	+ +		<.1	✓
β alanine		48	110	33	33	20	- - -	+ + + +		10	✓
ɣ aminobutyric acid (GABA)		1000	1000	1000	1000	1000	- - -	+ + + +		1000	✓
δ aminovaleric acid		71	40	140	20	50	- -	+ +		48	
ε aminocaproic acid		9.5	20	2.4	.5	<1	-	0		<.1	
7 aminocaprylic acid			1				0				
derivatives											
N-methyl glycine	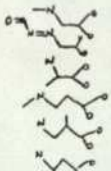						-				
N-formimino glycine							-				
∝ alanine (D & L)							- -				
N-methyl β alanine							- -				
β amino isobutyric acid							- -				
β amino butyric acid (β methyl δ alanine)		1.7	2		..3	<1	-	0		<.1	✓
2-4 diamino butyric acid		4.6	0			<10	-	+		1.2	
∝-fluoro-GABA							>GABA (J)				✓
β-hydroxy GABA			140		500		- -	+ + + +		270	✓
GABA choline	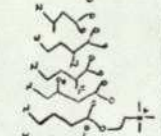		30								
4-methyl GABA							- - -				
N-methyl GABA	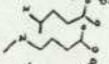									5	
4 aminotetrolic acid	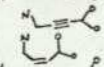						½-⅓ GABA(k)				✓
cis 4 aminocrotonic acid	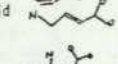						⅓ " "				✓
trans 4 aminocrotonic acid	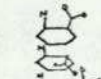						~ " "				✓
DL aminocyclohexane carboxylic acids											
1:2 cis	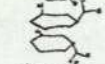								slight		
1:2 trans									~GABA		
1:3 cis									~⅓ GABA		
1:3 trans									v slight		
1:4 cis/trans	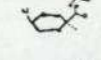								vv slight		
∝-ω guanidino acids											
∝ guanidinoacetic acid	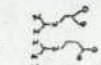	570	570		330		- - -	+ + + +		57	✓
β " propionic acid		710	1230		500		-	+ + + +		120	✓
ɣ " butyric acid		123	8		10		0	+ +		.7	✓
δ " pentanoic acid		5.3			1.4						
derivatives											
creatine	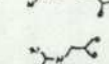	.9	0				0				✓
2 guanidinopropionic acid					12.5						
∝ " butyric acid		3.6			.5						
β " " "		109			140						
L 2 amino 3 guanidino propionic acid	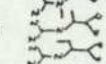		250								
hydrazino propionic acid							- - - (I)				
muscimol	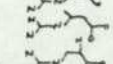						- - -				
imidazoleacetic acid			1520	300							✓
" propionic acid			25	50							✓
" carboxylic acid				0							✓
" lactic acid				3							
1-methyl imidazole 4 acetate	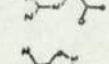		35								✓
taurine	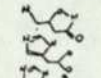	4.8	4			<20	- - -	0		1	✓
homotaurine							- - - -			3400	✓

Table 1.1 References

a) Edwards and Kuffler (1959)
b) McGeer et al (1961)
c) Swagel et al (1973)
d) Dudel (1965[a])
e) Robbins (1959)
f) Curtis and Watkins (1960)
g) Purpura et al (1959)
h) Segal et al (1973)
i) Bowery and Brown (1974)
j) Curtis et al (1972[a])
k) Johnston et al (1975)
l) Van Gelder (1971)

Table 1.2 References

a) Curtis and Watkins (1963) potencies approximate: ± 30%
b) Curtis and Watkins (1960)
c) Curtis and Watkins (1965)
d) Johnston et al (1968)
e) Johnston et al (1974)
f) Curtis et al (1972[a])
g) h) Biscoe et al (1975)
i) McDonald and O'Brien (1972)

TABLE 1.2

GLUTAMIC ACID ANALOGUES

RELATIVE POTENCIES

SUBSTANCE	STRUCTURE	Spinal inter-neurones		Frog spinal motor neurones	Insect neuro-muscular j[n].
		ref: a	g	h	i
Amino malonic acid	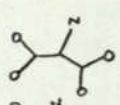	0.2[b]			
Aspartic acid D	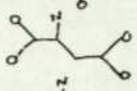	0.70			
L		1.00			
Glutamic acid D	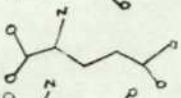	0.7			
L		1.0	1.0	1.0	1.0
∝amino adipic acid DL	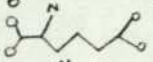	0.2			
∝amino pimelic acid DL	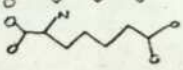	0.2[b]			
N methyl aspartate DL	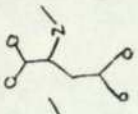	4.0			
D		6.5			
L		0.7			
N methyl glutamate DL	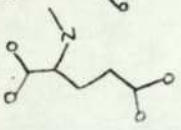	1.0			
D		1.0			
L		1.0			
NN dimethyl asp DL	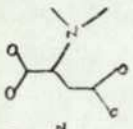	0.7			
D		0.2			
2 amino 3 sulphino n propionate DL	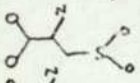	1.3			
L					.133
2 amino 4 sulphino n butyrate DL	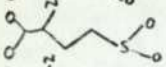	1.5			
2 amino 5 sulphino n valerate DL	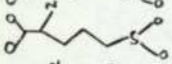	0.7			
cysteic acid D	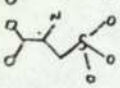	0.7			
L		1.3			.154
homocysteic acid DL	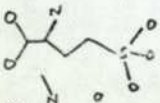	3.0	3-5	11	.015
D		4.5			
L		1.0			
N methyl cysteate DL	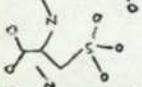	0.7			
L		0.2			
N methyl homocysteate DL	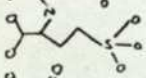	0.7			
βN oxalyl L ∝,β diamino propionate	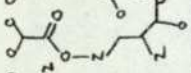	3.0[c]			
Ibotenic acid	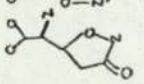	3.0[d]			
			40-200	127	
Kainic acid	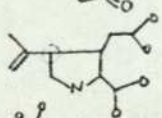	1.3		0.4	
∝Allokainic acid					
Cycloglutamate	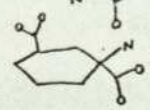		0.7 - 0.8[e]		
Quisqualic acid	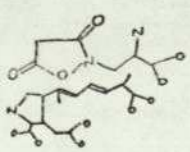		25 - >200	389	
Domoic acid			50 - >200	293	
O phospho L serine					.004
2-amino 3 phosphopropionate	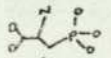				.002
2-amino 4 phosphobutyrate	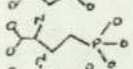				.011
γ methylene glutamate	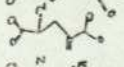	1.0[f]			
γ fluoro glutamate	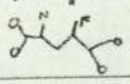	1.0[f]			

(+) bicuculline, is effective as an antagonist (Hill, Simmonds & Straughan, 1974; Collins & Hill, 1974). This finding has important implications as regards receptor investigation (1.3.3a).

Picrotoxin does not antagonise GABA on cortical neurones or Purkinje cells and is not considered to be a competitive antagonist (Obata, Takeda & Shinozaki, 1970). No evidence of a competitive action of benzyl pecicillin is available, although, again, structural considerations suggest such a possibility (Curtis et al, 1972b; Beart, Curtis & Johnston, 1971).

In contrast to the results quoted above, GABA exerts a depolarising effect at mammalian dorsal root ganglia, where it appears to act as a transmitter at primary afferent neurones (Bowery & Brown, 1974). The mechanism is not yet clear; it could involve increased membrane conductance to K^+ or to Na^+ and may be similar to that involved in presynaptic inhibition by GABA in the mammalian CNS (Feltz & Rasminsky, 1974).

It is probable that the pharmacological action of GABA is terminated by uptake of the transmitter into the presynaptic nerve terminal (Iversen, 1972) or possibly nearby glial cells (Hutchison, Werrbach, Vance & Haber, 1974) by a specific sodium-dependent high-affinity transport system (Fig 1.7). This type of process, rather than enzymic hydrolysis, appears to be implicated as the normal mode of transmitter inactivation (Bennett, Mulder & Snyder, 1975). Inhibitors of GABA transaminase, the GABA metabolising enzyme, do not in fact prolong GABA action (Curtis & Johnston, 1970). Moreover, there is good evidence that GABA pharmacological and uptake receptors are distinct, since blockers of one leave the other unaffected (see 1.3.3).

(b) L-glutamate pharmacology

L-glutamate and its analogues possess an asymmetric α carbon atom and thus each exist in two enantiomeric forms. The differences in pharmacological action between enantiomers are somewhat variable, and although most analogues are more potent

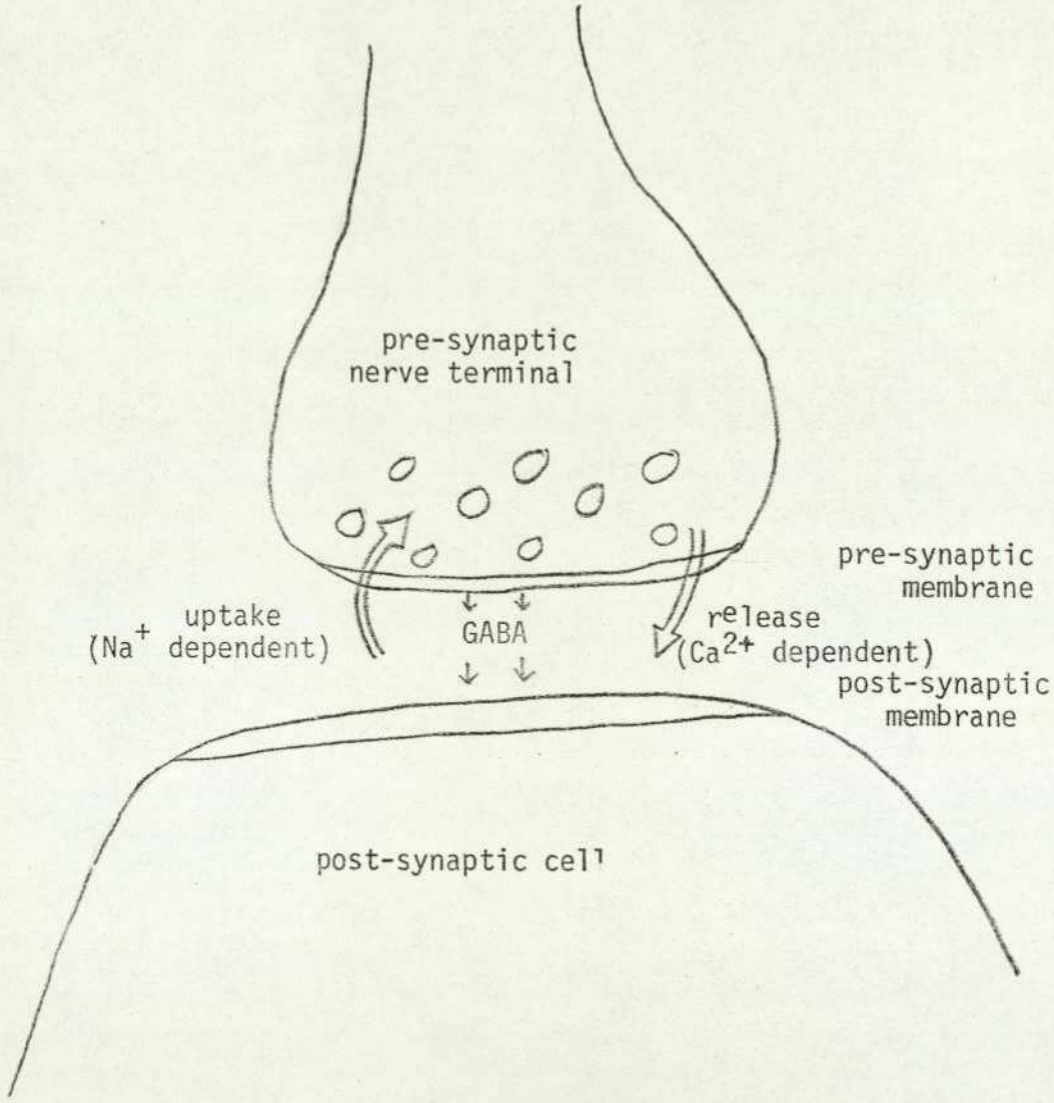

Fig. 1.7 Uptake and release of GABA at an inhibitory synapse (from Iversen, 1972)

in their L form, the D forms of some of the more powerful agonists are the more potent (Table 1.2). Pfeiffer's rule (Pfeiffer, 1956) is observed to apply; the differences in potency between enantiomers increasing with the mean potency of the compound. The discussion below assembles some of the relevant pharmacological data on the synaptic activity of glutamate, and the antagonism and termination of its action.

(i) Invertebrate

L-glutamate depolarises crayfish muscle, particularly when applied at synaptic regions (Takeuchi & Takeuchi, 1964). GABA responses on the muscle are unaffected, suggesting that the sites of action are distinct (Takeuchi & Takeuchi, 1965). However, GABA/glutamate inhibitory/excitatory systems appear in close apposition in invertebrate muscle (Johnson, 1972). L-glutamate mimics the excitatory motor axon transmitter for crayfish, cockroach and crab (Johnson 1972) and is also likely to have a transmitter role at insect neuromuscular junctions (Usherwood, 1972) where two distinct populations of glutamate receptors have been identified (Lea & Usherwood, 1973). L-glutamate and L-aspartate are likely transmitters at various neurones in snails (Kerkut et al, 1974). At the crayfish neuromuscular junction, synaptic and L-glutamate induced depolarisation are both mediated by Na^+ currents across the post-synaptic membrane, with a small component involving Ca^{2+} (Takeuchi & Onodera, 1973). There is also evidence (Florey & Murdock, 1974) that Na^+ and Cl^- channels are activated by L-glutamate on crustacean muscle.

Some glutamic acid esters (L-glutamic acid methyl ester, dimethyl ester, monoethyl ester and diethyl ester) have been shown to antagonise glutamate at the crayfish neuromuscular junction (Lowagie & Gerschenfeld, 1974). On the basis of differential antagonistic effects, it is likely that glutamate receptors in mammalian spinal neurones differ from those in invertebrate neurones.

(ii) Vertebrate

L-glutamate has no effect at mammalian neuromuscular junctions, its effects being confined to the CNS. L-glutamate and many structural analogues rapidly depolarise feline spinal (Curtis 1963) and cerebral neurones (Krnjevic & Phillis, 1963) such as primary sensory nuclei of the caudal medulla, reticular formation, thalamus, corpus striatum, caudate nucleus, hippocampus and cerebral cortex (Johnson 1972). The evidence supports a transmitter role for L-glutamate at the axon terminals of primary afferent fibres in the spinal cord, while L-aspartate may be the transmitter at spinal excitatory interneurones (Duggan 1974). Depolarisation may involve a simultaneous Na^+ and K^+ membrane conductance increase (Bradford & McIlwain, 1966), although technical difficulties preclude a clear experimental demonstration of ionic mechanism (Johnson, 1972). There is evidence for a glutamate/GABA excitatory/inhibitory synaptic input system in CNS neurones of lower vertebrates such as the goldfish Mauthner cell (Diamond 1968). L-glutamate release is lower in sleeping than aroused animals (opposite to GABA). Stimulation of the reticular activating system (arousal centre) increases L-glutamate release six-fold over sleep (Jasper & Koyama, 1967).

A number of glutamate analogues and other substances have been reported to antagonise L-glutamate in the CNS; notably glutamic acid diethylester (GDEE), α methyl glutamate (αMG), 2S-SR methionine sulfoximine (MSO) (which is not very specific (McLennan, 1974)) and 2/methoxy aporphine (2MA) (Curtis et al, 1972[a]; Haldeman, Huffman, Marshall & McLennan, 1972). There is evidence for competitive antagonism by GDEE and αMG (Haldeman et al, 1972; McLennan, 1974). Certain brain stem neurones which are excited by both serotonin and L-glutamate are blocked by LSD 25 (Boakes, Bradley, Briggs & Dray, 1970). The most effective specific glutamate antagonist so far discovered is 1 hydroxy-3-aminopyrolid-2-one (HA966). Structural considerations support the idea that HA966 acts competitively. It does not affect GABA or glycine receptors (Davies & Watkins, 1973[a,b]).

As with GABA, glutamate transmitter action is probably terminated by a high-affinity uptake system (Haldeman & McLennan, 1973). In common with other transmitter inactivation systems of this kind, high-affinity glutamate uptake is highly sodium dependent (Bennett, Logan & Snyder, 1973).

1.3.3 Present state of amino acid receptor theory

The authors of early pharmacological work on GABA, L-glutamate and their respective agonists were able to make suggestions as to the salient features of GABA and glutamate receptors. Curtis and Watkins (1960) in a study of the effects of GABA and L-glutamate on mammalian spinal neurones, drew attention to the possibility that the active moieties receptor were located on chains with a considerable degree of flexibility. This was deduced from the wide range of molecules which could apparently interact with amino-acid receptors, from short ones such as glycine and aminomalonic acid to the much longer ε aminocaproic acid and αaminopimelic acid. It seemed that receptor flexibility was a likely explanation, since GABA and L-glutamate respectively produced the strongest tissue responses, and molecules which could exhibit only smaller inter-charge distances mediated weaker responses. If the receptors were rigid and larger molecules had to fold up in order to act, the shortest molecules would be expected to mediate the strongest responses.

The receptors for inhibitory and excitatory amino acids were assumed to be geographically the same, the inhibitory transmitters making a 'two-point' contact with a pair of negative and positive sites, and the excitatory transmitters making a 'three-point' contact, including an extra positive site. The specificity of neurotransmitter activity may imply a more detailed recognition process than this, however (see below). On the basis of desensitisation experiments it is now known that inhibitory and excitatory amino-acid receptors are distinct (Curtis & Johnston, 1970).

(a) Theories of the GABA receptor

The present work is mainly concerned with the behaviour of GABA at postsynaptic receptors. It seems likely that pre and postsynaptic receptors and uptake receptors may each have their

own molecular geometry. The evidence suggests that GABA uptake receptors are distinct from those involved in transmitter action: this has been demonstrated for GABA by Iversen and Johnston (1971) and by Zukin, Young & Snyder (1974) in a comparison of GABA uptake inhibition and postsynaptic binding inhibition by a number of GABA analogues. Those which are good uptake inhibitors are not necessarily good GABA agonists or antagonists. The observation (Segal, Sims, Maggiora & Smissman, 1973) that 1-2 trans aminocyclohexane carboxylic acid (ACCA) is a GABA-mimetic transmitter as effective as 1-3 cis ACCA in rat hippocampal neurones, while the 1-3 cis compound is by far the better uptake inhibitor, may shed some light on the difference between uptake and transmitter receptor sites. ACCA molecules are semi-rigid, possessing a restricted range of possible charge separations. 1-3 cis ACCA can approximate extended GABA, while 1-2 trans ACCA is reminiscent of a partially folded GABA molecule. This may evidence involvement of a range of conformers of GABA in its transmitter action, embracing extended and partially folded forms, while, in uptake the fully extended rotamer is exclusively implicated. Iversen and Johnston (1971) point out the geometrical specificity of the uptake mechanism (in contrast to the apparent flexibility of the postsynaptic GABA receptor) and Beart, Johnston and Uhr (1972) quantify this statement by showing that competitive GABA uptake inhibitors, including the rigid 4 aminotetrolic acid (ATA) possess a charge separation of between 5Å and 6Å, probably nearer 6Å. They conclude that extended conformations of GABA are important in its initial binding to the transport carrier. In the present work crystal structure results from a number of GABA agonists have enabled the distinction between these receptor types to be further examined (3.3.2).

Before further suggestions about postsynaptic GABA receptor geometry are discussed, an important point should be made. Much of the literature on GABA pharmacology (e.g. Curtis & Watkins, 1960; Krnjevic & Phillis 1963) has concerned mammalian CNS neurones, many of which appear to possess glycine receptors rather than or as well as GABA receptors. Glycine receptors appear to predominate

in the cord, while GABA receptors predominate in supraspinal regions (Curtis et al, 1968; Straughan, 1974). The conductance change mediated by either receptor is the same (Straughan, 1974). Pharmacological investigation of GABA receptors is obviously impossible if there are uncertainties in the origin of measured responses, (i.e. the smaller GABA agonists (e.g. β alanine and taurine) possibly acting at glycine rather than GABA receptors). In receptor investigations, then, it is better to use data from highly GABA-specific preparations such as the crayfish abdominal stretch receptor (Edwards & Kuffler, 1969; McGeer, McGeer & McLennan, 1961; Swagel, Ikeda & Roberts, 1973). Mammalian CNS responses to the larger molecules which act specifically as GABA agonists (i.e. those with chain lengths > GABA), however, seem to parallel those in the stretch receptor, so, tentatively, we can conclude that the GABA receptors in these very different preparations may have some structural similarity. This possibility is noted by Krnjevic and Phillis (1963) in cerebral and cerebellar neurones. Moreover, studies on BIC antagonism have shown the likelihood of smaller molecules than GABA interacting with GABA receptors in the cerebral cortex and other supraspinal regions, as they do in invertebrate preparations (Curtis et al, 1970[a]; Straughan, 1974). Some pharmacological data for larger molecules from the mammalian CNS have thus been included in the SAR studies (3.2.2-3) and are considered to relate to GABA receptors comparable to those in invertebrate preparations. Data for smaller molecules, which may also interact with glycine receptors, are taken from GABA-specific preparations only.

Following the suggestion of Curtis and Watkins (1960) (see above) further proposals about the structure of postsynaptic GABA receptors have been made by McGeer, McGeer & McLennan (1961) experimenting on the crayfish abdominal stretch receptor. They deduce that GABA interacts with receptors in a partially folded conformation, on the basis of the inactivity of m-aminobenzoic acid, which can only exhibit a conformation like that of extended GABA. (This inactivity may be explicable on other grounds, however, such as electromeric effects or steric hindrance due to

the benzene ring.) They propose that the charge separation for the GABA receptor at the crayfish abdominal stretch receptor is ~ 4Å, and that active substances should possess such a charge separation with no interpolated groups causing steric hindrance.

Van Gelder (1971) also suggests that GABA acts in a folded conformation with charge centres less than 4.4Å apart. He considers transmitter action and uptake to occur consecutively at the same receptor, however, which is unlikely, as explained above.

Competitive antagonists might also be expected to show some structural complementarity to receptors. Thus there has been much discussion in the literature about stereochemical congruences between BIC and GABA agonists (Curtis et al, 1970[a]; Steward, Player, Quilliam, Brown & Pringle, 1971; Beart, Curtis & Johnston, 1971; Gilardi, 1973; Steward, Player & Warner, 1973[a]). Beart, Uhr & Johnston (1971) favour the involvement of an extended conformation of GABA in its transmitter action on the basis of the GABA-like activity of ATA and possible congruences between GABA, ATA and BIC. The diagram they present, however, shows a partially folded GABA molecule.

Kier and his co-workers (Kier & Truitt, 1970; Kier & George, 1973; Kier, George & Höltje, 1974) have developed a model for the GABA "pharmacophore" (i.e. the arrangement of atoms or groups in a GABA agonist molecule which are necessary for inhibitory activity) on the basis of low-energy conformations of GABA agonists and HBIC predicted by Extended Huckel Theory (EHT) molecular orbital calculations. (This method neglects electron-electron interactions and results are not generally in agreement with ab initio methods.) A number of agonists are shown to possess a congruent arrangement of a nitrogen atom and an oxygen atom at 5.8 ± 0.2Å separation (Fig 1.9). (This corresponds to the fully extended GABA molecule in Kier's work.) Kier, George & Höltje (1974) consider the GABA receptors on postsynaptic membranes, those associated with GABA uptake systems and those of the enzyme GABA-transaminase to be similar. It seems clear from the

pharmacological results, however, that GABA receptors (e.g. of the crayfish stretch receptor or neuromuscular junction) which interact with molecules of wide ranging size cannot be as inflexible as the Kier "pharmacophore" implies.

While there is no reason to believe that fully extended GABA cannot interact with the GABA receptor, there is also good evidence, as mentioned above, that molecules such as β alanine (which cannot exhibit a charge separation as great as that of extended GABA) also interact with GABA receptors (Straughan, 1974). Thus, the evidence supports the more flexible type of receptor proposed by Curtis & Wakins (1960) and developed quantitatively by Steward & Clarke, (1975). Details of the derivation of this quantitative model are presented in Appendix 6. A further development of it is reported in 3.2, where some important inferences concerning GABA receptor theory are made (3.2.3).

Smythies (1974) has proposed a detailed molecular receptor model for GABA which can explain the action of GABA agonists and antagonism by BIC. The GABA receptor is considered to consist of a ladder structure of hydrogen bonded arginine and glutamate moieties (Figs. 4.2 and 4.3) which permits the flexibility that the pharmacological results imply. This model is discussed in detail, with respect to the results of the present work, in chapter 4.

A further point of interest is whether two or three sites of interaction are necessary for a GABA agonist to bind to a receptor. All GABA agonists so far investigated possess two or more negatively charged atoms and one or more positively charged atoms which can take part in a hydrogen bonding interaction. Thus, GABA, for example, could interact with one negative and two positive sites on the receptor or one negative and just one positive. The pharmacological evidence is inconclusive, although the fact that esters of GABA are inactive (Curtis & Watkins, 1960) may imply that both negatively charged atoms are necessary. The problem is somewhat academic with regard to the present work,

however, since the gross charge separation of the GABA molecule is probably the most important feature for recognition (see 2.1). The detailed processes of binding are of interest, ultimately, and are discussed in chapter 4, but the SAR studies of chapter 3 do not depend on such knowledge.

The nature of GABA antagonism by BIC may provide a clue to the 2 or 3 point binding question. It has been shown by Collins and Hill (1974) that only one enantiomer of BIC (the (+) form, see fig 1.8) is active as a GABA antagonist. The conformation of BIC in aqueous solution where it exists in the protonated form (HBIC) is known with a fair degree of confidence (Andrews & Johnston, 1973; Gilardi, 1973; Kier & George, 1973). A recent study of the electronic charges in HBIC by the CNDO/2 MO method has provided evidence for the suggestion (Steward et al, 1971) that the oxygen atoms A and B (fig 1. 8) and the nitrogen substituents are important in congruences between GABA and the antagonist molecule (Steward, Borthwick, Clarke & Warner, 1975). The (+) and (-) forms possess the same distances between these functional moieties, but, of course, their atomic arrangement is enantiomorphic (Fig 1.10). If a three atom interaction is necessary for effective binding to the receptor, there should be a difference in the activities of the two enantiomers, as is observed. However, the sheer size of the BIC molecule may disallow interaction of the (-) with the receptor on steric grounds alone.

The pharmacological investigation of enantiomorphic BIC derivatives may ultimately reveal a great deal about the structure of GABA receptors (Collins & Hill, 1974; Steward, Borthwick, Clarke & Warner, 1975). As mentioned above, however, ambiguities remain, and it is still uncertain whether BIC acts at exactly the same site as GABA (Straughan, 1974). Hence, the present work has not dwelt on the question of BIC action.

(b) Theories of the glutamate receptor

From relative potency measurements (Table 1.2) and differential antagonistic effects (Lowagie & Gershenfeld, 1974)

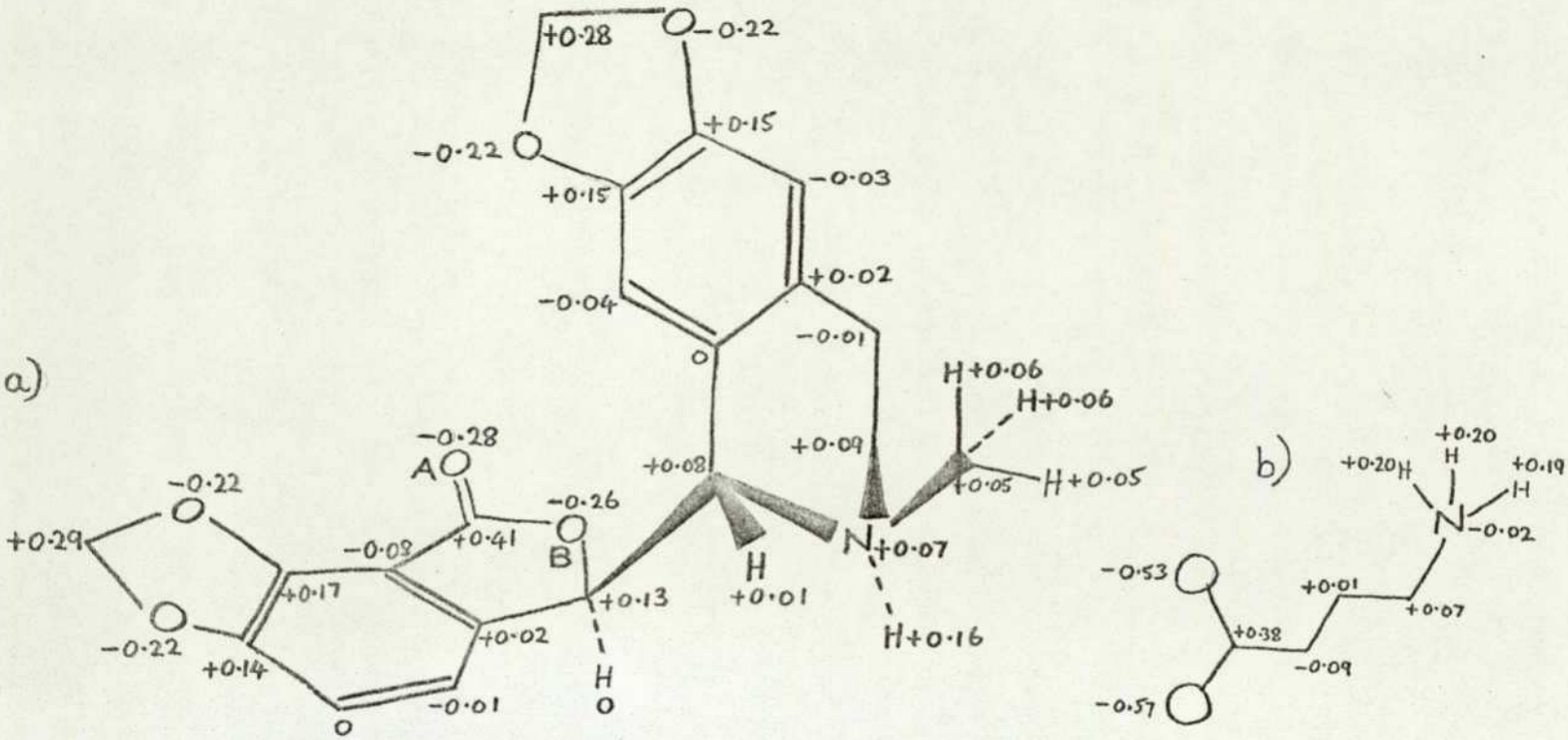

Fig. 1.8 a) The (+) bicuculline molecule in its protonated form, b) GABA zwitterion for comparison.

The approximate charge distribution derived from CNDO/2 calculations is indicated. The charges on the likely receptor-active atoms of bicuculline (lactone oxygens (A and B) and $NHCH_3$ group) show differences cf agonists (see Fig. 1.2). The charges on the oxygens are halved in magnitude and the positively charged region is more diffuse in the antagonist (Steward, Borthwick, Clarke and Warner, 1975). Units: e

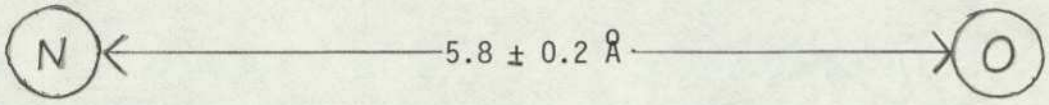

Fig. 1.9 The Kier "GABA pharmacophore"

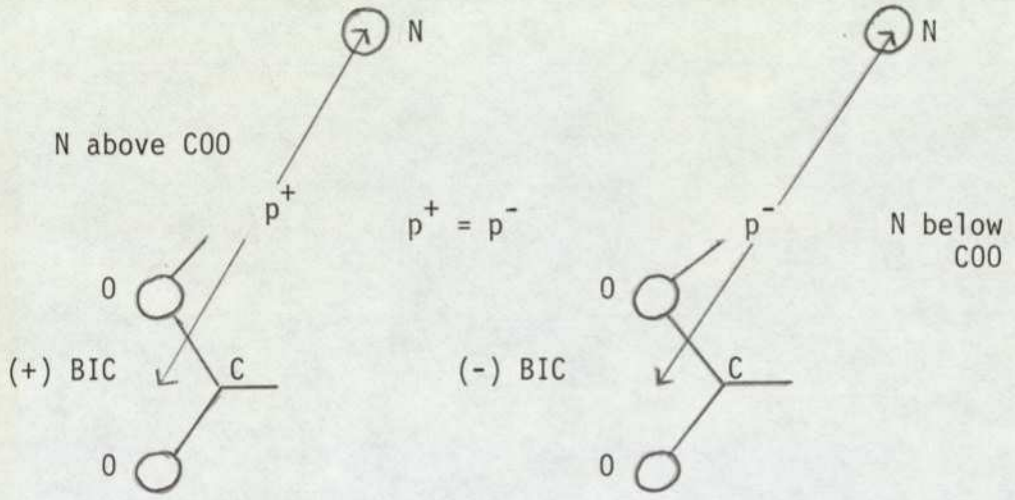

Fig. 1.10 Bicuculline and GABA receptor congruence

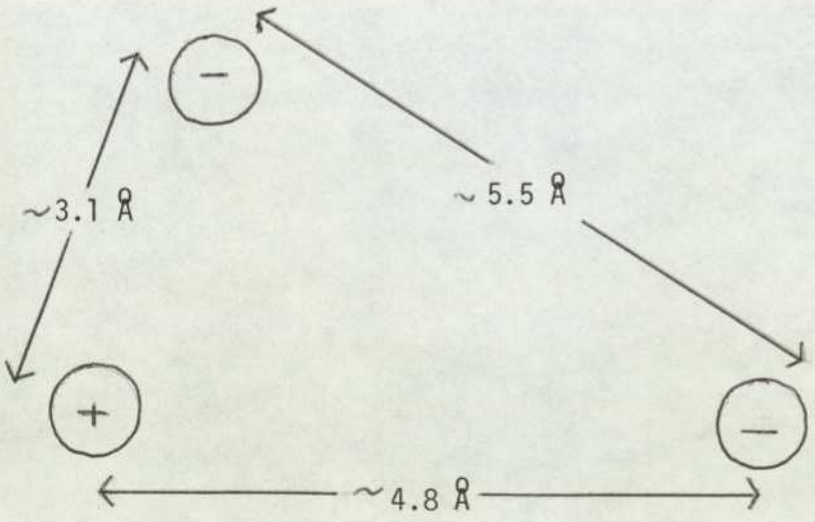

Fig. 1.11 The Johnston glutamate receptor model

it seems that the glutamate receptors on vertebrate spinal neurones are different from those found at invertebrate synapses. It is with the former that the present work has been concerned (3.2.4, 3.3.3).

The widespread occurrence of L-glutamate and L-aspartate as metabolic substances in the body, and their non-specific depolarising action on many excitable neurones has made the study of specific transmitter properties of these materials a difficult task. Moreover, in the mammalian CNS itself, distinctions must be made between different excitatory amino-acid receptors. Firstly, several glutamate analogues which have strong excitatory or antagonistic effects at glutamate-sensitive synapses fail to show any specific or potent influences on glutamate uptake by rat-brain synaptosomes (Bennett, Logan & Snyder, 1973). Moreover, the glutamate uptake inhibitor glutamate di-methyl ester does not affect glutamate-sensitive synapses (Haldeman & McLennan, 1972). Thus, the latter authors suggest a configurational difference between the excitation receptor and the uptake receptor. This is in contrast to the proposal of Van Gelder (1971) that glutamate acts in a highly folded conformation at a receptor responsible for both excitation and uptake.

As regards mammalian synaptic glutamate receptors, a number of observations and proposals have been made. Curtis & Watkins (1963) suggest that the excitatory action of glutamate analogues is so widespread, that some form of glutamate 'receptor' may be a fundamental structural component of central neuronal membranes. More recently, however, specific actions of glutamate and aspartate have been observed (McLennan, 1974) which indicate the existence of separate synaptic glutamate and aspartate receptors. Renshaw cells, for example, are more sensitive to L-aspartate than to L-glutamate, whereas spinal interneurones are more sensitive to L-glutamate than L-aspartate (Duggan, 1974). On this basis Johnston, Curtis, Davies & McCullough (1974) investigated the potencies of several conformationally restricted L-glutamate analogues, including the highly potent kainic acid, on spinal

interneurones and found a unique possible disposition of charged groups corresponding to a partially extended glutamate molecule (C_α - C_β eclipsed, C_β - C_γ trans). The charge separations in this conformation would be 4.8Å and 5.5Å (see Fig. 1.11). The powerful excitatory amino acid N Methyl-D-aspartate, and aspartic acid itself cannot attain such a charge separation, so it is proposed that excitation by L-glutamate and L-aspartate results from preferential interaction with different receptors. L-glutamate, however, might also interact with 'aspartate preferring' receptors in a more folded form. In the present work crystal structure congruences among excitatory amino acids have been examined which may relate to these distinct receptor types (3.3.2).

Following the discovery of the excitatory properties of kainic acid (Shinozaki & Konishi, 1970; Johnston et al, 1974), several other highly potent ring-containing glutamate analogues have been found. Domoic and quisqualic acids (Biscoe, Evans, Headley, Martin & Watkins, 1973; Shinozaki & Shibuya, 1974) together with kainic acid, have potencies at least two orders of magnitude greater than L-glutamate on rat and frog spinal interneurones (Table 1.2). Domoic and kainic acids possess an unsaturated side chain and a carboxy-methyl group (see Table 1.2) in a cis relationship to one another. Allokainic acid, in which the ring substituents are trans to one another, has a much lower potency. This suggests (Biscoe et al, 1975) a synergistic effect between the unsaturated group (perhaps via hydrophobic bonding) and the conventional three-point receptor. Increased agonist potency in these cases is unusual among amino-acid transmitters, since substitution of extra hydrophobic groups often produces antagonism (Paton, 1970; Curtis et al, 1972; Haldeman et al, 1972). It would appear, then, that the effects of these compounds are not mediated by the conventional glutamate receptor alone, so such results should be employed cautiously in SAR studies (3.2.4, 3.3.2).

A number of glutamate analogues with differing ω acidic groups have been reported (Biscoe et al, 1975). Increased electro-

negativity of the ω group seems to enhance excitatory activity, particularly in the case of quisqualic acid (Table 1.2).

By the complementarity principle, then, the glutamate receptor at vertebrate spinal interneurones may be considered to possess a sizeable electropositive region at the ω position, and nearby groups which can interact synergistically with unsaturated side chains of agonist molecules (Biscoe et al, 1975).

Nevertheless, the conformational aspects of transmitter receptor complementarity are just as important for excitatory amino acids as for other neurotransmitters (Johnston et al, 1974), so conformational analysis may reveal useful information about glutamate and aspartate receptors. Accordingly, such studies have been carried out in the present work (2.2.3, 2.4.4) and have enabled suggestions to be made concerning the respective receptor geometries (3.2.4, 3.3.2).

1.4 AIMS AND SCOPE OF THE PRESENT WORK

The pharmacological results described in 1.3 as well as the suggestions of allosteric mechanisms and flexible receptor sites described in 1.2. support the original proposals of Curtis and Watkins (1960), that the receptor sites for GABA and glutamate exhibit flexibility. The more recent work of Kier et al (1970, 1973, 1974) who propose, on the grounds of isolated molecule conformational results, that the GABA receptor is closely limited geometrically, would appear to be at variance with much of the pharmacological data. In particular, the distinction between presynaptic, postsynaptic and uptake receptors is ignored and the range of size of the drugs which are active at GABA receptors is not taken into account. On the other hand recent pharmacological work (Bowery & Brown, 1974) notes the wide range in size of transmitter molecules which can be recognised by the GABA receptor but makes the tacit assumption that all these molecules act in their fully extended conformations. A similar situation exists for the glutamate system, in which pharmacological evidence, though sparse, favours particular molecular conformations for optimum glutamate-like activity (Johnston et al, 1974). There is as yet, however, no clear evidence that such optimum conformations are energetically favoured.

Confronted with the state of knowledge summarised in this chapter, it was decided to attempt a study drawing together available pharmacological results and extensive conformational investigations. Thus, in chapter 2, conformational results for the GABA and glutamate systems are reported. 2.1 contains a discussion of the usefulness of conformational analysis in transmitter-receptor studies and the likely limitations of the approach. In 2.2 X-ray crystal structure conformations, two of which were determined in the course of this work (Appendices 2 and 3) are collated, compared and contrasted. The comparisons are made within both the GABA and glutamate systems with a view to SAR investigation later on (3.3.2).

A notable omission in the reported theoretical studies on the conformation of amino-acid transmitters is the consideration of solvent effects on conformation. For zwitterionic molecules in water, particularly, these effects are likely to be profound (Warner & Steward, 1975). In the present work, therefore, two approaches to conformational analysis in solution have been examined. In 2.3, a contribution to solvent effect methodology using MO calculations is reported, together with its application to a number of GABA agonists of similar chain length. In 2.4 a more widely applicable, but less precise, PE method is applied to a wide range of GABA agonists and a smaller number of glutamate agonists.

In 2.4 the results of conformational analysis in solution obtained in the preceding sections, are compared with each other and with such experimental results as are available. The preferred conformations exhibited by molecules in the gas phase, in solution and in the solid state are also compared, in order to ascertain the relevance of isolated molecule and crystal structure studies to the biophase.

In chapter 3, the conformational results of chapter 2 and the pharmacological evidence collated in 1.3 are drawn together. The SAR studies reported fall into qualitative and quantitative categories. In 3.2 the PE conformational results (2.4.3) for GABA agonists in aqueous solution provide the basis for a quantitative SAR study using potencies from experiments on the crayfish stretch receptor - a GABA-specific preparation - (1.3.3). Results from mammalian spinal neurones supplement the others, but are such that it is reasonable to assume that GABA receptors are mediating the response measured (1.3.3a). All the pharmacological data employed in 3.2 relate to postsynaptic GABA receptors, and as such this work is an extension of that reported in Steward and Clarke (1975), details of which are presented in Appendix 6. Inferences from the results are described in 3.2.3 and related to the conventional drug-receptor theories detailed in 1.2.2. 3.2 closes with a brief semi-quantitative study of a similar kind on glutamate and a small number of its agonists.

3.3 contains SAR results of a qualitative nature based on crystal structure conformations for both GABA and glutamate agonists. The GABA agonist BIC is also briefly considered. In the same section, the remaining conformational results, those of the MO solution-conformation method, are employed in a quantitative SAR study.

The SAR results are discussed in 3.4, where the relative merits of different types of conformational data in SAR work are considered, and the use of electronic and physicochemical parameters is discussed.

Section 4 proceeds from the results of 3.2 and some principles of protein structure to examine likely molecular arrangements for the GABA receptor. These suggestions are compared with the GABA receptor model proposed by Smythies (1974), which was derived somewhat differently.

In conclusion, the main results are summarised and discussed in section 5, where suggestions for further work are also made.

2. CONFORMATIONAL STUDIES ON SOME AMINO-ACID TRANSMITTER MOLECULES

2.1 Introduction

(a) Transmitter conformation at receptors

Conformational analysis has become an important tool in the elucidation of the mode of action of drugs (Gill, 1965; Kier, 1970, 1971). Few drug molecules are rigid enough to exist in a unique conformation by virtue of their chemical structure alone, but energy considerations generally preclude the existence of a wide range of conformational modes. Evidence has been presented (Lambrecht & Mutschler, 1974) that in the case of acetylcholine agonists, at least, a drug molecule is unlikely to undergo changes in conformation which are more expensive than a few Kcal/mole when leaving the biophase to bind to a receptor. Hence, the conformation of the drug molecule in solution is the most important aspect of conformational study (Gill, 1959, 1965). It is notable, however, that conformational preferences in isolated neurotransmitter molecules, in crystal structures and in solution often show marked correspondences (Pullman & Courriere, 1973; Beveridge, Radna, Schnuelle & Kelly, 1974), for molecules which are uncharged or singly charged. Hence, correlations between conformational preferences of such molecules in the solid state or in isolation and their biological activities have often been apparent (e.g. Chothia & Pullman, 1969; Beers & Reich, 1970; Kier, George & Höltje, 1974; Richards, 1974). Isolated-molecule MO calculations, moreover, have been employed extensively in the mapping of receptors (Kier, 1970). Congruent dispositions of atoms or groups likely to be involved in the transmitter-receptor interaction are frequently discovered in the preferred conformations of series of transmitters with similar biological function. Of the studies mentioned above, however, only that of Kier et al (1974) concerns amino-acid transmitters.

The success of conformational work in SAR studies provides some support for the underlying assumption that drugs act in an energetically preferred conformation or conformations at receptors.

Theoretically (Kier, 1975) it is reasonable to believe that a drug molecule must be recognised by the receptor while in the biophase, since, as soon as the process of attraction is under way and the drug molecule can be affected by the receptor environment, recognition must already have occurred. The fact that transmitters of different chemical structures but similar preferred conformations can act at the same receptor also favours the assumption above. If it were incorrect, these different molecules would each be required to adopt some other, less favourable congruent conformation to act (Kier, 1970).

In solution, many transmitter molecules possess a range of conformational flexibility (Beveridge, Radna & Kelly, 1974) around a unique preferred mode or indeed a number of preferred modes (2.5). Thus, the precise conformation which is recognised by the receptor may not be that which the drug molecule exhibits when finally bound. Burger (1966) suggests that there is time for molecules to adapt in conformation during the interaction process. Large energy changes are, however, probably precluded (Lambrecht & Mutschler, 1974), 6 Kcal/mole being a possible upper limit, although an earlier suggestion (Beveridge, 1973) took the limit to be an order of magnitude higher. Since conformational changes in the membrane-bound macromolecules which mediate the biological response to the transmitter are very likely to occur (1.2.2) the flexible transmitter molecules might also become involved. A bound transmitter molecule, having lost much of its charge would be capable of changing conformation with its receptor site quite drastically, since uncharged molecules are far less dependent upon intramolecular stabilising forces than charged ones, particularly zwitterions (Warner, 1975). 10 Kcal/mole, for example, would allow GABA non-zwitterion almost complete conformational freedom (Warner, 1975), but would limit GABA zwitterion to a small range of flexibility only (2.3). Perhaps the traditional 'lock and key' mechanism is an insufficient description of transmitter-receptor interaction processes. Richards, Aschman and Hammond (1975), in fact, suggest that a 'hand (receptor) in glove (transmitter)' metaphor would be more appropriate, both parties being able to adapt their shape to ensure perfect fit.

(b) Conformational effects in GABA and glutamate

The importance of conformation in the interaction between GABA agonists and receptors is emphasised by the fact that physicochemical parameters do not yield clear correlations with the pharmacological activity of GABA-like molecules (Appendix 5). Furthermore, the electronic structure of the functional groups of GABA agonists has been shown by MO calculations to be remarkably consistent from one molecule to another (1.3.1). Thus, it is not simply differences in electronic or physicochemical parameters which affect the ability of a molecule to interact with GABA receptors; molecular geometry - the ability of the molecule to present the appropriate disposition of active sites to the receptor - is intimately concerned. Once conformational preference has been taken into account, the role of other parameters, particularly electronic ones, can be more readily resolved (3.4).

The same arguments apply in the case of glutamate agonists, making it possible for Johnston et al (1974) to propose a description of receptor geometry from a study of the pharmacological activity of some semi-rigid glutamate agonists.

The conformational preferences exhibited by singly-charged transmitters (see e.g. Pullman & Courriere, 1973), and GABA, which is a zwitterion at physiological pH are fundamentally different. Most transmitters, as mentioned above, show some correspondence between isolated molecule, solid state and putative solution conformations; GABA agonists, being zwitterions, do not. Isolated-molecule preferred conformations are highly folded rotamers (Pullman & Berthod, 1974; Warner & Steward, 1975; Warner, 1975; Borthwick, Livingstone & Steward, 1975), whereas experimental solution conformations (Edward, Farrell & Job, 1973; Ham, 1974) and crystal structure conformations (2.2) tend towards extended forms. This discrepacy is a consequence of the strong electrostatic attraction between the charged ends of the conservative molecule, which is much reduced in an environment where dielectric effects or inter-molecular forces assume greater importance. As a result, isolated-molecule preferred conformations

are in themselves uninformative in the GABA system. They are, however, most useful as a basis for calculations on the effect of solvent on conformation (2.3).

Glutamate agonists possess three ionised groups at physiological pH (Fig. 1.5) and may also possess highly folded preferred conformations for conservative molecules, but as yet, no such calculations have been attempted.

In the present work, a variety of methods have been employed to study the conformation of amino-acid transmitters, aiming particularly at identifying congruent conformations which may be relevant to transmitter-receptor interactions. X-ray crystal structure analyses have been carried out for the partial GABA agonist β guanidinopropionic acid (Appendix 2) and the powerful glutamate agonist DL homocysteic acid (Appendix 3). Crystal structure conformations of GABA and glutamate agonists from the literature have been compared (2.2). Theoretical calculations of solvent effects using a continuum model, based on isolated molecule MO calculations have been carried out for a number of GABA agonists (2.3). Simple classical potential energy calculations allowing for solvent via dielectric constant have been attempted (2.4) for a range of GABA and glutamate agonists, many of which are not amenable to the more sophisticated treatment at present. The results of the different methods are compared with each other and with NMR and experimental dipole moment measurements in 2.5, where the general trends of the results are also discussed.

(c) A useful conformational parameter

The parameters usually employed in conformational studies on transmitters are distances between sites in the molecule where interactions with the receptor can take place, such as highly charged atoms, hydrogen-bonding sites or non-polar groups which may take part in hydrophobic bonding. The probable active sites of GABA agonists are the oxygens of the negatively charged group, (oxygen and nitrogen in muscimol) and hydrogens of the positively charged group (1.3.1). In many GABA agonists several distances

between positively and negatively charged atoms or H-bonding sites could be critical, so a simplified description of critical distance is desirable to make comparisons possible between agonists possessing different functional groups. Consideration of the flexible nature of macromolecules and the likely recognition properties of receptors reveals a useful and novel parameter for comparison of critical distances.

In the initial transmitter-receptor recognition process, the transmitter is more likely to be attracted by the time averaged charge characteristics of its own site, than to a precisely specified disposition of atoms, since electrostatic forces have a much longer range than other forces involved. For this reason, the discussion in the present work concerned with interaction between, for instance, GABA and its receptor, takes the transmitter to have an effective charge separation (x_T) equal to the distance between the mean charge centres of its receptor-active groups defined as follows. The negative mean charge centre is taken to be the mid-point of the two oxygen atoms and the positive mean charge centre as the centroid of the triangle formed by the three amino hydrogens (fig 2.1). For muscimol, the negative charge centre is taken as the mid-point of the ring nitrogen and exocyclic oxygen atoms, since these appear to be approximately equivalent to the carboxyl oxygens of GABA (fig 1.4). x_T values for the guanidino acids are measured from the mid-point of the oxygen atoms of the carboxyl group to the mid-point of the hydrogen atoms on each of the terminal nitrogens (fig 1.4). Thus, two x_T's occur for each compound (2.4.2). For the sulphonic acids, the oxygen atoms are taken in pairs, giving three x_T's for each molecule.

The matching receptor is similarly considered to consist of two charge centres with a mean separation x_R. An interaction is postulated to occur when a transmitter encounters a receptor whose x_R is equal, or can adjust to become equal, to the transmitter's x_T. Since both transmitter and receptor possess a degree of flexibility, x_R and x_T can exhibit a range of values. The

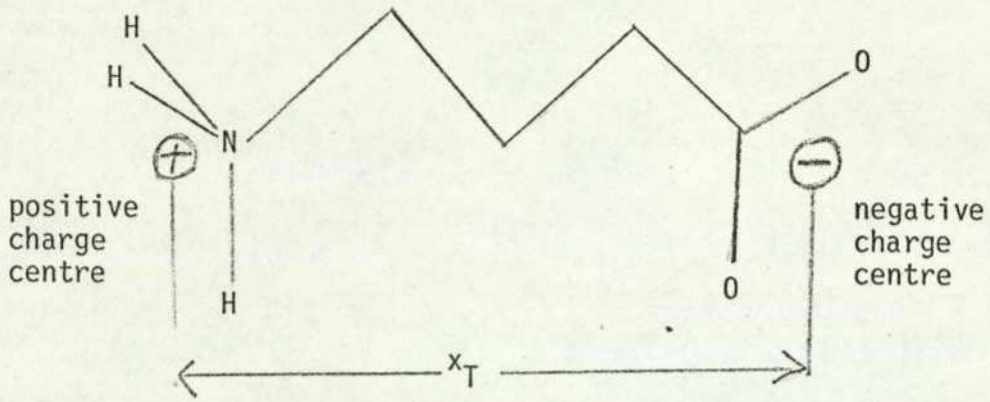

Fig. 2.1 The x_T parameter for GABA

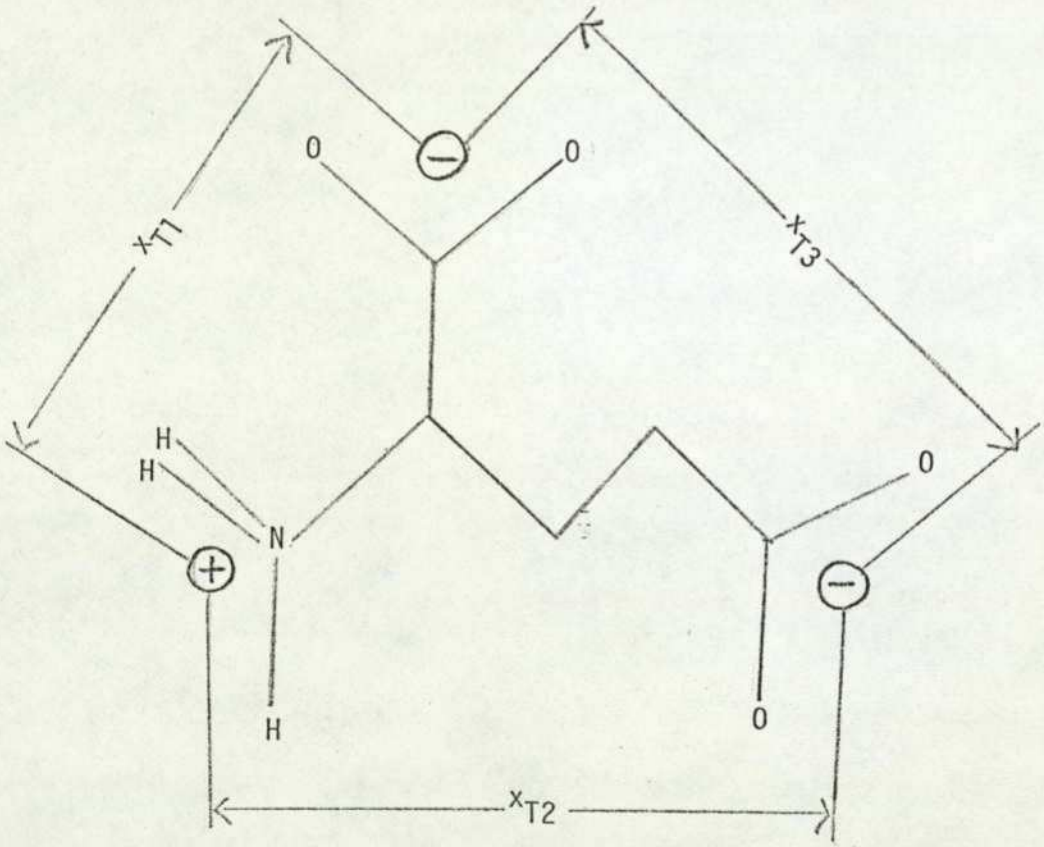

Fig. 2.2 x_T parameters for glutamate

values of x_T for each transmitter are determined from the results of conformational analyses. Using a simple Boltzmann function of the energy of any conformation and normalising, the probability of an agonist possessing an x_T within a small range can be determined (Gill, 1959). These values, calculated for all the available x_T's are then set out as an x_T probability distribution in histogram form for each agonist (2.3.3 and 2.4.3). The distribution can be used to build up SAR correlations for a series of agonists based on a receptor model which represents the flexibility of x_R (3.2 and 3.3). In the case of glutamate and its agonists, the situation is more complicated since there are three x_T's for each transmitter and three x_R's for the receptor (fig. 2.2). Otherwise, though, the method is directly applicable (3.2.4).

This simplified picture makes SAR studies possible without precise knowledge of transmitter-receptor binding processes (1.3.3). No decision about the 2-3 point binding question for GABA, for example, (1.3.3) is required.

The x_T parameter is also a useful guide to the relative degrees of folding of a molecule or a series of molecules. It can thus be employed as an indicator of correspondence between the results of different methods of conformational analysis. In GABA homologues - the α-ω amino-acids - x_T in any conformation closely parallels dipole moment in size and direction. However, in guanidino acids and glutamate analogues, where more than one positive or negative charge centre exists, this correspondence does not occur. x_T is then purely a molecular geometry parameter.

2.2 GABA AND L-GLUTAMATE AGONISTS: X-RAY CRYSTAL STRUCTURE INVESTIGATIONS

2.2.1 Introduction

X-ray structure analysis can give a precise and accurate picture of the solid state conformation of small organic molecules. Results present a snapshot of the molecule in one of its preferred conformations. It is possible to compare the crystal structure conformations, in terms of torsion angles and interatomic and intercharge distances, of a number of pharmacologically active compounds, and to seek correlations between degree of biological activity and the occurence of particular features of molecular geometry. It is difficult to find an a priori reason to justify the relevance of solid-state conformations to transmitter-receptor interactions, but nevertheless, some success has been forthcoming in the past using this technique (e.g. Beers & Reich (1970) on some acetylcholine agonists and antagonists). It is possible that the solid-state environment, where molecules exist in a closely packed form usually bound together by electrostatic, hydrophobic, hydrogen bonding and Van der Waal's forces, approximates in some way to the bound state of a transmitter at a receptor, where the same forces are involved. The solid-state conformation may thus approximate to a conformation involved in the transmitter-receptor interaction, although it is not necessarily a likely conformation in solution or in free space. In contrast to the highly folded conformations predicted by MO calculations for isolated GABA agonists, then, conformations of amino-acid transmitters in the solid state may provide some information about receptor geometry.

A number of crystal structure and biological activity studies have been carried out in recent years on acetylcholine and its agonists and antagonists which provide an illustration of the method (Beers & Reich, 1970; Chothis, 1970; Chothia & Pauling, 1969; Pauling & Petcher, 1972 and references therein). The discussion has centered on common dispositions of charged sites, hydrophobic groups, and hydrogen bonding sites in the crystal

structures of series of molecules of similar chemical structure but different degrees of biological activity. This information is supplemented by measurements from models of semi-rigid similar molecules and is presented in terms of torsion angles and interatomic distances. Beers & Reich (1970) point out that increasing hydrophobicity and structural rigidity of ACh analogues are usually associated with antagonism. They then suggest a tentative semi-quantitative scheme of structure-activity relationships among ACh agonists where the ability of molecules to adopt conformations in which functional groups are separated by optimum distances is an important factor. The results may be envisaged as relevant to detailed binding between transmitter and receptor, rather than recognition.

In the present work a similar kind of structure-activity analysis has been attempted (3.3.2) but is limited by the lack of antagonists for comparison.

Crystal structure conformations have been compared and contrasted for sixteen GABA agonists (2.2.2) and ten glutamate agonists (2.2.3). Comparisons of preferred conformation have been made from consideration of torsion angles and various molecular geometry parameters. Although congruences in atomic arrangements in the crystal structures may relate to complementary binding sites on the receptor, x_T values (more relevant to recognition (2.1)) have also been examined. These charge separations are useful both in SAR studies (3.3.2) and in comparisons with preferred conformation in solution (2.5.2).

In order to extend the number of available structures of powerful agonists, crystal structure determinations were carried out for β guanidinopropionic acid (Appendix 2) the powerful GABA agonist and suspected antagonist in some preparations (1.3.2), and for DL homocysteic acid, the powerful glutamate agonist (Appendix 3).

All the dimensions in the comparisons were calculated from co-ordinates given in original papers (listed in tables 2.1 and 2.3) using the molecular geometry package MOGEO, programmed by Borthwick and Warner (1973) and implemented interactively on the ICL 1905E computer at the City University.

TABLE 2.1 CRYSTAL STRUCTURE CONFORMATIONS OF GABA AGONISTS

	∘C - C	α - β	β - γ	γ - δ	δ - ε	Reference for co-ordinates
Glycine α	19°					Jönsson & Kvick (1972)
β	27°					Iitaka (1960)
γ	21°					Iitaka (1961)
β alanine	10°	(84°)				Jose & Pant (1965)
GABA	9°	(73°)	185°			Steward, Player & Warner (1973[b])
GABA HCl	2°	171°	180°			Steward, Player & Warner (1973[c])
α-γ diamino butyrate HCl	(61°)	(264°)	174°			Hinazumi & Mitsui (1971)
β hydroxy GABA	11°	174°	191°			Tomita, Harada & Fujiwara (1973)
ε amino caproate	(81°)	178°	173°	179°	175°	Bodor, Bednowitz & Post (1967)
α guanidino acetate HBr	11°	C 216° N	N 340° C			Roy, Majumdar & Saha (1967)
Creatine monohydrate	(43°)	C (14°) N	N 349° C			Jensen (1955)
β guanidino propionate	1°	(83°)	C (254°) N	N 12° C		Steward, Warner & Clarke (1974)
γ guanidino butyrate HBr	4°	180°	178°	C 180° N	N 359° C	Maeda, Fujiwara & Tomita (1972)
Taurine	S (58°) C	(70°)				Okaya (1966)
Homotaurine	S (0°) C	180°	180°			Ueoka, Fujiwara & Tomita (1972)
Muscimol	0°	180°	(122°)			Brehm (1973) (private communication)

Circled figures are exceptional (see text)

2.2.2 GABA agonists: comparison of crystal conformations

(a) Preferred conformations

The torsion angles displayed by GABA agonists in crystal structures are presented in Table 2.1 and compared below. It should be noted that the crystal conformations reported for GABA and GABA HCl are also found in copper-GABA complexes (Tomita, Higashi & Fujiwara 1973) so that extra weight may be assigned to preference for these conformations.

Out of thirteen compounds possessing a carboxyl group, ten show conformations in which the carboxyl group lies approximately in the plane of $C_{carboxyl}$- C_{α} -C_{β}. The exceptions are ε aminocaproic acid, α-γ diaminobutyric acid and creatine. The second of these possesses an α-amino group with which the carboxyl group tends to align (section 2.2.3). Therefore, in general a carboxyl group configuration in which oxygens are approximately cis and trans to the chain is preferred. In muscimol the equivalent charged atoms (the ring N and the exocyclic O) are held cis and trans to the chain by the ring structure, and in the case of the sulphonic acids, taurine has one oxygen trans to the chain and homotaurine one oxygen cis to the chain. The torsion angle of the oxygen nearest to cis is given in Table 2.1 for each compound.

The positive terminal groups in all the compounds except β alanine, taurine and muscimol line up trans to the chain. The behaviour of β alanine and taurine is explicable by the proximity of the negative terminal group, and that of muscimol by the effect of the nearby ring structure. For the guanidino compounds, one terminal nitrogen trans to the chain makes the other cis. In Table 2.1 torsion angles for the cis nitrogens are given.

Gauche preferences are exhibited by GABA, α-γ diaminobutyrate and βGP for the α-β torsion angle, which for the former pair is also the adjacent rotation to that controlling the terminal nitrogen alignment. βGP also shows a gauche conformation for the latter rotation, which is represented by the β-γ torsion angle

in this case. All other non-terminal rotations show trans preferences, except for the α-β configuration of creatine which is cis.

Overall, therefore, it can be concluded that trans rotational preferences are most commonly found among these compounds in the crystalline state. The exceptions comprise some gauche terminal group configurations, and some intermediate gauche configurations in molecules about the size of GABA. The exceptional results are marked in Table 2.1. There does not appear to be any correlation between the occurrence of gauche conformations and the state of the compound. Free acids show fully trans conformations and so do hydrochlorides, etc.

Comparisons between preferred conformations for some GABA agonists in the solid-state, in aqueous solution and in the gas phase are reported in 2.5.2, indicating a degree of similarity between conformational preference in crystal structures and in aqueous solution.

(b) Molecular dimensions

The N-O distances exhibited by GABA agonists in isolated molecule low-energy conformations have previously been employed in attempts to elucidate the geometry of the GABA receptor (Kier et al, 1974, see (1.3.3)).

Kier and his co-workers employed the EHT MO method (1.3.3) in this study, which fortuitously (Pullman, 1974) predicts extended conformations for GABA agonists. More sophisticated MO methods (Warner & Steward, 1975; Pullman & Berthod, 1975) predict highly folded conformations which are unlikely to be relevant to the pharmacological action of these compounds. Hence, N-O distances occuring in the crystalline state, which may have some relevance to the receptor environment (2.2.1), could be of greater pharmacological interest than those reported for isolated molecules.

TABLE 2.2 MOLECULAR GEOMETRY COMPARISON OF CRYSTAL STRUCTURE CONFORMATIONS OF GABA ANALOGUES

SUBSTANCE		$N - O_1$ (Å)	$N - O_2$ (Å)	$O_1 - O_2$ (Å)	$N\hat{O}_1O_2$ (°)	x_T (Å)
Glycine α		3.607	2.695	2.223	48.2	3.279
β		3.571	2.700	2.206	48.0	3.221
γ		3.497	2.690	2.162	50.3	3.138
β alanine		4.314	3.339	2.308	50.0	3.877
GABA		5.652	4.219	2.223	40.6	5.111
GABA HCl		6.103	5.103	2.226	53.5	5.776
α-γ diamino butyrate HCl		5.552	4.300	2.238	45.7	5.137
β hydroxy GABA		6.053	5.027	2.218	52.7	5.716
ε amino caproate		8.274	7.914	2.204	73.5	8.246
α guanidino acetate HBr	(1)	4.685	4.592	2.399	72.9	4.679
	(2)	5.630	4.375	2.399	47.3	5.215
Creatine monohydrate	(1)	4.111	3.493	2.195	58.2	3.877
	(2)	5.451	4.054	2.195	40.9	5.163
β guanidino propionate	(1)	6.116	4.645	2.217	40.1	5.680
	(2)	4.784	2.810	2.217	20.2	3.747
γ guanidino butyrate HBr	(1)	7.535	7.152	2.169	71.575	7.684
	(2)	8.315	7.329	2.169	56.072	7.916
Taurine	(1)	4.536	3.818	2.433	57.3	4.165
	(2)	4.536	2.924	2.428	35.6	3.742
	(3)	3.818	2.924	2.408	50.0	3.259
Homotaurine	(1)	5.356	5.356	2.418	77.0	5.535
	(2)	6.347	5.356	2.423	55.4	6.090
Muscimol		5.773	4.272	2.293	39.8	5.125
ATA						5.65
BIC crystal [1]		5.581	3.700	2.232	25.8	
" in water [2]		5.313	3.159	2.232	11.6	

1 Gorinsky and Moss (1973)

2 see Steward, Borthwick, Clarke and Warner (1975)

The N-O interatomic distances found in the crystal structures (Table 2.2, Fig. 2.3[a]) fall mainly in the range 4.0-6.5 Å. Some concentration of examples seems to occur at 4.2 (7 values), 4.6 (5), 5.3 (4), 5.7 (4) and 6.2 Å (4) with a spread in each case of 0.3-0.4 Å. These groups are not well defined, however, particularly those at 5.3 and 5.7 Å, so they may not be maintained when further structures become available. A fairly compact group of 4 distances also occurs at 3.4 Å, consisting of contributions from the smaller molecules glycine, β alanine, taurine and creatine. The larger molecules ε aminocaproic acid and γ guanidinobutyric acid display no N-O distances less than 7 Å.

More striking is the occurrence of consistent N-O-O angles in the triangle formed by these atoms in nearly all the compounds studied (Fig. 2.4). Although the spread of angles in Fig. 2.4 seems wide, inspection reveals that each of the agonist molecules, with the exception of ε aminocaproic acid shows at least one N-O-O angle of $50^{o} \pm 10^{o}$. The relevant triangles for all the compounds are illustrated in Fig. 2.5. It is clear from this figure that three clusters of triangles are identifiable, the clustering effect being far more pronounced than that of the N-O distances themselves (cf. Fig 2.3[a]). The first cluster ($\sim$ 4.0 Å along the abscissa of Fig. 2.5) contains the small molecules glycine, β alanine and taurine. The second ($\sim$ 5.5 Å) and the third ($\sim$ 6.1 Å) contain all the molecules of similar size to GABA itself.

In view of the discussion above (2.1), any congruences between the inter-charge distances (x_T) which occur in the crystal structures may be of considerable interest. The x_T values are illustrated in Fig 2.3[b], where it is clear that preferred values do occur. Three notable clusters appear which are much more concentrated than those for N-O distances (cf. Fig 2.3[a]). The first is at 3.8 Å (4 values), the second at 5.15 Å (5) and the third at 5.65 Å (4). The spread of these groups is less than 0.3 Å. The only substances which do not display at least one x_T value within the compact groups are glycine and the longer molecules ε aminocaproic acid and γ guanidinobutyric acid. The rigid agonist

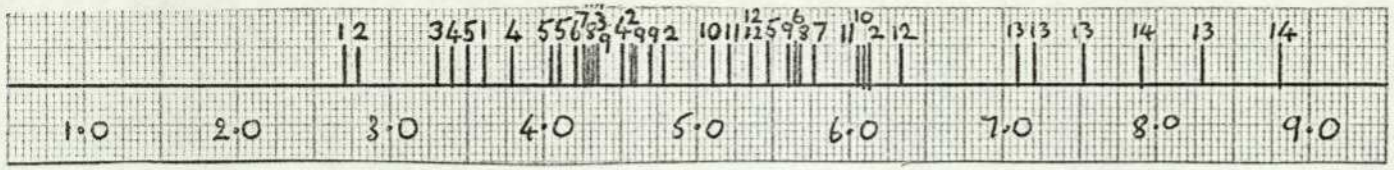

a) N-O distance (Å)

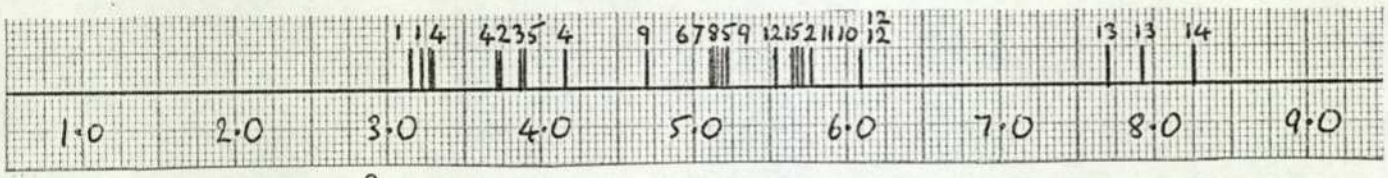

b) x_T (Å)

Fig. 2.3 Crystalline GABA agonists: N-O distances and x_T values

Key

1 glycine
2 βGP
3 β alanine
4 taurine
5 creatine
6 GABA
7 muscimol
8 α-γ diaminobutyrate
9 αGA
10 GABA HCl
11 βHG
12 homotaurine
13 γGB
14 εACA
15 ATA

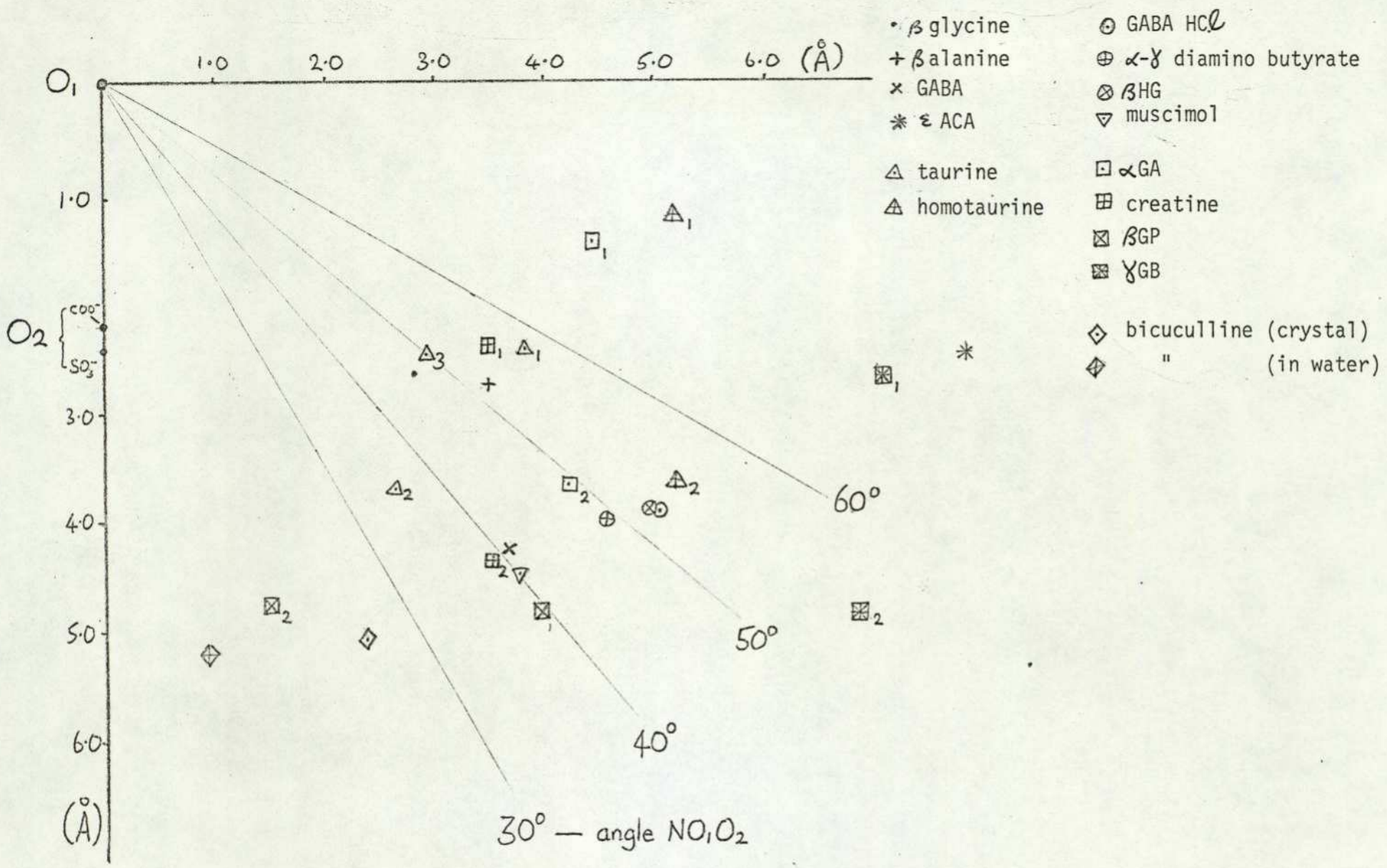

Fig. 2.4 Distribution of N atom positions with respect to pairs of oxygen atoms in GABA analogues 2cm ≡ 1 Å

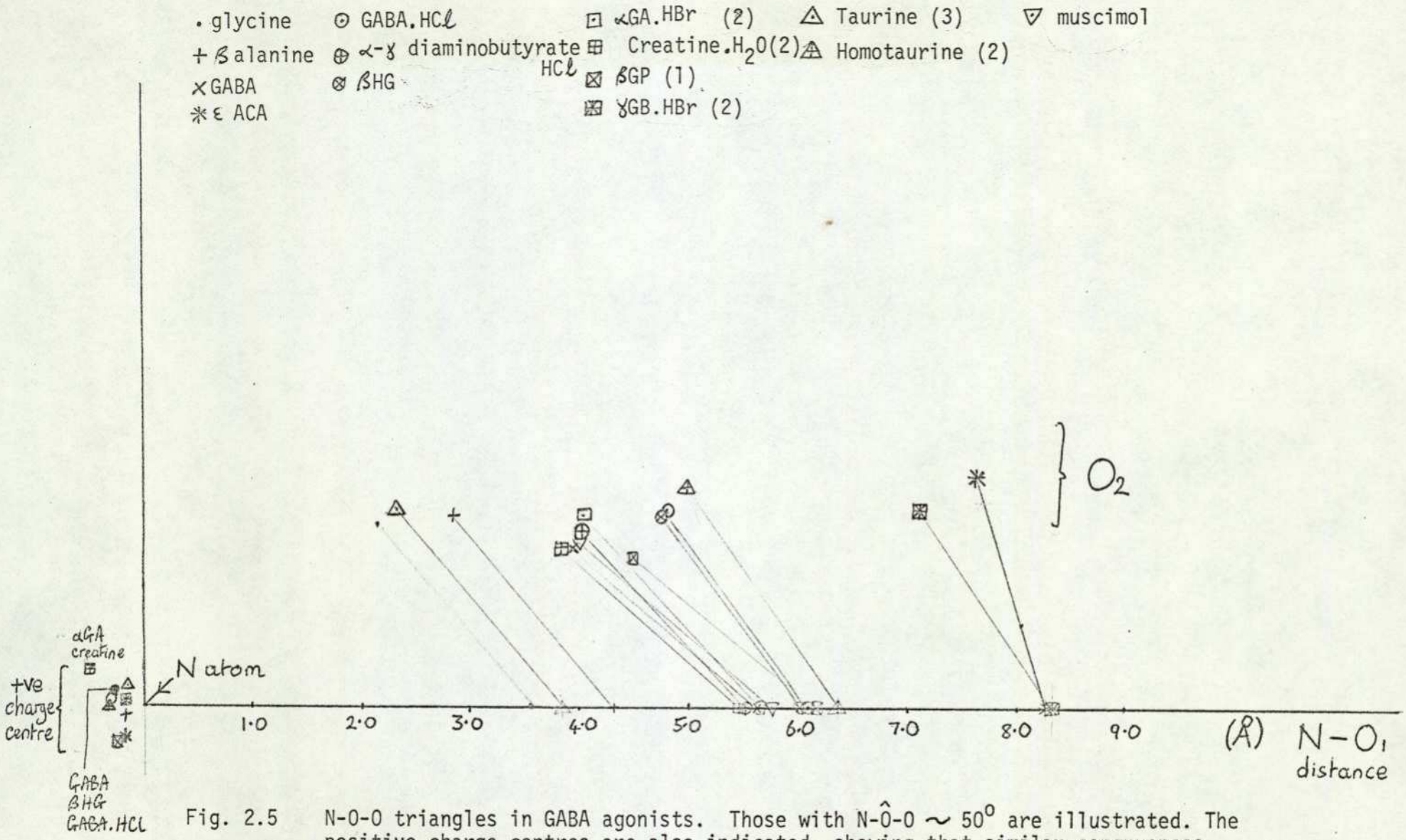

Fig. 2.5 N-O-O triangles in GABA agonists. Those with N-$\hat{O}$-O $\sim 50^{o}$ are illustrated. The positive charge centres are also indicated, showing that similar congruences would be obtained for ⊕-O-O triangles.

ATA (which possesses a conformationally invariant x_T value of 5.65 Å) would also fall into the third cluster.

In Table 2.2 and Fig 2.4 data for the GABA antagonist BIC are included for comparison with the agonists. Two conformations of BIC are examined; the crystal conformation (BIC) (Gorinksy & Moss, 1973; Gilardi, 1973) and the solution conformation (HBIC, see. 1.3.2) upon which there is a fair measure of agreement between methods and authors (see Steward, Borthwick, Clarke & Warner, 1975). It is notable that in both these conformations the disposition of N-O-O atoms displayed (see Fig 1.8) does not match the preferred arrangement in the crystal conformations of GABA agonists (Fig. 2.4). The disagreement is less marked for the BIC crystal conformation than for the HBIC solution conformation. Nevertheless, in each case one N-O distance (viz that to the exocyclic oxygen) is comparable with distances favoured by the agonists (Table 2.2).

The biological significance of the results of this section is discussed in 3.3.2.

2.2.3 Glutamate agonists: comparison of crystal conformations

(a) Preferred conformations

The solid-state conformations of glutamate agonists may, as in the case of GABA agonists, indicate common rotational preferences of interest in the elucidation of receptor geometry (see 3.3.2). The torsion angles exhibited in crystal structures by the ten glutamate agonists whose solid-state conformations have been determined are listed in Table 2.3.

The close proximity of α-amino and carboxyl groups in α-amino-acids appears to favour an O - C - C_α - N configuration between cis and gauche. The torsion angles exhibited for this rotation by the L forms of the molecules vary between 314^o and 352^o on the one side of cis, and between 12^o and 46^o on the other.

TABLE 2.3

GLUTAMATE AGONISTS: TORSION ANGLES IN CRYSTAL STRUCTURE CONFORMATIONS Terminal O. closest to cis is tabled

	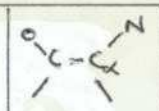	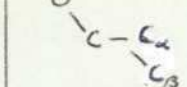	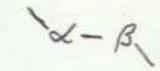	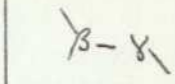	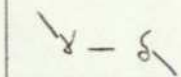	References
Amino malonate	46°	166°	68°			Kanters, Kroon, Bewskens and Vliegenthart (1966)
L aspartate	322°	83°	178°	309°		Derissen, Endeman and Peerdeman (1968)
DL aspartate (L form)	351°	121°	175°	0°		Thyagaraja Rao, Srinivasan and Valambal (1968)
L glutamate HCℓ	339°	101°	171°	187°	15°	Sequeira Rajagopal and Chidambaram (1972)
L glutamate	314°	78°	189°	283°	25°	Hirokawa (1955)
ℓ cysteate	352°	115°	162°	45°		Konishi, Ashida and Kakudo (1968)
L cysteate monohydrate	12°	140°	290°	53°		Ramanadham, Sikka and Chidambaram (1973)
DL homocysteate (L form)	335°	97°	177°	195°	311°	Clarke and Steward (1975^b)
Allokainic acid (L form)	38°	160°	103°	282°	274°	Watase (1958)
Kainic acid (L form)	12°	127°	161°	283°	36°	Watase, Tomiie and Nitta (1958)

The L form possesses a C_α - C_β bond at $\sim +120^o$ from the C_α - N bond looking along $C_{carboxyl}$ - C_α. Accordingly, the O - C - C_α - C_β torsion angles vary widely, between 78^o and 166^o.

The $C_{carboxyl}$ - α - β - γ rotation in most of the ten examples assumes an approximately trans configuration, the exceptions being one of the crystal forms of l-cysteic acid, allokainic acid and aminomalonic acid. In the latter, α-β is a terminal rotation (see below).

Of the five examples of non-terminal β-γ rotations, two show approximately trans configurations and the other three show almost identical torsion angles of 282-3^o (approaching gauche).

In the main, the terminal rotations are such that one oxygen of the terminal group is gauche to the chain. The two forms of L-glutamate and one of L-aspartate, however, show approximately cis-trans oxygen configurations.

Overall, then, the glutamate agonists show a greater tendency towards gauche configurations than do the GABA agonists. The conformational preferences at the α end of the molecules are governed by interaction between the α amino and carboxyl groups. There appears to be a particular preference for an O - C - C_α - N torsion angle of $\sim \pm 30^o$. This configuration is also found in the crystal structure of glycine (Table 2.1), the simplest α amino-acid.

(b) Molecular dimensions

Since atomic dispositions in crystal structures may be useful in the elucidation of GABA receptor geometry (2.2.2b), common atomic configurations among glutamate agonists in the solid-state also merit investigation. However, all glutamate analogues possess at leave five hydrogen-bonding sites, making molecular geometry comparison a complicated procedure. Hence, in order to discern significant common features which may relate to biological activity, a simplifying assumption will be made. Since carboxyl rotations in α amino-acids tend to be governed by interaction

TABLE 2.4

GLUTAMATE AGONISTS: CRYSTAL CONFORMATION/MOLECULAR GEOMETRY COMPARISON (Å)

	⊕ - O_1	⊖ - O_1	⊕ - O_2	⊖ - O_2	O_1 - O_2	x_{T1}	x_{T2}	x_{T3}	∅°
Amino malonate	3.931	3.387	2.839	3.860	2.219	3.250	3.244	3.457	66
L Aspartate	3.836	5.254	3.600	4.864	2.216	3.228	3.551	4.940	79
DL aspartate	4.433	5.397	2.994	4.862	2.215	3.246	3.616	5.015	58
L glutamate HCl	5.539	6.604	5.386	5.325	2.226	3.266	5.348	5.894	37
L glutamate	5.017	6.436	4.139	5.082	2.200	3.172	4.458	5.685	56
l cysteate (1)	4.388	5.613	4.192	4.955	2.429	3.221	4.117	5.150	72
(2)	4.388	5.613	2.761	5.059	2.441	3.221	3.457	5.205	49
(3)	4.192	4.955	2.761	5.059	2.430	3.221	3.337	4.859	16
L cysteate monohydrate (1)	4.688	4.961	3.785	3.707	2.448	3.248	4.086	3.994	59
(2)	4.688	4.961	2.903	4.436	2.408	3.248	3.708	4.545	74
(3)	3.785	3.707	2.903	4.436	2.380	3.248	3.158	3.680	77
DL homocysteate (1)	5.649	6.834	5.746	5.741	2.411	3.224	5.574	6.202	30
(2)	5.649	6.834	5.323	5.671	2.406	3.224	5.350	6.158	56
(3)	5.746	5.741	5.323	5.671	2.409	3.224	5.394	5.566	85
Allokanic acid	5.921	4.374	5.207	3.768	2.276	3.065	5.463	3.928	87
Kainic acid	5.692	6.179	4.466	4.442	2.229	3.198	4.993	5.265	44

with the nearby amino group (see above), the configuration of α carboxyl groups is considered constant, and no interatomic distances from individual α oxygens are considered. Instead, distances are measured to the mean charge centre of the group (Fig. 2.2) which, in any case, is not affected by the carboxyl rotation. Furthermore, the inter-charge distance between the two groups (x_{T1} in Fig. 2.2) is fixed by molecular geometry. Thus, the position and orientation of the ω acidic group in each of the molecules, with respect to the α groups, is the sole subject of this comparison. The molecules are considered in their L forms, but this does not affect the measured dimensions, which are the same for either enantiomer.

In Table 2.4, distances from the positive and negative α charge centres to the ω oxygen (x_1 and x_2 respectively), and to the mean charge centre of each pair of ω oxygens (x_{T1} and x_{T2} respectively) are indicated. (As before, ω oxygens are considered pairwise in SO_3 groups, since it is not likely that all three oxygens are simulteneously involved in the transmitter-receptor interaction. As a result of this, cysteate and homocysteate each display three x_{T2} and x_{T3} values.)

Fig 2.6 shows the combinations of distances between the α charge centres and the ω oxygens. The distances appear fairly random, but two somewhat compact regions (x_1 = 5-6 Å, x_2 = 5½-6½ Å and x_1 = 4-5 Å, x_2 = 5-5½ Å) can be delineated, the first containing distances from the longer molecules, and the second distances from the shorter ones. The clustering is not even as marked as GABA N-O distances, however, and may not be of particular significance.

A much more notable clustering effect occurs for the combinations of x_{T2} and x_{T3} distances illustration in Fig 2.7. Again, two groups occur. The group with the longer distances (centred at x_{T2} = 5.0 Å, x_{T3} = 5.7 Å) contains the larger molecules; glutamate, homocysteate and kainate. The semi-rigid agonist ibotenic acid, which possesses conformationally invariant x_T's, also fits into

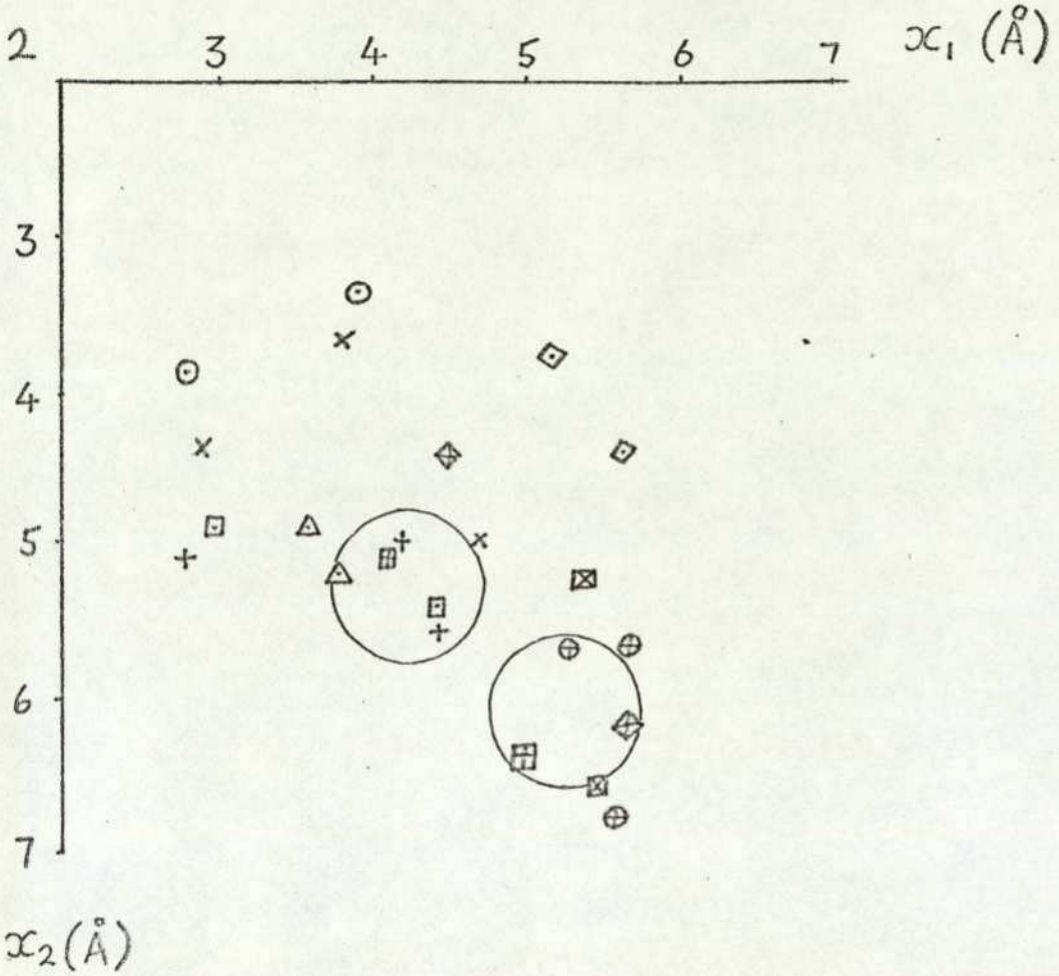

Fig. 2.6 Occurrence of combinations of α charge centre to ω O distances in crystal structures of glutamate agonists. $x_1 = \oplus_\alpha - O_\omega$, $x_2 = \ominus_\alpha - O_\omega$. The circles, diameter 1Å, indicate slightly favoured regions, but are probably of little significance.

For key see Fig 2.8.

this cluster. The second group (centred at 3.7, 4.9) contains aspartate and cysteate. Aminomalonic and allokainic acids fit into neither group. The distribution of terminal charge centres in space with respect to α charge centres is illustrated in Fig. 2.8. Two groups are again apparent, aminomalonic and allokainic acids being the only compounds which cannot be readily associated with either.

The last parameter listed in Table 2.4 is $\emptyset$, the angle between the planes defined by $C_{carboxyl} - C_{\alpha} - N_{\alpha}$ and $N_{\alpha} - O_{\omega 1} - O_{\omega 2}$. This expresses the spatial relationship between the orientation of the fixed α end of a molecule and the ω group. The angle varies over a wide range among the molecules considered, although all of them show at least one value within the range 37^{o}-87^{o}, measured as the acute angle.

Some comparison of solid-state and solution conformation for glutamate itself may be found in 2.5.2. The biological significance of the results reported above is discussed in 3.3.2, where the common charge-centre configurations found are interpreted in the light of pharmacological data on glutamate and its agonists.

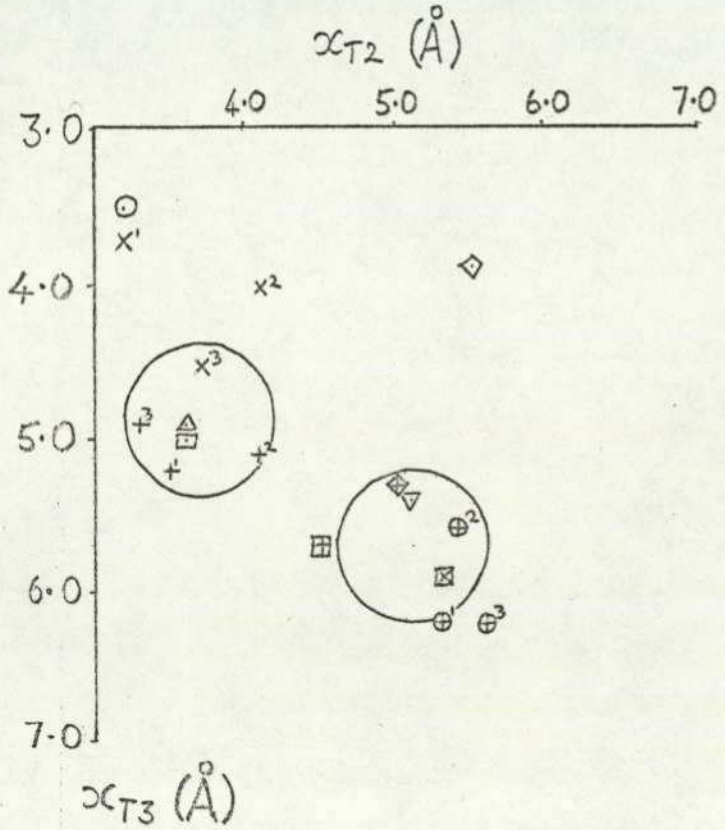

Fig. 2.7

Favoured combinations of x_{T2} and x_{T3} in crystal structures of glutamate agonists. The circles (centred at x_{T2} = 3.7 Å, x_{T3} = 4.9 Å; x_{T2} = 5.0 Å, x_{T3} = 5.7 Å) have diameter 1 Å. They indicate clusters of preferred distances.

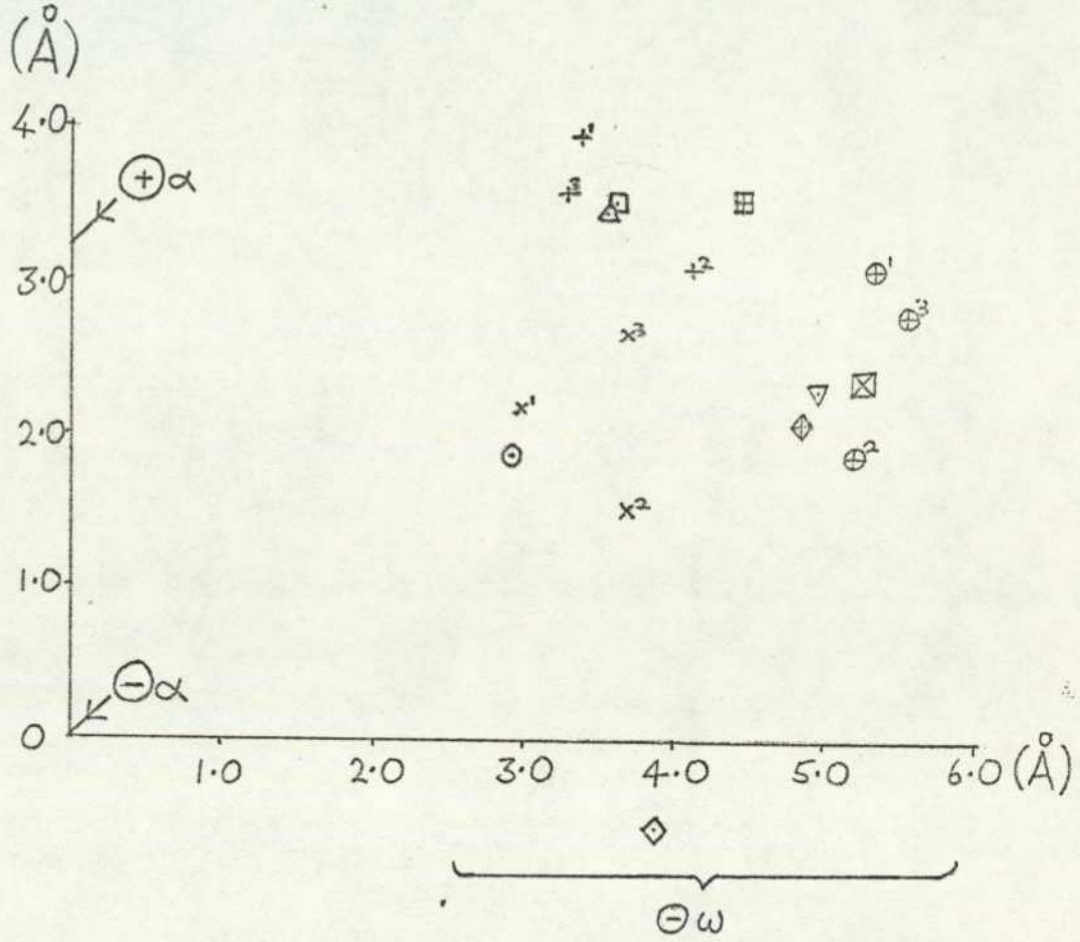

Fig. 2.8

The spatial distribution of ω acidic groups in crystal structures of glutamate agonists with respect to α charge centres.

Key:

○ aminomalonic acid	+ ℓ cysteate	⊞ L glutamate
△ L aspartate	× ℓ cysteate mono-hydrate	⊠ L glutamate HCl
□ DL aspartate	⊕ homocysteate	◇ allokainate
	▽ ibotenate	⊕ kainate

2.3 GABA AGONISTS: A CONTINUUM MODEL TREATMENT OF SOLVENT EFFECTS ON CONFORMATION

2.3.1 Introduction

(a) Aims

In this section, an attempt to adapt isolated molecule MO calculations to aqueous and lipidic environments is described. No calculations of this kind on GABA agonists have previously been reported in the literature. The calculations take as their starting point MO calculated energies and dipole moments for arrays of conformations defined by the two major torsion angles of the molecules considered. The effect of an aqueous medium on a number of small GABA agonists has been investigated, together with a more complete study of GABA itself in water, varying three of the torsion angles of the molecule. The results obtained are compared with experimental values (NMR and dipole moment measurements) in section 2.5. The solvent effects of octane and octanol, possibly analogous to a lipid milieu, have also been investigated for the major rotations of the GABA molecule. The results indicate some interesting general principles of solute-solvent interactions.

Since MO calculations are voracious in terms of computer time, the methods described below cannot conveniently be applied to molecules with a large number of rotational degrees of freedom. Thus it is not possible to develop a comprehensive SAR scheme based on these conformational results as yet. Some structure-activity correlations are apparent, however, and are described in section 3.3.3. The simple classical PE calculations of the next section (2.4) are on the other hand readily applicable to larger molecules and enable SAR to be developed on a conformational basis (section 3.2).

(b) Background

The advent of large computers has enabled quantum mechanical MO calculations to progress to a state where agreement can be achieved between experimental measurements and calculated values

of the gas phase dipole moments and rotation barriers of small molecules (Bastiansen, Seip & Boggs, 1971; Dewar, 1969).

A variety of MO techniques are available (reviewed by Golebiewski & Parczewski, 1974) but the most sophisticated ("ab initio" methods) require so much computer time that conformational studies on molecules as large as GABA are precluded. Hence in the present work a semi-empirical self consistent field method using the second parameterization of the Complete Neglect of Differential Overlap approximation (CNDO/2) (Pople, Santry & Segal, 1966) has been adopted. This method has been widely used for conformational studies and is fast enough to be economic for such purposes. Whilst the results may not necessarily be exact in absolute terms, comparison of conformational energy in series of similar molecules may be expected to yield meaningful information. The method and its advantages and disadvantages have been detailed by Warner (1975). In the literature, theoretical studies of a similar kind have been carried out on other series of related isolated transmitter molecules and relationships formed between the populations of low-energy conformational modes and pharmacological activities (Richard, 1974). While this kind of correlation does appear to have predictive value, it seems doubtful whether the low-energy conformations found in isolated molecules are likely to reveal much about receptors unless biophase conformations are similar. It is more useful to attempt to determine the conformations which these molecules adopt when actually in the vicinity of receptors.

There is no reason to suppose an exact correspondence between the conditions at the proteinaceous receptor site and the biophase itself, but a sensible starting point may be to consider an aqueous or lipidic receptor environment. SAR studies using calculated conformations in aqueous solution (Gill, 1959) have proved successful in the acetylcholine system, although experimental solution conformations (Partington, Feeney & Burgen, 1971) do not correlate with biological activity.

A number of experimental techniques are available for the estimation of conformation in solution, such as nuclear magnetic

resonance and other spectroscopic methods, circular dichroism and dipole moment measurements. Unfortunately, the interpretation of results is fraught with difficulty, especially for such molecules as GABA which possess a large degree of flexibility. Theoretical solvent effect calculations, therefore, would be of great value in the study of flexible molecules in both aqueous and lipid media (Pullman & Pullman, 1975).

This is particularly important in the case of amino acid transmitters, both excitatory and inhibitory, since they are highly charged in the biophase (1.3.1) and will interact strongly with polar solvents such as water. The isolated zwitterions of these flexible molecules, as mentioned above, show overwhelming preference for folded conformations (Warner, 1975) with a possibility of stabilisation by intramolecular hydrogen bonding (Borthwick, Livingstone & Steward, 1975). In solution, however, dielectric considerations suggest that more extended forms predominate (Warner & Steward, 1975). This is in contrast to singly charged transmitters, such as acetylcholine, which have lower dipole moments and are thus not so profoundly affected, in terms of conformation, by an aqueous environment (Beveridge, Radna, Schnuelle & Kelly, 1974).

Since MO calculations are probably the most reliable means of calculating conformational energy, the solvent effect calculations reported in this chapter were based on MO results. CNDO energy surfaces for some GABA agonists (Warner, 1975; Borthwick, Livingstone & Steward, 1975; Borthwick & Steward, 1975[c]; Livingstone, unpublished work) were modified via a 'continuum model' for the solvent as described below.

(c) Methods

Theoretical techniques allowing for the effect of environment in MO conformational studies have been described in the literature. The first of these was the continuum model suggested by Sinanoglu (1967, 1968, 1974) and applied by Beveridge, Radna & Kelly (1974) to acetylcholine. The solute molecule is considered to lie in a spherical cavity in a continuum of dielectric material which represents the solvent. The total energy for each conformation of

the solute molecule is taken to be the isolated molecule energy + terms allowing for the solvent effect. Hence:

$$E_{tot} = E_{isol} + E_{solv}$$

E_{isol} is the internal energy of the solute molecule calculated by molecular orbital methods. E_{solv} consists of two parts: (a) the interaction energy of the solute molecule with the solvent and (b) the energy required to create a cavity in the solvent to accommodate the solute molecule.

The second type of approach to the problem of solvation is that due to Pullman (see e.g. Pullman, Maigret & Berthod, 1974; Pullman & Pullman, 1975) known as the 'supermolecule' method. Here water molecules are specifically attached to the solute molecule and molecular orbital calculations are carried out on the solute and water 'supermolecule'. The hydration sites are determined by consideration of the hydrogen-bonding capability of the solute molecule and the positions and orientations of the water molecules are refined using ab initio calculations. Strictly speaking, this refinement should be carried out for each conformation considered.

Clearly, these two methods are extremes, the continuum method considering only long-range forces and the supermolecule only short-range ones. The contemporary conception of water structure can lend support to either, as follows. While it seems likely that a short-range ordered arrangement of water molecules can nucleate from a solute molecule, forming a cage framework reminiscent of the super-molecule, it is unlikely that such a situation persists for long. The solvent cage may be continually breaking up and reforming, thus approximating to a continuum on a time average basis (Symons, 1974). Ultimately, a combination method, considering one or more solvation shells surrounded by a continuum would be more realistic. This conclusion is reached on statistical thermodynamic grounds by Beveridge and Schnuelle (1974) who discuss relationships among the current approaches to the problem. At present, however, the computer time required for conformational studies of this kind on molecules the size of GABA is prohibitive and, indeed, for the purpose of comparison in series of similar molecules, one of the simpler approaches is probably adequate.

Beveridge and Schnuelle (1974) point out that the continuum and supermolecule approaches have specific advantages and disadvantages. The continuum model may fail when specific solute-solvent binding sites are moved from exposed to protected regions by conformational change or when intramolecular hydrogen bonding is present. In the case of GABA and its agonists, these points are significant for highly folded conformations, but the latter are energetically unlikely on dielectric grounds (see above). Indeed, extended conformations have been shown by dipole moment measurements (Edward, Farrell & Job, 1973) to be predominant in aqueous solution. The supermolecule method, however, is inadequate for solute molecules whose dipole moments vary greatly with conformation. This is the case for amino-acids, and since their dipole moments are not only sensitive to conformation but are also large in magnitude, it would seem that the continuum model, which takes account of solvent dielectric/solute dipole interactions would be preferable. Accordingly, the continuum model was adopted in the present work, but modified to enhance its suitability for aspherical solute molecules by using Buckingham's (1953 a,b) spheroidal cavity approximation rather than Onsager's (1936) spherical one. In the original work Buckingham (1953b) stated that the method was likely to be reliable for highly polar solutes in media of low dielectric constant, but as in the present work, physically reasonable results were obtained for small α-ω amino acids in aqueous solution.

2.3.2 Derivation of Solvent Effect Algorithms

In this section the algorithms used in calculating solvent effect energies by the continuum model are described and explained. As stated above, the modifications in isolated molecule energy due to solvent can be divided into (a) an interaction term and (b) a cavity term.

(a) Interaction term

This term accounts for the energy of interaction between solute and solvent is expressed in terms of Kcal/mole of solute. It consists, in our model, of two parts: i) an electrostatic term (Ees) and ii) a dispersion force term (Edis).

i) The electrostatic interaction energy

Since the molecules with which we are concerned are highly polar (making the Ees term large) and unsymmetrical in most conformations, a more complex electrostatic interaction calculation was employed than the Onsager expression (Onsager, 1936) used by Sinanoglu and Halcioglu (1968) and Beveridge et al (1974). The Onsager method considers the solute molecule to be a dielectric sphere with a point dipole situated at its centre; the method used in the present work was based on Buckingham's theory (Buckingham 1953[a]) considering the molecule as a similar dielectric spheroid. This should give considerably better results in extended conformations where the molecule approximates quite closely to a prolate spheroid but not at all closely to a sphere. Moreover, Buckingham's theory has been shown to give consistent results in computing dipole moments of α-ω amino acids from dielectric constant data (Edward, Farrell & Job, 1973).

The spheroid size and axis direction are calculated from the atomic co-ordinates of the molecule in the conformation under consideration. The axis of the spheroid is taken as the length of the molecule along the best least squares line through the atomic co-ordinates, + 2 Å, to allow for the Van der Waals radii of the

extreme atoms. The equatorial radius of the spheroid is then taken as the distance of the furthest atom from the axis + 1 Å. The details of this calculation may be found in Appendix 4.

The molecular dipole is considered to reside at the centre of the spheroid and to be oriented as calculated in the MO calculations. In some conformations the dipole is a little way from the centre of the sphere, which could lead to a result low by a factor of 1.5 or so (Sholte, 1949). In such instances, however, the molecule is folded and has a very low electrostatic energy in any case. The effect is unlikely to be significant in important conformations.

The molecular dipole is resolved in two directions: parallel and perpendicular to the axis of the spheroid, and the interaction energies for the two components are calculated independently from the energy of each in its own reaction field. This has a value:

$$Ees = -7.19\ \underline{\mu}.\underline{R}\ \text{ Kcal/mole}\quad \text{(Beveridge et al, 1974}^{a,b}\text{)}$$

where μ is the molecular dipole moment as modified by the reaction field $\underline{R}$. Hence, from Buckingham 1953[a]:

$$Ees = -7.19 \times \frac{3\mu_o^2}{ab^2} \frac{A(1-A)(\varepsilon-1)\left[1+(n^2-1)A\right]^2\left[\varepsilon-(\varepsilon-1)A\right]}{(\varepsilon+(n^2-\varepsilon)A)^2}$$

$$= -7.19 \times \frac{3\mu_o^2 F(A)}{ab^2}$$

where μ_o is the isolated molecule dipole moment (as calculated by CNDO/2), a is the semi axis of the spheroid and b is the radius of the spheroid at its equator. A is an internal field factor and ε and n are the dielectric constant of the solvent and the refractive index of the ellipsoid material (solute) respectively. n^2 is taken to be 2.5 (Beveridge et al, 1974[a,b]).

The internal field factors parallel and perpendicular to the axis, A_1 and A_2 are given by the equations of Osborn (1945) for a prolate spheroid:

$$A_1 = \frac{1}{m^2-1}\left[\frac{m}{2(m^2-1)^{\frac{1}{2}}} \times \ln\left(\frac{m+(m^2-1)^{\frac{1}{2}}}{m-(m^2-1)^{\frac{1}{2}}}\right)-1\right]; \quad m = \frac{a}{b}$$

$$A_2 = \frac{m}{2(m^2-1)}\left[m - \frac{1}{2(m^2-1)^{\frac{1}{2}}} \times \ln\left(\frac{m+(m^2-1)^{\frac{1}{2}}}{m-(m^2-1)^{\frac{1}{2}}}\right)\right]$$

and for an oblate spheroid:

$$A_1 = \frac{m^2}{m^2-1}\left[1 - \frac{1}{(m^2-1)^{\frac{1}{2}}} \times \sin^{-1}\left(\frac{(m^2-1)^{\frac{1}{2}}}{m}\right)\right]; \; m = \frac{b}{a}$$

$$A_2 = \frac{1}{2(m^2-1)}\left[m^2(m^2-1)^{-\frac{1}{2}} \times \sin^{-1}\left(\frac{(m^2-1)^{\frac{1}{2}}}{m}\right)-1\right]$$

Thus, for the two components of μ_o:

$(Ees)x = \frac{-7.19x3}{ab^2}(\mu_o\cos\theta)^2F(A_1)$ for the component along the spheroid axis

and $(Ees)y = \frac{-7.19x3}{ab^2}(\mu_o\sin\theta)^2F(A_2)$ for the component perpendicular to the axis

Total Ees is then given by Ees = (Ees)x + (Ees)y.

ii) The dispersion energy

This term is based on a gas-phase Kihara potential (Kihara, 1953). The potential is modified by a term due to Sinanoglu et al (1968) to make it valid for the case of a liquid, the final potential being $\upsilon_{eff}(r)$.

The dispersion energy is given by Sinanoglu (1969) as:

$$E_{dis} = d_b \int_0^{\infty} \upsilon_{eff}(r) g^{(2)}(r) 4\pi r^2 dr$$

d_b is the number density of the solvent, r is the distance out into the solvent from a given solute molecule, $g^{(2)}(r)$ is a radial distribution function for solvent molecules about a central solute molecule. ($g^{(2)}(r)$ is taken as 0 for $r < (r_a + r_b)$ and 1 for $r \geq (r_a + r_b)$ where r_a and r_b are the radii of solute and solvent molecules respectively.)

Kihara (1953) assumes a core of any shape within each molecule and then takes the intermolecular potential as the Lennard-Jones potential for the shortest distance (ρ_{ab}) between the outer surfaces of the molecular cores, hence the intermolecular distance r_{ab} of a Lennard-Jones potential function is replaced by $\rho_{ab} = r_{ab} - (\frac{\ell a+\ell b}{2})$ where ℓ_a is the core diameter of the solute and ℓ_b that of the solvent. We then write:

$$\ell_{ab} = \frac{\ell a + \ell b}{2}$$

σ_{ab} is the collision distance parameter, again derived from $\sigma ab = \frac{\sigma a+\sigma b}{2}$ where $\sigma_a = \rho^o_{aa}/2^{1/6}$ and ρ^o_{aa} is the ρ value in pure liquid a for the minimum of the Kihara potential function.

The form of the gas phase Kihara potential is then:

$$v_{ab} = Cab\left[\frac{\sigma^6_{ab}}{\rho^{12}_{ab}} - \frac{1}{\rho^6_{ab}}\right]$$

σ_{ab} and ρ_{ab} can be estimated from kinetic theory as follows:

From Sinanoglu (1967) $r^o_{ab} = 2^{1/6}\sigma_{ab} + \ell_{ab}$ (1)
where r^o_{ab} is the distance between molecular centres at the potential energy minimum. Also in a pure liquid:

$$3\ell a / (r^o_{aa} - \ell_a) = 7\omega + 0.24, \quad (2)$$

where ω is the 'acentric factor' (Donan & Pitzer, 1962; Pitzer, 1955) derived from the second coefficient of the virial equation for the substance concerned:

$$\omega = - \log Pr - 1$$

where Pr is the reduced vapour pressure P/pc of the pure liquid at a temperature $Tr = T/Tc = 0.7$. Tc values (critical temperatures) were obtained from Kaye and Laby (1966). For polar substances, ω should be taken from a nonpolar analogue of the molecule concerned (Sinanoglu, 1968).

From the above $r^o_{ab} = \rho^o_{ab} + \ell ab$ (3)

$$\rho^o_{ab} = 2^{\frac{1}{6}}\sigma ab \quad (4)$$

and from Sinanoglu (1967)

$$2r_i = 2(\tfrac{3}{4}\pi d_i)^{\frac{1}{3}} = \beta r^o_{ii} \quad (5)$$

where the constant $\beta \approx 1.15$.

From (2) $\ell a = \left(\frac{7\omega+0.24}{7\omega+3.24}\right) r^o_{aa}$

Using (5) $\ell a = \frac{2r_a}{\beta}\left(\frac{7\omega+0.24}{7\omega+3.24}\right)$

From (3) and (4) $r^o_{ab} = 2^{\frac{1}{6}}\sigma ab + \ell ab$, which for a pure liquid becomes:

$$r^o_{aa} = 2^{\frac{1}{6}}\sigma a + \ell a$$

Thus $$\sigma a = \frac{r^o_{aa} - \ell a}{2^{\frac{1}{6}}} = \frac{r^o_{aa}}{2^{\frac{1}{6}}}\left(1 - \frac{7\omega + 0.24}{7\omega + 3.24}\right)$$

and from (5) $$\sigma_a = \frac{2r_a}{\beta 2^{1/6}}\left(\frac{3}{7\omega + 3.24}\right)$$

These formulae for σ and ℓ differ from those used by Sinanoglu et al (1968, 1969) and Beveridge et al (1974), but they do relate the values of ω, r_a and σ_a, ℓ_a for various substances in table III of Sinanoglu's 1967 paper, and agree with the formula for ℓ given in Sinanoglu (1974). Moreover, they appear to give values of greater physical significance than the alternative formulae.

Cab in the kihara potential equation is the London dispersion coefficient:

$$Cab = \frac{3}{2} \alpha_a \alpha_b \frac{\delta a \delta b}{\delta a + \delta b} \quad \text{(Sinanoglu, 1967)}$$

where α's are polarisabilities for solvent and solute, obtained from

$$\alpha_i = \frac{n_i^2 - 1}{n_i^2 + 2} r_i^3 \; (= D_i r_i^3)$$

where n_i is the refractive index of i; and $\delta i - \mu Ii$. Ii are ionisation potentials obtained from Kaye and Laby (1966) for analogous compounds

and μ is a constant ≈ 1.35 (Sinanoglu, 1967).

Thus $$Cab = \frac{27}{32\pi^2} D_a D_b \times 1.35 \times \frac{IaIb}{Ia+Ib} \; VaVb \quad eV/mol\text{Å}^6$$

Va (solute) is the volume of the spheroid used in the Ees calculation, r_a is obtained from a spherical approximation:

$$r_a = \left(\frac{3Va}{4\pi}\right)^{1/3}$$

$$V_b = 1/d_b$$

and $$r_b = \left(\frac{3V_b}{4\pi}\right)^{1/3}$$

Converting to Kcal/mole:

$$Cab = 46.70 \left(DaDb\frac{IaIb}{Ia+Ib} \; r_a^3 \; r_b^3\right)$$

The liquid phase potential function $\nu eff(r) = \nu_{ab} B'ab$ where B'ab is the correction factor described by Sinanoglu et al (1967, 1968, 1969)

$$B'ab = \left[\frac{1 - B}{1-(\sigma ab/\rho ab)^6}\right] \text{where } B = \tfrac{1}{2}\left[\frac{Ia + 2Ib}{2(Ia+Ib)}\right]\left[\frac{Db}{1+Db}\right] L'ab$$

L'ab is a dimensionless function of r and the relative sizes of solute and solvent molecules (Sinanoglu, 1967). For our purposes L'ab ~2, and Ia ~Ib, so:

$$B \approx \tfrac{3}{4} \frac{Db}{1+Db}$$

Thus, the complete expression for dispersion energy becomes:

$$Edis = d_b \int_{(r_a+r_b)}^{\infty} 46.70 \left(DaDb\frac{IaIb}{IaIb} \; r_a^3 \; r_b^3\right)\left[\frac{\sigma ab^6}{\rho_{ab}^{12}} - \frac{1}{\rho_{ab}^6}\right]\left(1 - \frac{\frac{3}{4} Db}{(1+Db)(1-(\sigma ab/\rho ab)^6)}\right)$$
$$\times \left(4\pi(\rho ab + \ell ab)^2 \, d\rho ab\right)$$

which can be integrated analytically to give:

$$Edis = d_b Cab 4\pi \left[(1-B) \frac{1}{3\rho_{ab}^3} + \frac{\ell ab}{2\rho_{ab}^4} + \frac{\ell_{ab}^2}{5\rho_{ab}^5} - \sigma_{ab}^2 \left(\frac{1}{9\rho_{ab}^9} + \frac{\ell ab}{10\rho_{ab}^{10}} + \frac{\ell_{ab}^2}{11\rho_{ab}^{11}} \right) \right]_{\rho ab=(r_a+r_b)}^{\infty}$$

b) Cavity Term, Ecav

This is the energy required to form a cavity in the solvent to accommodate the solvent molecule. Its calculation is based on surface energy, such that for a solute molecule of radius r_a, the energy required is $4\pi r_a^2 \gamma$ where γ is the surface tension of solvent. A correction factor is required (Sinanoglu et al, 1968, 1969) for working at microscopic dimensions, so, converting to Kcal/mole:

$$E_{cav} = 6.903 \times 10^{-3} \gamma V_a^{\frac{2}{3}} Kb(Vb/Va) \left[1 - \frac{\partial \ln \gamma}{\partial \ln T} - \frac{2}{3} AT \right] \text{ Kcal/mole}$$

for γ in dynes/cm

$Kb(Vb/Va) = (1 + (Vb/Va)^{\frac{2}{3}} (Kb(1)-1))$ is a constant, $Kb(1)$ being the microscopic cavity factor for pure liquid b. A is a coefficient of thermal expansion appropriate to the cavity. It should have a value between those for pure solvent and pure solute, but calculations show that solvent expansivity is a good approximation (Sinanoglu et al, 1969).

Bringing $Kb(1)$ explicity into the equation:

$$Ecav = 6.903 \times 10^{-3} \gamma (Va^{\frac{2}{3}} + Vb^{\frac{2}{3}} (Kb(1)-1)) F(\gamma, A)$$

where $F(\gamma, A)$ is the function of γ and expansion:

$$\left[1 - \frac{\partial \ln \gamma}{\partial \ln \gamma} - \frac{2}{3} AT \right]$$

hence $$Ecav = 6.903 \times 10^{-3} \gamma \left(\frac{4}{3}\pi\right)^{\frac{2}{3}} (r_a^2 + r_b^2 (Kb(1)-1)) F(\gamma, A)$$

$$Ecav = .01809 \gamma (r_a^2 + r_b^2 (Kb(1)-1)) F(\gamma, A) \text{ Kcals/mole.}$$

A computer program (SOLVEFF) was written to calculate the values of Ees, Edis, Ecav and Etot (= Eisol + Ees + Edis + Ecav) for any conformation of a molecule consisting of up to thirty atoms. Spheroid dimensions and x_T values may also be obtained from the program. A description of SOLVEFF, its input requirements and output options is presented in Appendix 4, together with flow charts. The values of the parameters required for the calculations with water, octane and octanol as solvents are tabulated, also in Appendix 4.

2.3.3 Results of solvent effect calculations

The solvent effect program (SOLVEFF) was used to calculate energy corrections to the isolated molecule energy surface of the zwitterions of GABA and several of its agonists. The results are presented here in the form of energy surfaces and x_T distributions. (All contours are at 10 kcal/mole intervals unless otherwise stated.) The findings are discussed with respect to other methods (NMR, dipole moment measurements and theoretical approaches) in Section 2.5. The pharmacological significance of the results is discussed in Section 3.3.3

(a) Results for GABA

1) Initial calculations for aqueous solution

The most extensive calculations were carried out on the GABA zwitterion itself. The results illustrate some of the more general features of the method. Initially, 20^o grids of aqueous solvent effect energies were calculated for the assymetric part of the T_2-T_3 energy surface ($T_2=0^o$-180^o, $T_3=0^o$-360^o) with T_1 and $T_4=180^o$ (Fig. 1.3). Isolated-molecule energies and dipole moments were taken from MO calculations of the CNDO/2 type (Warner & Steward, 1975; Warner, 1975). The contoured T_2-T_3 maps of cavity energy, dispersion energy and electrostatic energy for the GABA zwitterion are shown in Fig. 2.9. Clearly, electrostatic energy is by far the largest effect. It is also the most variable with conformation, owing to the dependence of Ees on (dipole moment)^2 (see below) and the fact that dipole moment itself, for zwitterions is highly dependent upon conformation. Total energies were calculated for each point on the grid so that the minimum-energy conformations in solution could be located. The total-energy surface, and isolated-molecule energy surface for comparison, are illustrated in Fig. 2.10.

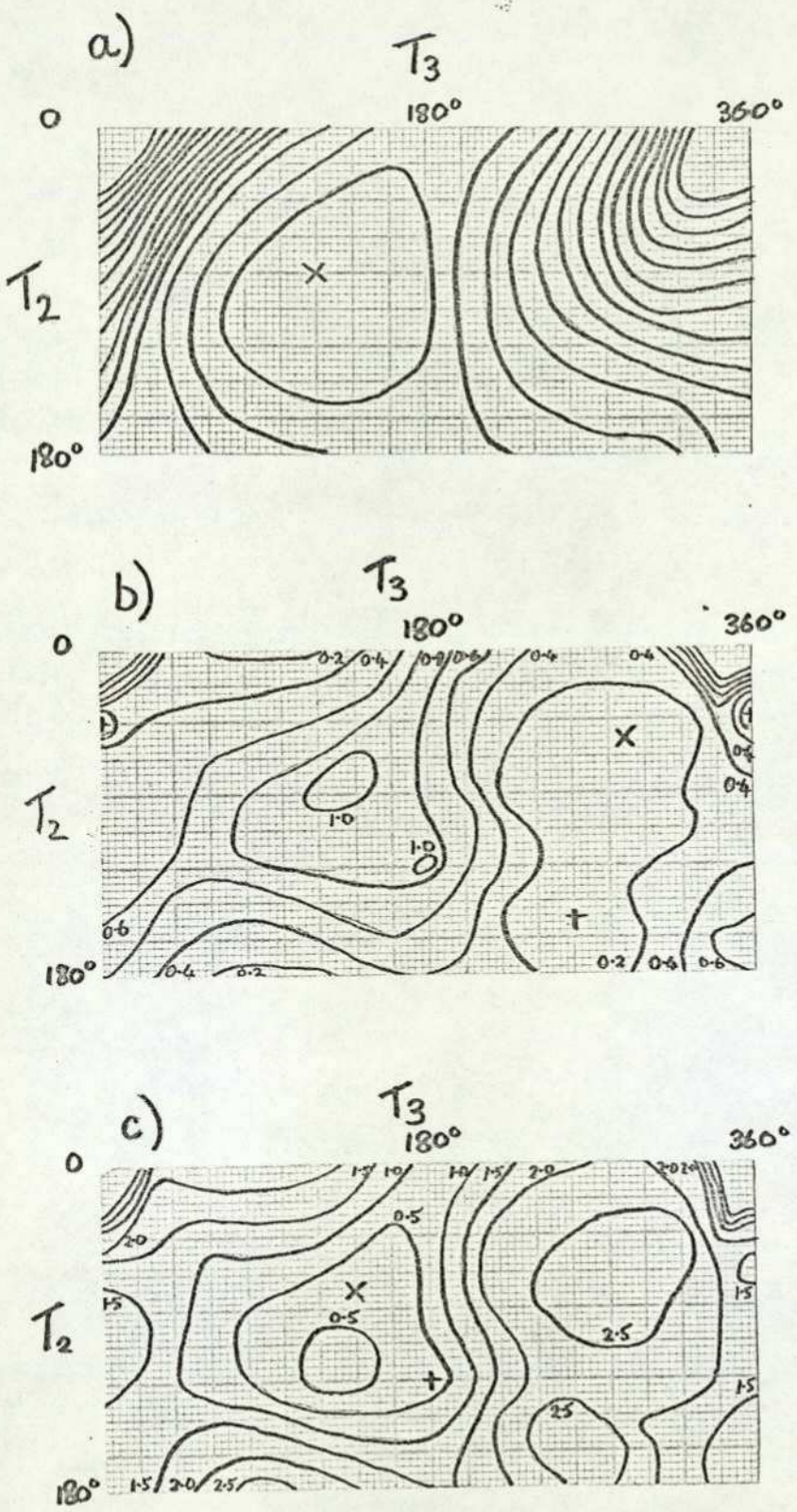

Fig. 2.9 GABA zwitterion solvent effect energies: asymmetric part of T_2-T_3 energy surfaces

a) electrostatic energy (EES)

b) dispersion energy (EDIS)

c) cavity energy (ECAV)

Contours in all energy surfaces are 10 Kcal/mole unless otherwise stated

+ local minima

× global minima

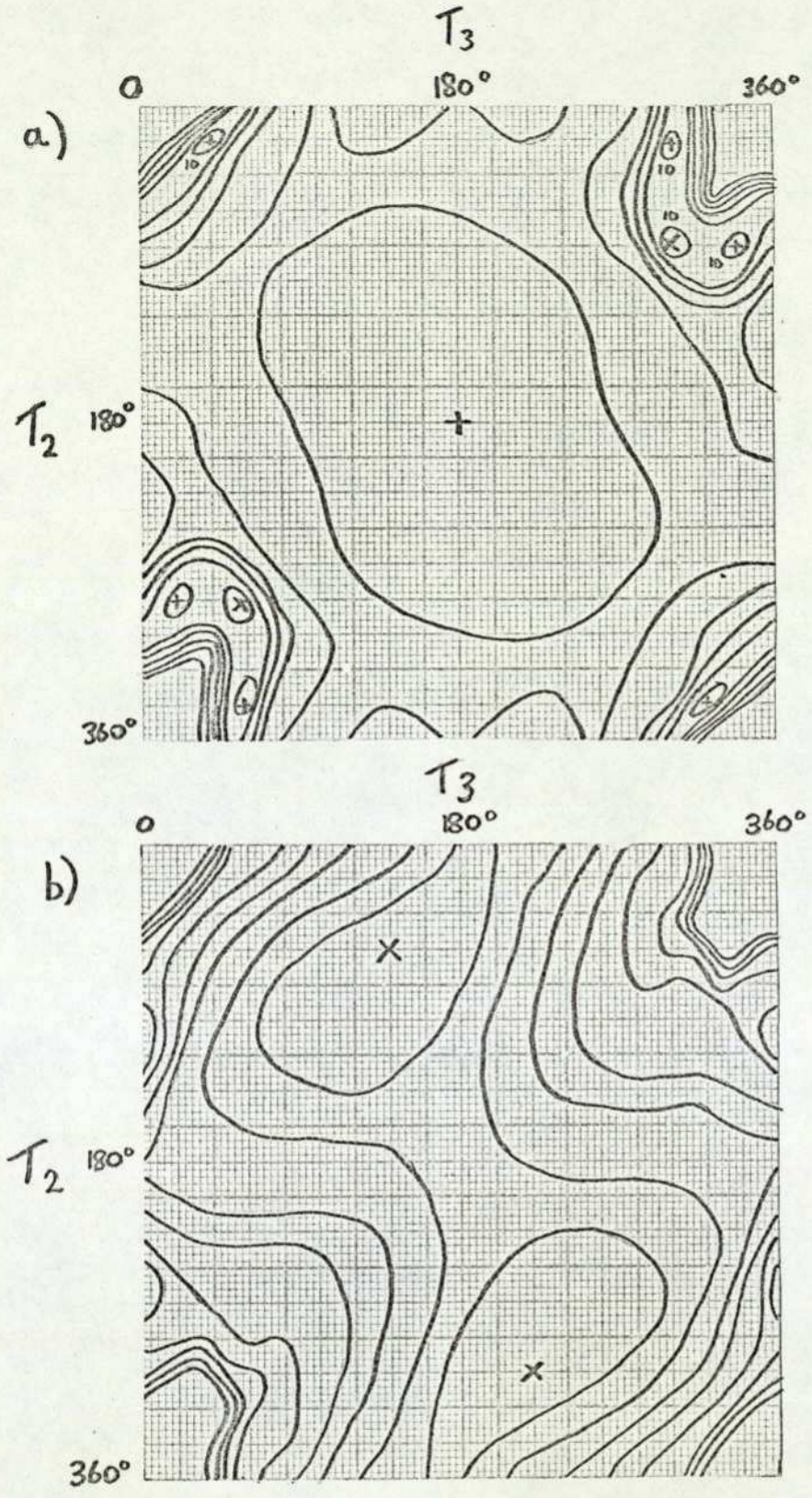

Fig. 2.10 GABA zwitterion T_2-T_3 energy surfaces

a) isolated molecule energy

b) total energy, including aqueous solvent effects

Contours 10 kcal/mole intervals:

+ local minima x global minima

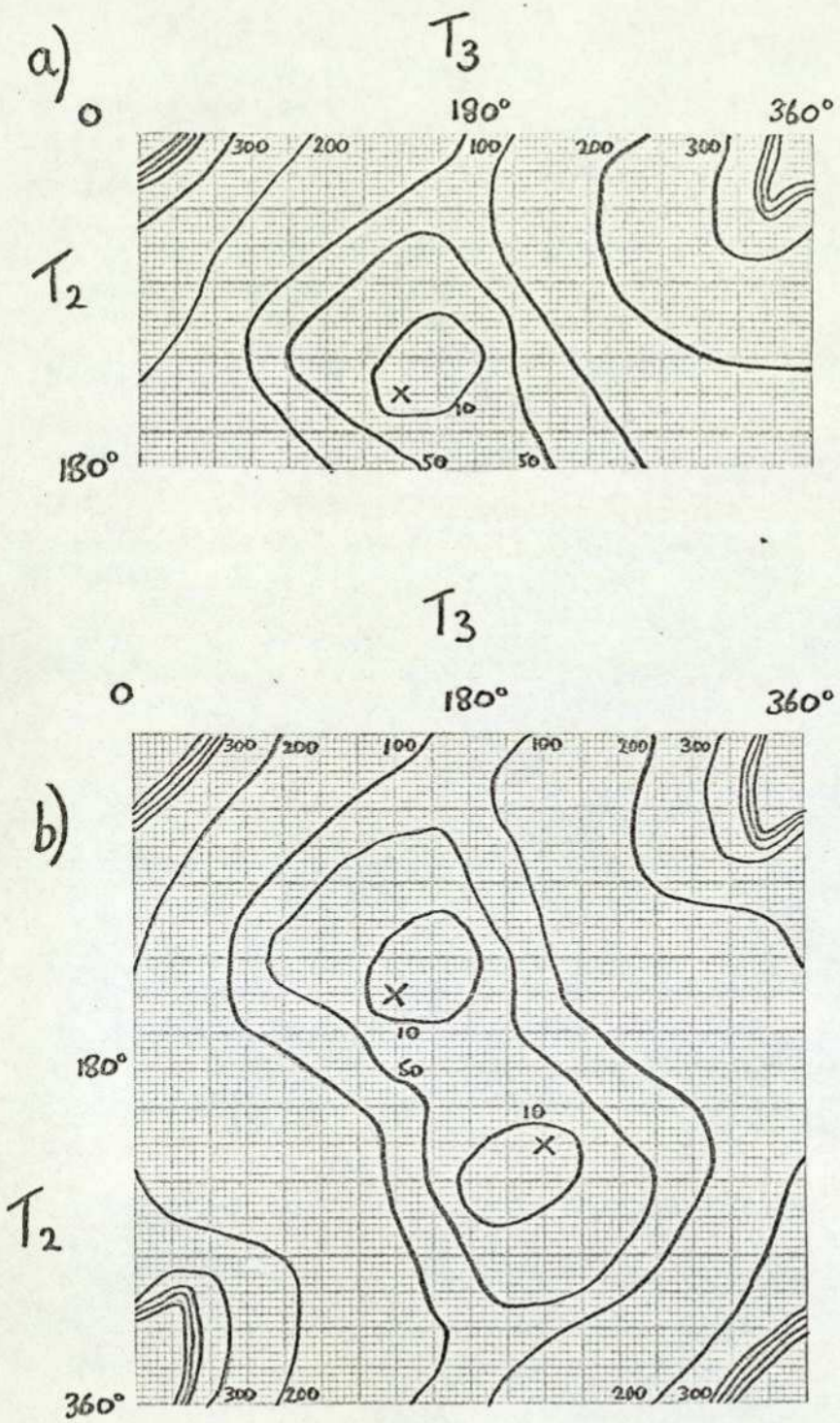

Fig. 2.11 Sphere approximation solvent effects

a) electrostatic energy

b) total energy

for GABA zwitterion

Contours kcal/mole: x global minima

A single pair of equivalent partly-folded energy minima was found in the total energy surface at $T_2 = +60^o$ and $T_3 = +140^o$. This result contrasts sharply with the isolated molecule minima which are highly folded, due to the strong attraction between the ionised terminal groups. In water, this attractive effect is counterbalanced by the energy gain obtained in extended conformations whose higher dipole moments interact strongly with the dielectric environment.

The conformational energy map for the electrostatic interaction calculated with a spherical instead of a spheroidal cavity, and the corresponding total-energy map (Fig 2.11 a,b) show more extended minimum-energy conformations. The use of a spherical cavity tends to increase the magnitude of the electrostatic term, and, not unexpectedly, to reduce the importance of molecular shape. The maximum electrostatic energy for the spherical model tends to occur at or near the conformation with the maximum x_T. In the spheroid model, on the other hand, shape effects introduced via the internal field factors (2.3.2) counteract this tendency. The spheroid model is theoretically more subtle than the spherical model on this point, and furthermore, experimental results tend to support the more folded GABA molecule predicted by the former (see 2.5). Accordingly, the spheroid model was employed for the remainder of the solvent effect investigations.

Interpolation of the energy surface around the minimum-energy region calculated on the spheroidal model showed that, on a 5^o grid, the minimum-energy position was at $T_2 = +65^o$, $T_3 = +140^o$ (Fig. 2.12). The interpolation was carried out using a bicubic spline function surface fitting routine (ISIR, programmed by P.W. Borthwick).

2) Population and x_T distribution

A population map of the interpolated minimum energy region was calculated (Fig. 2.13) using a simple Boltzmann function. Each point on the grid with an energy within 6 Kcal/mole of the global minimum was used in the calculation (points of higher energy have negligible populations owing to the exponential in the Boltzmann function). This method is analogous to the 'free-energy' population analysis of Gannellin, Farnell & Richards (1974) taking into account the curvature of the energy surface via an ensemble of states (see below).

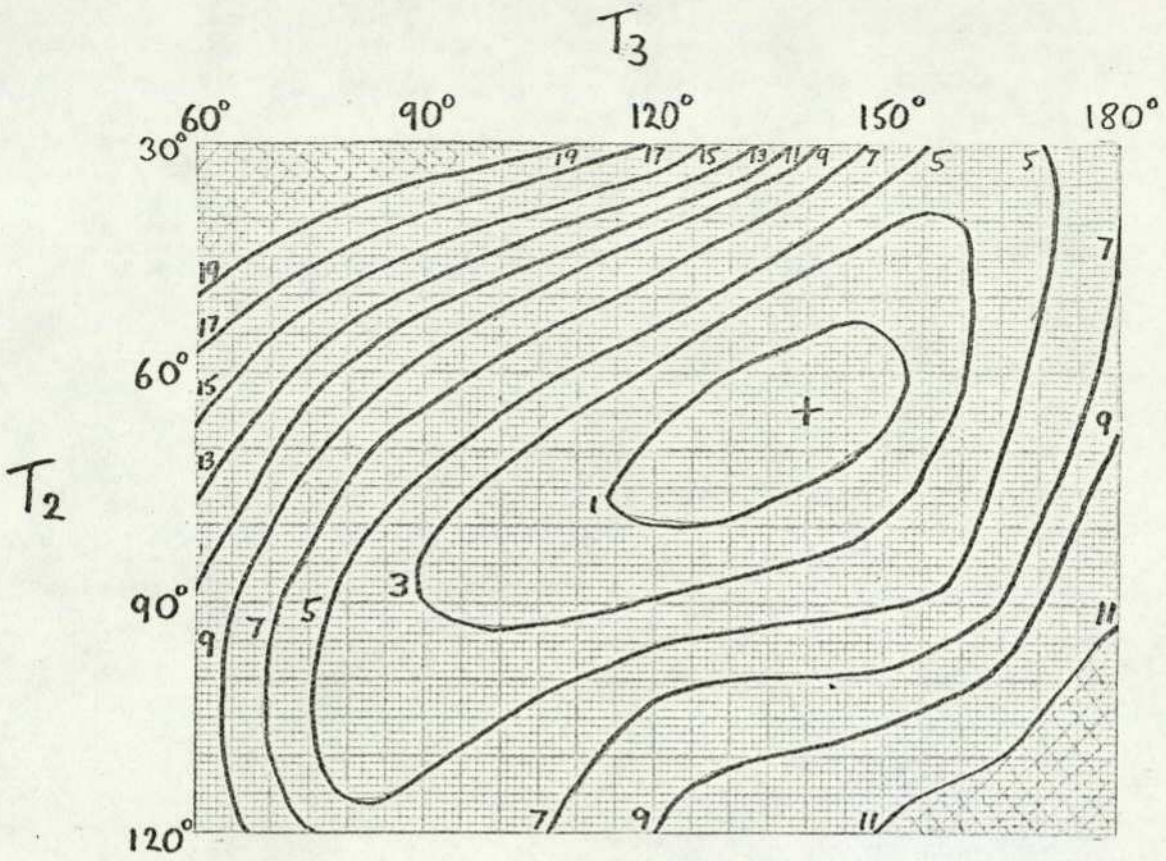

Fig. 2.12 GABA zwitterion in aqueous solution: interpolated minimum energy region (kcal/mole)

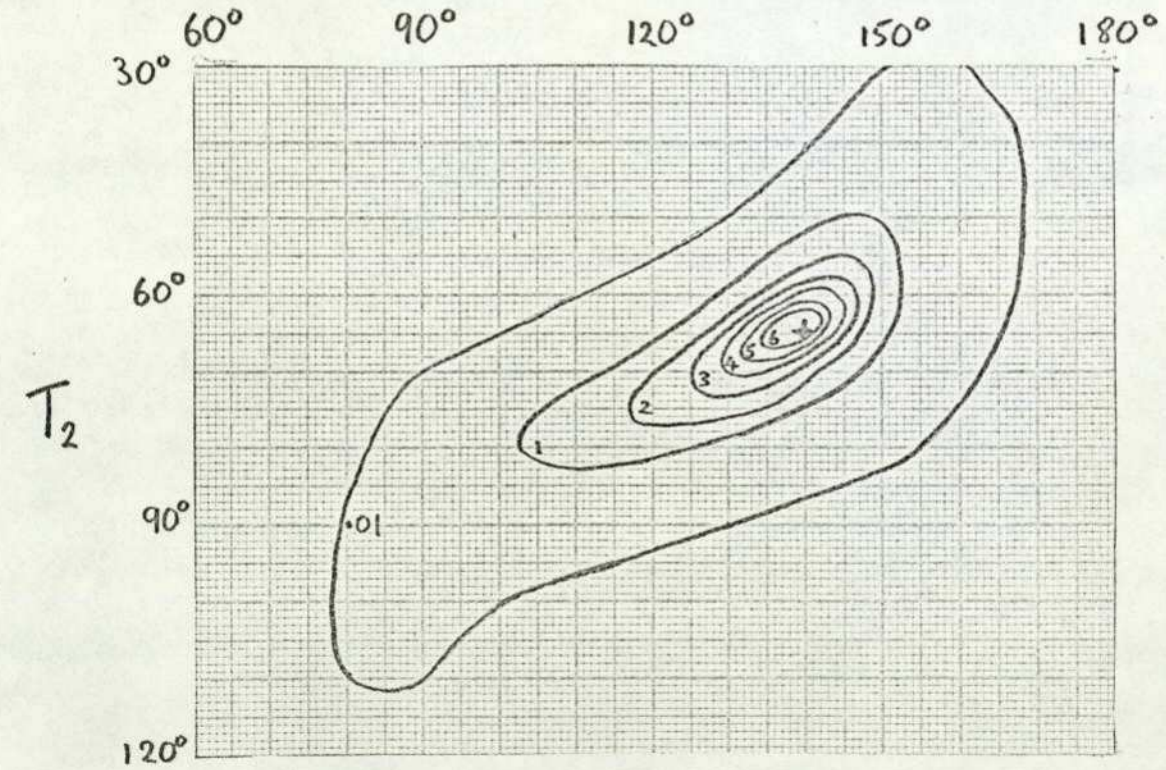

Fig. 2.13 Population density map from Fig. 2.12. Within countour ∩, each 5° square contains at least ∩% of the total number of molecules.

The fractional population of each point is given by:

$$fi = \frac{e^{-\Delta E_i/RT}}{\sum_{\substack{\text{all } E_i\text{'s} \\ <6\text{kcal/mole}}} e^{-\Delta E_i/RT}}$$

From these population values and the x_T values obtained from SOLVEFF, an x_T probability distribution was derived (Fig. 2.14a) using a simple computer program. Intervals of 0.1 Å in x_T were considered, so that the resulting distribution is a histogram with ordinates of 0.1 Å width. The segment centred on 5.15 Å, for example, contains the sum of the populations of all the conformations whose x_T falls between 5.10 Å and 5.19 Å. The peak population value of 0.50 occurs at x_T = 5.2 Å.

An x_T distribution based on the 20° grid was also calculated (Fig. 2.14b). This showed a sharper peak than the former distribution because of the lower number of contributions used, but the peak occurred in the same segment and the general shape of the two distributions was comparable.

All the remaining x_T distributions presented in this section are calculated from 20° grids. This should provide useful comparative information, although a finer grid would produce a somewhat smoother distribution. The population values used in the distributions are assembled in Table 2.7.

The relative populations of minima can be calculated using the method suggested by Farnell, Richards and Gannellin (1974) taking into account the shape of the minimum as well as the depth. A broad minimum will possess a higher number of populated states than a sharp one so a comparison of population based only on the lowest energy values of each minimum region may give misleading results. It is necessary instead to consider each populated state (i.e. within ~ 6 Kcal of the global minimum) in each minimum region and sum the populations over each region. Clearly, in the case of the T_2-T_3 GABA energy surface, the minima are equally populated, since they are symmetrically equivalent, but in other compounds, notably α-fluoro GABA (see below) minima of slightly different energy appear. In such

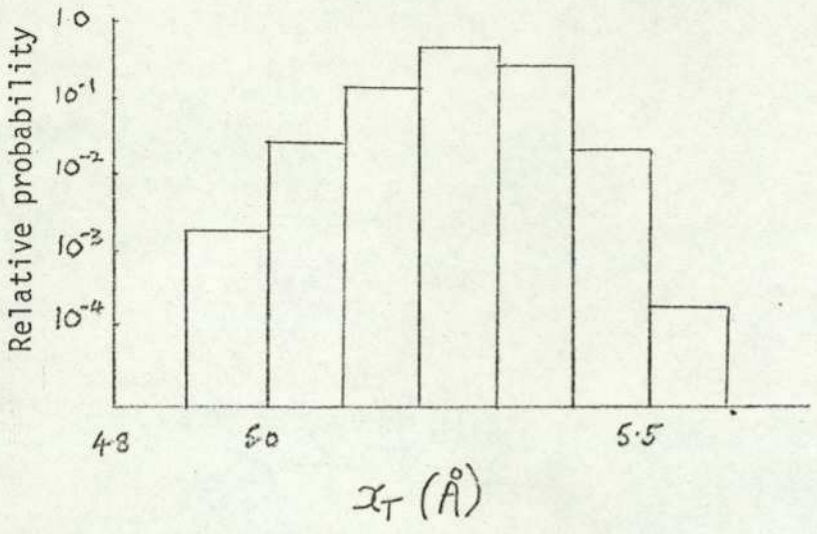

(a) distribution based on interpolated 5^o grid

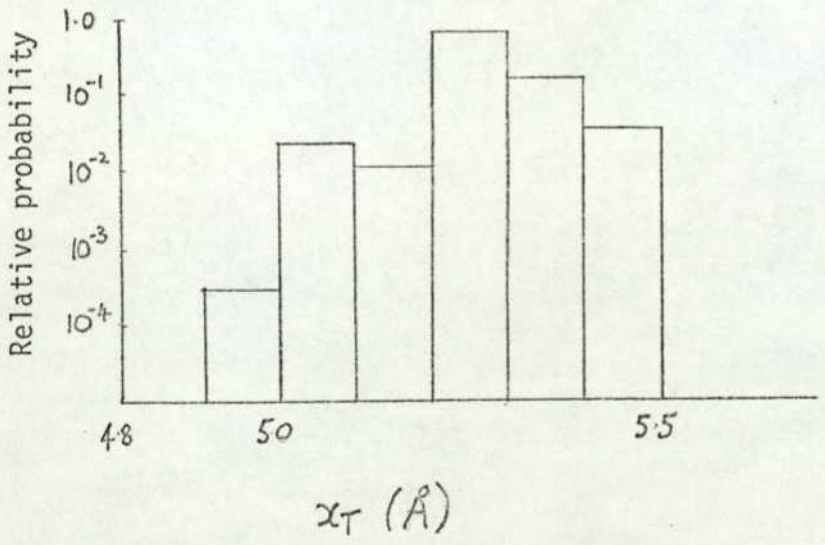

(b) distribution based on 20^o grid

Fig. 2.14 x_T distributions for GABA zwitterion in water From T_2-T_3 SOLVEFF energy surface with $T_4 = 0^o$

cases, the summed populations over each minimum energy region provide a much better estimate of relative population than comparison of population at the minimum energy points alone. Few of the compounds examined, however, actually exhibit more than one significantly populated minimum.

The x_T distributions, of course, allow for contributions from each populated state.

3) Rotation of the carboxyl group

The effect of the carboxyl group rotation was also investigated. With the carboxyl torsion angle T_4 (Fig. 1.3) set at multiples of 20^o, CNDO/2 and SOLVEFF calculations were carried out for the GABA molecule over likely low-energy regions of the T_2-T_3 surface on a 40^o grid. The results are illustrated in Fig. 2.15. Rotation of T_4 from the symmetric position causes the T_2-T_3 surface to lose its centre of symmetry. Hence, one of the global minima (60^o, 140^o) of the T_2-T_3 surface moves to a three-dimensional global minimum of $T_2 \simeq 140^o$, $T_3 \simeq 60^o$, $T_4 \simeq 60^o$, as T_4 rotates in the positive sense, while the other stays in place as a local minimum only. The three-dimensional global minimum is $\sim$27 Kcal/mole lower than that for the $T_4 = 0$ surface (Table 2.5). As T_4 proceeds through 90^o, the process is seen in reverse. A second, equivalent, three-dimensional global minimum occurs at $T_2 \simeq 220^o$, $T_3 \simeq 300^o$, $T_4 \simeq 120^o$, and as T_4 approaches 180^o, the T_2-T_3 global minimum returns to -60^o, -140^o, the $T_4 = 180^o$ surface being the same as the $T_4 = 0^o$.

Despite the change in conformational preference revealed by investigation of the T_4 rotation, the preferred x_T value remains the same, 5.21 Å. In fact, x_T values at global minima in each of the T_2-T_3 surfaces are remarkably consistent (Table 2.5).

Thus, broadly speaking, the carboxyl group rotation affects the minimum-energy conformation but does not alter the gross charge-separation of the molecule. If anything, the molecule tends to be slightly more extended when the carboxyl group is in its optimum position.

TABLE 2.5

Minima of the T_2-T_3 energy surface for GABA at various settings of T_4. DISMAX is the length of the spheroid representing the solute molecule and RADMAX is its radius. A is the radius of the sphere of equal volume.

T_2 °	T_3 °	T_4 °	ETOT Kcal/mole (rel. to global) min	x_T A°	DISMAX Å	RADMAX Å	A Å
60	140	0	27.17	5.21	7.99	2.57	2.97
80	100	20	20.42	5.19	7.75	2.60	2.97
100	80	40	9.24	5.19	7.50	2.60	2.94
140	60	60	0	5.21	7.32	2.61	2.92
180	20	80	6.57	4.83	6.88	2.76	2.97

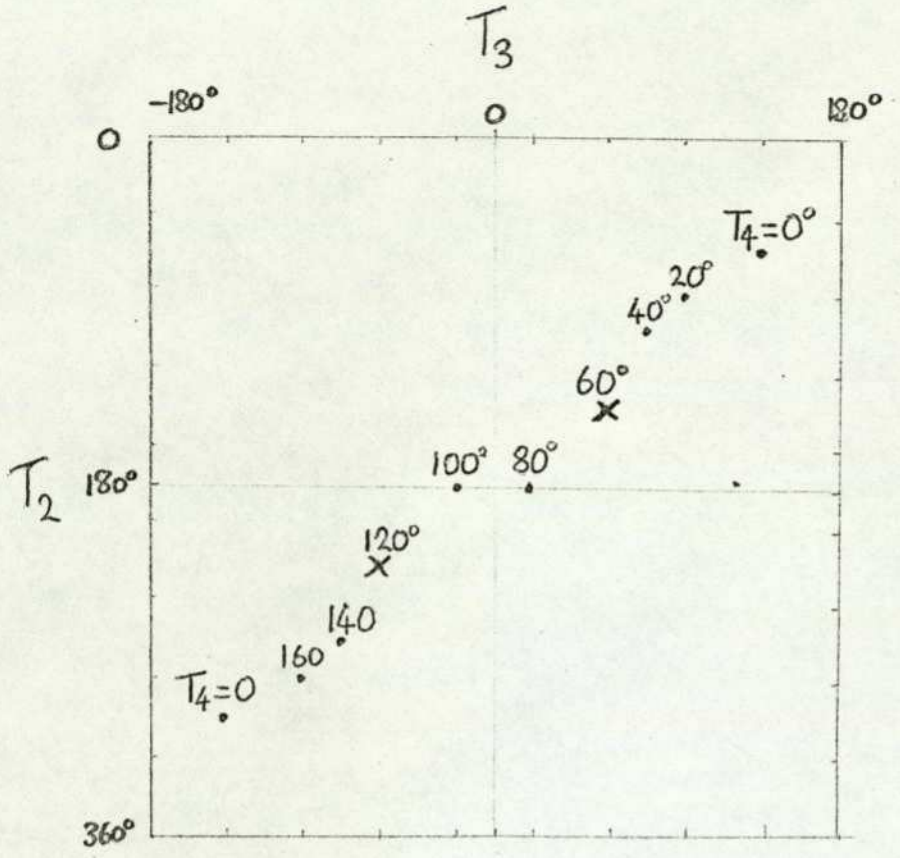

Fig. 2.15 Positions of global minima in T_2-T_3 energy surfaces for various settings of T_4 ; GABA zwitterion in water

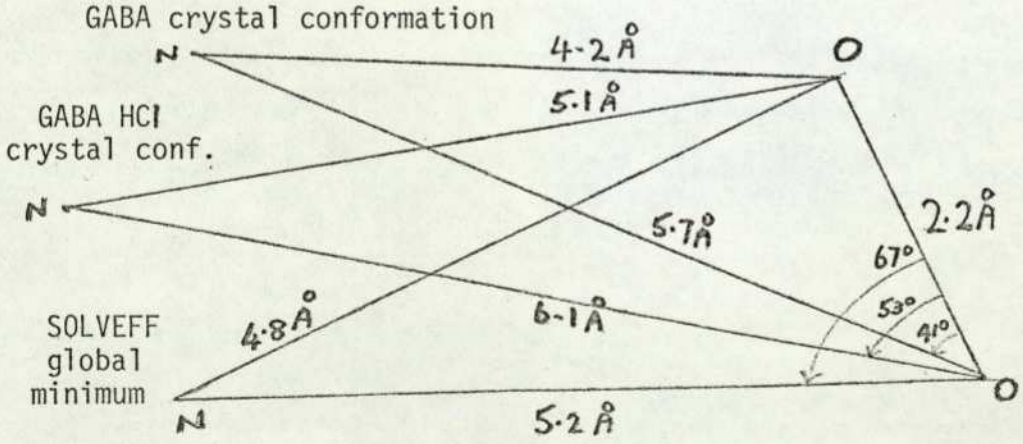

Fig. 2.16 N-O-O triangles for GABA zwitterion at its global minimum energy conformation in aqueous solution, and in crystal conformations

In comparison with the X-ray results, the N-O-O triangle for the SOLVEFF global minimum is shown in Fig. 2.16. The N-O-O angle is $\sim 67^{o}$, considerably higher than that found commonly in crystal structures (Table 2.2).

4) Other solvents

Two more T_2-T_3 grids were calculated using other solvents - octanol and octane - in an attempt to investigate the effect of a lipid milieu on conformation. Octanol is often used as a model for a lipid medium in partition function experiments (Hansch, 1963) but it has a higher dielectric constant ($\sim$10) than a lipid milieu ($\sim$2). Hence the solvent effect of octane which has a dielectric constant of $\sim$2 was also tested. The results were surprising at first sight, since the octanol total-energy surface looked almost identical to that for water as solvent (Fig. 2.10b) and the octane surface looked like the isolated molecule surface (Fig. 2.10a). The x_T distributions for GABA in octanol and octane are shown in Fig. 2.17. The octanol x_T distribution is slightly smoothed compared to that for water (20^{o} grid). That for octane is virtually identical to that which would be obtained for the isolated molecule. The reasons for these results are discussed below.

5) The effect of solvent and solute parameters

The differing effect of organic solvents is due to a sharp drop in electrostatic interaction energy which occurs when ε for the solvent drops below about 10. This is illustrated in Fig. 2.18 where electrostatic energy in an arbitrary conformation is plotted against dielectric constant. As ε increases above 10, there is little further change in energy. Since the electrostatic term is the major one, the total energy results tend to reflect this variation.

The solvent effect energies of a molecule of lower dipole moment would similarly be greatly reduced, due to the reduction of the electrostatic term. The relationship between molecular dipole moment and interaction energy is illustrated in Fig. 2.19.

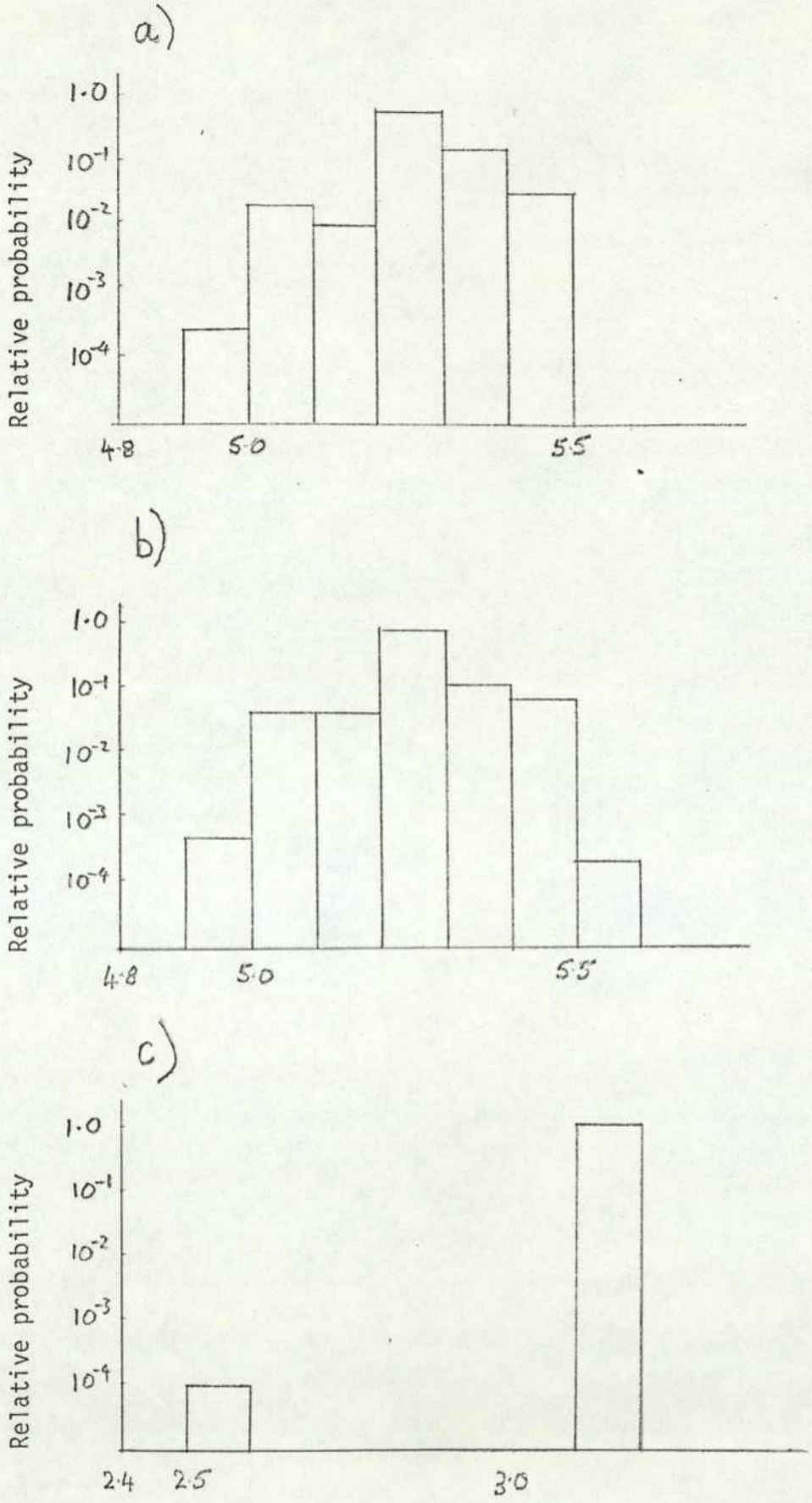

Fig. 2.17 x_T distributions for GABA zwitterion T_2-T_3 surfaces in various solvents (a) water (b) octanol (c) octane $T_4 = 0^o$

$E_{es} = -\frac{9\mu^2}{4a^3}\frac{(\varepsilon-1)(2\varepsilon+1)}{(2\varepsilon+2.5)^2}$ in the spherical approximation. For GABA zwitterion a^3 remains at ~27 Å^3 in most conformations. For high ε

$E_{es} \simeq -\frac{9\mu_o^2}{8a^3}$

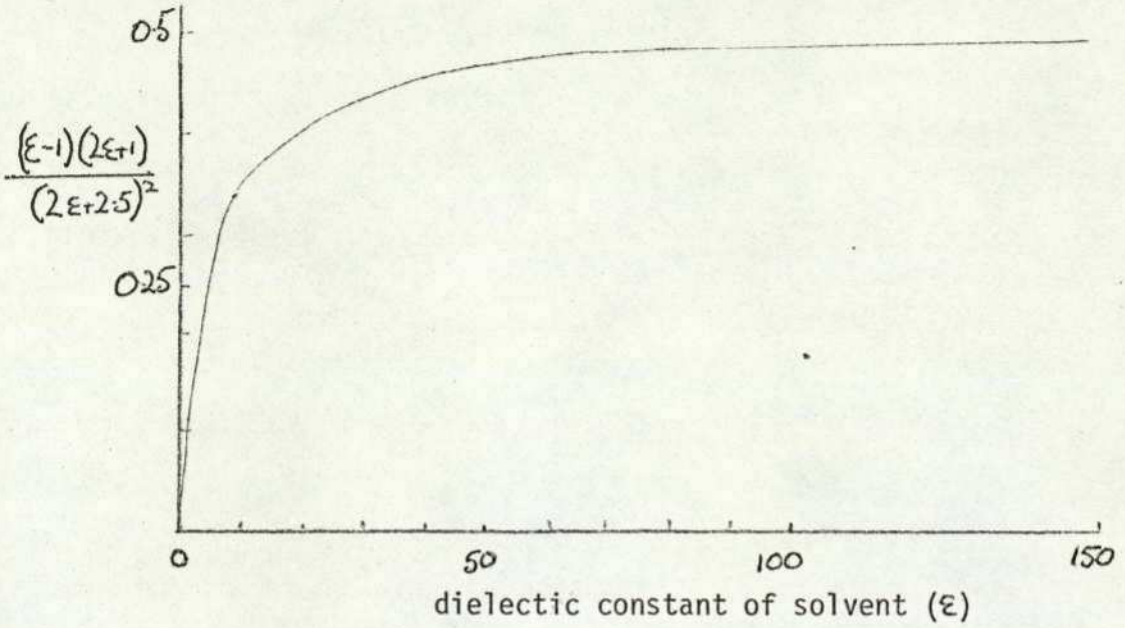

Fig. 2.18 Dependence of Ees on ε in the spherical approximation. The general shape is the same in the spheroidal case (see equations for Ees in section 2.3.2)

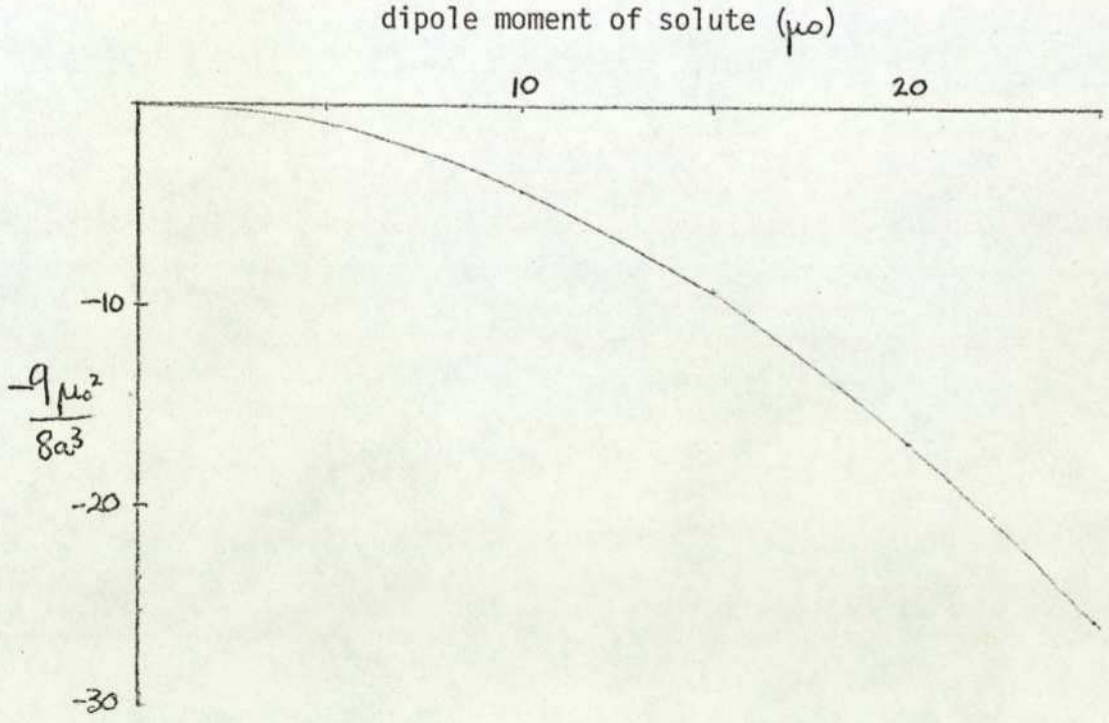

Fig. 2.19 Dependence of Ees on μo for high dielectric constant solvents

The volume of the molecule (as measured by the radius A (see 2.3.2)) is usually low in low-energy conformations since electrostatic energy depends on the reciprocal of the volume. In many surfaces, in fact, the global minimum coincides with the minimum molecular volume. The three-dimensional minimum-energy conformation of GABA also possesses a low molecular volume (Table 2.5), but this is not the lowest volume which the molecule can attain.

Despite this observation, molecular volume is not the most important factor in the solvent-effect calculations since it does not vary greatly with conformation. The total variation is ~10% from the mean. Dipole moment, in contrast, varies by over 30% and, moreover, appears as a squared term in the electrostatic interaction (2.3.2). Cavity energy and dispersion energy depend almost linearly on molecular volume alone, for given solvent and solute, so their variation is far less significant than that of the electrostatic term.

b) Results for GABA agonists with water as solvent

Solvent-effect calculations were carried out on six GABA agonists treated as zwitterions. Two-dimensional 20^{o} grids of total energy were produced. The results, with isolated-molecule energy maps for comparison, are shown in Figs. 2.20-25. The rotations involved are illustrated with the maps. x_T probability distributions were also calculated and are presented in Fig. 2.26. For clarity a logarithmic scale is used. The minima located are listed in Table 2.6 and population values for x_T's in Table 2.7.

1) ∝ Fluoro GABA

In common with GABA itself, the ∝ Fluoro GABA (∝FG) molecule possesses four degrees of rotational freedom. Only the two central torsion angles, T_2 and T_3, which define the gross shape of the molecule, were varied in this study (Fig. 2.20). T_1 and T_4 were set at 180^{o}.

∝FG contains an asymmetric ∝ carbon atom, so two enantiomers can exist. This study employs the (R) stereoisomer (Fig. 2.20).

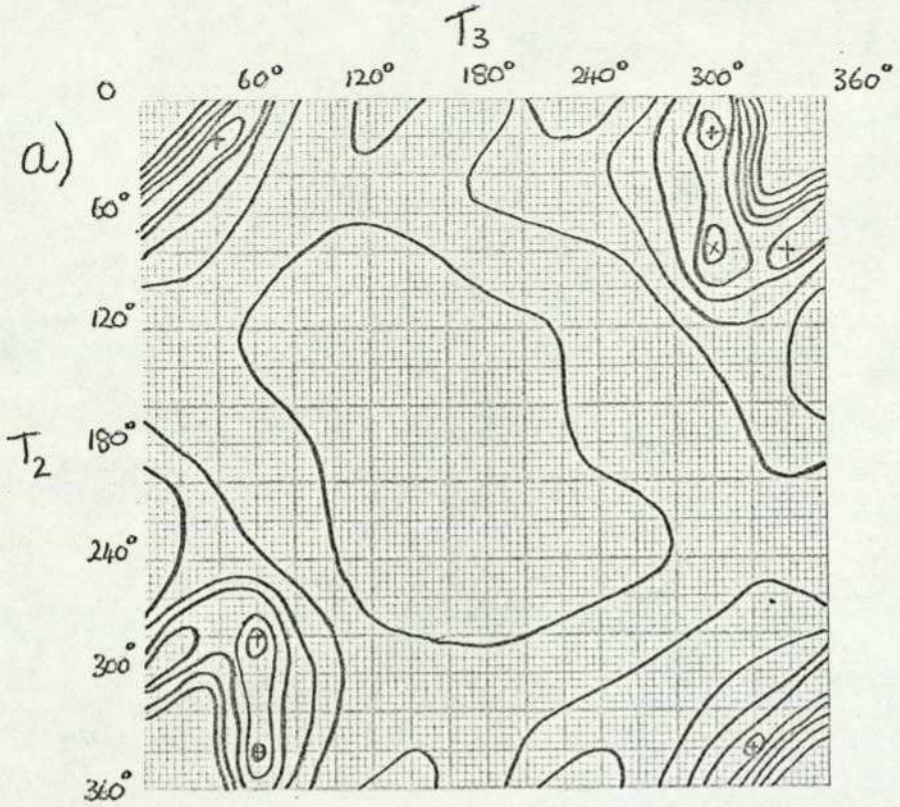

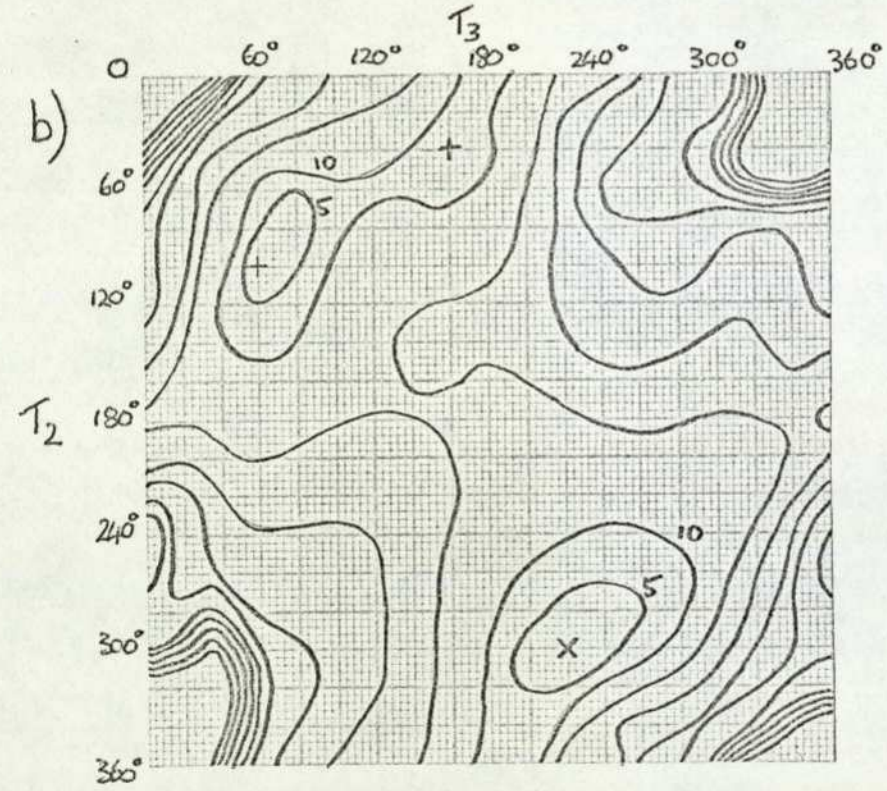

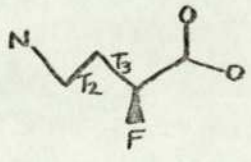

Fig. 2.20 α fluoro GABA energy surfaces

(a) isolated molecule

(b) with aqueous solvent effects

Contours 10 kcal/mole intervals unless otherwise stated

\+ local minima

x global minima

Isolated molecule energies and dipole moments were obtained from CNDO/2 calculations (Borthwick & Steward, 1975[c]).

Two minimum-energy regions of appreciable population were found. The global minimum, at -60^{o}, -140^{o}, corresponds exactly to one of the pair of global minima in the GABA T_2-T_3 surface. The second minimum is at 100^{o}, 60^{o} with an energy 3.2 Kcals/mole above the global minimum. Another local minimum occurs at 40^{o}, 160^{o} (close to the second global minimum for GABA) but this is barely populated, being 5.7 Kcals/mole above the global minimum. T_2-T_3 solvent-effect maps for GABA (Fig. 2.10) and αFG (Fig. 2.20) show marked similarities, but the comparison illustrates that the effect of α branching on chain conformation in solution is considerable. It is likely that, in common with GABA, investigation of the carboxyl group would reveal considerable changes in the minimum energy conformation but that the preferred charge-separation of the molecule would remain much the same.

2) β guanidinopropionic acid

β guanidinopropionic acid (βGP) possesses six possible rotations, but again, the gross shape of the molecule is controlled by the central pair T_2 and T_3 (see Fig 2.21). All other bonds were set trans in this study. Isolated-molecule energies and dipole moments were obtained from CNDO calculations (Warner, 1975). Two pairs of minimum-energy regions appear in the complete T_2-T_3 solvated energy-surface which, as in the case of GABA, possesses a centre of symmetry (Fig. 2.21).

The global minima occur at $\pm$ (60^{o}, 80^{o}) and local minima of 9.5 Kcal/mole higher energy, occur at $\pm$ (140^{o}, 280^{o}).

The x_T distribution shows two peaks (at 4.8 Å and 5.7 Å) corresponding to charge separations at the global minimum between the carboxyl group and the two terminal amino groups. The N-H group within the chain is not considered to be a likely point of interaction with the receptor since N substituted GABA analogues are usually inactive (Curtis & Watkins, 1960). Moreover, the charge associated

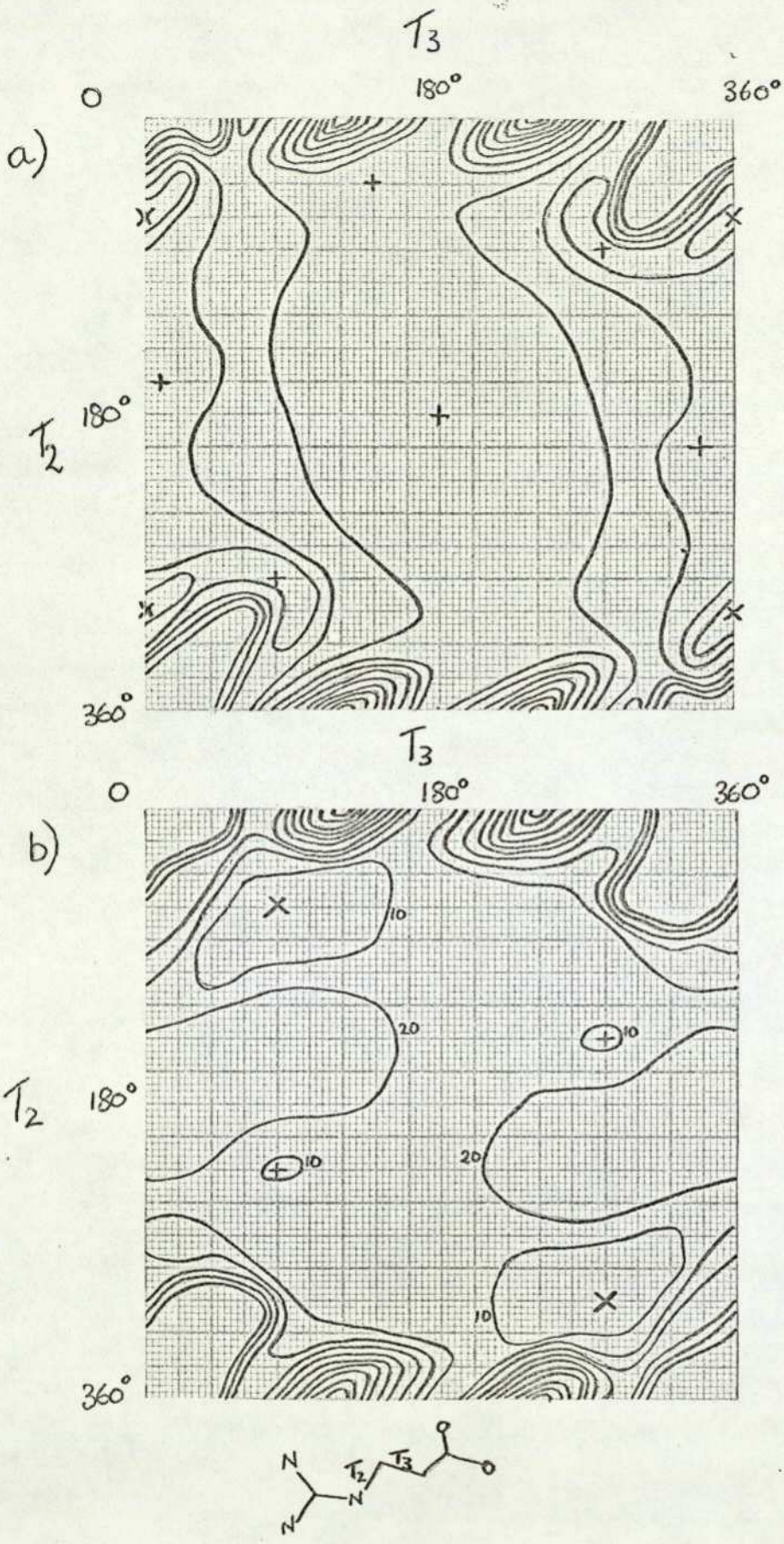

Fig. 2.21 β guanidinopropionic acid

(a) isolated molecule

(b) with aqueous solvent effects

Contours 10 kcal/mole intervals

+ local minima, x global minima

with each terminal group is twice that associated with the N-H group (Fig. 1.4). The positive charge-centres are thus taken as the mid-points of each pair of amino hydrogens.

3) Trans 4-aminocrotonic acid

The conformation of trans 4-aminocrotonic acid (trans ACA) is completely defined by three torsion angles (Fig. 2.22). In this study, only the rotation of the protonated amino group (T_1) was neglected, being set in the trans position. A complete T_2-T_3 energy surface for this molecule is 180^o x 360^o, since a carboxyl group rotation is involved (T_3). The surface itself consists of two equivalent parts related by a centre of symmetry. Isolated molecule energies and dipole moments were obtained from CNDO/2 calculations (D.I. Livingstone, unpublished work).

Two pairs of minima were found in the total-energy map. The global minima occur at 100^o, 120^o and 260^o, 60^o (see Fig. 2.22) and the local minima, only 0.01 Kcal/mole higher in energy (an insignificant difference), occur at 160^o, 100^o and 200^o, 80^o. The map shows a broad region within the 5 Kcal/mole contour, indicating a wide range of possible conformations. The entire energy surface is unusually flat, variations being no larger than 25 Kcal/mole. This is due to the absence of close approaches of the terminal groups.

The x_T distribution shows two peaks corresponding to the global and local minima at 5.4 Å and 5.7 Å respectively.

4) Cis-4-aminocrotonic acid

Cis-4-aminocrotonic acid (cis ACA) possesses the same symmetry properties as the trans epimer, so the rotations investigated correspond directly. The features of the energy surfaces however are very different, since close approaches between terminal groups occur in the cis compound. A strong preference is shown for maximally extended conformations of T_2, in which the carboxyl rotation, T_3, remains fairly free, the barrier to rotation being about 2½ Kcal/mole (Fig 2.23).

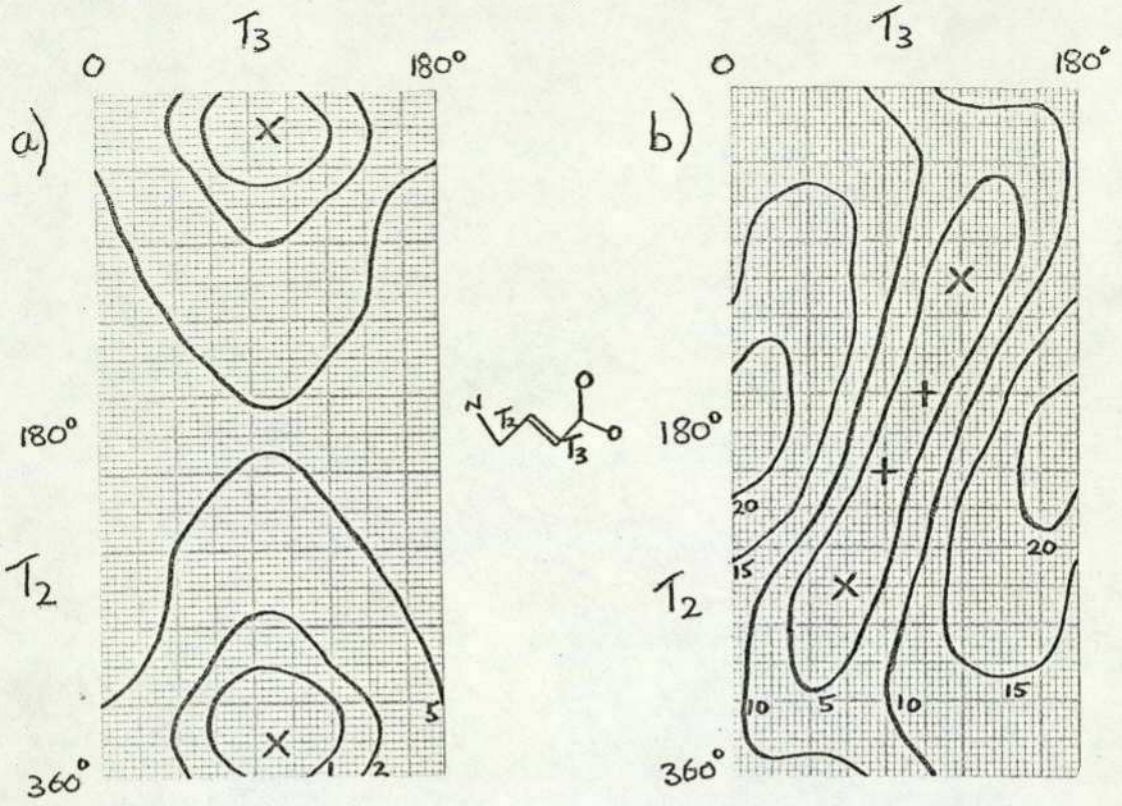

Fig. 2.22 Trans 4 aminocrotonic acid

(a) isolated molecule

(b) with aqueous solvent effects

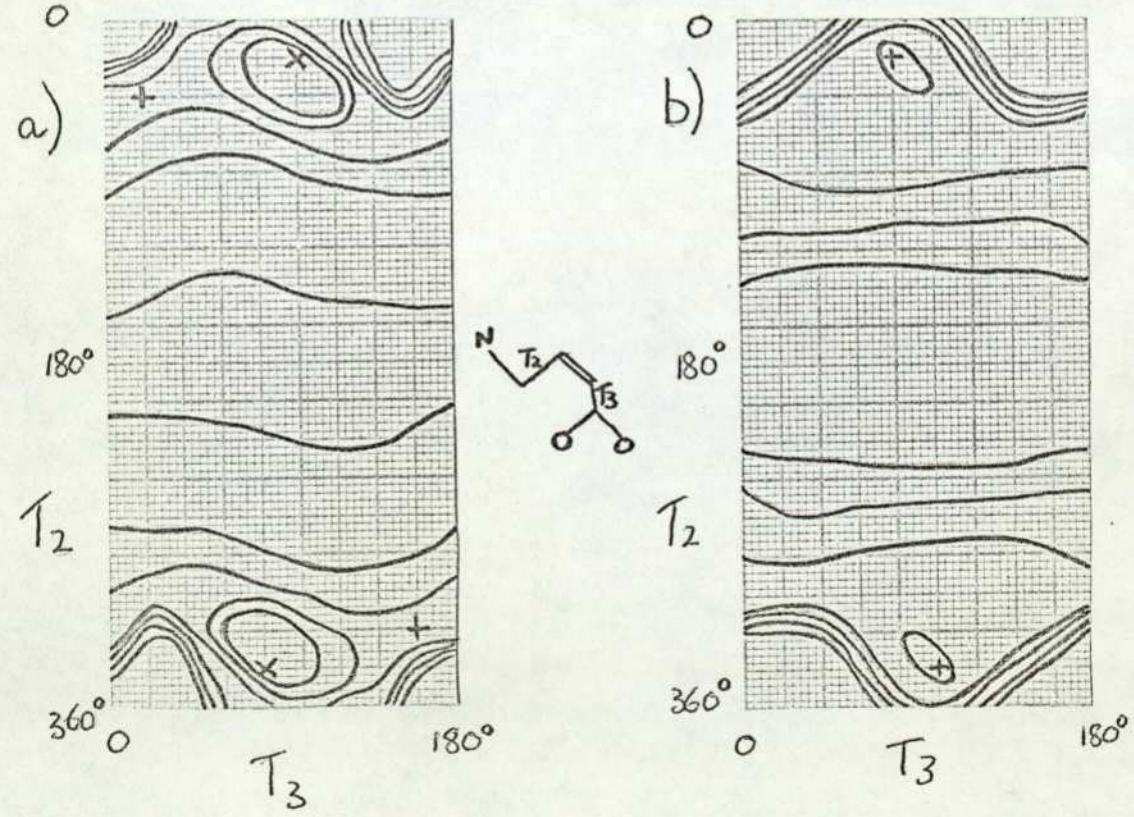

Fig. 2.23 Cis 4 aminocrotonic acid

Contours 10 kcal/mole intervals, unless otherwise stated: + local minima
x global minima

The global minimum occurs at 180^{o}, 0^{o} and is thus unique. A pair of local minima of 29.3 Kcal/mole higher energy occur at 20^{o}, 80^{o} and 340^{o}, 100^{o}. These correspond to the isolated molecule preferred conformation (Livingstone, unpublished work).

Since T_2 defines x_T completely, the entire population of molecules possesses a charge separation of $\sim$5.0 Å.

5) β alanine

The conformation of β alanine is also defined by three torsion angles but lower total energies are displayed overall when the rotation of the protonated amino group (T_1) is set trans. The T_2-T_3 energy surface shown in Fig. 2.24 is that for the trans T_1 case. Isolated molecule energies and dipole moments were taken from CNDO/2 results (Livingstone, Borthwick & Steward, 1975).

A unique minimum energy conformation occurs at 180^{o}, 90^{o} and the region within the 5 Kcal/mole contour is not extensive. The peak of the x_T distribution occurs at 4.6 Å.

6) β Hydroxy GABA

There is a strong possibility that, in solution, β Hydroxy GABA (βHG) possesses an intramolecular hydrogen bond between the hydroxyl oxygen and one of the carboxyl oxygens (Borthwick, unpublished work). This suggestion is based on the structure of salicylic acid which has a similar grouping. For salicylic acid the existence of an intramolecular hydrogen bond has been demonstrated in solution by spectroscopy of various kinds and in the solid state by X-ray crystallography (Catalan & Fernandez-Alonso, 1975). The crystal structure of βHG (Tomita, Harada & Fujiwara, 1973) also shows such a bond, although it is bifurcated. No relevant data is avilable for βHG in solution, but the analogy with salicylic acid suggests that an intramolecular hydrogen bond may well exist, creating a pseudo six-ring at the acidic end of the molecule. The possibility is also mentioned by Kier and George (1973) in an EHT MO study of βHG.

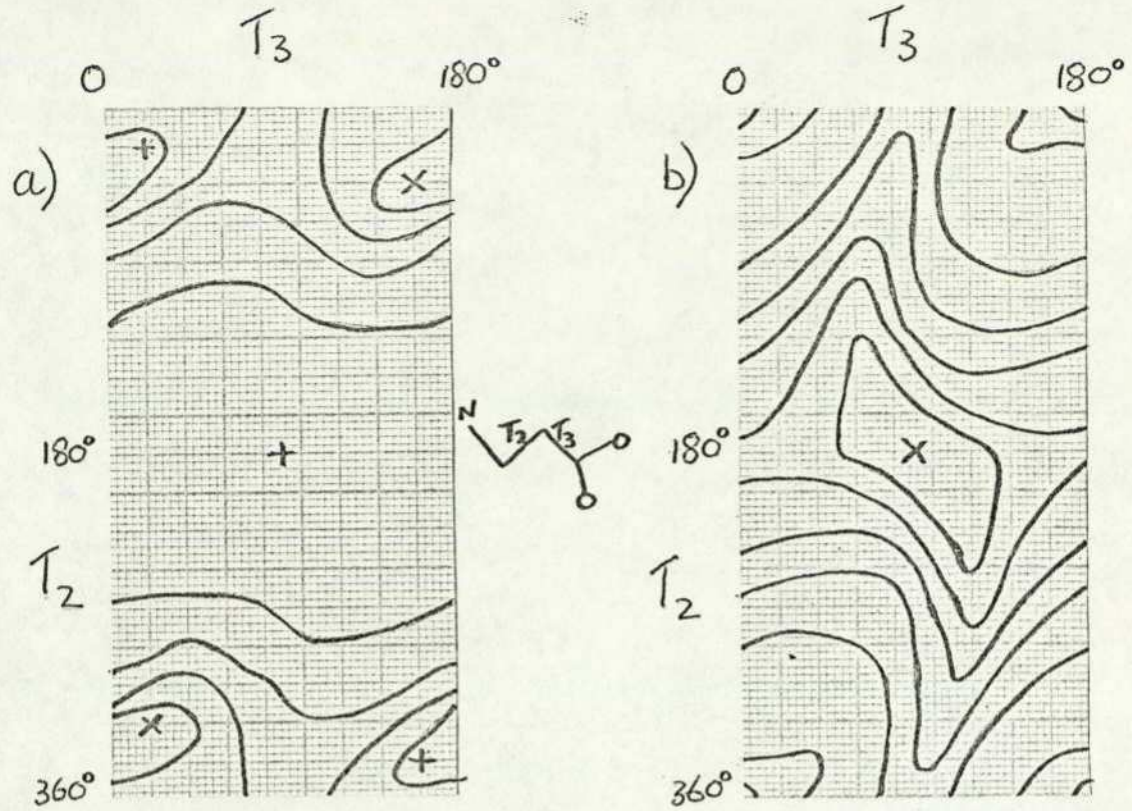

Fig. 2.24 β alanine

(a) isolated molecule

(b) with aqueous solvent effects

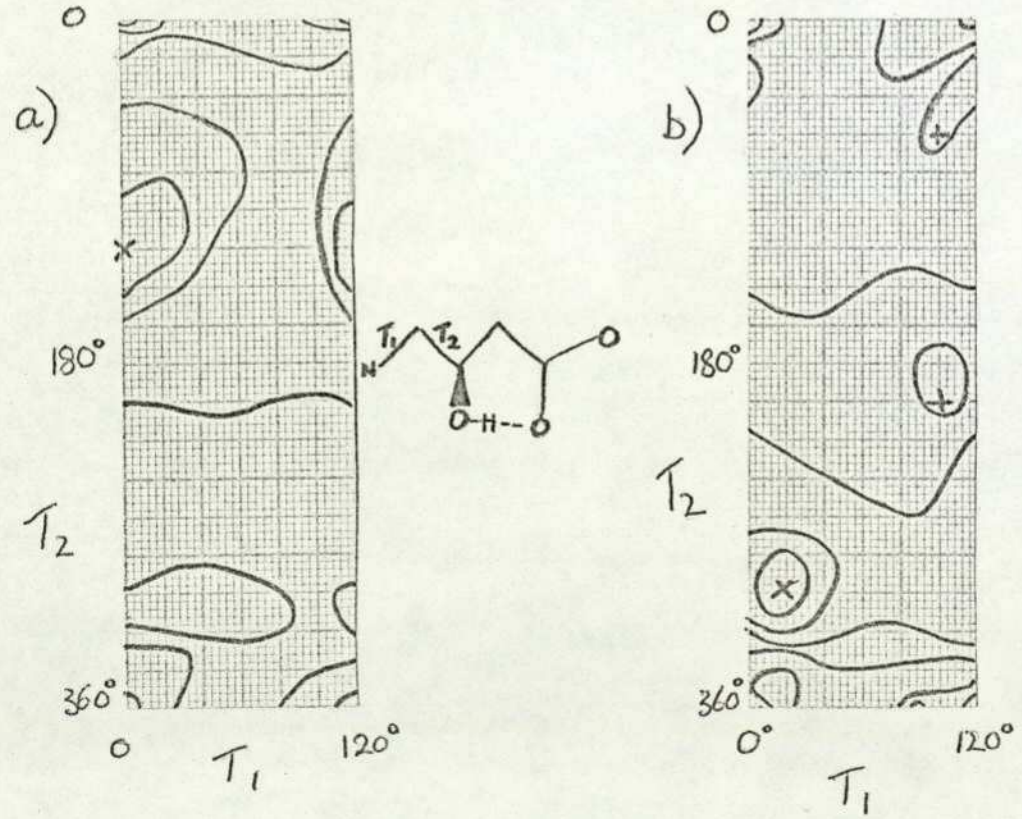

Fig. 2.25 β hydroxy GABA

(a) isolated molecule

(b) with aqueous solvent effects

Contours 10 kcal/mole intervals
+ local minima, x global minima

The present conformational study of βHG was carried out on the assumption that the pseudo six-ring is formed. This reduces the possible rotations to two, so a complete study is feasible. Since one of the rotations (T_1) is that of a protonated amino group, the complete energy surface is only 120^o x 360^o. There is no further symmetry. The (R) stereoisomer was employed, and isolated molecule energies and dipole moments were obtained from CNDO/2 calculations (Borthwick & Steward, 1975c).

Three minima were found for the βHG molecule in aqueous solution. The global minimum occurs at 20^o, 300^o, the second at 100^o, 180^o (17 Kcal/mole higher energy) and the third at 100^o, 60^o (28 Kcal/mole above the global minimum). T_2, it may be noted, takes up classical low energy positions. The position of the global minimum would be unaffected if the T_1 rotation were not considered. This may be an indication that the approximation of ignoring amino group rotations in the other compounds should not cause large errors, where close approaches are precluded.

The maximum value of the x_T distribution occurs at 5.1 Å and there are no subsidiary peaks.

c) Discussion of the results for aqueous solution

Overall, the total energy surfaces for water as solvent show a small number of conformations around the global minimum which have energies within 6 Kcal/mole of the minimum, and hence appreciable populations. The global minima are mainly in partially extended conformations. This is in contrast to the isolated molecule results, which generally show very deep sharp global minima in highly folded conformations. The effect of water as solvent is thus to extend the molecules, as would be predicted on grounds of decreased electrostatic attraction between the charged ends of the molecule when a dielectric medium is interposed (Warner & Steward, 1975). Moreover, the low energy region is smoothed out a little, allowing greater flexibility about the minimum energy conformation. Nevertheless, the range of highly populated conformations at room temperature is very restricted, as is illustrated for GABA in Fig. 2.13.

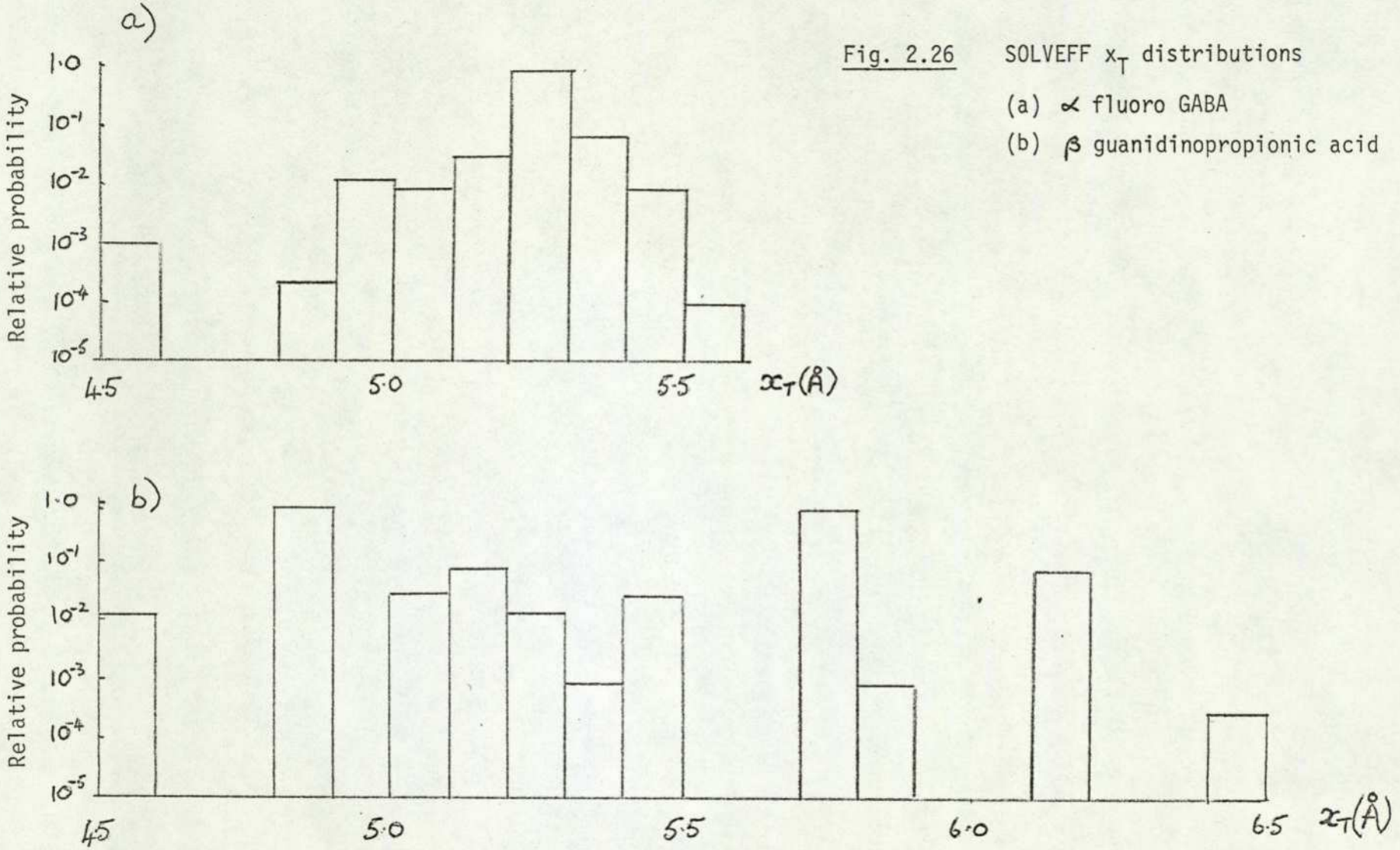

Fig. 2.26 SOLVEFF x_T distributions

(a) ∝ fluoro GABA

(b) β guanidinopropionic acid

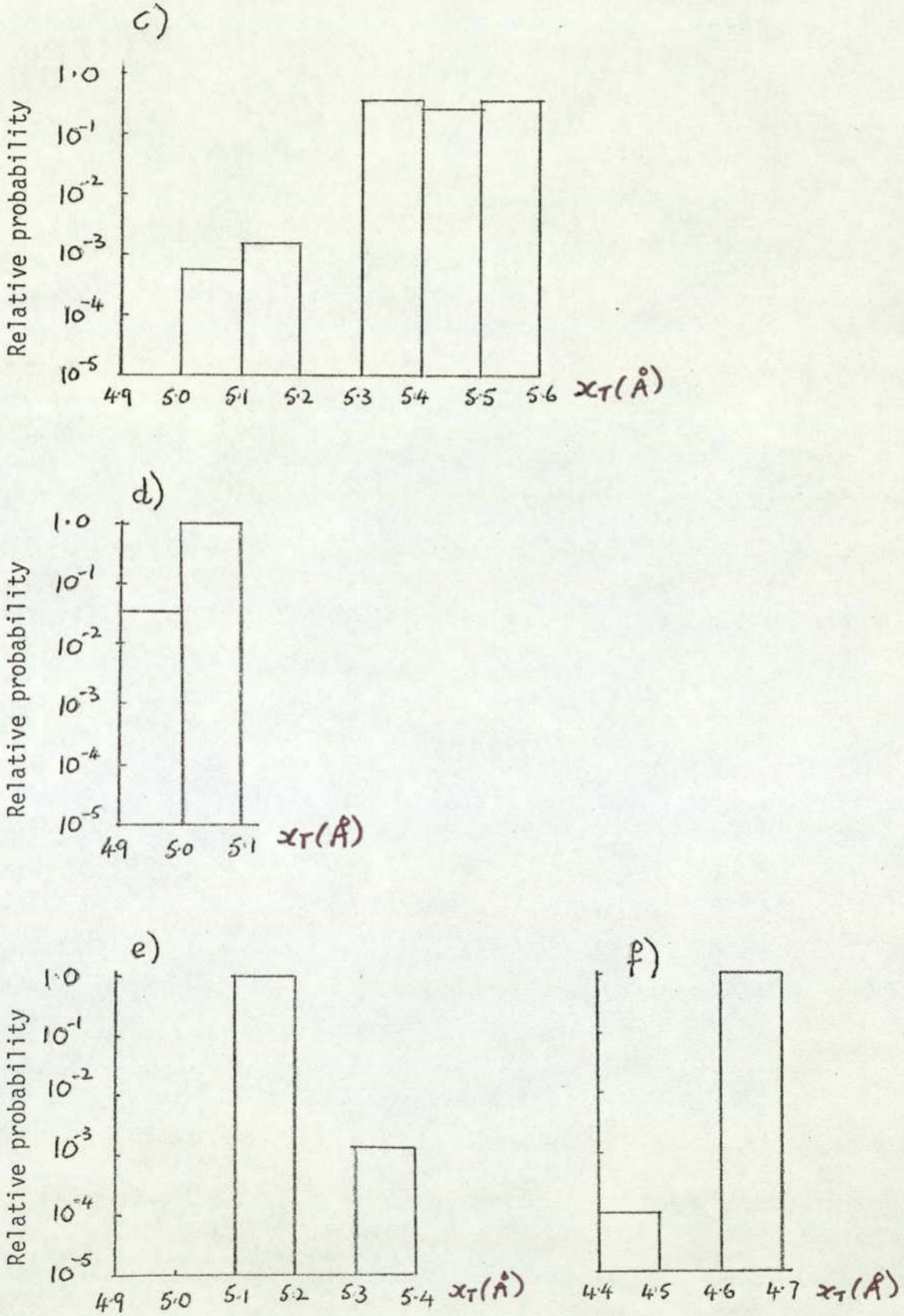

Fig. 2.26 (c) - (f) SOLVEFF x_T distributions

(c) trans 4 aminocrotonic acid

(d) cis 4 aminocrotonic acid

(e) β hydroxy GABA

(f) β alanine

TABLE 2.6

Minima of the SOLVEFF energy surfaces for zwitterions of GABA agonists (Two-dimensional surfaces only)

Substance	Solvent	Figure	SOLVEFF minima Ta	Tb	Energy rel. to global minima kcal/mole
GABA	water	2.10	± (60°	140°)	0
	octanol	~2.10 b	± (60°	140°)	0
	octane	~2.10 a	80°	300°	0
			20°	300°	3.4
			80°	340°	9.5
			20°	40°	9.8
			180°	180°	63.1
αFG	water	2.20	300°	220°	0
			100°	60°	3.2
			40°	160°	5.7
βGP	water	2.21	± (60°	80°)	0
			±(140°	280°)	9.5
trans ACA	water	2.22	100°	120°	0
			260°	60°	0
			160°	100°	0.01
			200°	80°	0.01
cis ACA	water	2.23	180°	0°	0
			20°	80°	29.3
			340°	100°	
β alanine	water	2.24	180°	90°	0
β HG	water	2.25	20°	300°	0
			100°	180°	17
			100°	60°	28

TABLE 2.7 SOLVEFF x_T probabilities for GABA agonists

For each x_T the first number given is the fractional population and the second is its logarithm to base 10, + 5. Any x_T with a population of < .0001 is not included, so that logarithmic values cannot be < 1.0.

SUBSTANCE	x_T values (Å) (The segment e.g. 2.5 contains total probabilities for x_T's from 2.50 to 2.59)																	
	2.5	3.1	4.4	4.5	4.6	4.8	4.9	5.0	5.1	5.2	5.3	5.4	5.5	5.6	5.7	5.8	6.1	6.4
GABA zwitterion																		
5° grid: water							.0020 2.30	.0278 3.44	.1550 4.19	.4999 4.70	.2851 4.45	.0240 3.38	.0002 1.30					
20° grid: water							.0003 1.48	.0243 3.39	.0204 3.31	.7588 4.88	.1619 4.21	.0343 3.54						
20° grid: octanol							.0005 1.70	.0442 3.65	.0431 3.63	.7288 4.86	.1195 4.08	.0638 3.80	.0002 1.30					
20° grid: octane	.0001 1.00	.9999 5.00																
20° grid: isolated mol.	.0001 1.00	.9999 5.00																
20° grid: water																		
∝ fluoro GABA				.0010 2.00		.0002 1.30	.0109 3.04	.0089 2.95	.0298 3.47	.8579 4.94	.0722 3.86	.0090 2.95	.0001 1.00					
β guanidino propionate				.0123 3.09		.8830 4.95		.0258 3.41	.0777 3.89	.0126 3.10	.0008 1.90	.0258 3.41			.8830 4.95	.0008 1.90	.0777 3.89	.0003 1.48
Trans 4 amino crotonic acid									.0006 1.78	.0015 2.18		.3662 4.56	.2639 4.42	.3677 4.57				
Cis 4 amino crotonic acid							.0359 3.56	.9641 4.98										
β alanine			.0001 1.00		.9999 5.0													
β hydroxy GABA (with H-bonded ring)									.9986 5.00		.0014 2.15							

It is noteworthy that fully-extended preferred-conformations are not predicted for any of the compounds except β alanine and cis ACA. It might be expected that a polar solvent would favour the conformation with the highest dipole moment (Bastiansen, Seip & Boggs, 1971) but the effect of molecular volume appears to counter-balance this tendency as described above. Hence, partially folded conformations are preferred. This is evident in the x_T distributions determined here which indicate the predominance of charge separations of $\sim$5 Å in compounds which act as strong GABA agonists. The implications of this for the understanding of the GABA receptor are discussed in 3.3.

More extended conformations are preferred if a spherical cavity approximation is employed in the calculation of electrostatic energy rather than a spheroidal one, but as was discussed in 2.3.1., the spheroidal approximation is theoretically more precise.

A consistent feature of the results is the β-γ torsion angle T_2 in GABA, βGP, αFG and βHG at two-dimensional global minima. In each case $T_2 = -60^o$ (for GABA and βGP, T_2 can also be $+60^o$ at global minima). These are, of course, the classical gauche positions. Moreover, T_2 for the global minimum in trans ACA is $+ 100^o$, and cis ACA exhibits a local minimum with $T_2 = + 20^o$. Local minima for αFG and βHG with $T_2 = +60^o$ also occur. Thus β-γ gauche conformations would appear to be likely modes in solution for zwitterions the size of GABA.

Less consistency is observed for the carboxy rotation: (GABA: 60^o, trans ACA: 60^o, cis ACA: 0^o, βalanine: 90^o at global minima and trans ACA: 80^o, cis ACA: 80^o at local minima) and for the α-β rotation (GABA: $+140^o$, αFG: -140^o, βGP: $+80^o$, βalanine: 180^o at global minima, αFG: 60^o, 160^o at local minima). Overall, it would appear that there is a greater tendency to gauche configurations than trans, in contrast to the trans preferences which appear in crystal structures (2.2.2).

Comparisons of SOLVEFF predicted solution conformations with experimental data have been made with encouraging results.

The method appears to predict sensible conformations. The experimental data, based on NMR and dipole moment measurements, however, are sparse, and dependent on complex interpretation, so it would be unwise to place undue weight upon them. The comparison is discussed in detail in 2.5, where some interesting parallels with crystal structure results are also to be found.

d) Postscript

Although the SOLVEFF method produces worthwhile results, its applicability is limited at present. The computer time necessary for CNDO and SOLVEFF calculations is too great to allow the method to be employed for larger molecules, with a greater number of rotational degrees of freedom. Hence, it is apparent that a technique of wider applicability is required for conformational SAR to be investigated thoroughly. Such a technique is described in the next section (2.4). It is based on the classical PE calculations reported by Gill (1959, 1965), solvent effects being introduced via the bulk dielectric constant of the solvent. The method is computationally far less sophisticated and time consuming than SOLVEFF. It is applicable to larger molecules, but its results are probably less reliable in absolute terms.

Before the pharmacological implications of the conformational results are discussed, then, the application of PE calculations to a wide range of GABA agonists and some glutamate agonists is presented. Hence, a comprehensive set of conformational data for amino-acid transmitters in aqueous solution (both SOLVEFF and PE) will be available for SAR studies in chapter 3.

2.4 GABA AND L-GLUTAMATE AGONISTS: SIMPLE POTENTIAL-ENERGY CALCULATIONS IN AQUEOUS SOLUTION

2.4.1 Introduction

As mentioned above (2.3.3d), the calculation of conformational energy minima in aqueous solution by the methods described in the last section is easily applied to small molecules with one or two significant torsion angles, but molecules with a larger number of degrees of conformational freedom present difficulties. To calculate a precise minimum energy position for a molecule with two torsion angles on a 20^{o} grid requires the investigation of more than three hundred conformations, if the molecule possesses no symmetry. For a four-angle molecule, however, $\sim 300^{2} \doteqdot 10^{5}$ conformations require investigation, and although symmetry and the exclusion of sterically hindered conformations may reduce this total considerably, tens of thousands of calculations would still have to be performed. Even employing the extremely fast CDC 7600 computer, which was used for both the CNDO and the solvent effect calculations in the present work, each conformation of a compound with 20-30 atoms would require up to 10 seconds of computer time. It is clear, then, that exhaustive CNDO investigations of molecules with a greater degree of flexibility than GABA are precluded at present for economic reasons.

Nevertheless, a number of higher homologues of GABA are active as GABA agonists (Table 1.1) as are some α-ω guanidino acids of longer chain length. Thus, if a comprehensive study of conformational SAR was to be made in the present work, a method of conformational analysis for such molecules, even a very approximate one, was necessary. This was considered particularly important in view of the possibility (2.1) that the gross inter-charge distance of a GABA agonists may be the essential feature for recognition by a receptor. For the investigation of this possibility estimates of the inter-charge distance probability distribution for long and short-chain GABA agonists alike would be required. From this could perhaps be found the proportion of molecules of different agonists which are of appropriate size to engage with a receptor which has a limited geometry.

The work of Gill (1959, 1965) offered a possible method, in which polymethylene chains were treated as a series of independent links adopting classical trans and gauche minimum-energy positions. From experimental values of the rotational energy barriers between these positions Gill determined the relative probabilities of the gauche and trans positions for each link, using classical non-bonded potential energy calculations. The probability of any combination of trans and gauche links was then taken to be the product of the individual link probabilities. Electrostatic attraction or repulsion between terminal groups was also taken into account, environmental effects being introduced into this term via the static dielectric constant of the solvent.

Because independent links were assumed, geometry of terminal groups ignored and solvent effects considered very simply, it seems unlikely that the inter-charge distance probability distributions derived would have been quantitatively accurate in absolute terms. Nevertheless, we may expect that relative effects within similar homologous series would be represented in the results.

Hence, Gill's method (described in more detail in 2.4.2) was employed in the present work to investigate conformation in solution for a number of α-ω amino-acids and guanidino-acids of varied chain length (2.4.3). Several other GABA agonists including branched chain compounds and imidazole derivatives were also considered. A smaller number of glutamate agonists, dicarboxylic α amino acids of varied chain length, were investigated in the same way. The pharmacological implications of the results are presented in 3.2.

Gill (1965) gives evidence for the physical reasonableness of the method, while in the case of α-ω amino acids, dipole moment measurements in aqueous solution (Edward, Farrell & Job, 1973) support the general conclusions of a preponderance of fairly extended conformations obtained in the present work (2.4.3). The NMR results of Ham (1974) on βalanine, GABA and glutamic acid (which are interpreted in terms of classical energy minima) also lend some support for the results obtained (2.5.1).

2.4.2 Method

a) Chain conformation

A carbon-carbon bond in a polymethylene chain is considered to possess a rotation barrier (Emax) of 4.1 kcal/mole (Taylor, 1948; Szasz, Sheppard & Rank, 1948). Thus, by the classical energy equation for a four-carbon chain,

$$E_{\phi'} = \tfrac{1}{2}Emax(0.74(1-\cos 3\phi') + 0.26(1-\cos\phi')) \text{ (Gill, 1959)}$$

where $\phi' = 180^{o}-\phi$ and ϕ is the torsion angle of the chain. The minima occur when the bonds are staggered, and their relative probabilities can be calculated by a Boltzmann function

$$P_{\phi'} = P_{o}e^{-\frac{E_{\phi'}}{RT}}$$

This function has three maxima, one at the trans position ($\phi'=0$, $\phi = 180^{o}$) with a relative probability of 1.000 and two in the gauche positions ($\phi=\pm 60^{o}$) with relative probabilities of 0.272. These maxima are considered to be discrete allowed configurations for the rotation.

For a longer carbon chain an approximate probability distribution can be calculated by noting the positions of each link. The total probability of a conformation is then the product of the probabilities of the trans or gauche settings of each link. It is noteworthy that adjacent links with opposite gauche conformations may be discounted due to steric interference between the hydrogen atoms on C_{n} and C_{n+4}. This effect has also been noted by Abe, Jernigan and Flory (1966). Such conformations are assigned a probability of zero except in GABA itself where it is the two terminal groups which are involved and intramolecular hydrogen bonding may take place.

Branched chains can be treated in a similar way. In this case the trans and one gauche conformation have probabilities of 1.000 and the gauche conformation which brings the hydrogens on the two central carbons into closer proximity has a probability of 0.272.

In the present work inter-charge distance(s) for each conformation were measured from molecular models constructed with standard bond lengths and angles (Pople & Beveridge, 1970) for the carbon chain and functional groups. Some of the standard measurements have recently been criticised (Wertz & Allinger, 1974) but for comparison purposes they should be adequate. The charge centres were defined as described below.

b) Treatment of functional groups

1) The carboxyl group:

The charge centre is taken as the mid-point of the two oxygens as before. The orientation of the carboxyl group does not affect the position of the charge centre, so the physical disposition of the group is not considered except under circumstances where it may preclude conformations by steric hindrance. MO calculations on isolated molecules indicate that the carboxyl rotation is fairly free, the barrier to rotation being 1-2 kcal/mole.

2) The protonated amino group:

The charge centre is taken to be the centroid of the three hydrogen atoms as before. As for the carboxyl group, the rotation of the NH_3 group does not affect the position of the charge centre. MO calculations indicate a low barrier to rotation.

3) The guanidino group:

In contrast, MO calculations indicate that the guanidino group has, in general, a strong preference for a trans setting with respect to a carbon chain (Warner, 1975). The rotational energy barrier is about 12 kcal/mole (Fig. 2.27).

Hence, in the present work, the torsion angle $C_{n+1}N_1C_{n+2}N_3$ is fixed at 180^o. Two charge centres are considered as before, lying at the midpoints of the hydrogen atoms of each terminal nitrogen. Thus two inter-charge distances occur for each conformation. The hydrogen on N_1 is not considered as a charge centre, although it has the same charge as the other individual hydrogens of the group (-0.2e), because nitrogens substituted with bulky groups tend not to take part in interactions with GABA receptors (Curtis & Johnston, 1960).

4) The imidazole group:

A number of complications are involved here. Firstly, the pk of the imidazole group in imidazole acetic acid is $\sim$6.8 (Kier et al, 1974) and is lower ($\sim$ 6.0) in histamine, histidine and some histidine derivatives. Hence at physiological pH, only a proportion of molecules will be in the zwitterionic form (Fig. 2.28)

The significance of this is related to the operation of the zwitterion $\rightleftharpoons$ anion equilibrium. If this is faster than the association and dissociation rates of the transmitter-receptor complex, it would be possible for all the molecules which act at receptors to act as zwitterions. Since ionisation rates are normally fast, it may be reasonable to regard the total concentration of imidazole derivatives to be available for interaction. Since all other GABA agonists are zwitterions, it is to be expected that the zwitterionic form is involved in the interaction with GABA receptors.

Secondly, in contrast to N_1 which is effectively a terminal nitrogen, N_3 may be shielded to some extent by the

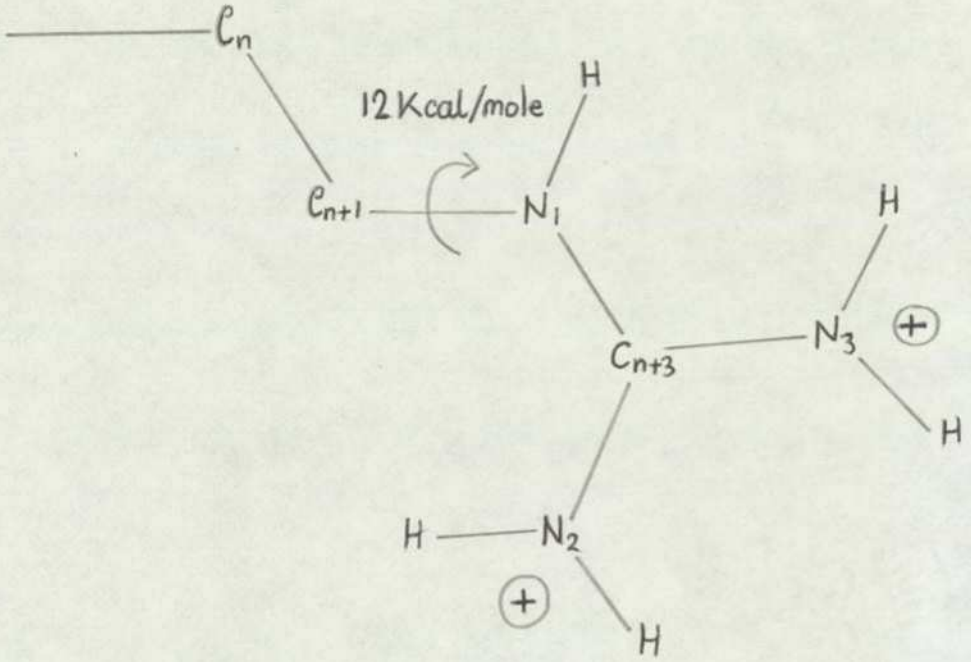

Fig. 2.27 The guanidino group in PE calculations

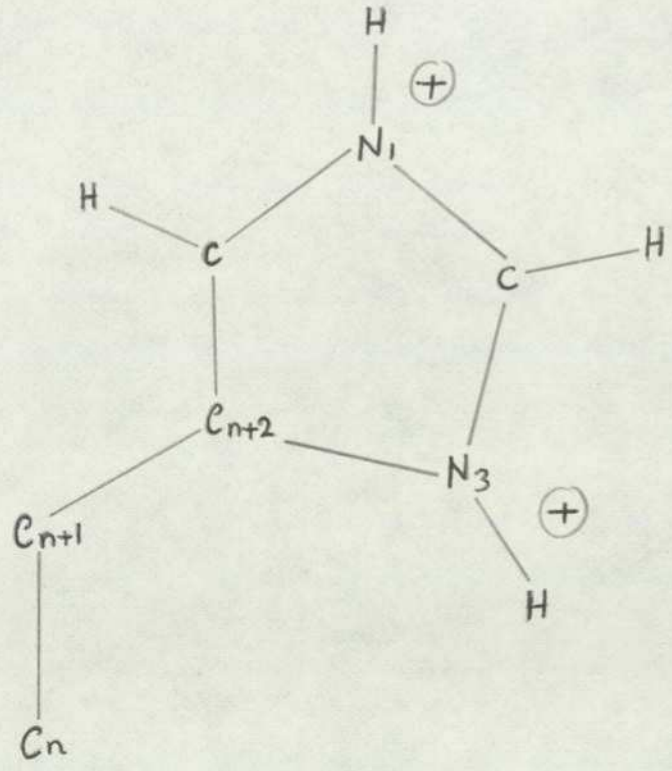

Fig. 2.28 The imidazole group in PE calculations

carbon chain and may not take part readily in interactions with the receptor. It may thus be necessary to down-weight its effect when considering structure-activity relationships of imidazole derivatives. Charge centres are taken to be the hydrogens on N_1 and N_3 as shown by CNDO calculations. Thus, again, two inter-charge distances occur for each conformation.

MO calculations (Kier et al, 1974) suggest a low rotation barrier for the bond C_{n+1}-C_{n+2}. Several crystal structures indicate favoured configurations about this bond when the torsion angle $C_nC_{n+1}C_{n+2}N_3$ is $\pm 60^o$ or $\pm 120^o$.

c) Electrostatic correction

The effect of the electrostatic attraction between terminal groups depends upon the dielectric constant of the medium separating them according to the equation:

$$E = \frac{-N_o q^2}{4\pi\varepsilon\varepsilon_o \ell}$$

where E is the electrostatic energy, N_o is Avagadros number, q is the total effective charge of the terminal group (taken to be e) ε is the dielectric constant of the medium and ℓ is the intercharge distance in metres (i.e. $\ell = x_T \times 10^{-10}$)

Gill (1965) suggests that it should be valid to use the bulk phase dielectric constant ($\simeq$ 80 for water) down to inter-charge distances of $\sim$4 Å, since the bulk phase value is maintained to within 4 Å of a univalent ion in dilute solution. Below 4 Å the dielectric constant will decrease, making electrostatic interactions increase considerably, but few conformations with inter-charge distances of less than 4 Å are sterically possible. Hence the bulk phase dielectric constant has been employed thoughout. The effect of this is to down-weight highly folded conformations, which in a more rigorous treatment, such as that of section 2.3, would be down-weighted by the greater electrostatic stabilisation of extended

conformations. This stabilisation is also neglected here, so the opposing errors reduce each other's effect, perhaps explaining the general agreement with NMR and dipole moment measurements which this simple treatment achieves.

The relative probability associated with the terminal group interaction is:

$$P_e = \exp\left(\frac{-E}{RT}\right) = \exp\left(\frac{6.70}{x_T}\right) \quad (x_T \text{ in } \text{Å})$$

Total probability for a conformation is then the product of the chain conformation probability and P_e. the value of P_e does not vary greatly for x_T's above 4 Å, so the electrostatic effect on conformation in this method is far less important than the effect of the rotational energy barriers.

d) The effect of hydrogen bonding

The heat of formation of N-H---O hydrogen bonds is $\sim$ 5 kcal/mole (Gill, 1965), so a considerable degree of stabilisation of conformations with possibilities of intramolecular hydrogen bonding might be expected. However, any group which will form hydrogen bonds will form hydrogen bonds with water in aqueous solution, so any stabilisation will be due to a difference in hydrogen bonding energy between intramolecular and intermolecular hydrogen bonds. This difference, particularly when entropy is taken into account, is likely to be small (Gill, 1965) so that intramolecular hydrogen bonding will not in general produce a stabilising effect. It is possible, however, that stabilisation occurs in β hydroxy GABA (βHG) where an O-H---O is involved (2.3.3).

e) Inter-charge distance probability distributions

For each compound the total probability of each conformation together with the measured inter-charge distance (x_T) was used to generate an inter-charge distance probability distribution. The conformations were divided into groups which span 0.1 Å in x_T and

the distributions are, accordingly, presented as histograms. Physically, factors such as thermal vibrations would easily encompass this order of uncertainty, and indeed a block diagram with larger units may well be more realistic than so sharp a distribution. However, 0.1 Å units are maintained here for ease of comparison with the results of 2.3 and others (see 2.5).

2.4.3 Results for GABA agonists

Conformational analyses were carried out for α-ω amino acids up to 7 aminocaprylic acid (7ACA), α-ω guanidino acids up to δ guanidinopentanoic acid (δGP), βhydroxy GABA (βHG), α-fluoro GABA (αFG), βaminobutyric acid (βABA), imidazoleacetic acid (ImAc), 1-methyl imidazoleacetic acid (MeImAc), imidazole-propionic acid (ImPr) and imidazolelactic acid (ImLa).

The results are presented in Table 2.8 and as inter-charge distance probability distributions in Figs. 2.29 a-p. Two sets of data are presented for βHG, one treating the molecule as a β branched chain, and one considering it to possess a hydrogen bonded pseudo ring in solution; for which there is some evidence (2.3.3): the hydrogen bond involved is between the hydroxyl oxygen and one of the carboxyl oxygens. O-O hydrogen bonds tend to have greater heats of formation and hence greater stabilising power than those involving nitrogen atoms, (Gill, 1965).

The most notable feature of the results is the fact that in most cases the fully extended conformation is not the most populated. Although for some molecules the fully extended conformer has the highest individual probability, there is nearly always a region of x_T (within say $\frac{1}{4}$ Å) which possesses a higher overall population. This is a consequence of the occurrence of different conformations with the same x_T, lower than the maximum. This effect illustrates the importance of considering all conformations, not just the fully extended ones, in the study of biologically active molecules (Schueler, 1953; Gill, 1959).

TABLE 2.8

CLASSICAL MINIMUM ENERGY CONFORMATIONS FOR GABA AGONISTS

SUBSTANCE	x_T(Å)	PROBABILITY
Glycine	3.3	1.0
β alanine	3.4	.493
	4.65	.507
GABA	2.75	.177
	4.1	.078
	5.0	.420
	5.7	.325
δ AVA	4.75	.061
	4.9	.058
	5.15	.068
	5.5	.180
	5.6	.174
	5.7	.047
	6.7	.152
	7.05	.260
ε ACA	4.2	.016
	4.3	.015
	4.8	.046
	5.9	.036
	6.0	.079
	6.1	.010
	6.2	.010
	6.3	.045
	6.6	.032
	6.7	.032
	7.0	.115
	7.1	.171
	7.2	.213
	8.1	.180
7 ACA	3.2	.005
	4.0	.012
	5.0	.016
	5.3	.009
	5.5	.009
	5.8	.007
	5.9	.007
	6.2	.023
	6.3	.023
	6.4	.046
	6.5	.023
	6.6	.029
	6.7	.018
	6.8	.052
	6.9	.021
7 ACA (cont.)	7.0	.027
	7.1	.050
	7.2	.072
	7.3	.025
	7.4	.011
	7.5	.007
	7.6	.001
	7.7	.097
	7.9	.092
	8.6	.020
	8.7	.020
	8.9	.145
	9.4	.133
α GA	3.2	.418
	4.8	.418
	5.3	.582
	5.7	.582
β GP	4.4	.078
	4.6	.223
	5.1	.078
	5.7	.698
	5.8	.288
	6.9	.223
	7.2	.410
γ GB	4.1	.051
	4.8	.170
	5.0	.049
	5.2	.176
	5.4	.054
	5.8	.067
	6.3	.014
	6.4	.104
	6.7	.051
	7.2	.176
	7.3	.492
	7.4	.343
	8.2	.282
δ GP	2.6	.015
	3.4	.015
	3.5	.052
	5.2	.033
	5.3	.018
	5.4	.113
	5.8	.075
δ GP (cont.)	5.9	.002
	6.1	.018
	6.2	.008
	6.3	.030
	6.5	.070
	6.6	.046
	6.8	.034
	6.9	.092
	7.0	.029
	7.2	.100
	7.3	.129
	7.4	.207
	7.5	.007
	7.7	.027
	8.0	.027
	8.1	.100
	8.3	.183
	8.6	.127
	8.7	.027
	8.9	.100
	9.3	.183
βABA	3.4	.705
	4.65	.295
β HG chain structure	2.75	.461
	4.1	.103
	5.0	.297
	5.7	.139
β HG with H-bonded ring structure	3.8	.189
	5.1	.394
	5.3	.417
α FG	2.75	.135
	4.1	.136
	5.0	.440
	5.7	.288
ImAc (N_3)	3.1	.541
	4.3	.459
(see fig. 2.28) (N_1)	5.4	.459
	5.8	.541
MeImAc (N_3)	3.1	.541
	4.3	.459
ImPr (2 + sites)	3.8	.124
	4.1	.113
	4.8	.311
	5.4	.413
	5.5	.124
	5.9	.152
	7.2	.300
	7.5	.311
ImPr (1 + site, N1)	5.4	.113
	5.5	.124
	5.9	.152
	7.2	.300
	7.5	.311
ImLa (2 + sites)	3.8	.191
	4.1	.173
	4.8	.204
	5.4	.371
	5.5	.191
	5.9	.234
	7.2	.198
	7.5	.204
ImLa (1 + site, N1)	5.4	.173
	5.5	.191
	5.9	.234
	7.2	.198
	7.5	.204

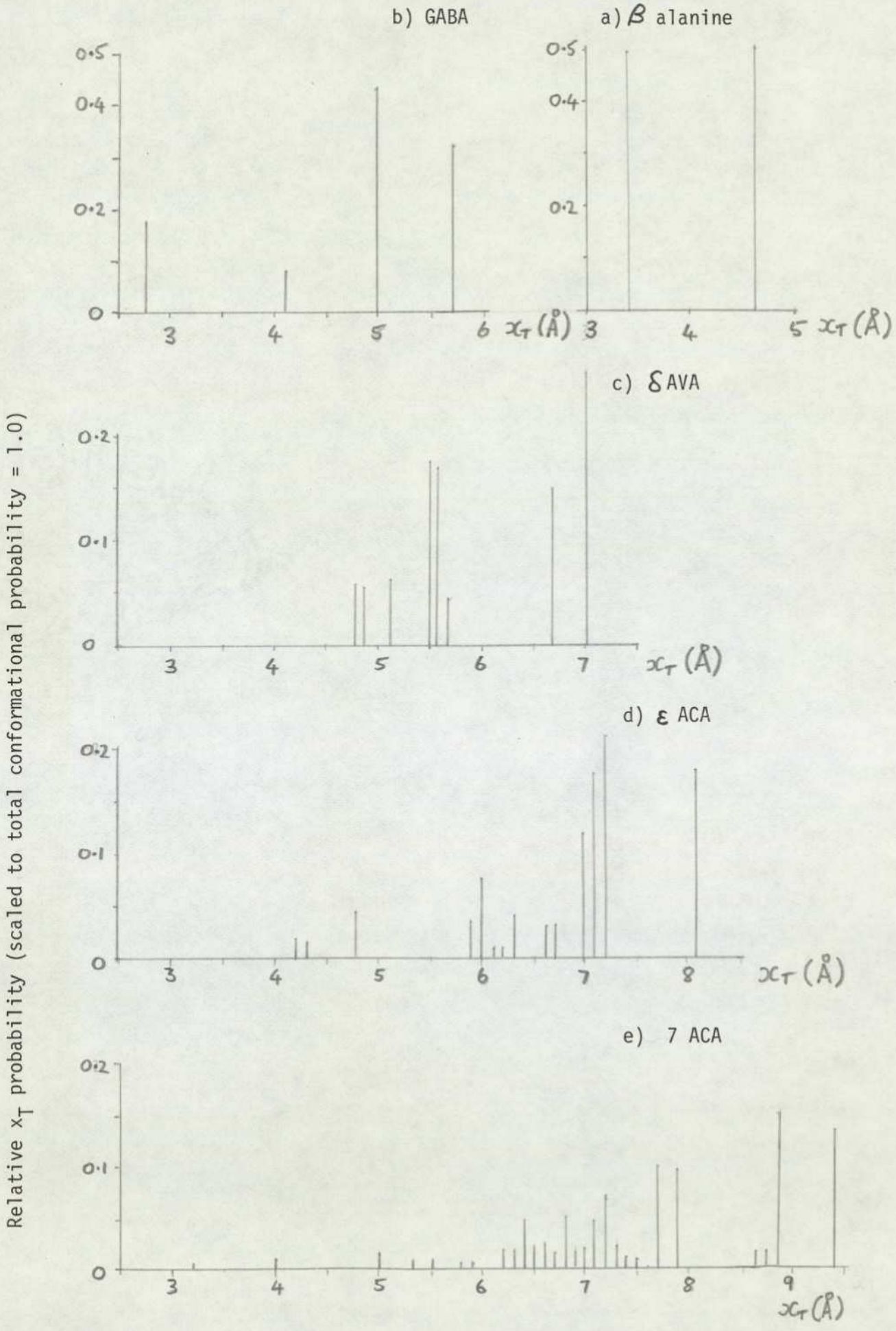

Fig. 2.29 (a-e) Classical PE results: α-ω amino acids

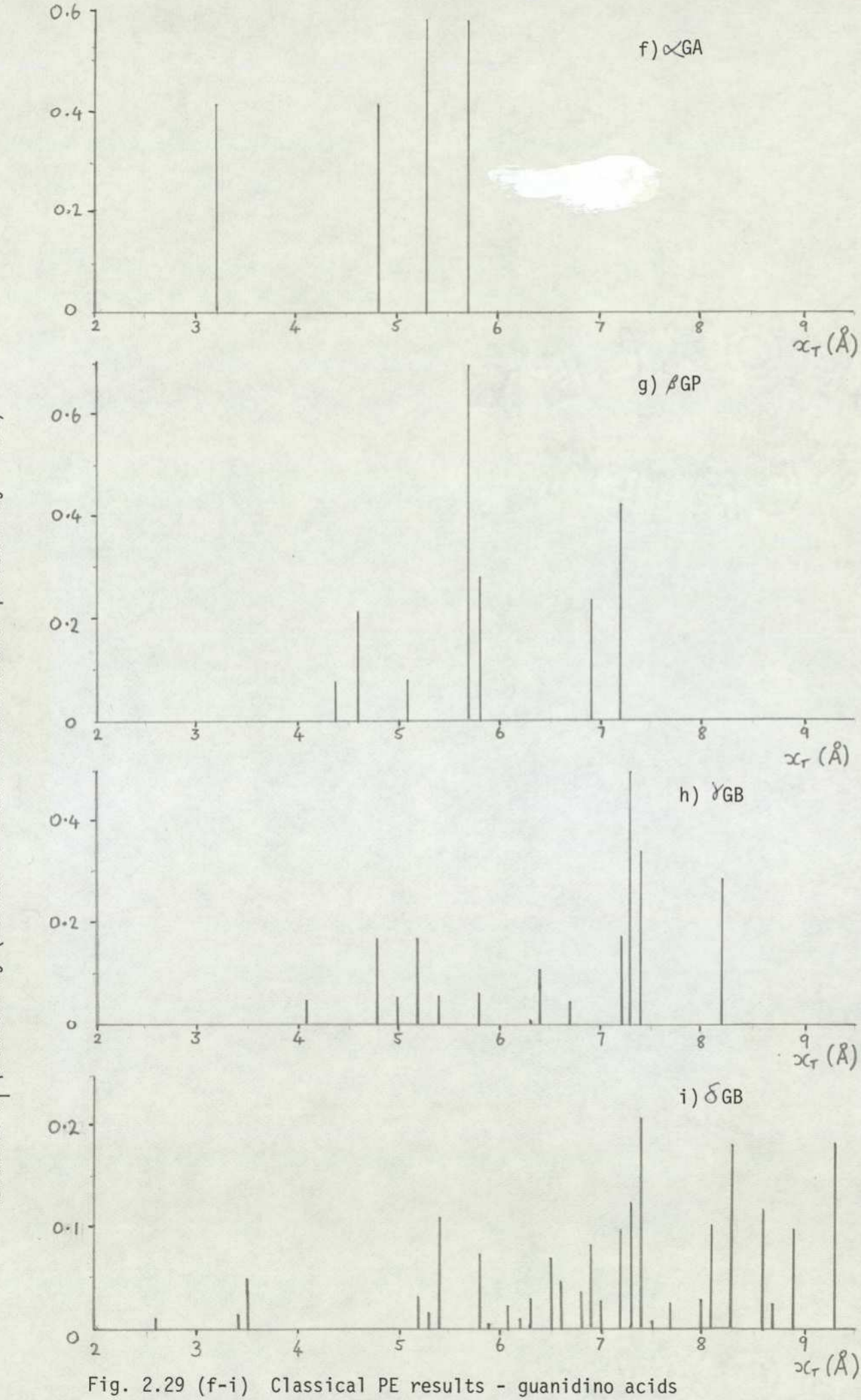

Fig. 2.29 (f-i) Classical PE results - guanidino acids

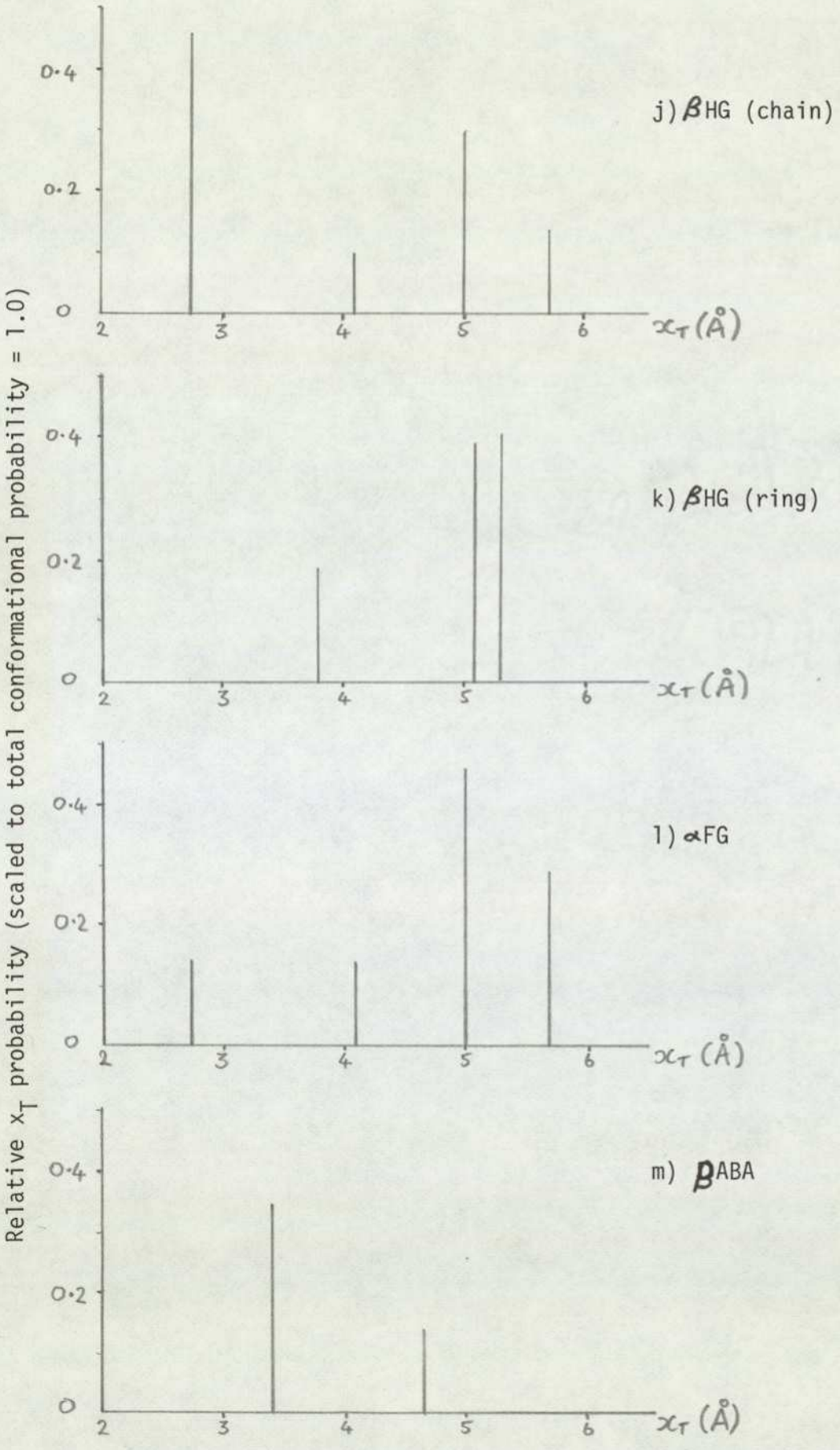

Fig. 2.29 (j-m) Classical PE results - branched chains

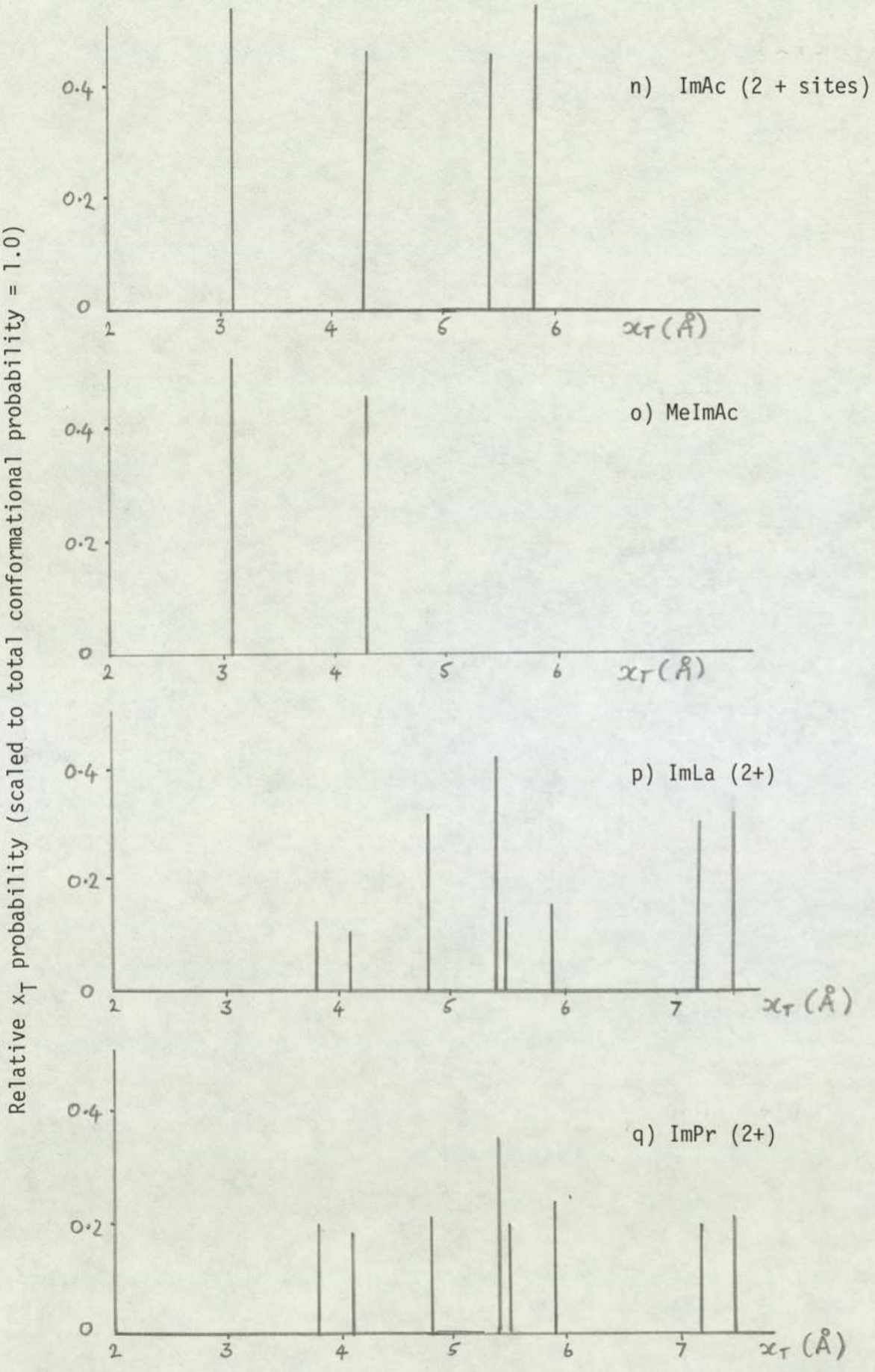

Fig. 2.29 (n-q) Classical PE results - imidazole derivatives

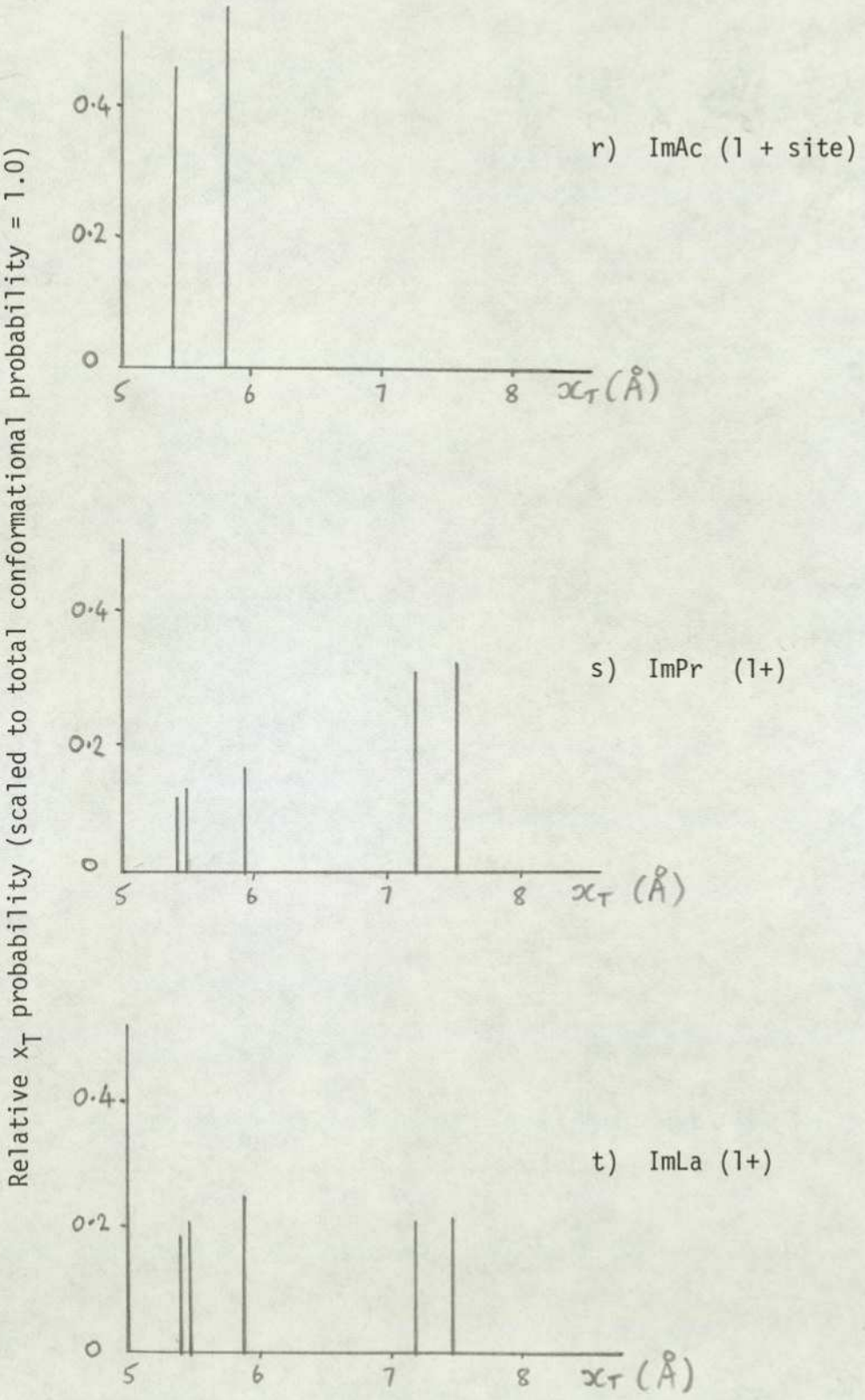

Fig 2.29 (r-t) Classical PE results - imidazole derivatives

2.4.4 Results for glutamate agonists

Glutamate homologues studied by the PE method were treated as branched chains in the manner described above (2.4.2). The molecules considered were the L forms of the first five homologues of the glutamate series: the semi-rigid aminomalonic acid (all x_T's fixed), aspartic acid, glutamic acid, aminoadipic acid and aminopimelic acid. The values of x_{T2} and x_{T3} (Fig. 2.2) were measured from models for each sterically permitted conformation (x_{T1} remains constant, see 3.2.4). The probabilities for each possible combination of x_{T2} and x_{T3} are indicated in Table 2.9 and illustrated in Figs. 2.30 a-f. The values for ibotenic acid, whose x_T's are all conformationally invariant, are included for comparison.

As a result of this study, a comprehensive set of consistent PE conformational data for amino acid transmitters is now available. In subsequent sections comparison with the results of other methods of conformational analysis are made (2.5), and structure-activity schemes are described (3.2) based on the PE data.

TABLE 2.9

x_T PROBABILITIES FOR GLUTAMATE AGONISTS

SUBSTANCE	x_{T2} (Å)	x_{T3} (Å)	PROBABILITY (scaled to 1.0)
Amino malonate	3.3	3.2	1.000
Aspartate	4.8	3.4	0.236
	3.5	3.5	0.114
	3.6	4.7	0.649
Glutamate	5.1	4.1	0.047
	2.7	4.2	0.043
	2.4	5.0	0.277
	5.1	5.0	0.063
	5.8	5.0	0.198
	4.1	5.1	0.090
	5.0	5.7	0.281
Amino Adipate	4.6	3.2	0.009
	5.2	4.9	0.016
	5.7	4.9	0.052
	6.0	4.9	0.014
	6.6	4.9	0.044
	5.4	5.4	0.074
	4.9	5.5	0.074
	5.8	5.5	0.059
	5.8	5.7	0.062
	7.1	5.7	0.185
	4.9	5.8	0.021
	5.6	5.8	0.066
	5.1	6.5	0.084
	5.6	7.0	0.296
Amino pimelate	6.9	4.5	0.007
	6.3	4.6	0.008
	6.4	4.7	0.002
	7.3	5.1	0.029
	6.2	5.2	0.009
	5.9	5.8	0.011
	7.2	5.8	0.034
	7.3	6.0	0.045
	6.0	6.1	0.012
	6.2	6.1	0.011
	4.5	6.2	0.022
	5.3	6.2	0.014
	6.3	6.2	0.011
	6.4	6.2	0.003
	6.3	6.3	0.003
	4.3	6.7	0.020
	7.1	6.7	0.040
	7.3	6.8	0.011
	5.7	7.0	0.053
	6.8	7.1	0.045
	5.2	7.2	0.061
	7.2	7.2	0.043
	7.3	7.2	0.084
	8.2	7.2	0.141
	6.2	7.3	0.064
	6.8	7.3	0.012
	7.2	8.1	0.175

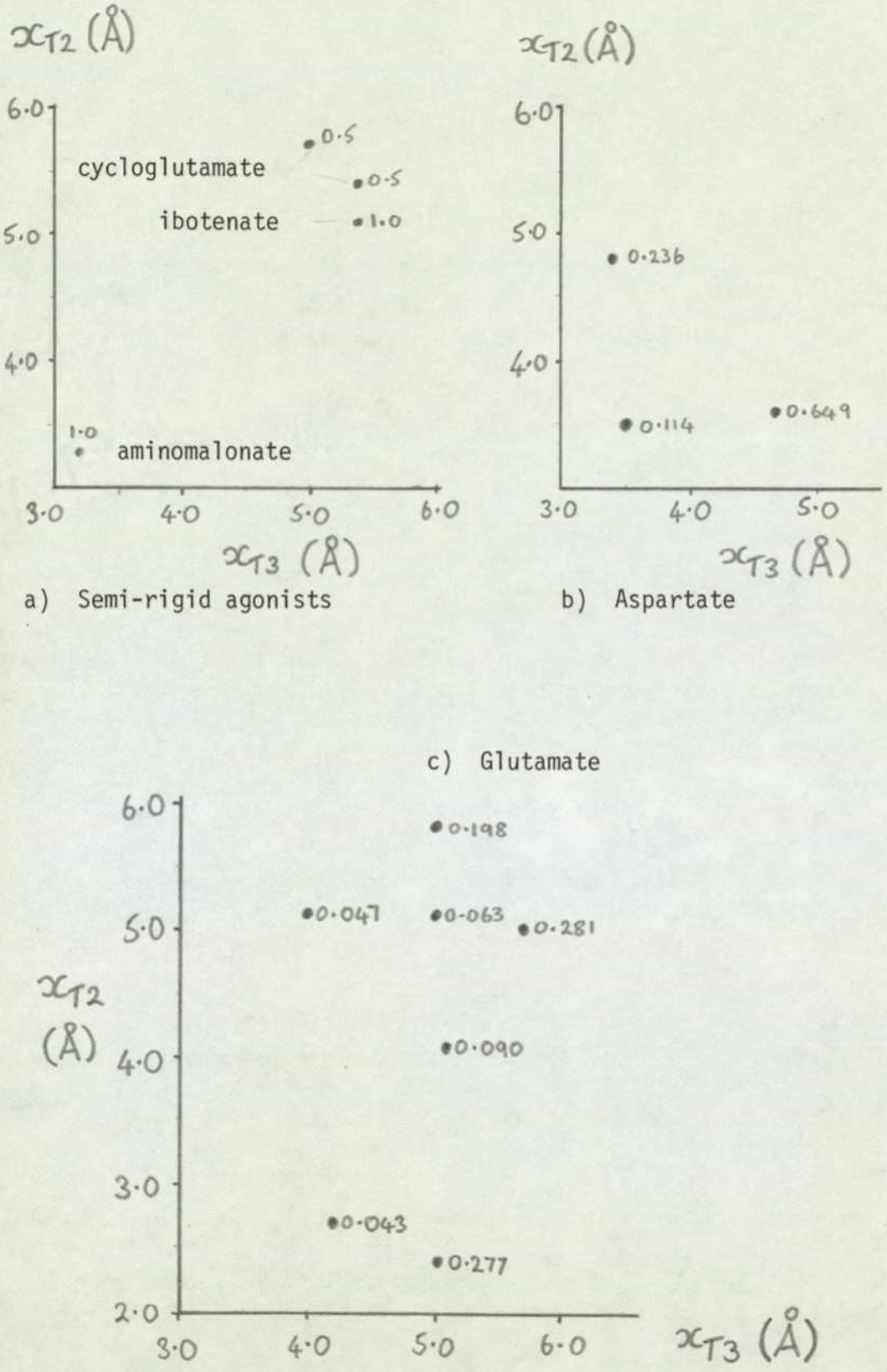

Fig. 2.30 a-c Classical PE results:

glutamate agonists

PE calculated conformational probabilities (scaled to total = 1.0) are indicated by each preferred conformation

d) Aminoadipate

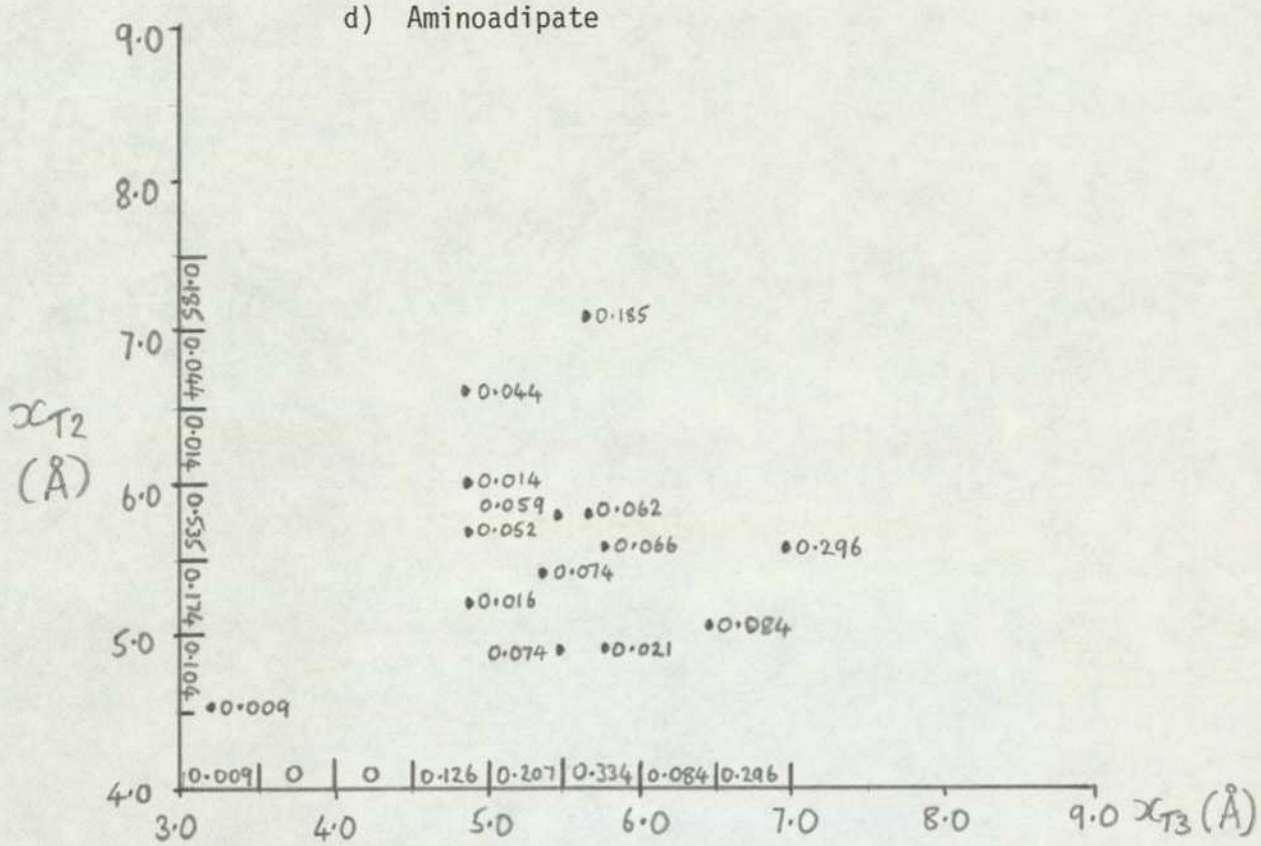

e) Aminopimelate

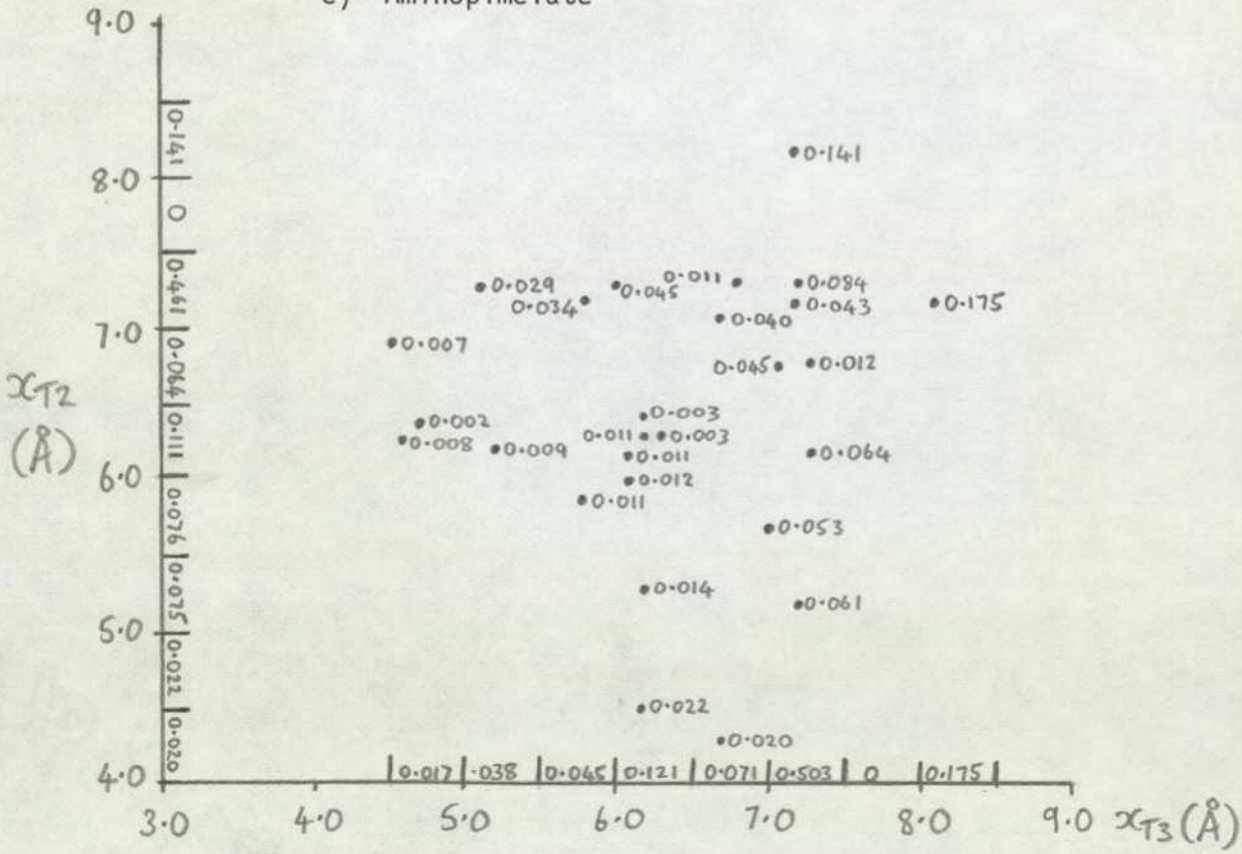

Fig. 2.30 d-e Classical PE results: glutamate agonists conformational probability shown by each conformation and aggregate probabilities over 0.5 Å intervals indicated along axes.

2.5 COMPARISONS BETWEEN PRESENT AND PREVIOUSLY REPORTED CONFORMATIONAL RESULTS FOR AMINO-ACID TRANSMITTERS

2.5.1 Experimental and theoretical conformations in aqueous solution

a) Introduction

In the present work, conformational preferences of a number of GABA agonists in aqueous solution have been calculated. Two methods have been employed: the simple PE method (2.4) allowing for solvent effects via the dielectric constant of the solvent; and the far more sophisticated, but computationally more involved SOLVEFF method (2.3) - a development of MO/continuum model solvent effect treatments. The former technique has also been applied here to glutamate and some of its agonists.

In the literature, the only other theoretical examination of conformation in solution for inhibitory amino-acid transmitters is that of Pullman and Berthod (1975) for GABA itself. These workers have employed the supermolecule method, briefly described in 2.3.1, and the PCILO MO formalism (see Warner, 1975). (The results of CNDO/2 and PCILO calculations on the isolated GABA zwitterion are substantially the same (Warner, 1975)). The only theoretical calculations on glutamate agonists yet published are those on the isolated ibotenic acid molecule by Borthwick and Steward (1975).

Two types of experimental study on the aqueous solution conformation of GABA agonists have been reported in the literature; viz NMR and dipole moment measurements. Some NMR results for glutamate are also available.

In view of the likely significance of conformational preference in solution for the pharmacological action of neuro-transmitters (2.1), a comparison of the conformational results obtained by these different methods would be useful. Compatible results, obtained by differing techniques employing different assumptions, may indicate a degree of validity over and above the

internal self-consistency of a single method for a number of substances. The application of conformational results to SAR studies is unlikely to prove fruitful if the methods used are failing to predict sensible conformations. Accordingly, in this section, the results obtained by experimental and theoretical investigations of the solution conformation of amino-acid transmitters are assembled and compared. Agreements and disagreements between the methods are noted and the validity of the preferred conformations predicted is discussed.

b) Experimental results: NMR and dipole moment studies

Two sets of NMR results are available. The first (Parry-Jones, Roberts & Ahmed, 1971) suggests, on the basis of the effect of temperature on the NMR spectrum, that GABA adopts a fully extended conformation in aqueous solution taking part in 'head to tail' interactions with other GABA molecules. These results rule out the possibility of a hydrogen-bonded ring structure for GABA in solution. Ham (1974), on the other hand, interpreting his NMR data in terms of classical gauche and trans minimum-energy conformations, suggests a spectrum of modes for GABA in solution. The most highly-populated mode is partially folded. β alanine, β hydroxy GABA, taurine and glutamate were also examined in the work by Ham. The interpretation of NMR data for a molecule as flexible as GABA is fraught with difficulty, and simplifying assumptions (such as Ham's classical minima) have to be introduced. Thus it would be unwise, at present, to believe that NMR results are unequivocal on this subject.

The dipole moment values determined by Edward, Farrell and Job (1973, 1974) for a series of α-ω amino acids are based on dielectric constant measurements interpreted via Buckingham's theory. An empirical correction factor was employed, calculated from results for the rigid molecule 4-amino bicyclo(2.2.2) octane carboxylic acid. The internal field factors used in the study were calculated by a different method from those in the present work (2.3.2) and did not consider the Van der Waal's radius of the extreme atoms. Using

a self-consistency argument, the authors conclude that fully extended α-ω amino acid molecules fit the data better than do molecules with freely rotating bonds. It should be stressed that this method is not very sensitive to conformational preference unless large differences in dipole moment and internal field factors exist between alternative conformations. Calculations using the T_4 = 0 minimum-energy conformation for GABA from SOLVEFF (section 2.3) and the algorithms of section 2.3.2 for the calculation of internal field factors show that this conformation fits the data marginally better than fully extended GABA, but the difference is very slight.

c) Theoretical results from the literature

Pullman and Berthod (1975), using the supermolecule method for treatment of solvent effects and the PCILO approximation for their MO calculations, suggest that the GABA molecule exhibits a spectrum of modes in solution not unlike the NMR results of Ham (1974). However, although such a superficial resemblance does exist in terms of torsion angles, the intercharge distance probability distributions (Fig. 2.32) do not corroborate the agreement (see below). The supermolecule results tend to weight folded-conformations much more highly than do the NMR results.

The supermolecule results are discussed below in comparison with (1) the continuum approximation calculations using the SOLVEFF program (2.3) and (2) the simple potential-energy calculations of section 2.4

d) Comparison between experimental and theoretical results

To permit comparison, calculations of a number of different substances have been made by two or more methods. Preferred x_T results are compared diagramatically in Figs. 2.31-2.34. (Corresponding tabulated results may be found in Table 2.3 (for SOLVEFF) and Tables 2.8-9 (for PE results).

a) SOLVEFF result

(in agreement with dipole moment measurements [Edward, Farrell & Job, 1973])

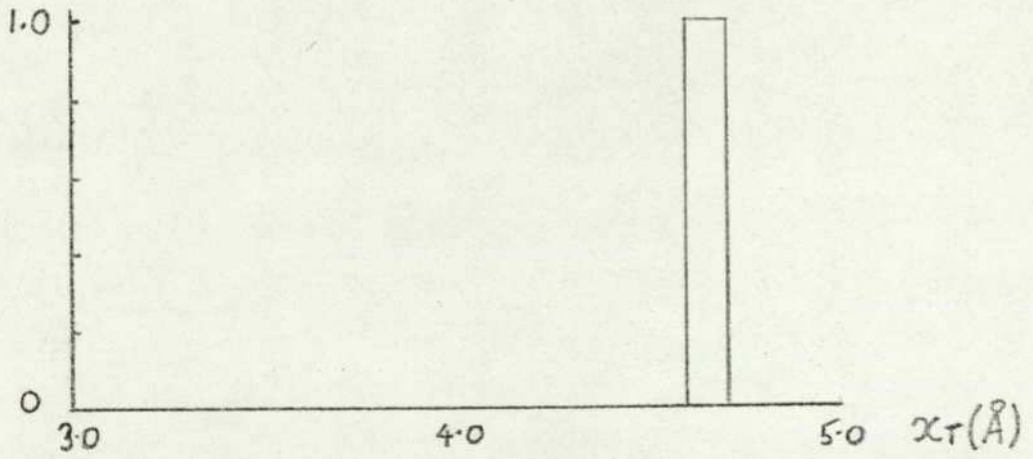

b) PE calculations

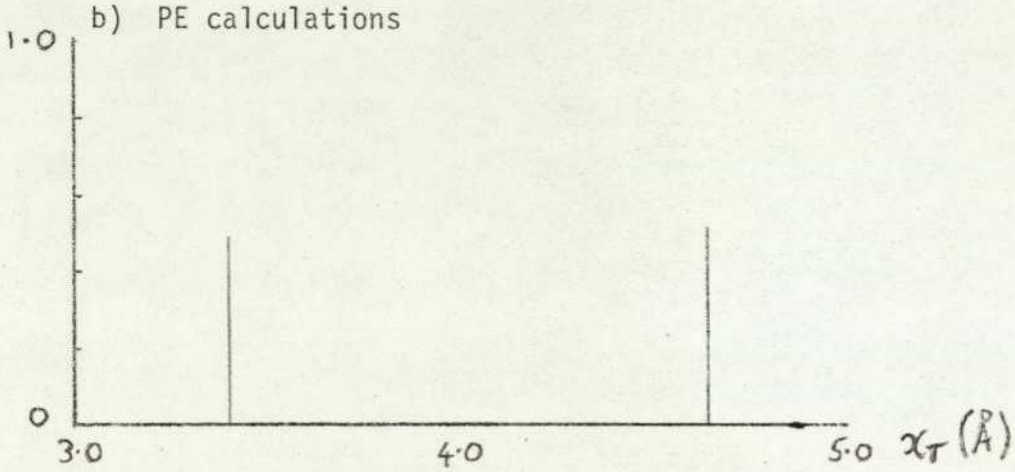

Relative x_T probability

c) NMR result (Ham, 1974)

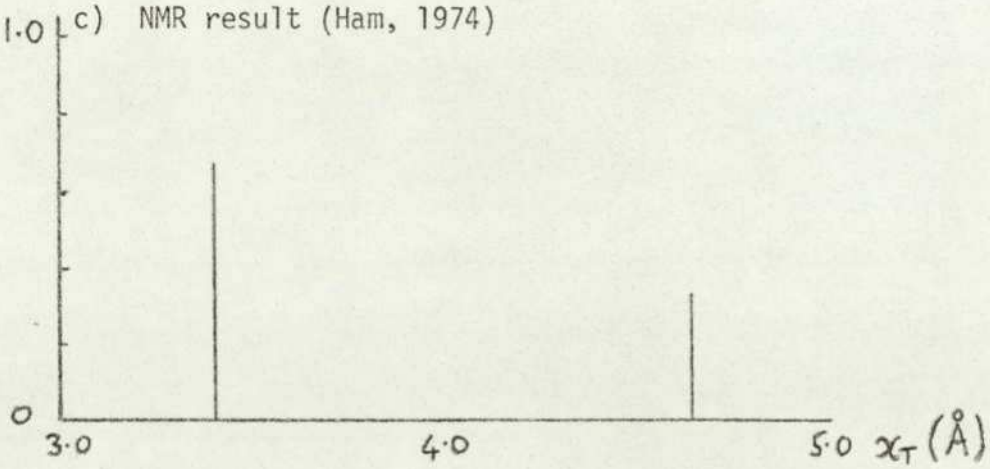

Fig. 2.31 Comparison of x_T distributions for β alanine zwitterion in water

1) β alanine

The conformation of β alanine in aqueous solution is predicted by SOLVEFF to be fully extended, with the carboxyl group at 90^{o} to the backbone of the molecule (2.3.3). Dipole-moment measurements (Edward et al, 1973) support a fully extended molecule, but do not examine the effect of carboxyl group rotation. The NMR results of Ham (1974), however, suggest no conformational preference about the central C-C bond, so that 1/3 of the molecules are in the trans conformation and 1/3 in each of the gauche conformations. The simple classical potential energy calculations of section 2.4.3 suggest 2/3 preference for the trans conformation over the gauche ones. The comparison of results is illustrated in terms of x_T distributions in Fig 2.31.

2) GABA

The SOLVEFF minimum-energy conformation (2.3.3) is not a classical rotamer, so that torsion angle comparison with the NMR results of Ham (1974) is not realistic. The peaks of the x_T distributions are, however, very close, NMR predicting $\sim$5.1 Å and SOLVEFF $\sim$5.2 Å (Fig. 2.32). As described above, the SOLVEFF results are consistent with the dielectric constant data obtained by Edward et al (1973). The fully extended GABA molecule predicted by the NMR studies of Parry-Jones, Roberts & Ahmed (1974) is not compatible with the results of Ham (1974) in which the fully extended rotamer has a 20% population only.

The classical calculations of 2.4.3 show qualitative agreement with the results of Ham, the population of the classical minima appearing in the same order. The NMR results give higher weight to the fully extended rotamer however and less to the fully folded rotamer.

The supermolecule theoretical results of Pullman and Berthod (1975) predict a more folded form for the GABA molecule than experimental results. The peak of x_T distribution for the supermolecule fall at 4.0 and 4.3 Å, while the other results all show preferred x_T values in the 5.1 - 5.7 Å region (Fig. 2.32).

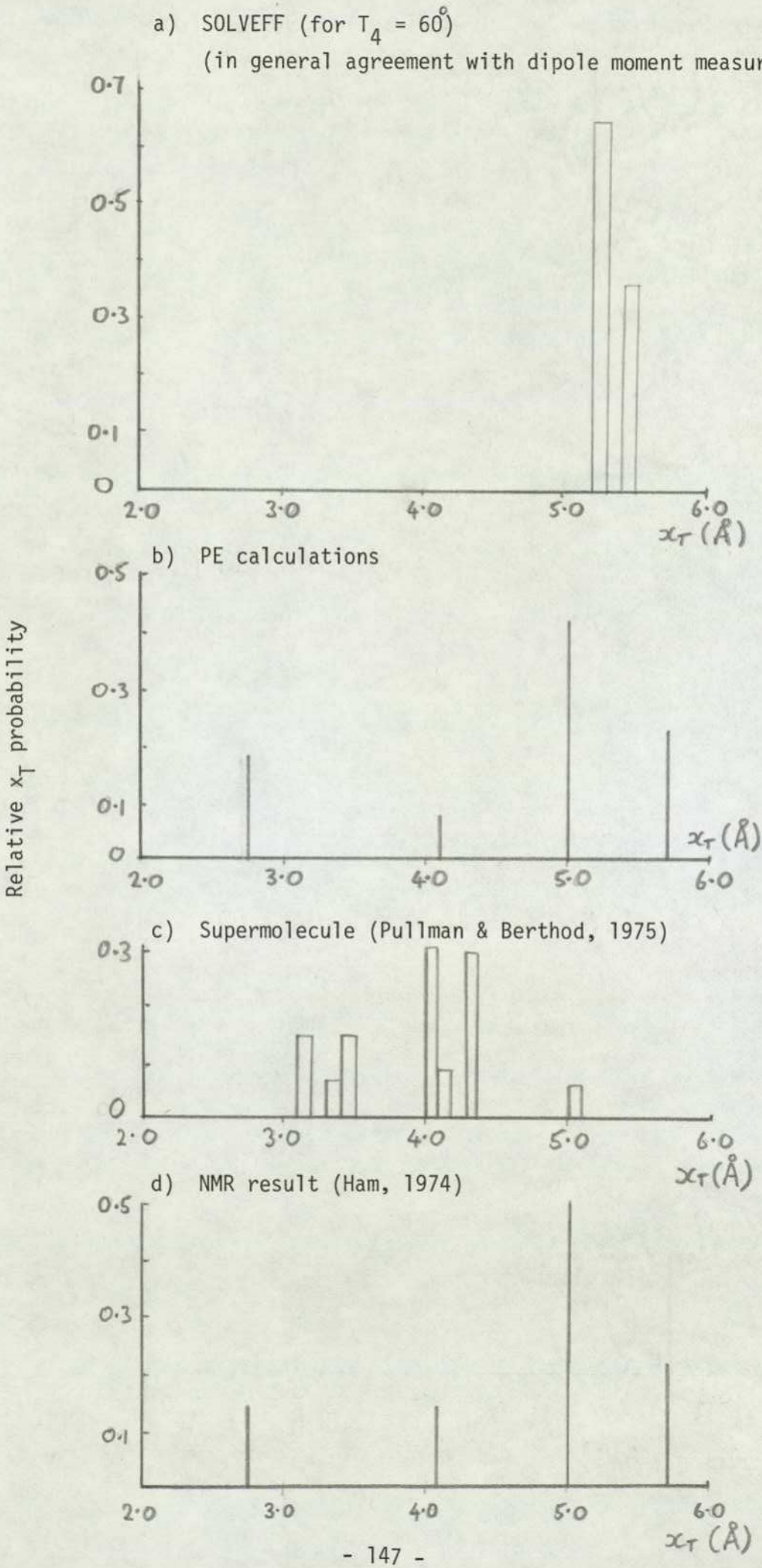

Fig. 2.32 Comparison of x_T distributions for GABA zwitterion in water

Thus agreement between results is somewhat incomplete, but it appears that the predictions of the SOLVEFF program compare more favourably with experimental values than do the supermolecule predictions.

3) β Hydroxy GABA

β Hydroxy GABA probably possesses an intramolecular hydrogen bond in solution, limiting the available rotations to one C-C bond and one C-N bond (2.3.3). SOLVEFF predicts minimum-energy conformations for the C-C bond in approximately classical positions, the global minimum-energy conformation being the gauche rotamer ($T_2 = -60^o$). Secondary minima occur for the trans and the other gauche conformations but these are of considerably higher energy (2.3.3). The NMR results of Ham (1974) predict the trans conformation as the global minimum (70% population) and a gauche conformation ($T_2 = 60^o$) as a secondary minimum (30% population). Technical difficulties preclude any NMR investigation of the carboxyl end of the molecule, so no evidence is forthcoming on the existence of an intramolecular bond. Classical calculations (2.4.3) predict the trans conformation and the gauche conformation ($T_2 = -60^o$) to be about equally populated ($\sim$40%) leaving the other gauche conformation ($T_2 = 60^o$) as a secondary minimum with appreciable population ($\sim$ 20%). Thus the methods do not agree on the relative populations of the classical minima.

A comparison of x_T distributions is presented in Fig. 2.33. Here it is apparent that the theoretical results place more weight on high x_T conformations than do NMR data. SOLVEFF, in fact, indicates appreciable populations exclusively in the high x_T region. Nevertheless, in each case, the preferred x_T value is similar; within the range 5.1 - 5.4 Å.

4) Glutamic acid

NMR results on this dicarboxylic acid (Ham, 1974) indicate a preference for partially folded conformations (C_β-C_γ trans; C_α-C_β gauche with respect to the C_α-N bond).

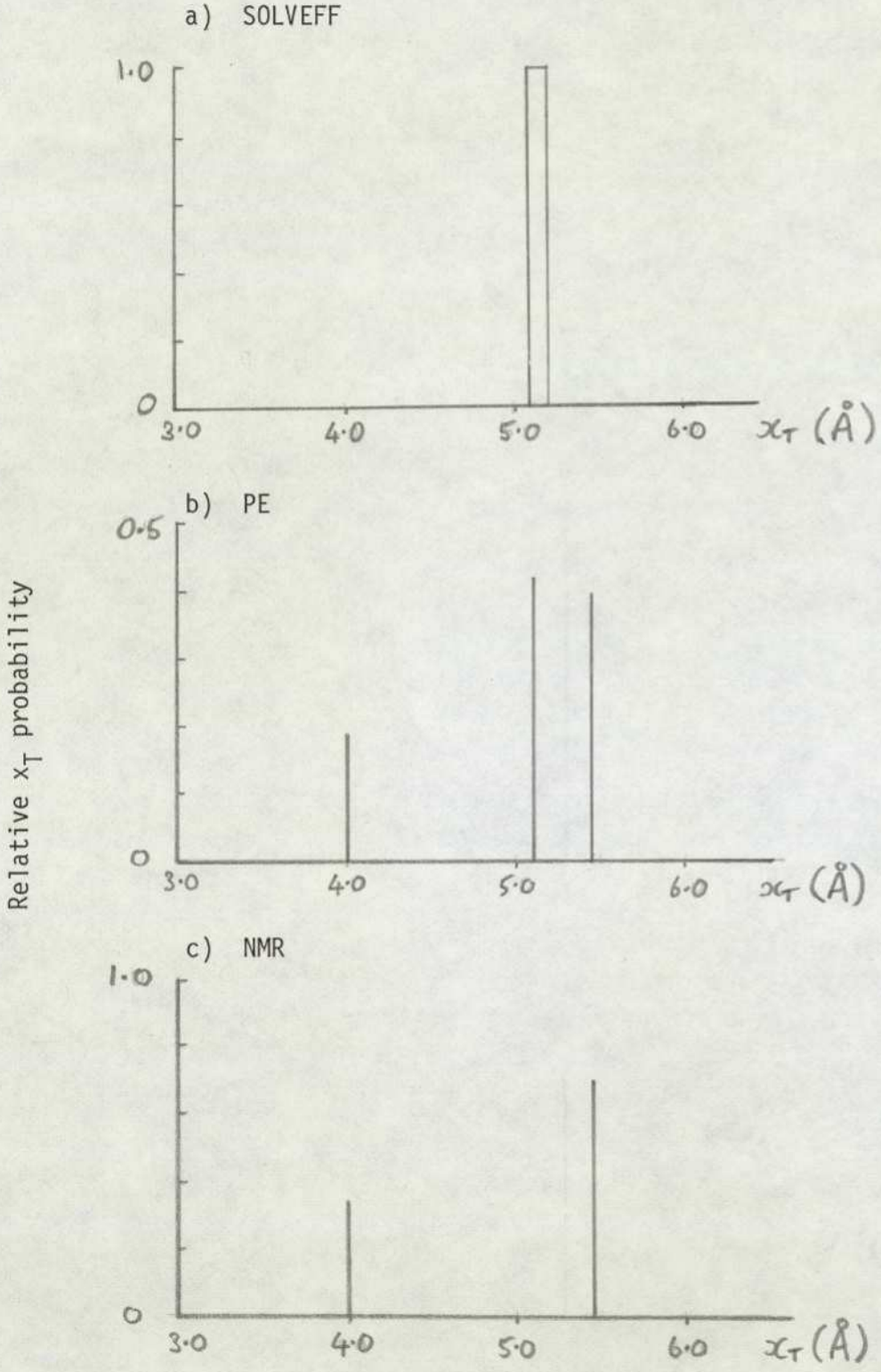

Fig. 2.33 Comparison of x_T distributions for β hydroxy GABA zwitterion in water
H bonded ring structure.

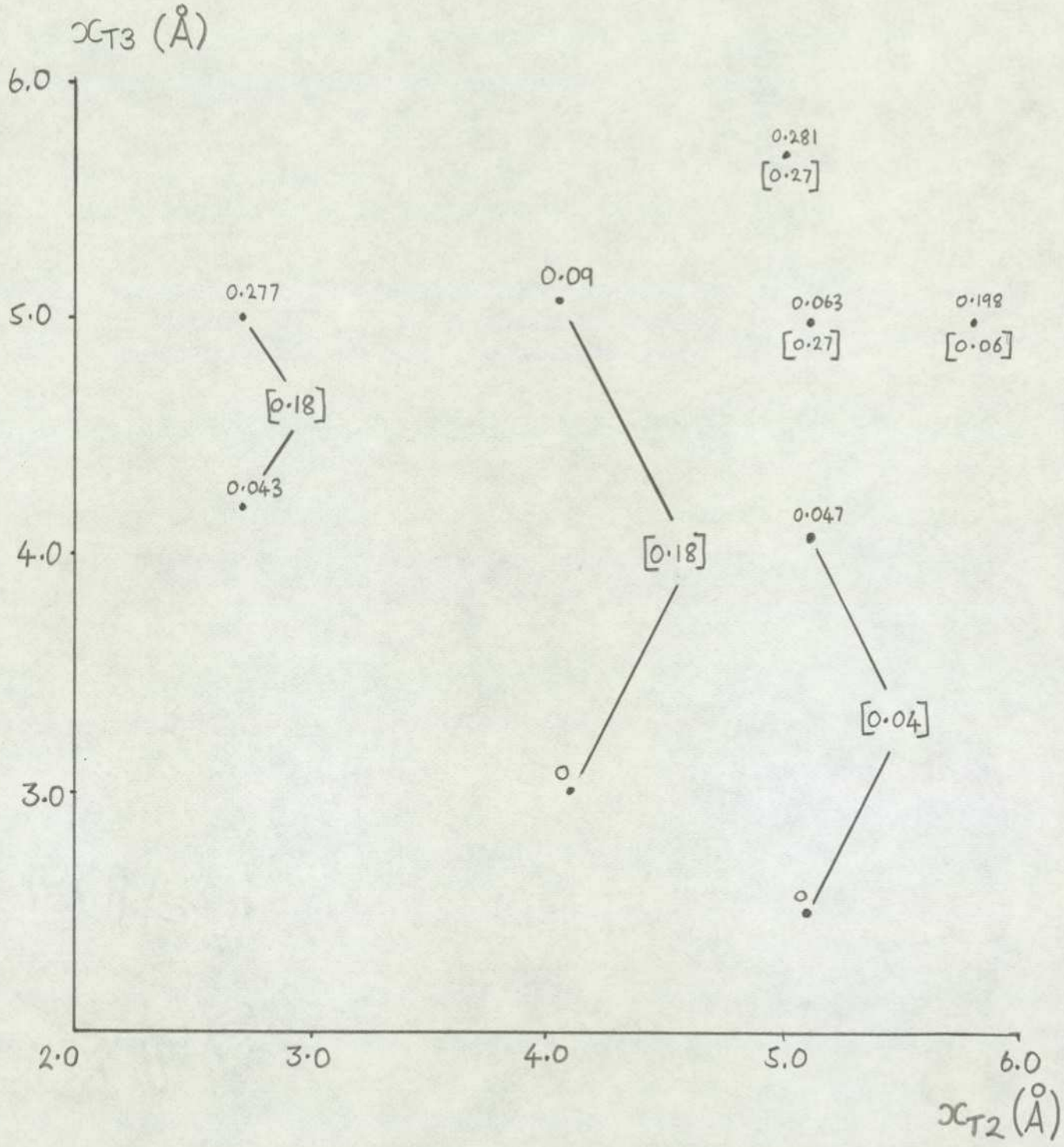

Fig. 2.34 Glutamate: Comparison of PE and NMR conformational populations [NMR figures are bracketed.]

Classical calculations (2.4.4) also suggest a preference for a partially folded molecule, although as in the case of GABA, the fully extended conformation (with respect to C_α-N) is given a higher weight than NMR would indicate.

A comparison of x_T distributions for both ⊕ - ⊖ and ⊖ - ⊖ charge separations is presented in Fig 2.34. Again, a qualitative agreement is apparent between theory and experiment, although in both cases the simplifying assumptions of the methods give cause for hesitancy in accepting their results as absolute.

e) Conclusion

The results for α-ω amino acids show general agreement in predicting that partially folded to fully extended conformers will occur in solution, rather than ring structures with intramolecular hydrogen bonds between amino and carboxyl groups. The extent of agreement on the actual preferred conformations is limited, however.

The SOLVEFF predictions seem to show sensible values, particularly for GABA itself, where general consistency with NMR and dielectric data is found. The agreement between theory and experiment in terms of x_T distributions is better than that in terms of torsion angles. The agreement between supermolecule results and experiment is less satisfactory than that of the SOLVEFF method.

Simple classical calculations show remarkable qualitative agreement with NMR results interpreted in terms of classical minima. This may provide some validation for the use of classical energy calculations in the structure-activity studies of section 3.2.

2.5.2 Comparisons between isolated molecule, solution and crystal structure conformations

a) Introduction

The relevance of crystal structure conformation to pharmacological activity is less certain than that of solution conformation (2.1). Nevertheless, there may be some similarity between the environment of a transmitter molecule at the receptor and in the solid state (2.2.1). Isolated molecule conformation is further removed from direct relevance to transmitter-receptor interactions, but like crystal structure results, has, in other transmitter systems, enabled SAR to be established on the basis of preferred conformation. A possible explanation for this is the striking similarities which occur, for singly-charged transmitters between preferred conformations exhibited in solution (NMR studies), in crystal structures (X-ray studies) and in conservative molecules (MO studies) (Partington, Feeney & Burgen, 1971; Pullman & Courriere, 1973; Beveridge et al, 1974[a]). Hence, it may not be any one of these molecular states which is actually involved in neurotransmitter activity, but since all investigations yield similar results, all can be used to establish conformational SAR. In fact, other considerations (2.1) point to the primary significance of conformation in the biophase (Lambrecht & Mutschler, 1974), i.e. solution conformation.

In the GABA system, the situation is different. Isolated molecules show strong calculated preferences for highly folded conformations (2.1) which are unlikely to be important at the receptor (1.3.3). The conformational preferences of GABA agonists in crystal structures however (2.2.2) show notable congruences which may relate to receptor activity (2.2.1) and in aqueous solution, calculated preferred conformations are similar for a number of strong agonists (2.3, 2.4, 2.5.1). It was thought to be constructive at this stage, therefore, to compare the conformational preferences determined for the solid state and for aqueous solution in order to ascertain any relationships between the results. X-ray crystal structure determination is a very precise technique,

whereas calculation of solution conformation is in the early stages of development and its results are not proven to be reliable. If the general features of solution conformation results for zwitterions in terms of inter-charge distances, etc., are compatible with those of X-ray crystal structure studies, the latter could be used to predict the former with sufficient accuracy to be useful in SAR. This may be an explanation of the success of the SAR studies on singly-charged transmitters using X-ray techniques (2.1).

Similar arguments apply for the mono-anionic glutamate agonists, where again, X-ray crystal structure determination can yield precise conformational information, while theoretical solution conformation calculations are, as yet, of unproven accuracy. Provided that some correspondence between crystal structure and solution conformation is demonstrable (see below), X-ray methods may provide less equivocal information than present theoretical treatments of conformational preference in solution.

b) Comparison of X-ray and solution conformation results

Electrostatic attraction between the charged ends of isolated zwitterions might be expected to produce the highly folded conformations which are predicted by MO calculations (Warner, 1975; Borthwick, Livingstone & Steward, 1975; Borthwick & Steward, 1975[b]; Pullman & Berthod, 1974). In the solid-state, however, where molecules are closely packed together, intermolecular interactions come into play, disrupting intramolecular forces and enabling the molecules to exist in more extended forms. (2.2.2). Again, in aqueous solution, the presence of water molecules results in extension of the zwitterionic amino-acids since electrostatic interactions favour conformations with large dipole moments. Hence, as might be expected from these considerations, the general features of X-ray structures do show some similarities with results for solution conformation. The detailed agreements are incomplete, but noteworthy nonetheless.

For GABA itself, the most highly populated classical conformation found by the NMR studies of Ham (1974) (2.5.1) and the potential energy calculations of 2.4.3 corresponds to the crystal structure of the pure compound (Steward, Player & Warner, 1973; Tomita, 1973) (2.2.2). The fully extended rotamer found in the crystal structure of GABA HCl is also well populated in both sets of solution results. The global minimum predicted by SOLVEFF for the three rotations T_2, T_3 and T_4 (Fig. 1.3) is at 140^o, 60^o, 60^o, whereas the crystal structure result gives 180^o, 80^o, 0^o. The degree of agreement reflects the general tendency of SOLVEFF results towards gauche rather than trans configurations.

The agreements in α alanine, βGP and βHydroxy GABA are not so striking, but in the latter case the NMR preferred conformation of the C_β- C_γ bond (Ham, 1974) corresponds to the crystal conformation, for which SOLVEFF also shows a minimum though only a local one. β alanine shows a gauche crystal conformation, a trans preference in SOLVEFF and no preference in NMR. βGP, while showing a similar degree of folding in the crystal and in two-dimensional SOLVEFF results, does not display precisely the same conformation. Judging by the GABA results, however, it is possible that the preferred two-dimensional conformation of βGP would be affected by rotation of the carboxyl group.

For the glutamate system, data is lacking, although for glutamic acid itself, as for GABA, the NMR results of Ham (1974) show a large population in solution for one of the solid state conformations (2.2.3). Isolated molecule calculations have not yet been performed on glutamate, but electrostatic considerations would again point to the likelihood of folded preferred conformations due to interaction between NH_3 and COOH groups, all three of which are ionised in solution at physiological pH.

c) Conclusion

Some correspondence between the degrees of folding of zwitterions in the solid state and in aqueous solution is found. This is not unexpected, since intermolecular forces in both cases predominate over intramolecular forces.

The limitation of crystal structure results in this kind of work is their uniqueness. In some compounds treated by the SOLVEFF method (2.3.3) a spectrum of conformations in solution was predicted. Indeed, such a result is almost inevitable for classical PE methods and NMR interpreted classically. X-ray results can only predict one conformation, unless, as in the case of GABA, more than one form of the compound is available and crystallises differently. Even then, the X-ray results cannot indicate the population of different conformational modes in solution. Hence, although, as is demonstrated in chapter 3, X-ray results can imply hypotheses about transmitter-receptor activity, they cannot be taken to indicate solution conformation without qualification. Independent studies of solution conformation remain desirable, since it remains probable that biophase conformation is more relevant to the receptor environment than is crystal structure conformation.

In the next chapter, the solid-state and solution conformation results are employed in the investigation of conformational SAR in the GABA and glutamate systems. Both types of results are shown to be useful in the establishment of SAR, although PE solution conformation data, allowing for flexible transmitter molecules, provides the basis for the most comprehensive scheme (3.2). Further discussion of the use of conformational information in SAR studies can be found in 3.4.1.

3 STRUCTURE ACTIVITY RELATIONSHIPS AMONG AMINO-ACID TRANSMITTERS

3.1 Introduction

(a) Background to structure-activity relationships (SAR)

The establishment of relationships between chemical structure and biological activity has a long history (Goodford, 1973). Two divergent approaches may be recognised, which have been termed structure-activity relationships (SAR) and physicochemical-activity relationships (PAR) (see 1.2.1c). The former usually describes the qualitative relationships between the molecular structure of drugs, including conformation, and their biological function (particularly in the context of 'receptor mapping' (1.2.1c)), and the latter correlates the physicochemical and biological properties of drugs in a quantitative manner.

As a result of the development of fast computers, it has become possible to carry out PAR studies without the need to vary only one physicochemical parameter at a time. This is achieved using multiple regression analysis as follows. Physico-chemical parameters for drugs are measured and then expressed in terms of related free-energy variables. The hydrophobicity of a molecule, for example, is often found to be strongly correlated with biological activity (Hansch, 1973) presumably because of the importance of hydrophobic bonding in drug-receptor interactions (1.2.1). Hydrophobicity can be estimated via the partition coefficient of the molecule between a model solvent (usually octanol) and water. The quantity log (partition coefficient) is then calculated, which is directly proportional to the free-energy of partition of the compound. The biological activity of a drug can also be expressed as a free-energy, since relative potency (1/C) as defined in 1.2.3, is related to the equilibrium constant (K_E) of the drug-receptor interaction and log (K_E) is directly proportional to the free-energy of the interaction.

The next step is to set up a 'linear free-energy relationship' between the terms measuring the biological activities and the physicochemical properties of a series of drug molecules. Hence:

$$\log(1/C) = a_1X_1 + a_2X_2 + a_3X_3 + \ldots\ldots + a_n$$

where the X_i's are physicochemical free-energy parameters and the a_i's are coefficients which are determined by multiple regression of the linear free-energy relationship by computer. The validity and usefulness of the relationship may be assessed by various statistical parameters (3.2.2) and X_i's can be included or not, according to their effect on the significance of the regression. The theoretical basis of these techniques, it is interesting to note, has only recently been demonstrated (Wold, 1974) although their empirical success has been documented for some time (see Hansch, 1973).

However, conventional PAR variables are not very useful for amino-acid transmitters, as is shown in Appendix 5, where the values of various physicochemical parameters for these substances are tabulated. The values fail to correlate with the observed peak activity of homologous series of excitatory and inhibitory amino-acid transmitters (1.3.3), since they exhibit only monotonic variation with increasing chain length. This lack of correlation is, of course, a consequence of attempting to ignore the geometrical specificity of GABA and glutamate receptors. Even a compound with ideal hydrophobicity for binding to the GABA receptor, for instance, will fail to bind if it does not fit. (The complementarity principle.) Hence, although physicochemical parameters may well exert significant influences on the activities of neurotransmitters, they are second-order influences compared to receptor fit.

Thus we return to SAR in order to consider how the molecular structure of an amino-acid transmitter molecule affects its biological activity. Clearly, after the chemical nature of the molecule, the most important factor affecting transmitter-receptor complementarity is conformation (2.1). The use of conformational parameters can enable SAR to be established without recourse to

physicochemical measurements as intermediaries, but these correlations are usually qualitative ones based on congruent conformations of a series of molecules (e.g. Beers & Reich (1970) on acetylcholine analogues). In contrast, though, Gill (1959) was able to demonstrate a semi-quantitative correlation between the biological activities of a series of competitive acetylcholine antagonists and parameters obtained from a complete conformational analysis of each of the molecules, albeit a simplified one. This study was based on the suggestion of Schueler (1953) that the probability of a molecule existing with a critical distance between receptor-active groups should relate quantitatively to its potency, the receptor being geometrically limited.

(b) SAR studies in the GABA and glutamate systems

The work reported in this chapter includes a development of Gill's method (3.2). An earlier version of this has already been published (Steward & Clarke, 1975) (see Appendix 6 for details) but a more refined method is presented here. The technique of multiple regression analysis, as described above, is employed to link biological activity and conformational (rather than physicochemical) parameters. Thus, a quantitative basis for SAR in the GABA (3.2.2-3) and glutamate (3.2.4) systems is provided, superceding the previous descriptive SAR based on molecular chain lengths alone (Curtis & Watkins, 1960; Bowery & Brown, 1974).

The chapter continues (3.3) with discussion of qualitative SAR based on congruent dispositions of atoms found in crystal structure (3.3.2) and solution (3.3.3) conformations of related molecules. The pharmacological data of 1.3 and the conformational results of Chapter 2 are thus drawn together.

In conclusion (3.4) the use of conformational preference as a predictor of biological activity is discussed, and the possibility of involving further parameters in quantitative structure-activity correlations is examined since it is not possible to account for the relative potencies of agonists entirely on conformational grounds.

3.2 SAR using PE conformational parameters

3.2.1 Introduction and method

The complementarity principle (1.2.1) implies that poor fit between transmitter and receptor leads to low transmitter potency. This emphasises the importance of knowledge of drug conformation in the study of drug-receptor interactions via the structure-activity properties of agonists. Not only are physicochemical and electronic properties of the drug molecules involved, but also the spatial disposition of functional and structural moieties.

(a) Aims

Having obtained quantitative estimates of conformer populations, the next step is to analyse the results in terms of molecular geometry parameters which may be associated with drug potency. Bowery and Brown (1974) have attempted to correlate the chain length of GABA agonists with potency, making the implicit assumption that it is a fully-extended molecule which is involved in the transmitter-receptor interaction. In 3.2.3 an attempt has been made to allow for the occurrence of other preferred conformations in such a correlation. All energetically possible conformations need to be considered (Schueler, 1953) since these are all available to the molecule. It may not be the most favoured conformation, or indeed any one conformation which is uniquely involved in the drug-receptor interaction.

The PE conformational analyses of 2.4.3 cover a wide range of GABA agonists of varying chain-length, a number of which are included in the study of Bowery and Brown (1974). Accordingly, these results are employed in 3.2.2 to produce structure-activity correlations which go further than chain-length comparison, and may have some predictive value for GABA-like activity. The results allow suggestions to be made about the structural properties of the GABA receptor, as discussed in Chapter 4, where a receptor model from SAR among GABA agonists is shown to be compatible with a

model deduced from studies of antagonists and protein structure (Smythies, 1974).

A conformational SAR study on some glutamate agonists is reported in 3.2.4, but a complete quantitative result is not forthcoming due to the lack of rigid glutamate agonists for comparison (see below).

(b) Description of the method

SAR studies employing conformational analysis have been described by Gill (1959) for a series of competititve acetylcholine antagonists, each consisting of a flexible chain with terminal quaternary nitrogens. Classical PE calculations as described in 2.4 were used to calculate conformational energies, and a simple Boltzmann function then provided population values for each energetically permitted rotamer. The molecular geometry parameter considered as a function of conformation was the inter-charge distance of the molecules. A probability-distance distribution was built up from the probability of each conformation and the inter-charge distance in each conformation.

The working hypothesis required at this point is that the receptor is geometrically limited so that it can only accept molecules with particular dispositions of active atoms. Hence, only that proportion of molecules possessing inter-charge distances within a certain range can interact with the receptor, the effective concentration of drug being therefore reduced. In order to ascertain which inter-charge distances may be important, an initial receptor model is required, giving the approximate distance or range of distances separating the active moieties of the receptor. In the work of Gill (1959), the ACh receptor was taken to consist of two negative sites (complementary to the positive terminal groups of the antagonists) with a separation of between 6 and 8 Å. The proportion of molecules of each antagonist possessing an inter-charge distance within this range was shown to bear a semi-quantitative relationship to the antagonistic potency. Thus, the simple receptor model provided a basis for consistent SAR results.

The model employed in the present work differs in that receptors are considered to be identical but flexible, where Gill's receptors were rigid but showed a variation in size between individuals. A rigid model would not be compatible with the pharmacological results for GABA and glutamate analogues, since muscimol, the strong GABA agonist, and ibotenic acid, the strong glutamate agonist, are themselves both rigid. A Gill type receptor model requires that rigid agonists are not very potent as they can only combine with a small proportion of the receptors. The present work, then, considers the flexibility of receptors as well as that of drug molecules, and is thus an extension of Gill's method. The development of the model for receptor flexibility is described below (3.2.2).

The existence of rigid analogues of transmitter molecules (agonists or competitive antagonists (see 1.2.1c)) is helpful in this connection; their molecular geometry can suggest the initial receptor model, which can be refined by the conformational results from flexible molecules. In the GABA system, a number of conformationally restricted analogues have been tested pharmacologically, enabling an initial picture of the flexible receptor to be built up (Steward & Clarke, 1975). In the present work, the initial model was refined, using multiple regression analysis to correlate activities and transmitter/receptor conformational parameters in a successive approximation process (3.3.2-3). Few rigid glutamate analogues have yet been reported, so the SAR scheme developed for the glutamate system (3.2.4) is not so comprehensive.

Gill's work concerned SAR among competitive antagonists. As discussed in 1.2.3c, this is impracticable for amino-acid transmission systems owing to the lack of such substances, so SAR among agonists is considered here. The mechanism of action of the agonists, beyond the initial interaction stage, is not investigated in this section; the question of receptor fit is the main subject and is treated from the recognition aspect as described in 2.1. Hence, a GABA agonist is treated as a pair of opposite charges separated by a distance x_T (Fig 2.1), and a glutamate agonist as

a system of three charges (- - and +) separated by distances x_{T1}, x_{T2} and x_{T3} (see Fig. 2.2). Interactions are presumed to occur when the receptor charge separation x_R can accommodate the transmitter's x_T (2.1). The results have a number of interesting implications concerning not only the geometry of receptors, but also the nature of efficacy and partial agonism in the GABA system. These are discussed in 3.2.3.

3.2.2. Extension of the method and its application to the GABA system

(a) Importance of rigid agonists

Owing to the existence of a number of GABA agonists possessing unique or restricted x_T values (Table 3.1), quantitative structure-activity correlations on GABA agonists are practicable. Glycine (x_T = 3.26 Å) has a potency $\sim$ 1/1000 that of GABA on the crayfish stretch receptor (Edwards & Kuffler, 1959); muscimol (x_T = 5.16 Å) has a potency about equal to GABA on feline spinal neurones (Johnston et al, 1968); 4-aminotetrolic acid (ATA) (x_T = 5.65 Å) has a potency $\sim \frac{1}{5}$ - $\frac{1}{2}$ GABA on spinal neurones (Beart et al, 1971); and imidazoleacrylic acid (x_T = 7.0-7.3 Å) is ineffective at the crayfish stretch receptor (McGeer et al, 1961). From these results an initial model for the GABA receptor (taken to be similar in these preparations (see 1.3.3) may be developed, the range in x_T values which can be accepted being taken to imply a range of flexibility in the inter-charge distance (x_R) of individual receptors (2.1). Thus, the low potency of glycine implies that, at any instant only a small number of GABA receptors will have an x_R equal to the x_T of glycine, such that only a small proportion of receptors can complex with glycine (2.1). (Efficacies must be taken as equal at this initial stage, in keeping with the 'concept of optimum stereoselectivity maximising efficacy' (Kier, 1970) (see 1.2.3)). On a simple occupation theory hypothesis, then, glycine occupies only a small number of receptors and is thus of low potency. Muscimol, on the other hand, must occupy a large number of receptors, for it has a high potency. It may be concluded that there are many receptors, at any instant, which have an x_R of 5.16 Å. Similarly, fewer receptors can complex with ATA so fewer have x_R = 5.65 Å at any instant. Immeasurably few have $x_R > 7.0$ Å or they would complex with imidazoleacrylic acid.

Rate theory would predict essentially the same model, since whatever the efficacy of a particular molecule (i.e. its dissociation rate from the receptor in rate theory) it can only interact with the proportion of receptors which, at the instant of impact, have a complementary inter-charge distance. A further, and perhaps more satisfactory, possibility is that the dimensions of an individual receptor are shifted away from equilibrium by the approaching transmitter (cf. Burgen, 1966; Richards et al, 1975). Here again, though, the same model of the receptor applies, since the energy involved in a large shift of x_R from the mean would be greater than that involved in a small shift, so the probability of interaction with, say, glycine would be smaller than that with muscimol, if the latter more closely matches the receptor at equilibrium.

(b) Development of a receptor inter-charge distance distribution

From the foregoing, it is apparent that the GABA system possesses features which allow some deductions to be made about receptor geometry; at any instant, there are less receptors with $x_R \sim 7$ Å than with $x_R \sim 3$ Å, less with $x_R \sim 3$ Å than ~ 6 Å, and less with $x_R \sim 6$ Å then ~ 5 Å. To be more precise, the assumption can be made as a first approximation, that the potency of an agonist with inter-charge distance x_T is proportional to the probability of the receptor having $x_R = x_T$:

$$1/C \propto P(x_R)$$

This may be too simple, as the relationship between $1/C$ and $P(x_R)$ need not be linear. The efficacy of interactions with x_R close to the equilibrium position, for example, may be greater than others. The relationship can be improved upon at a later stage.

At this point, it may be noted that the quantities $kT \log (1/C)$ and $kT \log (P(x_R))$ have dimensions of energy as mentioned above (3.1). Accordingly, a more useful expression connecting the terms $1/c$ and $P(x_R)$ could be the linear free-energy relationship:

$$\log(1/C) = m\log(P(x_R)) + p$$

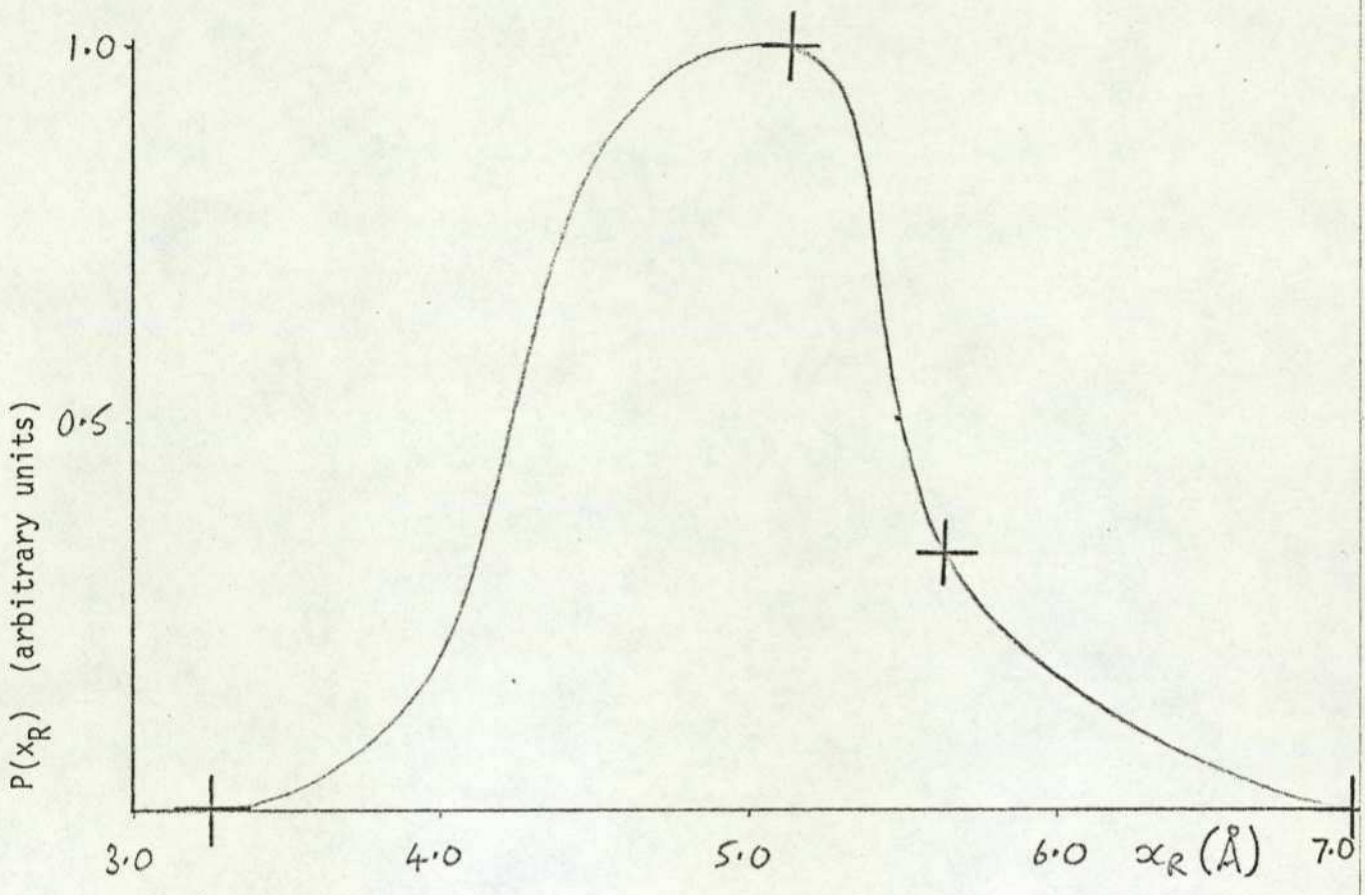

Fig. 3.1 Initial $P(x_R)$ model from results presented below

TABLE 3.1 Parameters for initial x_R model

Substance	1/C	$P(x_R)$	x_R
glycine	~1/1000	0.001	3.26
muscimol	~1	1.000	5.16
ATA	~1/3	0.333	5.65
imidazoleacrylic acid	0	0.000	7.0

although it should be noted that kT log ($P(x_R)$) is not strictly a free-energy term, since configurational entropy is neglected, conformational modes being treated as discrete states (2.4.2).

From this equation, an initial receptor-model can be developed, taking the simplest possible case (m = 1 and p = 0). The model can be refined by consideration of the potencies of flexible agonists, and later, by successive approximation.

The parameters of the initial model are given in Table 3.1 and the probability curve itself is illustrated in Fig. 3.1. This initial model is closely similar to that employed in the published work on this topic (Steward & Clarke, 1975) but the x_T values are more precise (see Appendix 6).

(c) Interaction probability for individual conformations

The situation for flexible molecules is complicated by the x_T distribution of the agonist itself. Taking β alanine, for example, the PE calculations of 2.4.3 indicate an x_T distribution containing two peaks within the range 3 - 7 Å. These peak x_T values (with probabilities in brackets) are: 3.4 Å (.493) and 4.65 Å (.507). From these figures, it is possible to define an 'interaction probability' for each x_T equal to (probability of drug molecule x_T) x (probability of receptor having matching x_R), so for β alanine:

Total interaction probability = $(.493)P(x_R=3.4)+(.507)P(x_R=4.65)$

$T_i = \sum_{all\,x_T\,in\,drug\,i} P(x_T) \times P(x_R)$

NB: T_i depends upon m and p via $P(x_R)$ since $P(x_R)$ may vary as m and p are refined (see (d) below)

The working hypothesis (3.2.1b) is that the conformational restriction on agonists which the receptor can accept reduces the effective number of drug molecules available to that number which have x_T within the geometrical constraints. The total interaction probability quantifies this concept. It is a measure of the proportion of drug molecules which actually interact with receptors.

The linear free-energy relationship above can now be restated in a more general form which allows for agonists with more than one possible x_T:

$$\log(1/C_i) = m\log(\Sigma P(x_T).P(x_R)) + p = m\log(T_i) + p$$

(d) Analytical $P(x_R)$ curve

The concept of interaction probability enables the potency results of flexible agonists to be used in the development of a more precise x_R distribution. In the case of β alanine, with its two x_T values, it is clear that molecules with the lower x_T (3.4 Å) will have low potency, since the potency of glycine (x_T = 3.26 Å) is low, x_T values being closely similar. Hence, most of the effect of β alanine is due to interactions at $x_T = x_R$ = 4.65 Å. This extra piece of information can be used in developing an analytical expression for x_R, which need not be physically meaningful, since it is merely a mathematical device, but which does provide a straightforward means of calculating $P(x_R)$ for any required x_R.

The initial curve of Fig 3.1 suggests that a Poissonian approximation may provide an appropriately shaped x_R curve. Hence:

$$P(x_R) = a \exp(-b(x_R - x_o)^2)$$

From the linear free-energy relationship with m=1 and p=0:

$$\log(1/C_i) = \log(\Sigma P(x_T) a.\exp(-b(x_R - x_o)^2))$$

So, for β alanine, ignoring the small effect of the conformations with x_T = 3.4 Å,

$\log(.06) = \log(P(x_T=4.65)\ a\ \exp(-b(4.65-x_o)^2))$. For Muscimol: $\log(1.0) = \log(P(x_T=5.16)\ a\ \exp(-b(5.16-x_o)^2))$. For ATA: $\log(.32) = \log(P(x_T=5.65)\ a\ \exp(-b(5.65-x_o)^2))$.

(approximate potencies are taken from Table 1.1)

As the x_R curve is refined, the value of m is adjusted successively from 1.0 to a self-consistent value (see below). The equations for individual substances then become of the form:

$$\log(1/C_i) = m\log(P(x_T)\ a\ \exp(-b(x_R - x_o)^2))$$

For each m assumed, the three equations representing the action of β alanine, muscimol and ATA are solved for a, b and x_o. The values of these parameters for various values of m are shown in Table 3.2.

(NB. A Poissonian approximation to the x_R probability curve is not subtle enough to fit the results for glycine as well as those for β alanine, muscimol and ATA. The addition of a constant term to the $P(x_R)$ expression for low values of x_R is required to represent glycine activity:

$$P(x_R) = a \exp(-b(x_R - x_o)^2) + c \quad (c=0 \text{ for } x_R > 3.5 \text{ Å})$$

(e) Regression analysis and refinement of $P(x_R)$ curve

The x_R distribution having been defined analytically, it is possible to proceed with the correlation of conformational data for a series of agonists with their biological activities. From the analytical x_R curve (initially, that with m = 1) and the x_T distribution for agonists from section 2.4.3, total interaction probabilities can be calculated for each substance as described above. A linear free-energy equation for regression is formulated as before:

$$\log(1/C_i) = m\log(T_i) + p$$

The values of $\log(1/C_i)$ and $\log(T_i)$ for the series of agonists considered are employed as data for a computer program which carries out a multiple regression of the equation above. The program finds the best straight line through the data points and calculates m and p together with the statistical parameters (Hansch 1973) described below. The value of m calculated by the program may not, of course, match the value of m assumed in the calculation of total interaction probabilities. Hence the input value of m is adjusted until the output value equals the input value, that is until self-consistency has been attained. The values of T_i for each value of m are calculated via a computer program.

(In general, the value of p (which depends upon the scaling of $P(x_R)$ apart from anything else) should be similarly

TABLE 3.2

$P(x_R)$ curve parameters for the GABA receptor model

slope m	a	b	x_o	c
1.0	1.0325	6.6789	5.2291	0.000708
1.5	1.010	4.0060	5.2095	0.0079
2.0	1.002	2.6626	5.1854	0.0266
2.5	1.000	1.8707	5.1538	0.0550

optimised, but in the present study output values of p did not vary significantly from the input value p = 0 in any of the regression analyses).

Two statistical parameters are calculated by the regression program to indicate the degree of validity of the correlation. These are the correlation coefficient, R, and the standard deviation of data points about the best straight line, σ, which are defined as follows:

If the values of the dependent variable (log(1/C) in this case) are Y_i and their mean is $\bar{Y}$, the squared deviation from the mean is

$$SS_1 = \sum_{i=1}^{n}(Y_i-\bar{Y})^2$$

where n is the number of data points.

The sum of the squares of the residuals of the dependent variable about the regression line is:

$$SS_2 = \sum_{i=1}^{n}(Y_i-\hat{Y}_i)^2$$

where $\hat{Y}_i$ is the ith value of the dependent variable predicted by the regression line from the values of the independent variables ($\log(T_i)$ and the constant term).

The correlation coefficient is then defined as:

$$R = \left\{1 - \frac{SS_2}{SS_1}\right\}^{\frac{1}{2}}$$

and the standard deviation as:

$$\sigma = \left\{\frac{SS_2}{n - 2}\right\}^{\frac{1}{2}}$$

The statistical significance of the result can be assessed by the F parameter, which compares a regression result either against chance or against a reference regression. If k_1 is the number of parameters in the reference regression (k_1 = 1 for chance) and k_2 is the number of independent variables in the regression under test,

F is defined by:

$$F_{(k_2-k_1),(n-k_1)} = \frac{SS - SS_2}{SS_2} \times \frac{(n-k_2)}{(k_2-k_1)}$$

SS is the reference sum of squares ($=SS_1$ for chance).

The value of F represents the degree of statistical significance of the regression over chance or over the reference regression, which can be ascertained by reference to statistical tables.

3.2.3 SAR results and inferences for GABA agonists

(a) Results of regression analysis

Regression analyses were carried out for a set of twelve GABA agonists:

- α-ω amino-acids up to 7ACA (6 compounds)
- α-ω guanidino acids up to δGP (4 compounds)
- muscimol
- ATA

for which $SS_1 = 14.84$.

The choice of these agonists is a compromise between limiting the number of chemical variables in order to free the correlation from electronic effects (see 3.4), and using a sufficiently large number of compounds to make the correlation worthwhile. Hence, straight-chain compounds only are considered (+7ACA) and imidazole derivatives are not used. The fit of some of the other compounds investigated conformationally in 2.4.3 is discussed below, however. The data points for all the agonists are shown in Table 3.3.

The results of the regressions for m=1.0, 1.5, 2.0 and 2.5 are shown in Table 3.4. The input value of p was zero in all cases and the output value was not significantly different from zero in any of the regressions employing an analytical x_R curve. $F_{1,11}$ measures the significance of each regression over chance, as shown in the adjacent column. The calculated value of m is higher than the input value in the first two cases, almost equal in

TABLE 3.3 PE SAR PARAMETERS FOR GABA AGONISTS

Substance	log (1/Ci) ref	log (Ti) m=1	m=1.5	m=2	m=2.5	3-7°A receptor
Glycine	-3.150 a,c	-3.150	-2.102	-1.575	-1.260	0.000
β alanine	-1.253 a,b,c	-1.240	-0.812	-0.625	-0.499	0.000
GABA	0.000 a,b,c	-0.418	-0.312	-0.261	-0.224	-0.085
δAVA	-1.130 a,b,c	-0.512	-0.414	-0.373	-0.340	0.000
εACA	-2.169 a,b,c	-1.751	-1.388	-1.218	-1.072	-0.361
7ACA	-3.000 b	-1.556	-1.455	-1.413	-1.325	-0.485
muscimol	0.000 d	0.000	0.000	0.000	0.000	0.000
ATA	-0.500 e	-0.500	-0.326	-0.249	-0.200	0.000
αGA	-0.244 a,b	-0.073	0.011	0.054	0.088	0.301
βGP	-0.028 a,b	-0.541	-0.314	-0.199	-0.118	0.201
γGB	-1.504 a,b	-0.492	-0.423	-0.384	-0.347	-0.133
δGP	-2.276 a	-0.804	-0.757	-0.737	-0.705	-0.197
βABA	-2.733 a,b			-0.860		
βHG	-0.854 b			-0.462		
" with H bonded ring	-0.854			-0.101		
αFG	> 0.000 f			-0.259		
IMAc	-0.041 b,c			-0.179 (-0.218)*		
MeImAc	-1.456 b			-1.081 (- ∞)		
ImPr	-1.426 b,c			-0.145 (-0.629)		
ImLa	-2.523 c			-0.166 (-0.443)		

Refs: a) Edwards and Kuffler, 1959
b) McGeer, et al, 1961
c) Swagel, et al, 1973
d) Johnston, et al, 1968
e) Beart, et al, 1971
f) Curtis, et al, 1972[a]

* Values in brackets for imidazole compounds consider the end nitrogen (N1) only (see Fig. 2.28)

Table 3.4 Results of Regression Analysis

Input m	Calc^{d}. m	Uncertainty	Calc^{d}. p	Uncertainty	SS_2	R	σ^2	$F_{1,11}$	Significance over chance
1.0	1.077	0.235	- 0.280	0.294	4.772	0.824	0.477	23.22	> 99.9%
1.5	1.618	0.244	- 0.154	0.227	2.750	0.903	0.275	43.95	> 99.99%
2.0	1.987	0.236	- 0.115	0.184	1.827	0.936	0.183	71.20	> 99.99%
2.5	2.267	0.246	- 0.138	0.167	1.560	0.946	0.156	85.10	> 99.99%
Step function x_R curve (see text)	3.597	1.266	- 1.044	0.274	8.209	0.668	0.821	8.07	~ 98%

the third and considerably lower in the fourth. Hence, although the regression for m = 2.5 has slightly better statistics than the others, the self consistency of m is best for m = 2.0. This regression line, with data points, is shown in Fig. 3.2 and the corresponding $P(x_R)$ curve is illustrated in Fig. 3.3.

The final set of results in Table 3.4 is a regression for a receptor model, which will accept with equal probability any molecule with x_T between 3 and 7 Å (i.e. for $3 \leq x_r \geq 7$, $P(x_R) = 1$; else $P(x_R) = 0$). This range allows all the known GABA agonists to be recognised. The corresponding regression is markedly poorer than the rest, demonstrating that the concept of a x_R flexibility curve fits the data better than the simpler model.

The statistics of the self-consistent regression line without the substances used in the development of the x_R curve are:

$R = .899$

$\sigma^2 = .299$

$F_{1,7} = 25.23$ (significant at 0.1% level)

The correlation is thus shown to be very significant, although the standard deviation is large. This is to be expected, however, since the standard deviations in the data points are also large (Table 3.3) as a result of the inherent inconsistencies in pharmacological measurements (see 1.2.3).

(b) Other agonists

The PE calculations of section 2.4.3 include results for some branched chain compounds and some imidazole derivatives which act as GABA agonists. Using the analytical $P(x_R)$ curve for m = 2, total interaction probabilities were calculated for these compounds (Table 3.3). Fig 3.4 shows the m = 2 regression line with the extra data points.

Branched α-ω amino acids show some agreement with the line, which would predict their potencies within an order of magnitude. The results for imidazole compounds are less satisfactory as there are uncertainties about which of the positive sites is likely to

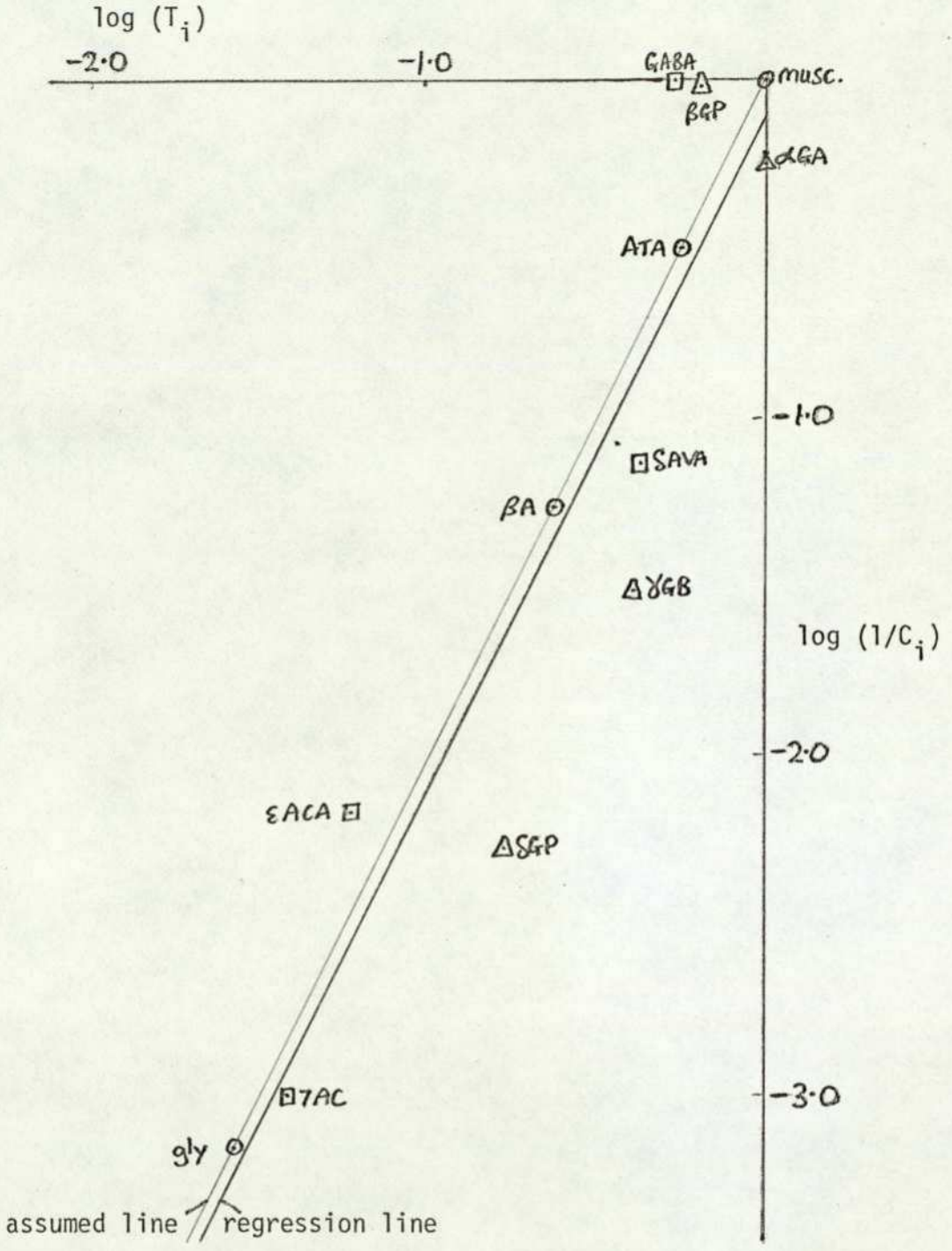

Fig. 3.2 Self consistent regression line for log ($1/C_i$) against log (T_i)

$\log (1/C_i) = 2.0\ (\pm 0.2)\log(T_i) - 0.1\ (\pm 0.2)$

$R = 0.936\ \sigma^2 = 0.183$ for all twelve substances

$R = 0.899\ \sigma^2 = 0.299$ for the eight substances not used in formulating the $P(x_R)$ distribution

⊙ = substances used in formulation

⊡ = other α-ω amino acids

△ = guanidino acids

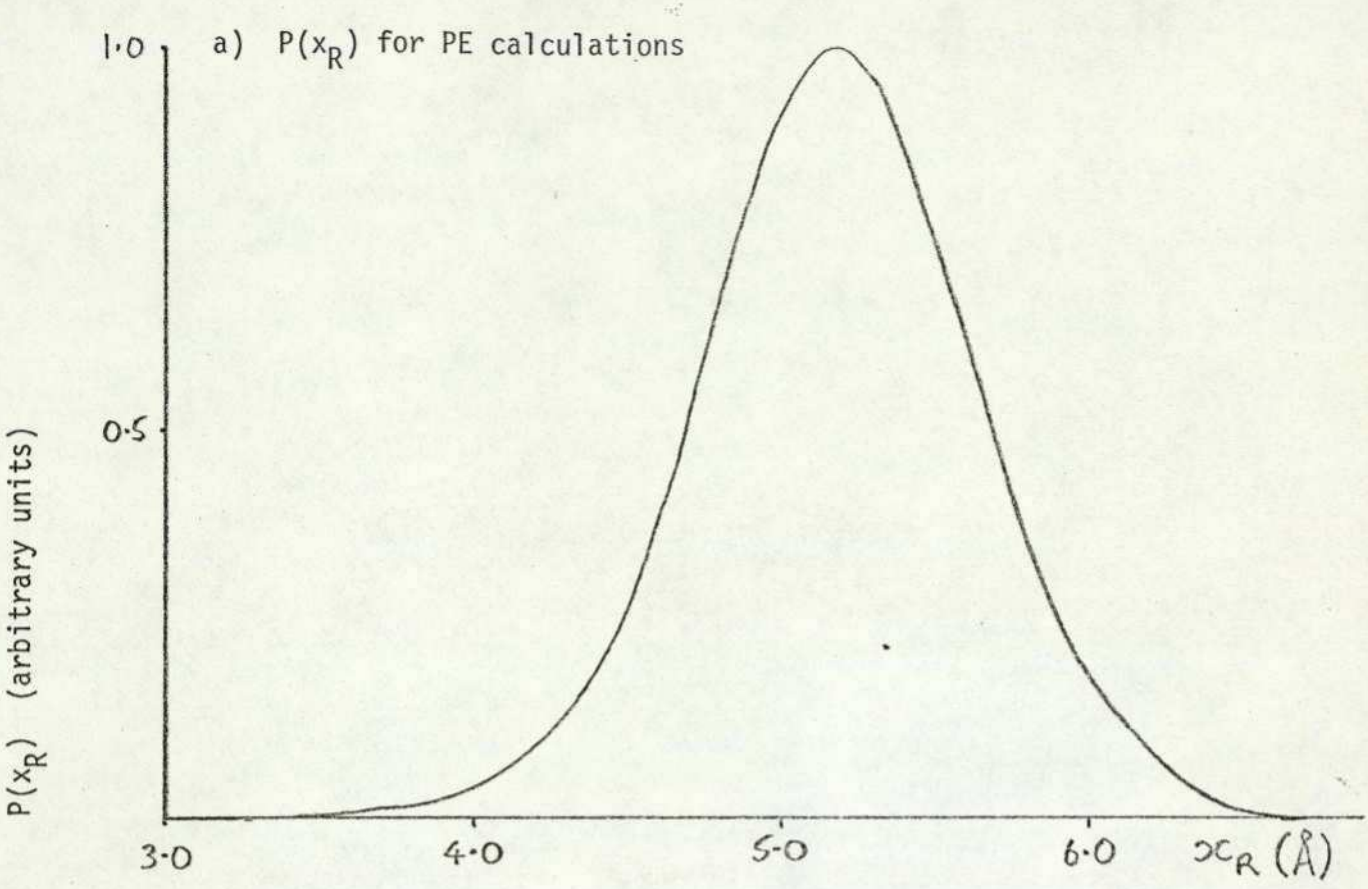

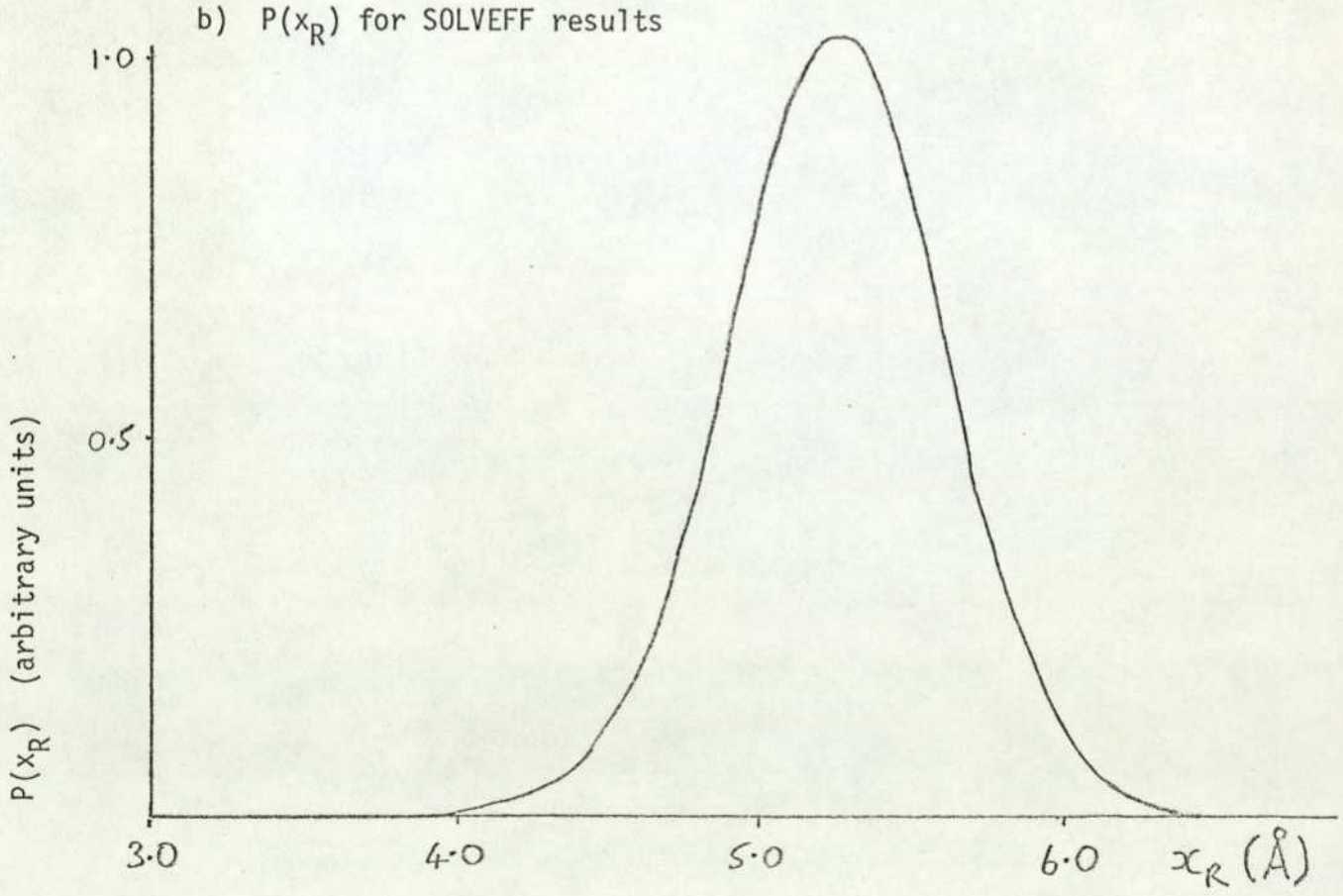

Fig. 3.3 Analytical $P(x_R)$ curves

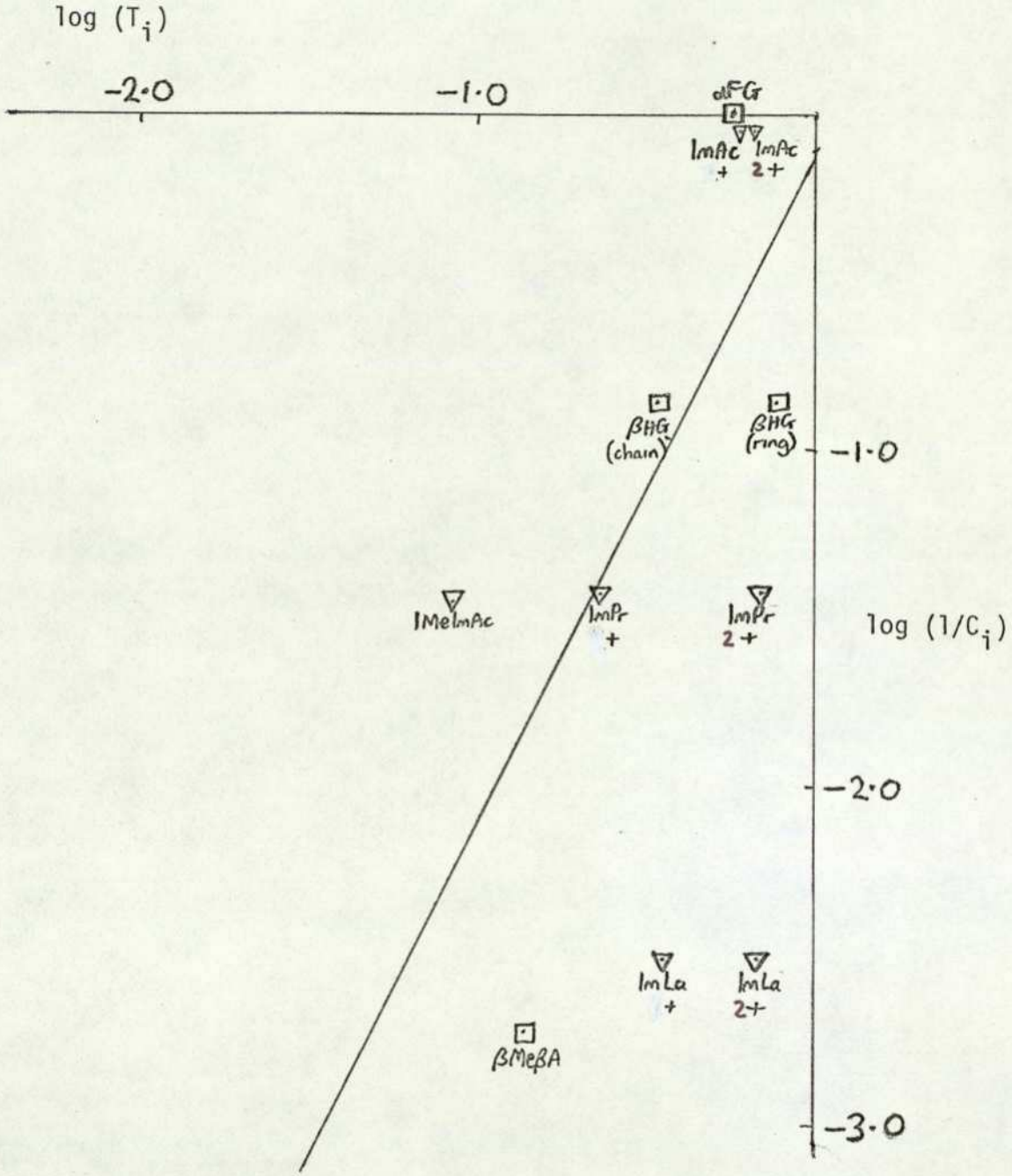

Fig. 3.4 Self consistent regression line with extra data points

⊡ branched α-ω amino acids

▽ Imidazole derivatives

be involved in the drug-receptor interaction (2.4.2). If only the N1 positive site is involved, the agreement with the line is good, but if either site can interact with the receptor the agreement is poor. It may be unwise to consider this result as indicating that N1 alone is involved, however, since the electronic nature of the imidazole group may be exerting a profound influence on the interaction.

(c) Implications of the results

(i) The $P(x_R)$ curve

The $P(x_R)$ curve can be mathematically represented by a Poissonian function. However, this does not necessarily indicate that a Poisson distribution is a good approximation to the real flexibility characteristics of the receptor charge separation. It would be necessary to involve a larger number of rigid agonists in the analysis, providing some redundancy in the equations, to show that such a representation were truly consistent. Indeed, the failure of the Poissonian curve to fit the glycine data could suggest that a more complex function is required.

Nevertheless, the Poissonian approximation is effective in producing a correlation between interaction probability and potency, so some examination of its physicial interpretation may be appropriate. Forces operating around the charged sites of the receptor constraining them loosely around an equilibrium position would cause Poissonian probability characteristics to be exhibited. The exponential term $(b(x_R - x_o)^2)$ would then be proportional to the energy involved in changing x_R from its equilibrium value of x_o, such that $b = \frac{\text{force constant}}{RT}$. The correspondence between this interpretation and possible receptor models is discussed in chapter 4.

(Some attempts were made to improve the curve by introducing a term to represent the electrostatic attraction between the charged groups of the receptor, assuming that the flexibility

of x_R was otherwise controlled by purely mechanical forces. Hence:

$$P(x_R) = a \exp(-b(x_R - x_o)^2 + c/x_R)$$

Solving this equation for a, b, c and x_o from the values of potency for glycine, β alanine, muscimol and ATA produced an unrealistic $P(x_R)$ curve. This showed an enormous peak, such that any compound with an x_T close to the peak x_R would exhibit almost infinite potency.)

(ii) The slope of the self-consistent regression line

The derivation of the straight line relationship between log(potency) and log(total interaction probability) has been couched in terms of linear free-energy relationship. Despite this, it is instructive to examine the relationship between C_i, T_i and potency in terms of drug-receptor theory, and to see whether the slope of the regression line implies anything about the parameters of the occupation theory and rate theory equations (see 1.2.2).

By definition (3.2.2c) T_i is a measure of the fraction of transmitter-receptor contacts which are fruitful. Hence the effective concentration of a drug is not its actual concentration $[i]$, but $[i]T_i$. Two cases may now be considered:

(1) On occupation theory:

$$\text{response, } y \propto \frac{e_i}{1 + 1/K_i(T_i[i])^n}$$

where K_i is the affinity constant of the drug, n is the molecularity of the reaction (2-4 for GABA (Feltz, 1971)), and e_i is the 'efficacy' of the drug.

In the simplest formulation of occupation theory ($e_i = 1$), $(T_i[i])^n$ must be a constant for any drug in the appropriate concentration to produce a standard response, y. For a half maximal response:

$$K_i(T_i[i])^n = 1 \qquad \text{——————————(1)}$$

The regression results, however, have produced the equation:

$$\log(1/C_i) = 2 \log T_i \qquad \text{——————————(2)}$$

where $(1/C_i)$ is a relative potency, i.e. the actual concentration of drug required for the standard response is:

$$[i] = C_i [Ref] \qquad \text{——————————(3)}$$

where $[Ref]$ is the concentration of reference compound required to produce the response.

From (1) and (3), for a half maximal response:

$$K_i (T_i C_i [Ref])^n = 1 \qquad \text{——————————(4)}$$

From (2) and (4)

$$[Ref]^n = T_i^n \qquad \text{——————————(5)}$$

Employing the same analysis, but including efficacies, again for a half maximal response:

$$K_i [Ref]^n \left(\frac{2e_i}{e_{ref}} - 1\right) = T^n$$

$$\text{or} \quad ei = \frac{e_{ref}}{2} \left(1 + \frac{T_i^n}{K_i [Ref]^n}\right) \qquad \text{——————————(6)}$$

In this formation, efficacy is linked directly to interaction probability, such that compounds with high T_i will be stronger agonists than concentration effects would predict. This is a more satisfactory result than equation (5) where efficacy was ignored and affinity connected with T_i, since affinity is a chemical effect and thus unlikely to be directly related to T_i, a conformational effect.

(2) On rate theory

$$\text{response, } y \propto \frac{(T_i [i]^n k_{2i}}{(T_i [i]^n k_{2i}/k_{1i}} \quad \text{(see 1.2.2a)}$$

where k_{1i} is the association rate of the drug-receptor complex and k_{2i} is its dissociation rate. The equation is equivalent

to that for occupation theory such that: $k_{2i} \equiv e_i$ and $k_{1i}/k_{2i} \equiv K_i$. Employing the same analysis as above, the equivalent expression for efficacy (k_{2i} in the rate theory case) is:

$$\text{form (6)} \quad k_{2i} = \frac{k_{2ref}}{2}\left(1 + \frac{T_i^n k_{2i}}{[Ref]^n k_{1i}}\right)$$

$$\text{which gives } k_{2i} = \left(\frac{2}{k_{2ref}} - \frac{T_i^n}{k_{1i}[Ref]^n}\right)^{-1} \qquad (7)$$

i.e. higher efficacy for higher T_i.

Thus in either case, high interaction probabilities correspond to higher potencies than concentration effects alone would predict. If T_i only affected potency by reducing the effective drug population, of course, the slope of the SAR regression line should be unity. The precise relationships between efficacy and T_i derived above ((6) and (7)) may not be reliable, since the standard deviations of the regression data and slope are large. Moreover, the assumption is made that efficacy and affinity remain constant for a particular compound in whatever conformation it interacts. This may not be the case. A simple physical interpretation of the effect could, in fact, be that interactions occurring with $x_T = x_R$ near the equilibrium x_R value have higher efficacy than those taking place further from equilibrium. This would require a different formulation of equations (6) and (7) with individual efficacies for each x_T involved in interations. The overall effect, however, would be the same: molecules possessing highly populated conformations with x_T values around the ideal would be efficacous and have high T_i; molecules possessing few such conformations would be less efficacious and have low T_i. Compounds which have high T_i, by virtue of their structure, but x_T values a little removed from the ideal, however, would constitute a special class - they would in fact be 'partial agonists' (see 1.2.2) which bind, but mediate a response only weakly (see below).

(iii) Partial agonism

It seems from the SAR results that potency is affected by interaction probability in a more complicated way than merely

reducing the effective drug concentration. As discussed above, drugs acting with x_T values far from the equilibrium x_R value may be less effective at mediating a response than those which have more ideal x_T values ($\sim$ 5.1 - 5.2 Å). This observation may furnish an explanation of the action of 'partial agonists' in the GABA system.

It is notable that the guanidino acids (particularly αGA and βGP) seem to possess partial agonist properties (Dudel, 1965; Feltz, 1971; Constanti & Quilliam, 1974), and also tend to exhibit high probabilities (i.e. $> \sim .5$) for x_T's a little removed from the ideal values. Most conformations displayed by other agonists in these regions possess quite low values of $P(x_T)$. This is, of course, a consequence of the chemical structure of the guanidino group, possessing as it does two positive charge centres which contribute to $P(x_T)$ for each conformation (see 2.4.2). If it is true that the efficacy of interactions away from ideal x_T become progressively lower, the partial agonism of guanidino compounds could be explained. Possessing large total interaction probabilities, the molecules will occupy a large number of receptors, but since most contributions to the total come from low efficacy regions of x_R, the mediation of response will be less efficient than the binding. Hence partial agonism may be the result.

This proposal is supported by the more sophisticated solvent effect calculations for β guanidinoproprionic acid described in 2.3. The high probability of x_T's a little removed from ideality is again observed (see 3.3.3).

On this theory, the action of ATA, and perhaps even β alanine, on GABA receptors should show some partial agonist properties (Fig. 2.2.9). Pharmacological experiments along these lines would provide a useful test of the hypothesis. In fact, the work of Swagel, Ikeda and Roberts (1973) indicates that β alanine produces a lower maximal response than GABA, a typical result of partial agonism.

An alternative explanation of the phenomenon may be revealed by equations (6) and (7) above, assuming this time that efficacy is a property of the drug rather than a property of the interaction. Equation (6) indicates that T_i and K_i, the drug-receptor affinity constant, oppose one another's effect. Thus a drug with high K_i will be less efficacious than one with low K_i, for the same T_i. Equation (7) shows a similar effect. Here drugs with high association constants will be less efficacious. Thus, strong binding militates against high efficacy, which is compatible with the tenets of rate theory. Some types of competitive antagonism could perhaps be explained on a similar basis, although antagonists can act in such a variety of ways that each case is best examined on its own merits.

3.2.4 Application of PE conformational SAR to some glutamate agonists

In this section a conformational SAR study on a small number of dicarboxylic excitatory amino acids is reported. The substances considered are mainly homologues of glutamic acid itself. No attempt has been made to explain the recently discovered high potencies of some heavily substituted glutamate analogues (see 1.3.3) since their potent action is not likely to be due to conformational effects. Synergistic action involving the hydrophobic side chains is a more reasonable explanation.

The glutamate system is less amenable to PE conformational SAR work than the GABA system because of the limitations described below. Hence, a clear quantitative result is not forthcoming from this investigation.

(a) Limitations

The first complication of excitatory amino-acids is the presence of three charged functional groups and thus three charge separations (Fig. 2.2). Fortunately, x_{T1} is constant for all α-ω amino acids due to the geometry of α carboxyl and amino groups in α amino acids (Fig. 2.2) so the problem can be reduced to two

parameters. x_{T2} and x_{T3}, however, are not independent for SAR purposes, since if a three point glutamate receptor is assumed (Curtis & Watkins, 1960), even with fixed x_{T1}, the x_{T2} and x_{T3} charge separations of an agonist both have to be correct for the third contact to be made.

Secondly, glutamate and its agonists possess an asymmetric α carbon atom and thus exist as enantiomorphic pairs. The potencies of each stereoisomer are different in general (Table 1.2), with L forms having the greater effect. The differences for glutamate itself, the most potent of the dicarboxylic amino-acids, is relatively slight, however, so the differences for agonists of lower mean potency is likely to be even less (Pfeiffer's rule, see 1.3.2). Hence the effect of enantiomorphism is ignored in this study and the potencies of racemic mixtures are considered. Accordingly, the more powerful agonists, such as N-methyl aspartate and homocysteate are not investigated here, since the neglect of enantiomorphism in those cases would be a gross approximation.

The third difficulty is the lack of known rigid glutamate agonists. The isoxazoline derivative, ibotenic acid, is a powerful glutamate agonist, and, by geometrical accident has x_{T2} and x_{T3} as well as x_{T1} independent of conformation. Only the racemic form has been pharmacologically investigated (Johnston et al, 1968) so enantiomorphism cannot be considered. Aminomalonic acid also possesses a unique set of x_T's. Cycloglutamic acid can attain only a limited range of x_T values and is $\sim$ 0.7-0.8 as potent as glutamate (Johnston et al 1974). The existence of only two completely rigid agonists precludes the development of quantitative flexibility curves for the glutamate receptor x_R values, and, in any case, the pharmacological data are themselves too imprecise to permit quantitative correlations to be made (Curtis & Watkins, 1963). Nevertheless, a crude correlation between preferred x_T values and potency can be established from the PE calculations of 2.4.4. The results are presented below.

(b) Results

The possible conformations of glutamate agonists can be expressed for SAR purposes as functions of x_{T2} and x_{T3} only, since

optimum values of these distances should correspond to optimum potency, other factors (electronic, physicochemical, steric) being discounted. As in the GABA system, members of homologous series of glutamate agonists, of wide ranging size, appear to interact with the same excitatory receptor, so flexibility in the receptor charge separations may be deduced.

Taking the x_{T2}/x_{T3} distributions of 2.4.4, it is possible to delineate regions of x_{T2} - x_{T3} space which correspond to high potencies. The values for ibotenic acid may serve as an optimum position, since this is the most powerful of the unbranched glutamate agonists. Then, taking the ibotenic acid values as centre, circles can be drawn of radius ½ Å, 1 Å, etc., which serve in an approximate way to represent regions of progressively decreasing x_R probability. As for the GABA receptor, then, the glutamate receptor is considered to possess optimum charge separations for which optimum potency is attainable. Interactions occurring at other separations are less probable and hence contribute less to the mediation of responses.

x_R probabilities are calculated on a linear scale, taking the ibotenic acid and aminomalonic acid potencies as base points. Potency is taken to be directly proportional to interaction probability. Hence x_R's within the ½ Å circle have a relative probability of 1.0 and those beyond the circle of radius 2 Å have a relative probability of 1/15, giving ibotenic acid and aminomalonic acid respectively, their correct potencies. The intermediate toruses are assigned values by linear interpolation (Fig. 3.5).

Now, calculating interaction probabilities as before, an order of potencies for the glutamate homologues can be predicted (Table 3.5). The results show some correlation between interaction probability and potency on this rough model. The major faults are that aspartic acid is assigned too low a potency and amino adipic acid too high. The aspartate result may be explicable on the grounds that much of its reported activity may be mediated via separate aspartate-specific receptors (see 1.3.3).

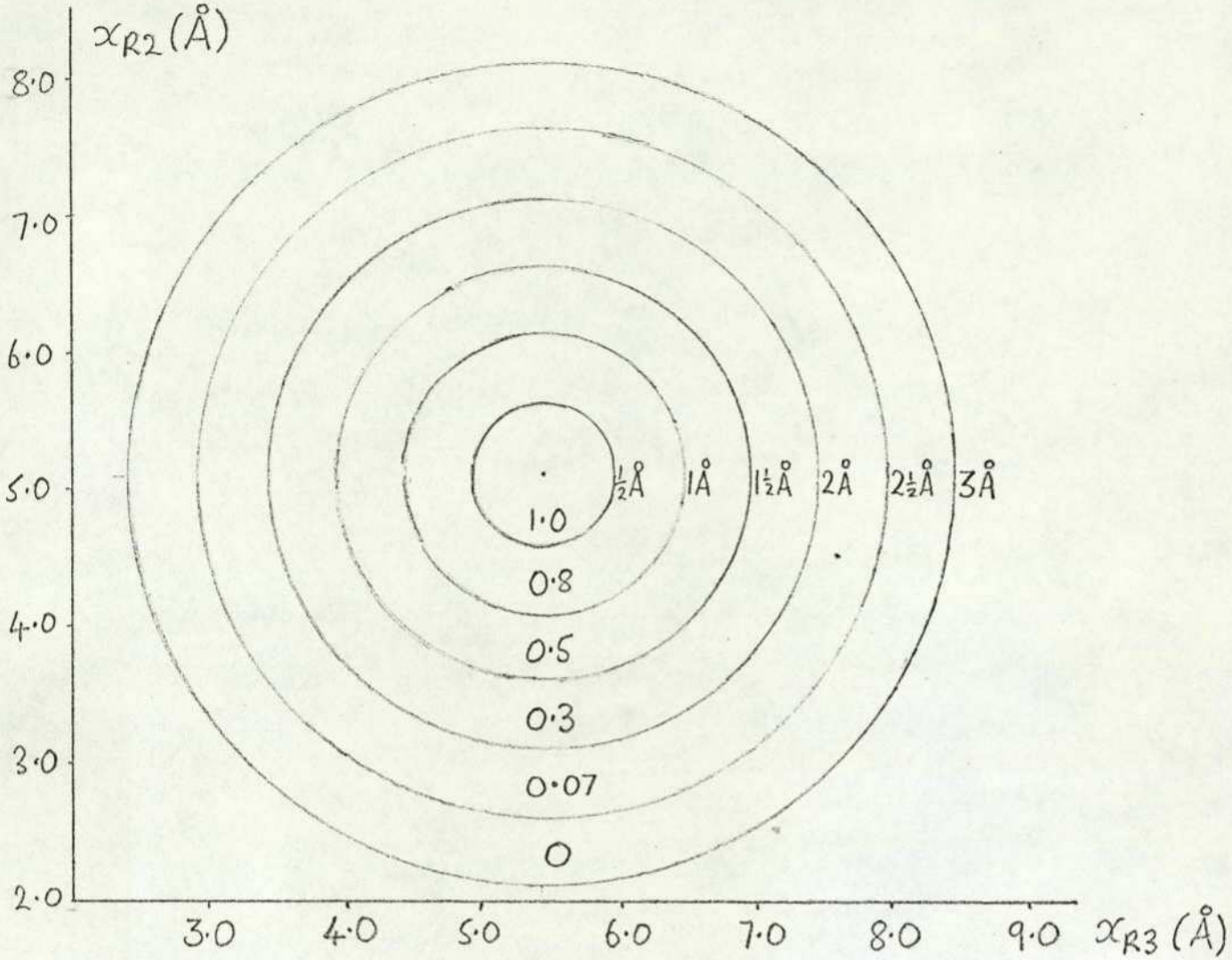

Fig. 3.5 $P(x_R)$ probability toruses for the glutamate receptor. Probabilities (arbitrary units) are indicated within each torus.

Table 3.5 Glutamate agonists: PE SAR results

Substance (i)	T_i	$1/C_i$
Aminomalonate	0.07	0.2
Aspartate	0.23	0.85
Glutamate	0.43	0.85
Aminoadipate	0.44	0.2
Aminopimelate	0.12	0.2
Cycloglutamate	0.90	0.75
Ibotenate	1.00	3.0

Total interaction probabilities (T_i) calculated by superimposing the $P(x_R)$ toruses above on the $P(x_T)$ distributions of Fig. 2.30. Relative potencies ($1/C_i$) from Table 1.2.

The relationship between conformational preference and potency found here is too restricted to be generally useful. It is, moreover, difficult to extend until the electronic effects of different functional groups can be taken into account. Many powerful glutamate agonists, for example, contain SO_3 groups (see Table 1.2) which complicate the PE analysis. Soon, however, the calculation of electrostatic potentials for functional moieties may become possible (see 3.4). Simple conformational considerations of this kind may then be useful in making allowance for the flexibility of molecules while electronic effects are under investigation.

3.3 SAR Using crystal structure and solution conformations

3.3.1 Introduction

So far, only SAR studies using simplified PE calculations have been described (3.2). This technique has the advantage of ready applicability to a wide range of polymethylene chain compounds, even those with a large number of conformational degrees of freedom. (Up to five rotations were treated in 2.4.3). Although the absolute predictions of preferred conformation may not be reliable, trends between them provide consistent results upon which SAR studies may be successfully based. More precise methods of conformational analysis both experimental and theoretical are limited by the number of degrees of freedom which can be treated at once. X-ray crystal structure determinations represent a snapshot of possible preferred conformations (2.2.1). A number of studies of the same molecule crystallised in different forms (e.g. hydrochlorides, hydrates, complexes) may reveal several solid state conformations but can provide no information about relative energies (2.5.2). Dielectric constant measurements will show only an average value of dipole moment in solution, which could be the result of a combination of many different conformations. Some NMR methods require input assumptions about the molecule and in any case become very difficult to interpret when a large number of degrees of freedom are present (2.5.1). Theoretical MO studies allowing for solvent effects (2.3) may provide physically reasonable x_T values (2.5.1), but the computer time required to carry out a full theoretical study for a molecule with more than about three degrees of freedom is prohibitive (2.4.1).

Hence, all methods of conformational analysis have their drawbacks for SAR studies covering a wide range of flexible homologues and analogues of active drugs. Nevertheless, for small molecules the more precise methods may make it possible to allow for conformation in a more realistic way than PE calculations, leaving the field clear for the investigation of finer electronic, physicochemical and steric effects. Accordingly, as mentioned in

2.5.2, the conformational information derived from X-ray crystal structures of GABA and glutamate agonists (2.2) and theoretical solvent effect studies on GABA agonists (2.3) is examined below with respect to biological activity. The intention is not to produce a comprehensive SAR scheme as in the last section, but rather to identify any correlations with biological activity which may be forthcoming from the more precise conformational data.

3.3.2 GABA and glutamate agonists: SAR using crystal structure conformational parameters

(a) Introduction

The usefulness of X-ray crystal structure determinations in neurotransmitter pharmacology (2.5.2) has often been questioned (Gill, 1965; Paton, 1970) since it seems unlikely that conformation in the solid state is a good approximation to conformation in solution. Despite this, however, it has been demonstrated (see 2.5.2) that X-ray and isolated molecule MO predicted conformations show considerable similarities for a wide range of neurotransmitter compounds (Pullman & Courriere, 1973) (2.1). Acetylcholine and some of its analogues in solution exhibit conformational modes which correspond approximately to crystal structure conformations (Partington, Feeney & Burgen, 1971; Beveridge, Radna, Schnuelle & Kelly, 1974) and in the present work some agreement between crystal structure and theoretical solution conformations has been obtained for GABA and glutamate (2.5.2). It may be, of course, that solid-state conformation has a more direct relevance to the receptor environment (2.2.1). Thus it is perhaps premature to discount the results of crystal structure analyses in SAR. They may give as good approximations to relevant transmitter conformations as other methods, particularly when few rotations are involved.

Further, when a number of similarly acting molecules display conformations in which the functional moieties involved in transmitter action exhibit a congruent disposition, it seems reasonable to believe that this may have some significance for

neurotransmitter activity (Kier, 1970). As described in 2.2.1, Beers and Reich (1970) were able to find such congruent dispositions of atoms among the X-ray crystal structures of acetylcholine analogues and relate them to biological activity. In a similar way congruences have been noted in the present work among the crystal structures of GABA analogues (2.2.2) and glutamate analogues (2.2.3) respectively. Thus, it seemed worthwhile here to investigate their possible biological significance.

Limitations of the usefulness of X-ray results in SAR have been mentioned above (2.5.2). In particular, the existence of congruences cannot provide information of relative potency, since the relative stability of different conformations remains unknown. Thus, while X-ray results can indicate common conformations which may relate to transmitter action, relative potencies will not be apparent (2.5.2).

The situation is complicated for amino-acid transmitters by the apparent flexibility of the receptors (3.2.). Any congruences found may relate perhaps to an ideal disposition of receptor-active moieties, but it may not be the only disposition which can be recognised by receptors.

(b) GABA agonists

Considering firstly the recognition aspect of the drug-receptor interaction (2.1), the x_T values of GABA agonists in crystal structures cluster in two narrow regions - $\sim$5.2 and $\sim$ 5.7 Å (Fig. 2.3). All the agonists of potency greater than 1/10 GABA show at least one x_T value in these two regions. The flexibility of the receptor implies that no one x_T is essential, but it is interesting to note that of the nine compounds (including ATA) which possess x_T's in the 5-6 Å region, seven have the same order of potency as GABA itself. Creatine and α-γ diaminobutyric acid also show crystal structure x_T's in the 5.2 Å region, but are of low potency. Although other factors, steric and electronic, may be involved, the implication could be that the crystal conformation of the latter pair of compounds is not that preferred at the receptor.

The long chain GABA agonists ε aminocaproic acid and γ guanidinobutyric acid exhibit fully-extended crystal conformations. It seems unlikely that the GABA receptor could extend far enough to accommodate the large x_T's these fully-extended molecules, so perhaps again, the crystal conformation is not that displayed at the receptor by these materials.

It is not known whether the shorter agonists, glycine, β alanine and taurine act at GABA receptors in their crystal conformations. It is interesting, however, that although these compounds do complex with GABA receptors (Edwards & Kuffler, 1959; Straughan, 1974), they are more often termed 'glycine-line agonists' (Curtis et al, 1968). Their interaction with GABA receptors may just be a side effect of receptor flexibility. The shorter x_T's of these compounds in crystal structures may thus be more indicative of the geometry of glycine receptors.

Although there is some danger in taking the results of one model such as the x_R distributions derived from PE calculations, and trying to fit the results from another, such as crystal structures, it is noteworthy that 5.2 Å appears as a favoured x_T value in both.

This may well be physically significant because the peak region of the x_R distribution is more or less fixed by results from rigid agonists and does not depend upon any assumptions about conformation or the relationship between potency and interaction probability. This being the case, an x_T of $\sim$ 5.2 Å would appear to be necessary for powerful GABA agonism, and moreover, the appearance of such an x_T value in the crystal structure implies powerful GABA agonism in most cases.

The appearance of two x_T congruences among the agonists ($\sim$ 5.2 Å and 5.7 Å), in parallel with pharmacological evidence concerning the differing geometry of postsynaptic and uptake receptors (1.3.3), may be interpreted to mean that the two receptor types respectively accept the two preferred conformations. In view

of the pharmacological (1.3.3) and SAR (3.2.3) evidence that a partially folded molecule is favoured for the postsynaptic receptor, the implication is that the uptake receptor prefers molecules with the larger charge separation. This is also in keeping with the pharmacological evidence (Beart et al, 1972). Thus, congruences of x_T in crystal structures are consistent with the preferred conformations predicted by pharmacological results.

As suggested in 2.2.1, precise congruent dispositions of atoms found in crystal structures may relate to the bound state of a transmitter molecule at the receptor, while x_T measurements relate to recognition. Hence, having considered x_T values, it is now appropriate, secondly, to investigate congruences of atomic disposition in crystal structures.

The derivation of a more detailed geometry of the GABA receptor in this manner is very uncertain. It is possible that a three point interaction is involved in transmitter-receptor binding (1.3.3), which may relate to the approximate congruences of N-O-O triangles in crystal structures, noted in 2.2.2. In two groups of powerful GABA agonists the angle N-O-O is $50^{o} \pm 10^{o}$ with the longer N-O distance about 5.7 Å in the first group and 6.2 Å in the second. These congruences are illustrated in Fig. 2.5. The two groups of agonists correspond to the two groups with x_T's 5.2 and 5.7 Å respectively, described above. This could indicate a disposition of three complementary hydrogen bonding sites on the receptors for transmitter action and uptake, but it does not prove that three points of interaction are involved. The N-O distances themselves for powerful agonists, which again may be complementary to hydrogen-bonding sites on receptors, fall into five loose clusters (Fig. 2.3); 4.2, 4.6, 5.3, 5.7 and 6.2 Å. The suggestion of 5.8 ± 0.2 Å for the GABA 'pharmacophore' made by Kier et al (1970, 1973, 1974) corresponds to a combination of the latter two groups.

The crystal structure and solution conformations of bicuculline show only limited congruence with crystal structure

conformations of GABA agonists, displaying N-O distances of 5.6 Å and 5.3 Å respectively, but very low N-O-O angles (see Fig. 2.5). One of the N-O-O triangles of βGP, also a GABA antagonist in some preparations, is closely similar. It is unlikely, however, that this congruence is significant for antagonistic activity, since electronic effects are likely to be more important (Steward, Borthwick, Clarke & Warner, 1975).

Thus X-ray crystal structure results for GABA agonists indicate conformational preferences which parallel those suggested by other methods (2.5.2). The congruences which are found are compatible with the properties of the GABA receptor derived from pharmacological results and from the PE SAR study of 3.2.2. They may also provide some support for the notion of different geometries for the uptake and transmitter receptors.

(c) L-glutamate agonists

Comparison of conformation results for L-glutamate agonists is much more complicated than for GABA agonists, owing to the presence of a third functional group. As mentioned above, however, (2.2.3, 2.4.4) simplifying assumptions can be made which enable comparisons to be effected. The α end of each molecule is thus considered constant, and the positional variation of the ω end between molecules is investigated.

Considering, firstly, the separations of the functional groups, it can be seen from Fig. 2.7 that the positions of many of the ω functional groups in crystal structures fall into two loose clusters; centred at x_{T2} = 5.0 Å, x_{T3} = 5.7 Å and x_{T2} = 3.7 Å, x_{T3} = 4.9 Å. The former cluster contains x_T's from all the most powerful glutamate agonists considered, except allokainic acid. Since kainic and allokainic acids differ only in inversion of a side chain, however, it is likely that allokainic acid could also exhibit a conformation having x_T's within the cluster.

The second cluster, with the ω group closer to the α end of the molecule, contains both crystal forms of cysteate and aspartate.

These are both glutamate agonists of potency ~ glutamate (Table 1.2) but there is evidence (1.3.3) that aspartate is a neurotransmitter in its own right. The implication from the crystal structure results, then, could be that the glutamate receptor is complementary to the disposition of functional groups represented by the first cluster, and the aspartate receptor is complementary to the second cluster.

Secondly, detailed examination of interatomic distances may reveal more precise information about glutamate receptor geometry. Many parameters could be considered, but this discussion will be limited to the distances between α charge centres and ω oxygens (Fig. 2.6). Clustering of distances is not clear in this case, since each compound shows at least two pairs of distances, one for each oxygen atom. Nevertheless, two regions in Fig. 2.6 include compact groups of distances from several substances. A circle of radius 0.5 Å centred at x_1 = 5.4 Å, x_2 = 6.2 Å contains distances for the powerful agonists homocysteic acid, kainic acid and the two crystal forms of glutamic acid itself. The range of distances which ibotenic acid can display also fall partly within this circle. In particular, the isolated molecule minimum-energy conformation predicted by CNDO/2 calculations (Borthwick & Steward, 1975) gives x_1 = 6.1 Å, x_2 = 5.9 Å for the exocyclic oxygen, which lies just at the edge of the circle.

The second group is centred at x_1 = 4.3 Å, x_2 = 5.3 Å. A circle, radius 0.5 Å, around this point contains distances for both forms of aspartate and cysteate and for one form of glutamate itself. (The minimum energy conformation of ibotenic acid predicted by SOLVEFF (Borthwick, unpublished work) possesses x_1 and x_2 values for the ring nitrogen atom within this circle.) The implication is, again, that the first group represents distances of importance for the glutamate receptor and the second distances for the aspartate receptor, but the looseness of the grouping precludes any firm conclusion.

The disposition of functional groups suggested by Johnston et al (1974) for the glutamate receptor, on the basis of molecular

models, corresponds to $x_{T2} \simeq 4.8$, $x_{T3} \simeq 5.5$; $x_1 \simeq 5.0$, $x_2 \simeq 5.2$. These distances fit into both the glutamate receptor clusters described above in the respective crystal geometry diagrams (Figs. 2.7 and 2.6). The conformation suggested for glutamate in the paper above is not far from its crystal conformation in L glutamic acid hydrochloride (Table 2.3). Hence, again, some correspondence is observable between crystal structure conformations and the predictions of pharmacological results. Prediction of pharmacological activity on the grounds of crystal structure conformation, however, remains hazardous, since the relative stability of different rotomers is unknown (2.5.2). The use of solid-state conformation in SAR studies is discussed further in 3.4.1.

3.3.3 GABA agonists: conformational SAR using SOLVEFF results

(a) Introduction

Both PE and X-ray conformational results from Chapter 2 have been employed, above, in establishing SAR among amino acid transmitters. The remaining conformational data obtained during the present work is that derived for GABA and some of its agonists by the SOLVEFF method (2.3), introducing aqueous solvent effects into the isolated molecule CNDO/2 energy surfaces for these substances. This method is theoretically the best reported in the present work for SAR studies on small molecules, since it combines complete conformational investigation (as in PE calculations) with precision of results (as in X-ray crystal structure determination). In practice, of course, there are limitations: complete conformational investigation is very expensive in terms of computer time, so in all the molecules investigated, some rotations have been permanently set in one position; and the accuracy of results, although in broad agreement with such experimental measurements as are available (2.5.1) cannot be shown to be comparable to crystal structure determination.

Despite this, it was considered worthwhile to attempt, with the limited number of results available, a similar SAR analysis

to that of 3.2. The more precise results from SOLVEFF should, it was hoped, allow for conformation more effectively than the PE analysis, and thus indicate the significance of other factors. A receptor model was developed, based on the results of 3.2, and a plot of log(1/Ci) against log(Ti) constructed. Details of the method and results are described below.

(b) Method

An analytical $P(x_R)$ curve for the SOLVEFF results was first calculated. The curve was slightly different from that in 3.2, since β alanine, whose conformation is used in the defining equations for $P(x_R)$ (see 3.2.2d), is predicted by SOLVEFF to exist exclusively trans, whereas PE calculations predict ~50% gauche. The defining equations became (retaining m = 2 for the assumed regression slope value (see 3.2.3)):

βalanine: $\log(.06) = 2(\log a - b(4.65 - x_o)^2)$
Muscimol: $\log(1) = 2(\log a - b(5.16 - x_o)^2)$
ATA : $\log(.32) = 2(\log a - b(5.65 - x_o)^2)$

Solving for a, b, x_o gave the equation for $P(x_R)$:

$$P(x_R) = 1.039(\exp(-4.007(x_R - 5.258)^2))$$

This curve is illustrated in Fig. 3.3 with the PE $P(x_R)$ curve for comparison. The 5.2 Å region again appears as the preferred x_T value for GABA-like transmitter action.

The SOLVEFF x_T distributions calculated in 2.3.3 (see Table 2.7 and Fig. 2.26) were then employed to calculate total interaction probabilities (T_i) for the seven substances considered (Table 3.6).

Taking approximate potencies from Table 1.1, $\log(1/C_i)$ (see Table 3.6) was plotted against $\log(T_i)$, as shown in Fig 3.6.

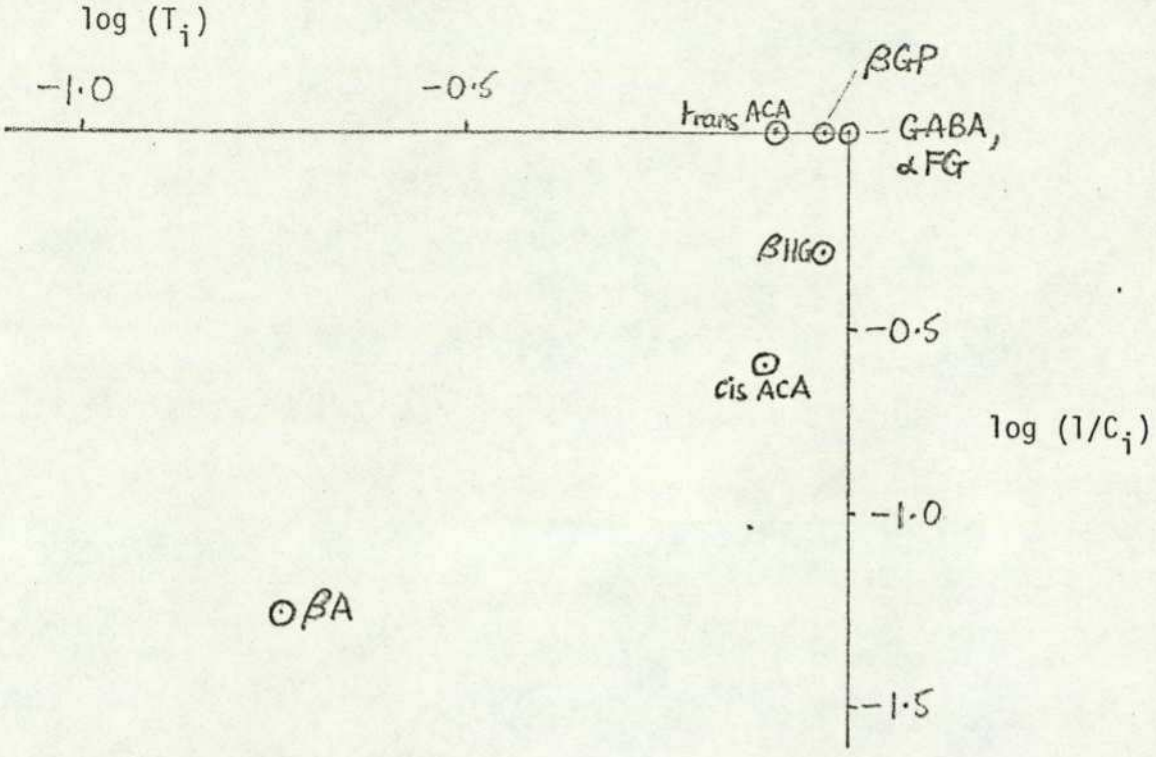

Fig. 3.6 SOLVEFF SAR results

Table 3.6 SOLVEFF SAR results

Substance (i)	log (T_i)	log ($1/C_i$)
GABA	.007	0
α fluoro-GABA	.007	0
β hydroxy-GABA	- .027	- .301
β alanine	- .737	- 1.253
cis ACA	- .103	- .602
trans ACA	- .092	0
βGP	- .020	0

for potency references, see Table 1.1

T_i = total interaction probability

$1/C_i$ = relative potency

(c) Results and discussion

With the exception of β alanine and βGP, all the compounds considered here are of the same chain length as GABA, and the conformational differences between them are small (2.3, 2.5). Conformation will thus not affect their potencies as profoundly as it does for compounds of widely differing chain length, and other factors are likely to be apparent. As might be expected, then, the results indicated in Table 3.6 and illustrated in Fig. 3.6 show that quantitative correlation between log(potency) and log(total interaction probability) is lacking for the SOLVEFF conformations. It is also true to say, however, that little relationship exists in the PE calculations for compounds of similar chain length. It is only when large ranges of x_T are apparent in the series of compounds under investigation that conformational SAR works well without considering other factors which affect potency.

The SOLVEFF method, although not immediately applicable to long-chain compounds, should in principle provide a better basis than PE calculations for allowing for conformational preference among a series of agonists. This should clear the way for the investigation of the effect of other parameters on potency (see 3.4.2) provided that SOLVEFF results for x_T's are physically realistic. As described above (2.5.1), experimental results provide some support for the predictions of SOLVEFF, but it cannot yet be shown experimentally whether the small differences in x_T between compounds of similar chain length are really significant.

The results for βGP are interesting in view of the possible mechanism of partial agonism suggested in section 3.2.2. The peak x_T values predicted by SOLVEFF for βGP are 4.8 Å and 5.7 Å, a little removed from the values for GABA etc. ($\sim$ 5.2 Å). The x_T probabilities at these peaks are high (see Fig. 2.26), such that although the binding of βGP to a GABA receptor would be efficient, it would occur at x_R values away from the ideal and may thus be less effective at mediating a response.

3.4 Discussion of SAR results

3.4.1 Preferred conformation as a predictor of amino-acid neurotransmitter activity

Conformational preference for α-ω amino acids is strongly influenced by the presence of the charged terminal groups (2.1). This causes isolated-molecule MO calculations to predict highly folded preferred conformations for these molecules (Warner, 1975; Pullman & Berthod, 1975). If such conformations were important at receptors, small molecules such as glycine and βalanine could be expected to exhibit higher potencies as GABA agonists than they do. Hence it is unlikely that the folded isolated molecule results are relevant to the biological activities of amino acid transmitters (2.1). The situation is different, however, for these molecules in the solid state or in solutions with dielectric constant greater than $\sim$10 (2.3.3). In such environments, intermolecular forces overwhelm intramolecular electrostatic attractions, causing the molecules to adopt more extended forms (2.5.2). SAR studies using crystal structure (3.3.2) and solution conformations (3.2, 3.3.3) have, accordingly, been more fruitful.

The conformation of molecules in the biophase is perhaps the most reasonable starting point for SAR studies on transmitter-receptor interactions (2.1). Experimental methods for the determination of solution conformation are not yet well developed (Pullman & Pullman, 1975) especially for molecules with large numbers of possible rotations about single bonds, so theoretical techniques as described in Chapter 2 are desirable. These have been shown to give results reasonably consistent with such experimental data as are available (2.5.1), particularly with regard to the separation of terminal groups as measured by the x_T parameters, which may relate to the separations of functional moieties at the receptor (2.1). The use of simple PE aqueous solution conformations has enable a quantitative structure-activity scheme for GABA agonists (3.2.2-3) and a semi-quantitative scheme for some glutamate agonists (3.2.4) to be developed. The success of such schemes

may provide some support for the use of the x_T parameter in these studies, rather than more complicated molecular measurements. Provided no gross steric effects are involved, preferred x_T in solution seems to predict biological activity in a significant way, although, as is usual in biological measurement, the margins of error are large (3.2.3).

Nevertheless, preferred x_T values do not account for differences in biological activity between agonists which display closely similar conformations in solution. This is apparent in the PE (3.2.3) and more sophisticated SOLVEFF (3.3.3) results for GABA. The calculations may well allow for conformation successfully in these cases, as they appear to do for agonists of wide ranging x_T, but the effect of other factors overwhelms conformational preference when differences in conformation are small. The other factors, electronic, physicochemical and steric, likely to be involved are discussed in 3.4.2.

Overall, then, aqueous solution conformation does appear to be a good starting point for studies of conformation effects on the biological activities of amino acid transmitters. The results make much more sense than comparison of isolated molecule conformations or conformations in lipid media, which are very similar (2.3.3). The question which now remains is what may be learnt from the third state in which transmitter molecules are frequently studied - crystal structures.

For GABA agonists, crystal structures show two sets of closely similar x_T's (at $\sim$5.2 Å and $\sim$5.7 Å) and, indeed, corresponding N-O-O triangles. One of the x_T groups, moreover, is in close agreement with the optimum x_T ($\sim$ 5.2 Å) for GABA-like transmitter activity found using pharmacological results, during SAR studies employing solution conformation (3.3.2). A similar, though less precise, result is found for the glutamate agonists (3.3.2). However, the agonists which exhibit crystal structure conformations with 'ideal' x_T's are not in every case the strong agonists, and some strong GABA agonists, for example, show x_T's in the second group ($\sim$ 5.7 Å). Hence, while congruences of conformational preference

found in crystal structures can indicate conformations or x_T's which are important in transmitter activity, other congruences may also appear. Further results from different methods are then required to resolve the ambiguities. In the case of GABA agonists, for example, pharmacological results suggest that the 5.2 Å x_T may be that involved in transmitter activity and 5.7 Å may be the x_T value important at the uptake receptor (1.3.3). The former suggestion is, of course, supported by the theoretical results (3.2.3, 3.3.3). In the case of glutamate agonists, the two regions of preferred x_T combinations found in crystal structures may relate to the distinct aspartate and glutamate receptors suggested by pharmacological results (Duggan, 1974), although such a conclusion is necessarily tentative.

The theoretical basis for the use of crystal structure conformations in SAR is by no means clear, but may rest on the similarities between crystal structure and aqueous solution preferred conformations as found here (2.5.2), particularly for GABA, and in other series of transmitters (Beveridge et al, 1974[a]). Similarities between structures around receptor binding sites and the crystalline environment of small transmitter molecules may also be a significant factor.

Thus, while preferred rotamers in aqueous solution remain the most reliable conformational predictors of biological activity for amino acid transmitters, crystal structure results may be a valuable source of information, revealing likely conformations at receptors via congruences in the solid state.

3.4.2 The importance of further parameters in SAR

Conformation profoundly affects the action of highly flexible drug molecules, such as neurotransmitters, but pharmacological activity is not dependent upon conformational preference alone. Although the SAR studies of the present chapter successfully allow for gross conformational effects, they do not predict well the relative potencies of molecules with similar conformational preference. The small differences in conformation observed in the

SOLVEFF results, for example, do not account for the differences in potency of the agonists (3.3.3).

For GABA and glutamate and their respective agonists, most of which can be considered to behave as a system of linked discrete charges, it may be possible to factorise the main features responsible for pharmacological activity into two major parameters. Firstly, conformational preference and, secondly, electrostatic potential due to the charged groups. The present work has considered the first of these only, so a brief discussion of the possible involvement of electronic parameters in subsequent SAR studies is presented here. The influence of physicochemical and other steric parameters is also considered.

Computer programs are now available to calculate the electrostatic potentials due to functional groups within molecules. Preliminary calculations of this kind have been carried out (Borthwick & Steward, 1975[c]) on the carboxyl groups of the GABA agonists α fluoro-GABA, β hydroxy GABA and GABA itself. These molecules have such similar conformational preferences, as predicted by SOLVEFF (2.3.3, Fig. 2.26), that conformation is effectively factorised out, as a first approximation. It would appear that the higher the electrostatic potential of the negative group, the higher is the potency of the compound.

The electrostatic energy of a point charge in the potential field of the molecule can be calculated from the potential itself, and is a measure of that potential. This leads to an interesting possibility; maximum or minimum electrostatic energy for respective ends of the molecule could be included in a linear free energy relationship together with total interaction probability from conformational calculations.

Then: $\log(1/Ci) = a \log(Ti) + bV^{+} + cV^{-} + d$

Multiple regression analysis could provide values for the coefficients, producing an equation which may be able to predict the pharmacological activity of a compound. Thus, the conformational

and electronic approaches to potency correlation could be harmonised. To be useful, a correlation of this kind would require the involvement of compounds of wide-ranging size, containing various functional groups. It is possible that this method would take account of electromeric effects, which may be responsible for the ineffectiveness of some aromatic GABA analogues (1.3.1) as GABA agonists.

Physicochemical parameters do not appear to correlate well with amino-acid transmitter activity (see Appendix 5). Sulphonic acid derivatives, for example, have very much lower partition coefficients between water and octanol (i.e. lower hydrophobicity) then corresponding α-ω amino acids, but their potencies do not differ accordingly. Most of the usual physicochemical parameters employed in PAR work are, in fact, highly dependent upon molecular size in homologous series of compounds, so they do not correlate with transmitter activity which peaks at a chain length of 3 (1.3.2). Receptor fit and the long range electrostatic forces involved in the transmitter-receptor interaction (2.1) override considerations of hydrophobicity and pk.

The problem of steric effects is limited to the interference of parts of the agonist molecule with its approach and/or binding to the receptor. Internal steric effects (limiting the flexibility of the molecule) are taken into account by conformational analysis. It may be that the inactivity of aromatic GABA analogues is due to steric rather than electromeric effects and that branched GABA agonists (e.g. β aminobutyrate, β hydroxy GABA, etc) may also encounter some steric hindrance in their interaction with receptors. The Taft steric parameter (Appendix 5) which provides some measure of the 'bulkiness' of a molecule, may be useful in this respect, but it is correlated with gross molecular size rather than branching alone. A systematic investigation of the effect of substitution on strong agonists could perhaps reveal details of receptor geometry.

Overall, then, conformational and electrostatic parameters appear the most important factors, while steric hindrance can also

influence potency to some extent. The effectiveness of conformational parameters, together with a flexible receptor model, in establishing SAR in the GABA system, has underlined the importance of flexibility in the transmitter-receptor interaction. Hence, in the next chapter the implications of the SAR results, particularly receptor flexibility, are taken further, and possible structures for the GABA receptor are discussed.

4. A PLAUSIBLE MODEL FOR POSTSYNAPTIC GABA RECEPTORS

4.1 Introduction

Structural theories about amino-acid receptors generally propose that charged sites in macromolecular proteinaceous receptor material are the units primarily involved in the interaction with transmitters. The separation of the charge centres and the associated molecular structures have been, nevertheless, a subject of debate, as was described in 1.3.3. The most recent and comprehensive attempt at a molecular description of the GABA receptor is that of Smythies (1974). This model is speculative in its details, but its basis - a pair of bridged β pleated sheets - has long been envisaged (Kutsnetsov & Ghokov, 1962) as a plausible model for receptor structure. Details of the receptor were developed via complementarity with the structure of antagonists.

The present chapter, drawing on inferences from the SAR studies of chapter 3, principles of protein structure and the bridged β-pleated sheet model for receptors, seeks to present a picture of the GABA receptor which may provide a useful basis for further work, (see 5.4). This discussion is necessarily speculative but is compatible with contemporary hypotheses on receptor mechanism (1.2.2) and the dimensions and flexibility of receptor sites indicated by the present work (3.2). A geometrical description of the transmitter-receptor interaction process which has received some support from MO calculations is also suggested here. The geometrical features of a bridged β-pleated sheet model are shown to be consistent with preferred conformations and charge-separations of GABA agonists.

It is noteworthy that inferences from SAR studies on agonists (4.2.1) lead to suggestions on receptor geometry compatible with Smythies' proposals (4.3) which are developed from considerations of protein structure (see 4.2.2) and the structure of antagonists. This correspondence between different approaches may perhaps be taken as an indication that the model produced is worthy of further investigation.

The extension of the model to glutamate receptors is also briefly examined.

4.2 Evidence

4.2.1 Inferences from SAR results

The results obtained from SAR studies on GABA agonists and on glutamate agonists support the suggestion (Curtis & Wakins, 1960) that the respective receptors are flexible, each possessing opposite charge centres which can vary in separation, x_R (3.2.3). The receptors can accommodate drug molecules which range in size, and more specifically in charge separation, x_T. For interaction to occur $x_R = x_T$. For GABA agonists, for example, each individual receptor can exhibit a continuous range of charge separations, x_R. Agonist molecules which possess x_T's the same as, or near, the equilibrium x_R distance will mediate a response more effectively than those which interact with receptors at low or high x_R. Moreover, flexing of the receptor to make $x_R = x_T$ may be envisaged, such that interactions at or near the equilibrium x_R are energetically more probable.

It should be stressed that x_R does not necessarily indicate an actual separation between groups in the receptor. It is merely a device to quantify the concept of receptor flexibility and is designed to complement the agonist x_T distance. For example, in Fig 4.1, it can be seen that either arrangement, a) or b), of receptor groups can interact with a transmitter molecule of length x_T but that only in a) does x_R equal the actual distance between active moities of the receptor. In situation b), although x_R is closely related to such an inter-group distance, it is not equal to it. Care must be taken, therefore, when possible receptor groups are examined, to allow some leeway (perhaps 2-4 Å) between x_R and the physical distance between groups.

The x_R distribution curves developed above, suggest that the receptor groups may be constrained in an equilibrium position by interatomic forces (mechanical and/or electrostatic) which allow a certain measure of flexibility in x_R, at least during the period

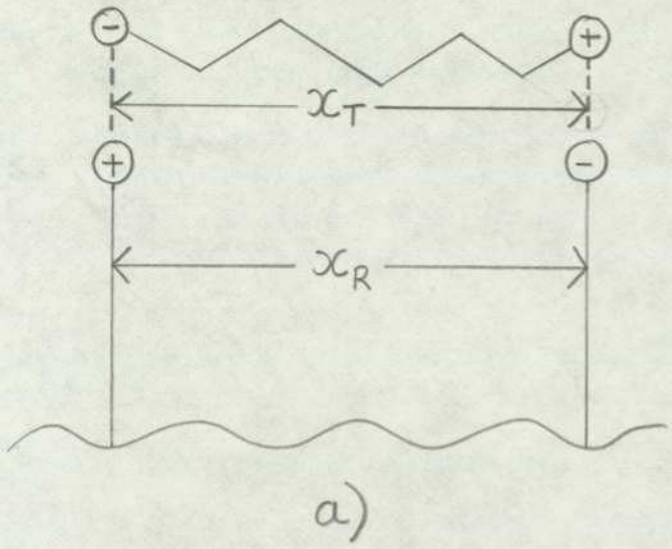

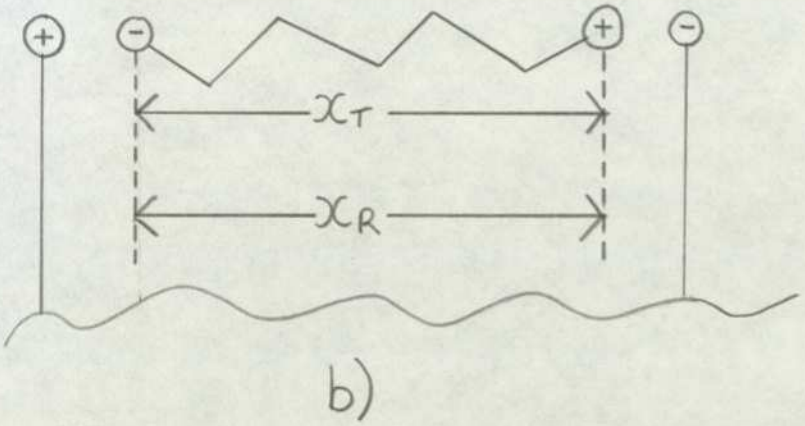

Fig. 4.1 Physical significance of x_R (see text)

of close approach of an agonist molecule. It is perhaps unwise to postulate further details than this on the basis of an approximate method, but further information about likely receptor structure may be gleaned from the growing fund of knowledge on protein architecture.

4.2.2 Inferences from protein structure

Gill (1965) draws together a number of important threads about protein structure, relevant to receptor theory and consistent with the observations in 1.2.3b about the generation of biological response. To begin with, the major force which constrains protein macromolecules in an organised secondary and tertiary structure is not hydrogen-bonding as is often supposed: rather, hydrophobic bonding and electrostatic interactions between amino-acid side-chains are the important agents. A recent study supports the role of side-chain interactions in secondary structure stabilisation (Ralston & De Coen, 1974). Although, the dielectric constant assumed for proteins by Gill may be too low by an order of magnitude (Tredgold 1973), it would still appear that electrostatic interactions of this kind make a major contribution to the stability of protein structure. A corollary of this is that a disruption of such interactions may be the modus operandi of transmitter molecules such as acetylcholine (Gill, 1959). The transmitter molecule could cause a disruption of structure which increases the permeability of the synaptic membranes; it could, for example, trigger a ferro-electric transition in a neighbouring part of the macromolecular receptor, opening ionic channels. This kind of allosteric transition is the process suggested by Changeux et al (1970) for the agonist protamer (1.2.1) and is consistent with the pore-forming model system described by Urry (1972) using the antiobiotic gramicidin (1.2.2b). GABA and glutamate, with their highly-charged functional groups, may well act in a similar way to that envisaged above.

For specific receptors to exist, it is reasonable to believe that receptor sites consist of ordered regions of protein secondary structure, that is of α helices and/or β pleated sheets.

In aqueous solution 15% - 50% of amino-acid residues in proteins are likely to exist in coiled arrangements (Gill, 1965). Overall, proteins in solution possess segments of helix or pleated sheet regions interspersed with extended open-chain ragions (Gill, 1965).

The most important forces in the drug-receptor interaction are likely to be hydrophobic and electrostatic (Gill, 1965). For the highly-charged amino-acidtransmitters electrostatic interactions probably predominate. If, accordingly, amino-acid receptors consist of charged moieties complementary to the charges on the agonists, the possible protein amino-acid units involved are limited to only five, three positively charged (arginine, histidine and lysine) and two negatively charged (aspartate and glutamate) at neutral pH. Moreover, the possible arrangements of such units in ordered protein segments is also limited. In α helices, adjacent β carbon atoms are 5.5 Å apart, and in β pleated sheets, 4-5.5 Å apart (Gill, 1965). Thus, since amino-acid transmitters are small molecules, it is unlikely that the receptor consists of more than three or four such functional groups. The flexibility of the receptor would depend upon the flexibility of the amino-acid side-chains which were involved. Clearly, arginine and lysine could exhibit most flexibility, glutamate somewhat less and aspartate and histidine little at all.

Thus, considerations of protein structure limit the range of possible molecular building blocks of which amino acid receptors could consist.

4.3 A model for the GABA receptor interaction

4.3.1 Receptor geometry

A detailed molecular description of the GABA receptor has been proposed by Smythies (1974) based on two β pleated sheets hydrogen bonded together by a ladder of arginine-glutamate bridges (Fig. 4.2). This type of grid structure for receptors was suggested by Kutsnetsov and Ghokov (1962). The geometry of the Smythies GABA receptor is developed from a Kutsnetsov-Ghokov grid by consideration

a)

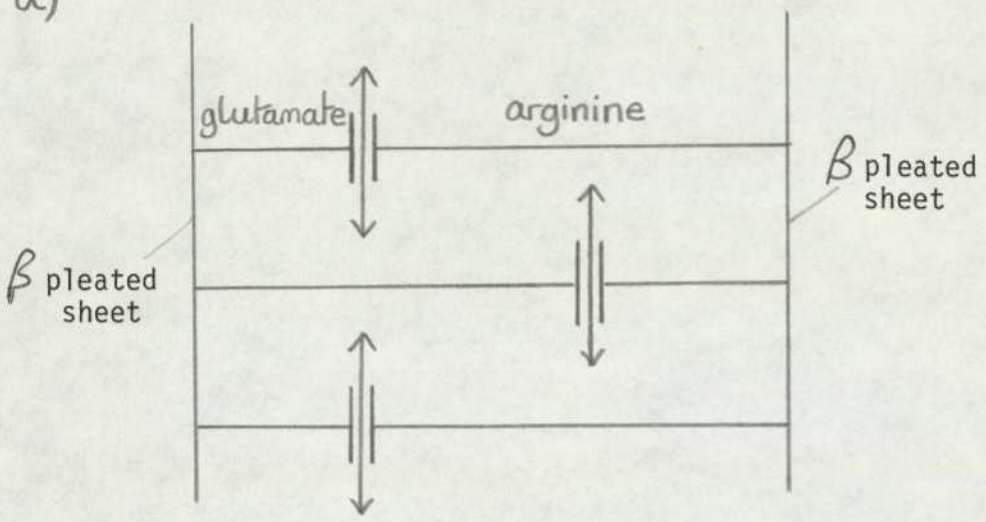

Schematic diagram of the bridged β pleated sheet structure. Arrows indicate directions of flexibility.

b)

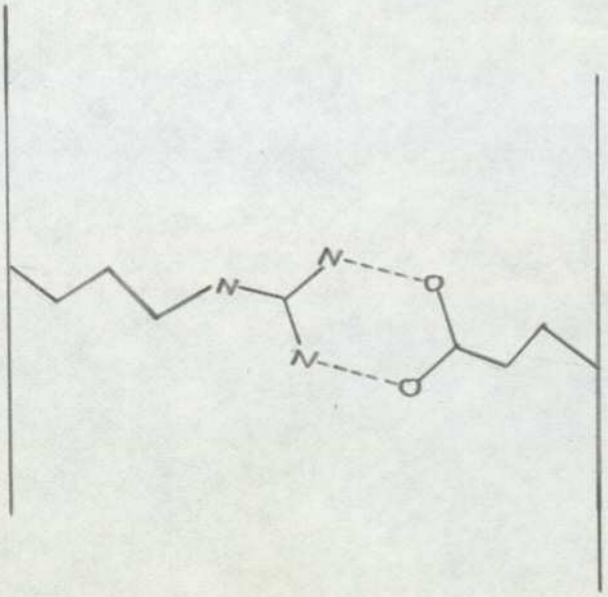

Fig. 4.2 Arginine-glutamate bridges between β pleated sheets

The arg-glu moieties can be arranged in a number of ways, but the vertical form illustrated here may be sterically favoured.

of the molecular structures of GABA, bicuculline and picrotoxinin and the constraints of protein architecture. It is doubtful whether picrotoxinin does in fact act at the GABA receptor (1.2.1) but the suggested model does fit the general principles of receptor structure discussed above. The details of the structure, including secondary chains around the receptor, are not yet vindicated by the limited evidence available, but the basic concept of the GABA receptor as a Kutsnetsov-Ghokov grid is not unreasonable. Four arginine-glutamate bridges are involved in the Smythies model (Fig. 4.3), but it is hard to justify this precise a picture on the data available. A GABA receptor of only two bridges is conceivable, or, alternatively, an extended ladder structure permitting co-operative interactions could be proposed.

The Smythies model is open to experimental investigation via pharmacological tests on a number of compounds which are predicted to display antagonistic activity. The results of such studies should prove most instructive but none have yet been reported. Alternative suggestions for the molecular structure of the GABA receptor could be made involving neighbouring pairs of amino-acid bridges on a single β pleated sheet or even on an α helix, but the paired β sheet model does seem most likely, since β sheets and α helices themselves normally appear to be stable.

It is likely that, if the receptor resides in an aqueous environment, the arginine-glutamate bridges will be unstable, since hydrogen-bonding between water and the arginine and glutamate terminal groups is energetically just as favourable as bonding between the terminal groups themselves. Electrostatic interactions between arginine and glutamate will be stronger. The approach of a GABA agonist could disrupt the electrostatic links and cause a change in the structure of the surrounding protein.

Consideration of a model of a Kutsnetsov-Ghokov grid as in the Smythies proposal (Fig. 4.3) indicates that flexibility in the distance between the arginine and glutamate terminal groups in adjacent rungs of the ladder is possible and could relate to the x_R

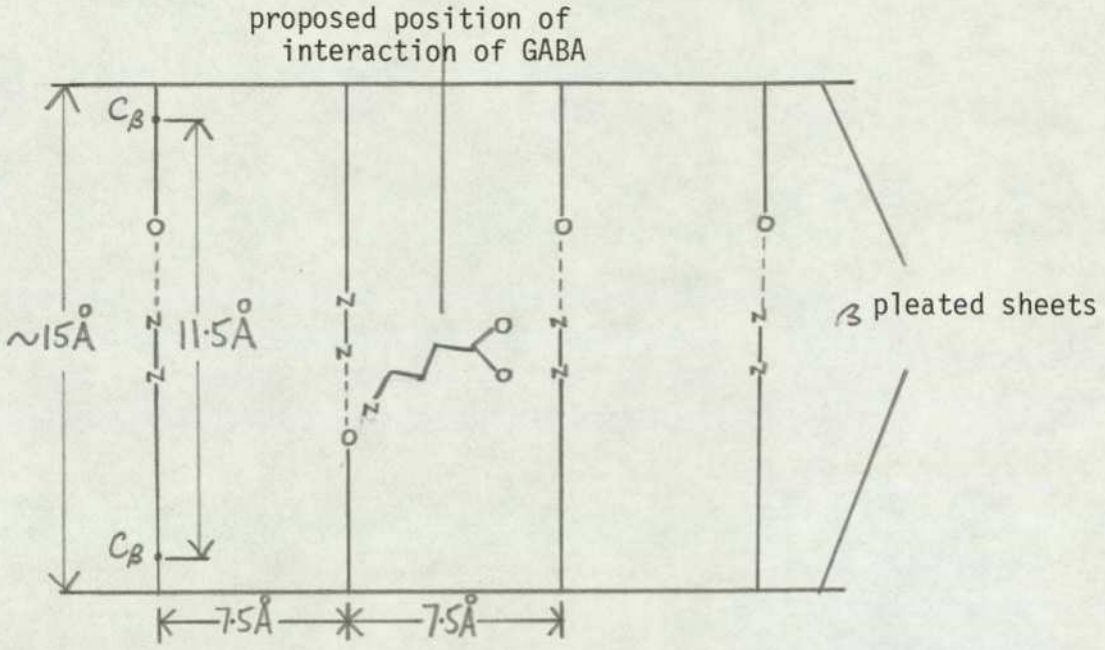

Fig. 4.3 The Smythies GABA receptor model-schematic diagram

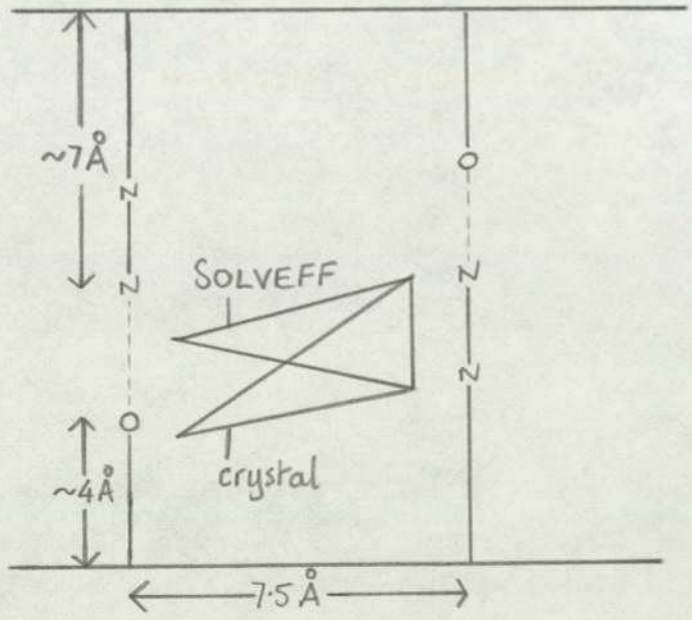

Fig. 4.4 Suggested geometry of the GABA-receptor interaction SOLVEFF and crystal structure GABA N-O-O triangles are indicated (cf. Fig. 2.16)

distribution predicted in the SAR studies above (3.2). Since the arginine-glutamate bridges would be held together largely by electrostatic interactions (see above) the functional groups would possess some freedom of movement, being constrained by the electrostatic forces and the rotational barriers of the chains. A mechanism of x_R flexibility may thus be envisaged (Fig. 4.2a). The α carbon atoms of the neighbouring arg-glu bridges are 7.5 Å apart, which makes the distance between the arginine guanidino group and the glutamate carboxyl group (not necessarily equal to x_R (4.2.1)) compatible with the convenient approach of a GABA molecule with $x_T \sim 5.2$ Å. Such an x_T value, of course, is not the only one which could be accepted by the receptor, but consideration of molecular models shows that such an arrangement could be an ideal one. The N-O-O triangles commonly found among the crystal conformations of GABA agonists with $x_T \sim 5.2$ Å (Fig. 2.5) fit neatly into the space between the hydrogen-bonding sites (see 4.3.2) on adjacent arg and glu moieties in the Kutsnetsov-Ghokov grid (Fig. 4.4). The SOLVEFF N-O-O triangle (Fig. 2.16) is not such a good fit, although the x_T value remains the same.

Model building, of course, has its limitations. The precision of measurement attainable, and indeed, the present state of our knowledge of receptor mechanism are insufficient to conclude from the above that any particular conformation is the ideal for GABA-like activity. Nonetheless, the consistency of this model with the results of conformational analysis (2.5) and the predictions of SAR studies (3.2) render further investigation along similar lines desirable. Proposals can be made, for instance, as to the geometrical interaction processes which may occur on transmitter approach.

4.3.2 Geometrical interaction processes

Taking the Smythies receptor model described above as a starting point, suggestions concerning the geometrical mechanism for the GABA-receptor interaction may be made as follows. The arginine-glutamate complex possesses a pair of hydrogen-bond accepting sites (the chain nitrogen and one of the terminal nitrogens

of the guanidino group) into which the carboxyl group of GABA could fit, being attracted initially by electrostatic forces (Fig. 4.5a). The effect of this could be to disrupt the arginine-glutamate electrostatic link (Fig. 4.5b). CNDO/2 reaction path studies (Livingstone, unpublished work) for this kind of interaction in isolated molecules have indicated a slight tendency in this direction. Little charge-transfer is observed, so the inherent flexibility of the transmitter will not be greatly affected (2.1). Solvent effects may be expected to increase the disruptive effect, since CNDO/2 calculations on isolated molecules predict very stable hydrogen bonds (Borthwick, Livingstone & Steward, 1975) which are unlikely to occur in solution (Gill, 1965). Finally (Fig. 4.5c) the positive tail of the GABA molecule could link up with an adjacent glutamate carboxyl group, breaking a second bridge and allowing the previously linked β pleated sheets to move apart. This may immediately form an ionic channel in the structure (cf the sodium channel model of Smythies et al (1974[b])) or may precipitate a structural transition elsewhere, resulting in channel formation. This would correspond to the allosteric receptor mechanism postulated by Changeux et al (1970) described in 1.2.2 and would be consistent with the observation (1.2.1) that the receptor and permeability mechanism for GABA-mediated inhibition are distinct although closely associated. The GABA molecule could be removed by diffusion as the concentration in the external medium drops, or be displaced by the reverse procedure to Fig 4.5, on the rebound. The uptake mechanism would then complete the process (1.3.2).

4.3.3 Extension to the glutamate receptor

A glutamate receptor could be constructed along similar lines, but involving a second positively charged group. This could be situated in an adjacent region of one of the β pleated sheets of the GABA receptor. Since similar x_T values seem to be favoured in both GABA and glutamate agonists (see 3.3.2), it may be reasonable to believe that the two receptors are themselves similarly constructed. It would perhaps be wiser, however, to wait for further pharmacological and structural evidence on glutamate analogues before attempting to develope a detailed molecular picture of the glutamate receptor.

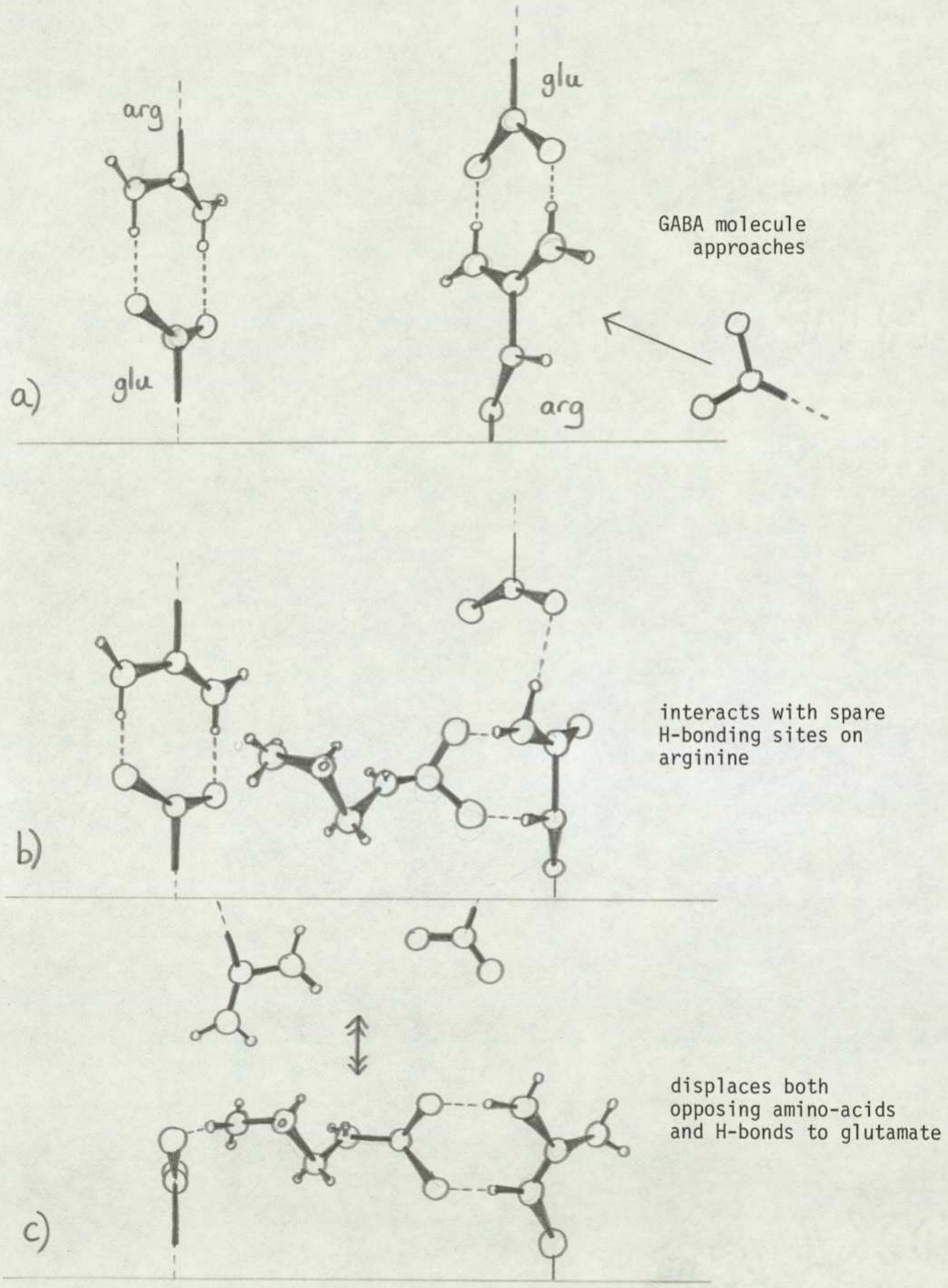

Fig. 4.5 Putative geometrical interaction process for the GABA receptor (viewed from above, with perspective)

4.4 Conclusion

The points made in this chapter may be summarised as follows:

The SAR studies of chapter 3 support the original proposals of Curtis and Watkins (1960) that synaptic GABA and glutamate receptors possess a degree of flexibility (4.3.1) rather than the closely constrained receptor geometry suggested by Kier et al (1971, 1973, 1974) (1.3.3).

The proteinaceous composition of receptor material (1.2.1) provides a starting point for investigation of the molecular nature of receptor sites (4.3.2). Charged sites, such as those implicated for GABA and glutamate receptors by the complementarity principle, required charged amino-acid residues, of which only a limited number exist and even fewer can exhibit significant flexibility, viz. arginine, lysine and glutamate. Interactions between charged residues are important in the maintenance of protein secondary structure (Gill, 1965). Interference with such interactions by the approach of transmitters could thus provide a mechanism for transitions in receptor material (Gill, 1965) which could trigger the opening of ionic channels in the postsynaptic membrane (Changeux et al 1970) (1.2.2b).

Thus, the present work and the implications of protein structure indicate that GABA and glutamate receptor sites are likely to involve arginine, glutamate and/or lysine moieties and may perhaps include aspartate or histidine.

Smythies (1974) has proposed a structure for the GABA receptor on the basis of a Kutsnetsov-Ghokov (1962) grid of parallel β-pleated sheets bridged by arginine and glutamate moieties (4.3.1). This β-pleated sheet model permits flexibility as implied by the SAR studies of chapter 3, involves appropriate amino-acids and has dimensions not inconsistent with the SAR findings. The details of the Smythies model, however, have yet to be vindicated.

Assuming that the GABA receptor did involve a β pleated sheet structure, consistent with the SAR results, it is possible to envisage a geometrical interaction process for the GABA receptor (4.3.2). The negatively charged carboxyl group would approach the guanidino group of an arginine molecule, disrupting the link with glutamate. The positive end of the transmitter could interact similarly with the glutamate carboxyl group of an adjacent bridge. The β pleated sheets could thus move apart slightly - a step in the chain of processes culminating in channel formation.

The parallels which exist between the flexibility and geometrical properties of GABA and glutamate receptors (3.2) suggest that the latter may be similar in molecular construction to the former. The evidence is flimsy as yet, however, so no firm conclusions may be drawn (4.3.3).

The consistency of implications between SAR results, protein structure considerations and the basic grid pattern of the Smythies model indicates that such a grid model may be a useful basis for further work (see 5.4).

5. CONCLUDING DISCUSSION

5.1 Introduction

The direct study of amino-acid transmitter-receptor interactions is only just beginning to become practicable. The isolation of GABA and glutamate receptor material (de Robertis and de Plazas, 1975; de Plazas and de Robertis, 1975) may eventually enable the geometry of receptor sites to be determined by X-ray crystallography, but until that time the understanding of transmitter-receptor interactions depends upon structural and pharmacological studies of the transmitter molecules and their antagonists. In the GABA and glutamate systems, data on antagonism is limited, and in any case is only like to relate to competitive antagonism in one or two cases. Hence antagonism cannot yet provide much information on GABA and glutamate receptors. In the present work, however, investigation of the conformational properties and hence the structure-activity properties of amino acid transmitters, has enabled some conclusions to be drawn about the geometrical features of transmitters and receptors, which are consistent with other approaches (Smythies, 1974). The use of standard response relative potencies, which do not distinguish between the affinity of a transmitter for receptors and its efficacy in promoting a response, has not precluded the establishment of quantitative correlations between structure and activity.

5.2 Synopsis of main findings

5.2.1 Conformational results

Studies of singly-charged or uncharged neurotransmitters often reveal conformational congruences between isolated molecule, aqueous solution and crystal conformation, which may relate to the biological activity of the compounds (2.1). For the zwitterionic amino-acid transmitters, this is not the case. Isolated molecule MO calculations do not predict similar preferred conformations to those found in crystal structures or aqueous solution and do not provide information about biologically important conformations (1.3.3, 2.1). However, the study of both the crystal structure and calculated

aqueous solution conformations of these molecules described in chapter 2 has revealed congruences in the dispositions of atoms and functional groups which may be biologically significant.

Although the theoretical calculations on solution conformation using the solvent effect calculation program SOLVEFF (2.3) or simpler PE solution calculations (2.4) cannot yet be shown to be accurate in an absolute sense, the degree of agreement with experimental results is encouraging (2.5.1). In terms of preferred functional-group separation (x_T) (Fig. 2.1) the SOLVEFF and PE results are in good agreement with each other and experimental data (see e.g. Fig. 2.32). Values of x_T of 5.0-5.2 Å are particularly favoured for GABA agonists indicating a small degree of folding in the preferred conformations. In terms of torsion angles, the agreement is not so striking, since SOLVEFF energy surfaces show only one or two non-equivalent broad minima in general, whereas PE and NMR results, by virtue of their fundamental assumptions, show a spectrum of classical conformational modes.

Such agreement between methods may indicate that at least as far as x_T is concerned, the results are physically reasonable. It might be expected that results on a series of molecules using a single method of conformational analysis would be self-consistent, allowing comparisons between substances to be usefully made. The fact that comparison of results between methods also shows limited self-consistency is an encouraging sign of the usefulness of the methods.

Overall, α-ω amino-acid zwitterions in an aqueous solution have been shown, both theoretically and experimentally to be slightly rather than fully folded (2.5). The attraction between the charged terminal groups which causes an isolated zwitterion to fold up, is counterbalanced in aqueous solution by electrostatic interaction between the large dipole of an extended zwitterion and the surrounding bulk dielectric (2.3.3). The continuum method used in the SOLVEFF program treats this long-range effect explicitly, which may account for its higher degree of agreement with experimental results than has been obtained by other workers using the essentially short-range 'supermolecule' solvent effect treatment (2.5.1) (see Fig. 2.32).

Although crystal structure conformations of GABA agonists show a greater tendency towards trans configuration of bonds than do SOLVEFF results, perhaps due to packing effects, consistency of x_T values is apparent between the methods (2.5.2). Both, of course, relate to environments where intermolecular rather than intramolecular forces predominate, so some similarity might be expected. Crystal structure results (2.2.2), however, show favoured x_T values of about 5.7 Å for GABA agonists as well as the preference for ~5.2 Å mentioned above. Congruences among the crystal structure conformations of glutamate agonists (2.2.3) are not so marked, but two particular positions of ω functional groups with respect to the α end of the molecule seem particularly favoured. These are also found in the PE preferred conformations of aspartate and glutamate respectively (2.4.4).

5.2.2 Structure-Activity Relationships

The conformational congruences discussed above for GABA and its agonists are closely consistent with the ideal value of the putative receptor charge separation ($x_R \simeq 5.2$ Å) developed in 3.2. The x_R probability curve is largely dependent on pharmacological results, so the agreement between this and conformational congruences for a series of agonists supports the validity of conformational studies in neurotransmitter research. The crystal structure results suggest a further point (3.3.2). The occurrence of a second group of x_T's in the region of 5.7 Å may relate to the possibility (1.3.3) that GABA uptake receptors preferentially recognise a fully extended GABA molecule, while synaptic receptors recognise a partially folded one (3.3.2).

The studies on glutamate, although less thorough than those on GABA, also indicate congruences of conformation which may relate to biological activity (3.2.4, 3.3.2). A combination of x_{T2}~5.0, x_{T3}~5.7 (see Fig. 2.2) may relate to the dimensions of the glutamate receptor considered as a three-point site, and x_{T2}~3.7, x_{T3}~4.9 may relate to those of the aspartate receptor. The former suggestion is supported by pharmacological results (Johnston et al, 1974) on semi-rigid glutamate agonists.

The quantitative SAR results of 3.2 not only corroborate the ideal conformations for GABA-like activity derived from crystal structure and solution conformation studies, but also provide a scheme under which the potency of an agonist can be approximately correlated with its structure via simple PE calculations. The flexibility of the charge separation of individual receptors is an essential feature of the scheme. It would appear that a transmitter acting at the ideal charge-separation mediates a response with greater efficiency than a transmitter with non-ideal separations of receptor-active moieties. This may provide an explanation for partial agonism at GABA receptors (3.2.3). Partial agonists possess highly populated conformations with charge separations a little removed from the ideal. Hence they will bind to the receptor more efficiently than they will mediate a response.

Conformational preference is not the only important factor in determining potency, however. Even when a number of molecules exhibit very similar conformations in solution, their potencies may differ by a factor of five or more. The electrostatic potential of the functional groups of agonists may provide an explanation for this, such that an SAR scheme involving electrostatic potential as well as conformational preference would be a closer approximation to the truth (3.4). Physicochemical and steric effects probably also contribute to agonist potency (3.4.2).

5.2.3. Possible models for amino acid receptors

The most plausible model for the GABA receptor so far suggested is that of Smythies (1974) based on a bridged β-pleated sheet structure (4.3). The approach of a transmitter may disrupt the bridges, leading to the formation of ionic channels in the receptor macromolecule or neighbouring units. The model was developed from principles of protein structure and the structure of GABA antagonists. The properties of the receptor suggested by SAR studies in the present work, notably its flexibility, are compatible with the Smythies model and the ideal inter-charge distances for agonists suggested by conformational studies are broadly complementary to the structure of the receptor (4.3.1). The agreement between

these completely different approaches to the problem provides some support for the suggested model. A proposal for the geometrical interaction processes occurring at the Smythies receptor has been made in the present work (4.3.2) and the extension of the model to glutamate receptors is not difficult to visualise (4.3.3).

5.3 Summary Tables

5.3.1 The GABA system

Table 5.1 illustrates the trends in conformational and pharmacological results in the GABA system. Substances are listed in order of approximate potency with charge separations x_T in aqueous solution and in crystal structures. The PE result shown for each substance corresponds to the $\frac{1}{2}$ Å range in x_T with the greatest population. The pharmacological results are taken from Table 1.1, including values from GABA-specific preparations alone for the shorter amino-acids which may also interact with glycine receptors.

x_T values in aqueous solution for strong agonists ($>\frac{1}{2}$ GABA) fall mainly between 5 and $5\frac{1}{2}$ Å. The exceptions are imidazoleacetic acid, whose relevant x_T values are not well established (3.2.3), and αGA and βGP which exhibit very high probability for x_T values a little removed from the others, providing a possible explanation for their partial agonist properties (3.2.3).

Moderate agonists (potency $\frac{1}{10}$ - $\frac{1}{2}$ GABA) show x_T's at or beyond the extreme of the range above, except for βHG, whose structure in solution is uncertain (2.3.3). Of the weaker agonists (potency $<\frac{1}{10}$ GABA) only imidazole derivatives show x_T's in the ideal range, and compounds with preferred x_T's < 5.0 Å or > 5.7 Å are all poor agonists.

The crystal structure x_T values are equivocal indicators of potency, but do effectively demonstrate conformational congruence. The preference for x_T's of ~ 5.2 Å and ~ 5.7 Å (3.3.2) is again apparent.

Used in conjunction, then, these two sets of x_T values shed some light on the pharmacological action of GABA agonists (3.2.3, 3.3.3) as well as their conformational preferences (2.5), and also provide clues about possible receptor geometry.

TABLE 5.1 GABA SYSTEM SUMMARY

Substance	Approx Relative potency (Table 1.1)	crystal x_T (Å) (2.2.2)	aqueous solution SOLVEFF x_T (Å) (2.3.3)	aqueous solution PE x_T (Å) (2.4.3)
Homotaurine	3000	5.5, 6.1		
ImAc[1]	1500			5½-6
∝FG	>1000		5.2	5-5½
GABA	1000	5.1, 5.8	5.2	5-5½
βGP[3]	1000	3.7, 5.7	4.8, 5.7	5½-6
muscimol	1000	5.2	5.2	5.2 (rigid)
trans ACA	1000		5.4, 5.6	
∝GA[3]	600	4.8, 5.2		5-6
ATA	300	5.7	5.7	5.7 (rigid)
cis ACA	250		5.0	
βHG[2, 4]	200	5.7	5.1 (ring)	2½-3 (chain) 5-5½ (ring)
δAVA	100			5½-6
β alanine	60	3.9	4.6	4½-5
γGB	50	7.7, 7.9		7-7½
ImPr[1]	35			5-5½ (1+) 7½-8 (2+)
MeImAc[1]	35			3-3½
εACA	10	8.2		7-7½
δGP	5			7-7½
∝-γ diamino butyrate	5	5.1		
taurine	5	3.2, 3.7, 4.2		
ImLa[1, 4]	3			5½-6 (1+) 5½-6 (2+)
βABA[4]	2			3-3½
7ACA[4]	1			7½-8
creatine[4]	1	3.9, 5.2		
glycine	1	3.2		3-3½

1 Imidazole derivatives: see 2.4.2, 3.2.3 on uncertainties in x_T

2 βHG: see 2.3.3 on alternative configurations in solution

3 Guanidino acids: see 3.2.3 on x_T values and partial agonism

4 Branched chains: see 3.2.3

5.3.2 The glutamate system

In Table 5.2 a number of glutamate agonists are tabulated in order of potency together with crystal structure and PE charge separations. Synergistic agonists (1.3.3) are not included.

The results are not as clear cut as in the GABA system, although the main trends are apparent.

Substances only displaying PE x_{T2} values outside the range $3\frac{1}{2}$ Å - $5\frac{1}{2}$ Å and x_{T3} values outside the range $4\frac{1}{2}$ Å - $5\frac{1}{2}$ Å are of low potency. Crystal structure x_T's indicate similar conformational preferences. Substances within these ranges are all of moderate potency, but appear to fall into two groups in crystal structures - aspartate, cysteate and one of the forms of glutamate having low x_T values and the rest higher values. The exception is allokainic acid which has high x_{T2}, but very low x_{T3}, illustrating again that crystal structure results on their own may be misleading (see 3.3.2).

It is conceivable that the two groups of preferred conformations may relate to specific glutamate and aspartate receptors (3.3.2), but such a conclusion is necessarily tentative on the limited evidence available. Further conformational studies on glutamate agonists would be valuable in this connection.

TABLE 5.2 GLUTAMATE SYSTEM SUMMARY

Substance (DL form)	Approx. Relative potency (Table 1.2)	crystal (2.2.3) x_{T2}	crystal (2.2.3) x_{T3}	PE (2.4.4) x_{T2}	PE (2.4.4) x_{T3}
Homocysteic acid	3000	5.6	6.2		
		5.4	6.2		
		5.4	5.6		
Ibotenic acid	3000	5.1	5.4	5.1	5.4
			rigid		
allokainate	2000	5.5	3.9		
glutamate	1000	5.3	5.9	5 - 5½	4½ - 5
aspartate	1000	3.6	4.9	3½ - 4	4½ - 5
		3.6	5.0		
cysteate	1000	4.1	5.1		
		3.4	5.2		
		3.3	4.9		
		4.1	4.0		
		3.7	4.5		
		3.1	3.7		
cycloglutamate	800			~5½	5 - 5½
aminoadipate	200			5½ - 6	5½ - 6
aminopimelate	200			7 - 7½	7 - 7½
aminomalonate	200	3.2	3.5	3.3	3.2

5.4 Possibilities for further work

The development of SAR schemes involving electronic and other parameters as well as conformational preference may permit more information about amino-acid receptors to be gathered. High precision would be necessary in the conformational calculations to resolve the finer electronic effects, so a method as (or more) sophisticated than the SOLVEFF program would be required. A combined supermolecule-continuum method is theoretically the most satisfactory approach.

Alternatively, a more fruitful line of enquiry may be to consider the properties of the receptor site itself, perhaps by MO studies of interactions based on, say, the functional portions of the Smythies model. Ultimately it should be possible to investigate receptor sites directly by X-ray crystallography, analysing the X-ray diffraction patterns due to pure receptor material and those due to receptor + transmitter. This is still some way in the future, but a start could be made by the X-ray crystal structure determination of GABA-peptide complexes of appropriate structure. The way in which the binding of a small molecule affects the structure of a larger peptide chain may indicate something of the processes which occur at the receptor itself.

Concerning the therapeutic use of amino acid transmitters, it is clear that GABA-mimetic compounds, in particular, may provide relief for sufferers with a variety of neurological disorders. The powerful GABA agonist imidazoleacetic acid is already being tested as a therapeutic agent in Huntington's chorea (Swagel, Ikeda & Roberts, 1973). It is to be hoped that greater understanding of the mode of action of neurotransmitter drugs will enable the development of safe and effective neuroactive substances to proceed more rapidly.

APPENDIX 1 A FEASIBILITY STUDY ON THE INVESTIGATION OF THE AXONAL MEMBRANE BY SMALL-ANGLE X-RAY SCATTERING

1. Background

The structural integrity of a living cell is maintained by means of its surrounding membrane. Biological membranes in different types of organism and different types of cell are chemically similar, consisting of lipid, water and protein in various proportions. Synaptosomal membrane preparations, consisting mainly of pre and post-synaptic membrane material (McBride & Van Tassal, 1972) have a lipid:protein ratio of 1:2 (Morgan, Zanetta, Breckenridge, Vincendon & Gombos, 1973) amounting to one protein molecule for every 60-80 of lipid. The lipid portion of synaptosomal membrane consists of cholesterol, phospholipids and gangliosides. The membranes contain a large number of polypeptide chains, several glycoproteins (molecular weights from 23,000 to 120,000) and about thirty protein consistuents of molecular weights between 12,000 and 210,000. Synaptic junction preparations, extracted from the synaptosomal material, show different ratios of protein constituents than do the less specific preparations.

The arrangement of lipid and protein in cell membranes has been the subject of recent controversy, as the early Davson and Danielli (1935) protein-lipid sandwich model has been improved in the light of experimental findings (Finean, 1972). X-ray crystallographic studies of various membrane preparations (Levine & Wilkins, 1971; Wilkins, Blaurock & Engelman, 1971) have demonstrated the validity of the lipid bilayer structure, but have shown that a continuous outer layer of protein is unlikely. The bilayer structure of myelin - the membranous sheath which surrounds fast-conducting nerve axons - has been extensively studied by X-ray diffraction methods (Worthington, 1971). The Singer and Nicolson (1972) fluid mosaic model in which protein units 'float' in the lipid bilayer seems to fit the evidence well (Fig. A1.1). Freeze-etch electron microscopy indicates that it is likely that some of the protein units span the entire membrane (Engstrom, 1972).

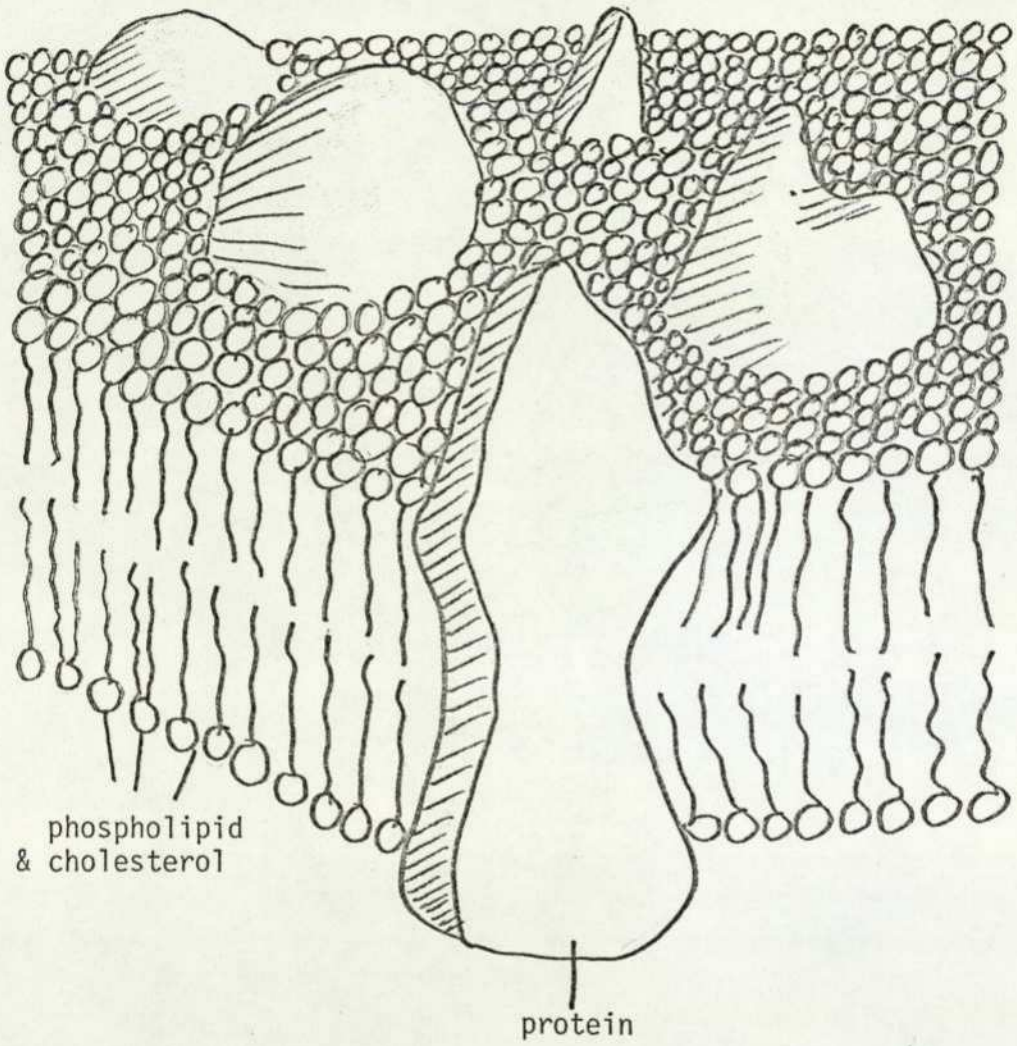

Fig. A1.1 The fluid mosaic model of membrane structure

It is possible that some membrane regions may consist of subunit structures, the lipid and protein molecules forming globular aggregates (Lucy, 1964). The experimental observations leading to this theory, however, were made by direct electron microscopy of membranes, where specimen preparation techniques can alter the structure drastically (Parsons, 1970).

As yet there is little evidence of organised structure in the plane of the bilayer. The freeze-etch experiments mentioned above show an irregular arrangement of protein molecules. Vasquez, Parisi and de Robertis (1971) in an electron microscope study of model membrane systems, have shown that acetylcholine receptor proteolipids in a lipid bilayer membrane tend to aggregate in the presence of acetylcholine. This, the authors suggest, may relate to the membrane conductance change due to acetylcholine, the aggregating macromolecules forming a transmembrane pore for ion transport. The permeability enhancing effect of protein aggregation in membranes has also been observed in various other situations Gingell, 1973). Other than these glimpses, very little is known about the arrangement of protein molecules in either somatic axonal or synaptosomal nerve membranes.

2. Unmyelinated nerve X-ray scattering patterns

In view of the lack of structural data on nerve membrane, a feasibility study was conducted as part of the present work, into the possibility of resolving the membrane structure of unmyelinated nerve by low-angle X-ray diffraction. Most X-ray studies on nerve have involved myelinated specimens (Worthington, 1971). Thus, the results obtained describe the structure of the myelin sheath, which is a set of stacked bilayers, rather than the actual axonal membrane. Studies on unmyelinated nerve (Schmitt, Bear & Clark, 1935; Blaisie, Goldman, Chacko & Dearey, 1972) are hindered by the lack of natural stacking of axonal membrane which renders the X-ray scattering pattern considerably more diffuse than that from the oriented multilayers of myelin.

There are two ways around the difficulties of interpretation inherent in such a diffuse pattern. Firstly, it is now possible to stack membranes artificially by ultracentrifugation (Worthington, 1970; Worthington & Liu, 1973). The single membranes take up an ordered planar multilayered arrangement which is eminently suitable for X-ray diffraction studies. However, such harsh treatment may well alter the in vivo structure of the membrane. Secondly, very high-intensity focussed X-rays can be used in order to obtain the resolution necessary to produce a measureable scattering pattern from unstacked specimens.

The second alternative was employed in the present work since equipment was readily available. The apparatus used consisted of an Elliott GX6 rotating-anode X-ray-generator and a Searle small angle scattering camera fitted with a toroid focussing system (Elliott, 1965). A single sector aperture was employed to minimise parasitic scatter. Nerve bundle specimens from the walking leg of the crab (Carcinus maenas) were used in this preliminary study since, although they do not contain such a large amount of membrane material as for example the olfactory nerve of the garfish used by Blaisie et al, (1972), they are easily obtainable and easily dissected from the animal. The nerve bundle specimens were placed in a humidity cell, on dissection, where they remained unchanged in appearance during the 2-7 hours before exposure.

The specimens were mounted in a humidity cell (Fig. A1.2) the design of which was the result of much experimentation. The specimens were maintained in a vertical orientation on a thin melinex sheet by surface tension. No stretching force was applied to increase the orientation of the fibres. The humidity could be altered without moving the specimen by changing the salt solution in the bottom half of the cell via a rubber tube. The liquid present made no difference to the scattering due to the cell. Water scattering peaks at 3.3 Å using Cuka radiation, so this does not interfere with the low angle pattern. During exposures the whole apparatus was enclosed by a lid and filled with hydrogen.

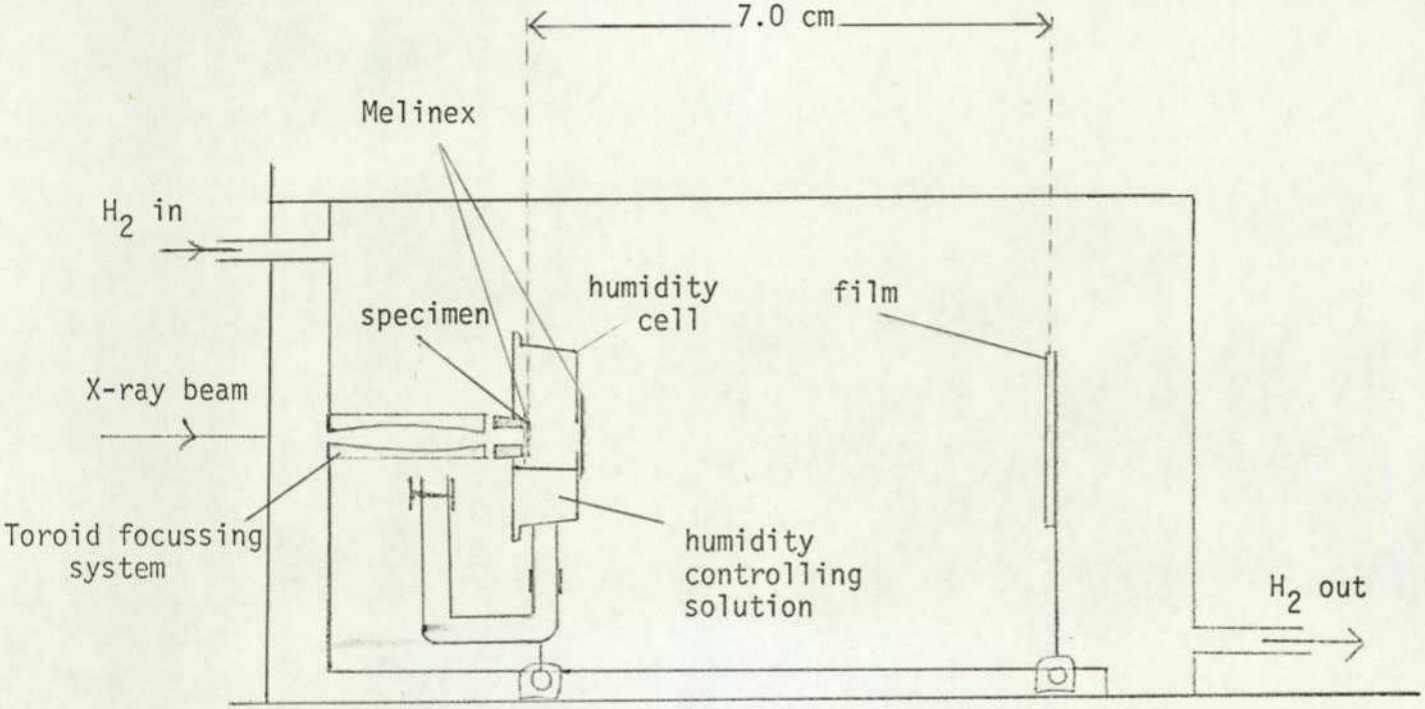

Fig. A1.2 Small-angle scattering apparatus for nerve bundle experiments

Photographs of the X-ray scattering patterns obtained are presented in Fig.A1.3. At humidities above 80% there was no visible structure in the patterns. At 75% and 65% a single sharp ring was visible, equivalent to spacings in the membrane structure of 53 and 50 Å respectively, but at 55% this was no longer apparent. At 44% preferred orientation began to appear and at 33% lamellar diffraction equivalent to a spacing of 61 Å was observed in the equatorial plane. A brief note of these findings has already been published (Clarke & Steward, 1975).

It is evident that changes in membrane stacking occurred with changes in humidity. The sharpness of the ring at 75% and 65% humidities suggests that the drying may cause lipid and protein to reorganise into a lamellar structure which probably does not correspond to the in vivo state. The tangled nature of the specimen prevents much preferred orientation at high humidities but at lower humidities, when some shrinkage will have occurred, the fibres experience longitudinal tension which promotes preferred orientation. Hence lamellar diffraction appears in the 44% and 33% photographs.

As only one order of diffraction was recorded, no attempts could be made to analyse the results in terms of the electron density profile of the membranes involved. Nevertheless, the spacings obtained are consistent with a lipid bilayer model. It is likely that the general structural features of the garfish olfactory nerve membrane studied by Blaise et al (1972) are similar to the crab walking leg nerve. These workers obtained four orders of diffraction and were able to derive an autocorrelation function for the axon membrane which was very similar to that for phospholipid/cholesterol bilayers. The differences could be explained by the presence in the axon membrane of protein molecules near the polar headgroups of the membrane phospholipids.

3. Critique of the study

It is possible to obtain interpretable X-ray data from crab nerve bundle specimens at certain humidities, but the diffuseness of the scattering makes detailed interpretation impossible. Ordered

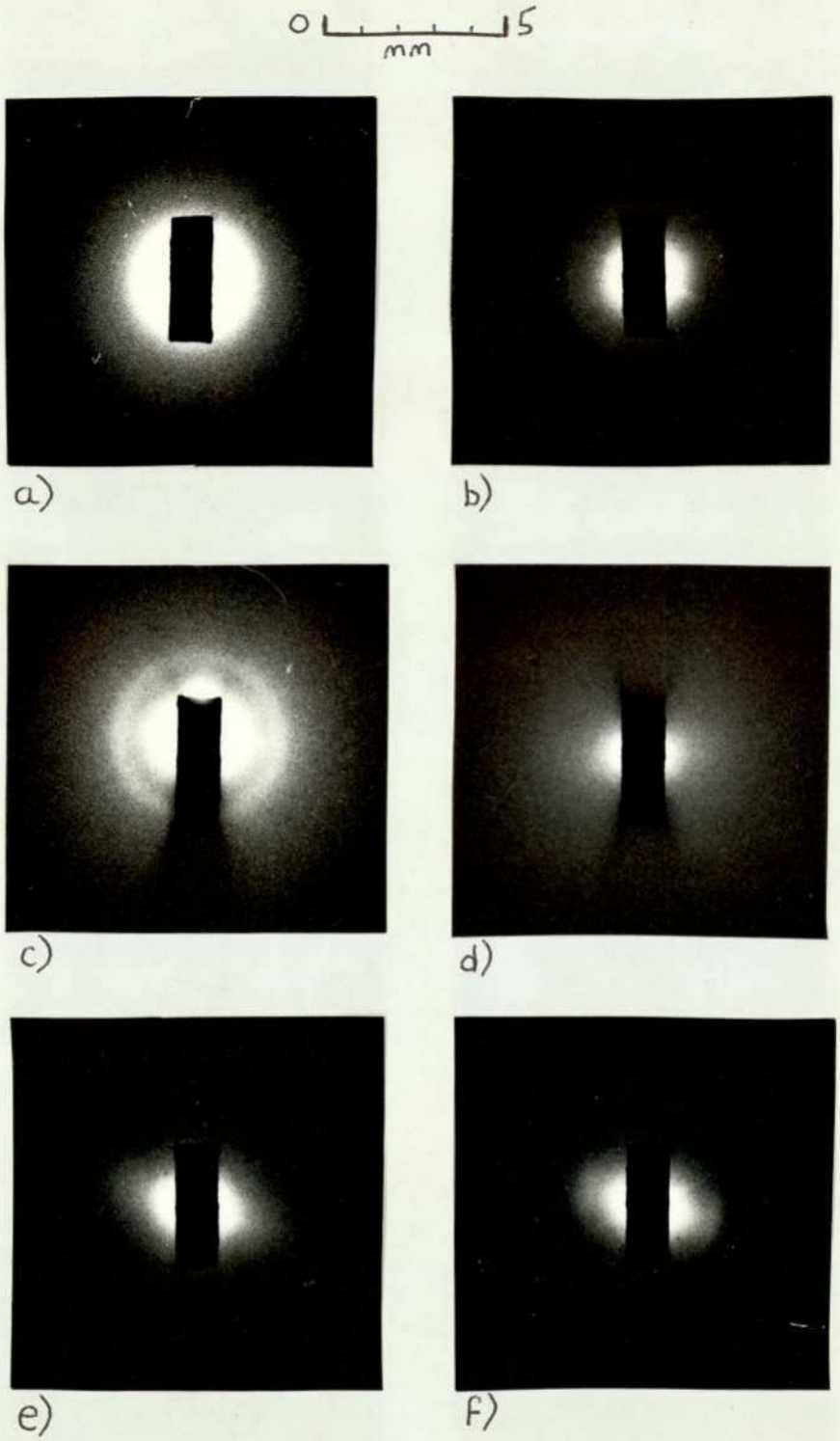

Fig. A1.3 Small-angle X-ray scattering from crab nerve bundles at various humidities; toroid optics

a) 80% humidity b) 75% c) 65%

d) 55% e) 44% f) 33%

Specimen to film distance 7.0 cm. Cuk_α radiation

phases appear to exist which probably do not correspond to in vivo membrane systems. It would appear necessary to treat the nerve bundle in some way for a structured pattern to appear at all, e.g. by changing humidity. The artificially stacked membranes described above are probably no further from the in vivo situation than membranes which have been subjected to humidity changes. Therefore, it could be useful to employ such techniques to improve the ordered nature of the specimen and the sharpness of the diffraction. Gain in information would probably be obtained at the expense of a possible loss in relevance.

Other possibilities, however, could usefully be investigated. Firstly, the orientation of nerve bundles could be improved by subjecting them to tension in glass capillaries. The nerve could be kept moist by Ringer solution in the tube. The increase in orientation obtained may be sufficient to reveal some pattern even for the high humidity case. Moreover, in interpreting diffuse diffraction, it is necessary to correct intensities by a factor of r^2 where r is the distance of a point on the pattern from the centre. This can reveal structure in an apparently featureless diffuse region.

Secondly, the resolution of the present high humidity photographs is insufficient to make use of this effect, but it could perhaps be employed in photographs obtained with a small-angle scattering camera using the more subtle Franks optics (Franks, 1958). This system enables finer focussing of the X-ray beam to be achieved, allowing spacings in the material under test of over 600 Å to be resolved. The exposure times required, however, are an order of magnitude higher. Some experiments were carried out using this system in the present work but the X-ray generator available in this case was of too low a power to enable scattering patterns from nerve bundles to be observed in a feasible exposure time. The resolution of the system is indicated by the photograph in Fig. A1.4. obtained during these experiments which shows twelve orders of diffraction from kangaroo tail collagen, giving a resolution of 640 Å.

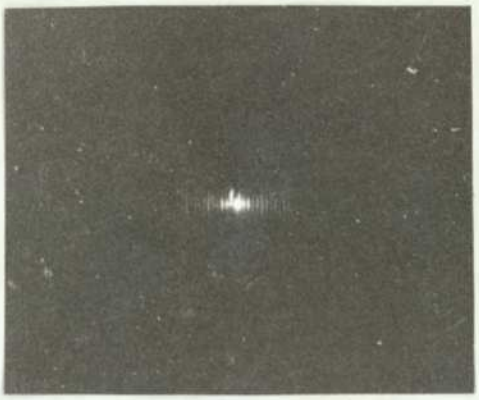

Fig. A1.4 High resolution X-ray scattering from kangaroo tail collagen using Franks optics. The first order of diffraction visible represents a spacing of 640 Å in the material.

Thirdly, despite the convenience of the crab nerve preparation, it is not the most suitable for this kind of work. The axons it contains are ~1.5μ in diameter, whereas those in garfish olfactory nerve are only ~0.1μ in diameter. Thus the latter preparation possesses a far higher proportion of axon membrane to axoplasm, etc. Moreover, any nerve bundle contains glial cells, sarcoplasmic reticulum, mitochondria etc. which all possess membrane structures. Hence the proportion of nerve membrane present needs to be as high as possible. The garfish preparation, however, is almost unobtainable in this country, but pike, or the more easily dissected dogfish olfactory nerve could be a useful substitute (D. Gilbert & A.E. Blaurock, private communication).

4. Possible use of nerve X-ray scattering

If the suggestions above were successful and permitted the observation of interpretable scattering from fully hydrated nerve, an exciting possibility could emerge. That is, the observation of the differences in scattering between resting and conducting nerve. The conduction of a nerve impulse along an axon is accompanied by successive permeability changes in the axon membrane. Permeability changes are probably due to conformational changes occurring in the protein macromolecules of the membrane (Section 1.2.1) or aggregation of these macromolecules (see above). At high resolution, then, it may be possible to detect differences in the arrangement of protein molecules in the plane of the bilayer between resting and conducting nerve. The problem here, over and above the difficulties already described, is that a nerve bundle cannot be continuously stimulated indefinitely (more than half an hour or so). Unfortunately, high resolution X-ray photographs with present day powerful generators would require 12-24 hour exposures to register structure in the bilayer plane. Perhaps the intense X-ray production associated with synchrotron operation may provide the answer to this, although the intensity produced may be too much for the nerve to stand.

Results indicating the type of mechanism involved in axon permeability changes would also be relevant to synaptic mechanisms, since it seems that similarities exist between the two

situations. Acetylcholine, for example, has been shown (Denburg et al, 1972) to exert an excitant effect on axon membrane as well as on synaptic membrane.

5. Acknowledgements

The bulk of the X-ray experiments described above were carried out at GEC-Marconi, Borehamwood, with the help and advice of [redacted], and at the National Physical Laboratory, Teddington, with [redacted]. [redacted] of St. Bartholomew's Hospital medical school provided the specimens. I would also like to thank [redacted] and [redacted] (King's College, London) for helpful discussions and advice.

APPENDIX 2 DETERMINATION OF THE CRYSTAL AND MOLECULAR STRUCTURE OF β GUANIDINOPROPIONIC ACID

1. Preliminary Work

1.1 Preparation of crystals

β guanidinopropionic acid (βGP) ($C_4H_9N_3O_2$) dissolves readily in water. Large, well-formed sphenoidal crystals were grown by slow evaporation in air.

Crystal habit diagrams are presented in Fig. A2.1.

1.2 Physical properties of the crystals

Heating the crystals in a vacuum at over 100°C for four hours caused no weight loss. The crystals were thus shown to contain no water of crystallisation.

The density of βGP, measured by the flotation method, was 1.403 g/cc.

A melting point determination for the crystals was carried out on a hot-stage microscope. This revealed a range in melting point between 215° and 221°C. The range may be due to some decomposition around the melting point. Dictionary of organic compounds 4th Ed. (1965) gives βGP melting point as 209°-11°C.

2. X-ray analysis

Ni filtered Cu radiation (Cukα, λ = 1.5418 Å) was used throughout.

2.1 Preliminary photographs

A crystal was aligned along a prominent morphological axis (subsequently defined as b) on the goniometer of a Nonius

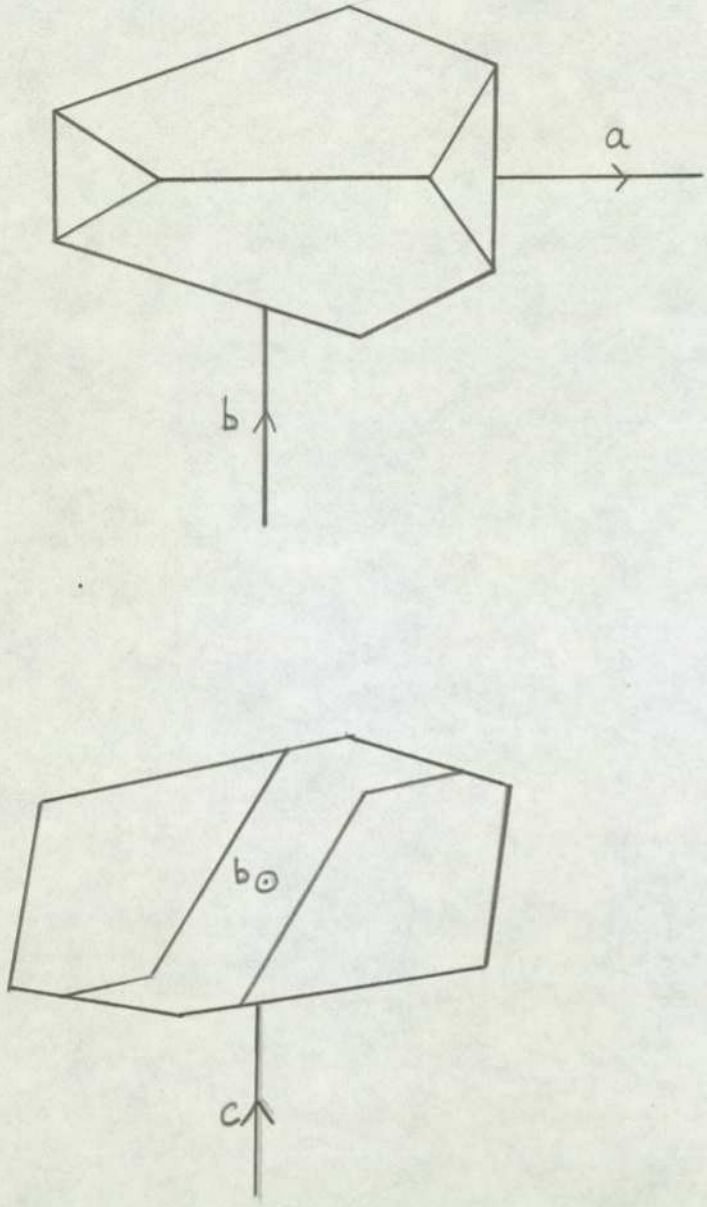

Fig. A2.1 Crystal habit diagrams for βGP crystals grown from aqueous solution by slow evaporation in air

Weissenberg camera, using double-oscillation photographs. Rotation photographs revealed the repeat distance along the axial direction and a Weissenberg photograph was also taken. The procedure was repeated using a second crystal aligned along a different prominent axis (subsequently defined as c).

Comparison of axial repeat distances in the rotation and Weissenberg photographs showed that the crystals were monoclinic with approximate cell dimensions:-

$a = 11.6 \pm 0.1$ Å
$b = 7.3 \pm 0.1$ Å
$c = 7.3 \pm 0.1$ Å
$\beta = 98.0 \pm 0.2^{o}$

The Weissenberg photographs were then indexed, taking care to maintain a right handed set of axes and the following systematic absences were revealed:

$h0l$, hodd
$0k0$, kOdd

This corresponds to the diffraction symbol $P\frac{2}{a}1..$ which defines the space group unambiguously as $P2_1/a$, a centrosymmetric space group.

The approximate cell dimensions, together with the measured density were used to calculate the number of molecules per unit cell:

$Z = 4$

2.2 Preliminary diffractometry

A Stoë-Guttinger linear diffractometer was employed in this study (see Hoyes, 1971). This has two movements, the crystal rotation (ω), and the diffractometer arm setting (2θ) which corresponds to the angle of deviation of diffracted beam from incident beam. A control tape was prepared which guides the diffractometer during automatic data collection (Section 2.3).

This requires more accurate cell parameters than the photographic ones above so, using approximate positional values (ω & 2θ) derived from the approximate cell parameters, various zero layer reflections were located and their 2θ and ω measured precisely on the diffractometer. This process was carried out for twelve pairs of reflections (e.g. $h0l$ and $\bar{h}0\bar{l}$) on the b axis zero layer and twelve pairs on the c axis zero layer. Different crystals were used for the respective axes.

A computer program, implemented by Mr. W.A. Sentance (City University Mathematics Department) on the ICL 1900 computer at City University, was employed to derive accurate cell parameters by least squares refinement from the precise positional parameters of the forty-eight reflections measured on the diffractomer. The final cell parameters were:

$$a = 11.818 \pm .004 \text{ Å}$$
$$b = 7.247 \pm .004 \text{ Å}$$
$$c = 7.311 \pm .004 \text{ Å}$$
$$\beta = 98.22 \pm .04^{o}$$

The calculated density of βGP was thus 1.403 g/cc, the same as the measured density.

Accurate cell parameters having been determined, control tapes which direct the diffractometer to the correct ω and 2θ values for each reflection to be measured on each layer were derived using a program implemented as above.

2.3 Data collection

For each reflection the diffractometer takes a one minute background count at $(\omega - 1)^{o}$, $(2\theta - 2)^{o}$, then counts during its two minute scan over ω and 2θ to $(\omega + 1)^{o}$, $(2\theta + 2)^{o}$, where a second one minute background count is taken. In each layer a reflection is periodically repeated to ensure that the intensities are remaining consistent.

Before data collection was commenced, the pulse height analyser was set up and test scans over several reflections were carried out to determine the best slit size to use in order to maximise the scanning count and minimise background counts. Both these procedures were necessary when a new crystal was to be used. The slit-size experiments were automated using a short hand-punched control tape.

For each layer to be investigated, the diffractometer was set at the appropriate equi-inclination angle, a reciprocal lattice net was then drawn out, to assist in identifying reflections so that the diffractometer could be zeroed correctly in both 2θ and ω movements. This process was carried out by manually identifying some dozen or so reflections detected by the diffractometer and finding the relationship between 2θ and ω on the control tape and the diffractometer, respectively.

Once the zeroes had been set for each layer, automatic data collection was commenced. The diffractometer results were automatically recorded on punched tape.

The reflections measured were those making up the asymmetric parts of the following layers:

b axis; layers 0, 1, 2, 3
c axis; layers 0, 1, 2, 3

3. Data Processing

3.1 Preparation of data cards

The punched data tape from the diffractometer was interpreted using the ICL 1900 computer. The reflection intensities, corrected for Lorentz and Polarisation factors, were punched on to cards in the format required by the X-ray 70 suite of programs (Steward, Kundell, & Baldwin, 1970) which was used to analyse the data.

In the course of the data collection, many reflections had been measured more than once (e.g. (213) was measured on the b axis first layer and the c axis third layer). The X-ray 70 suite requires a unique set of data cards, since all the others are generated by symmetry. Hence all the duplicate cards were removed, taking care that at least 50 reflections in each layer remained for scaling purposes.

The total number of unique reflections measured was 1127, of which 106 were systematically extinct and 85 designated as 'unobserved' i.e. with an integrated intensity less than 100 counts above background. The remaining 936 reflections were regarded as 'observed'. Measured reflections fell into eight layer groups as follows:

1	$h0l$	:	203
2	$h1l$	:	196
3	$h2l$	:	185
4	$h3l$	:	202
5	$hk0$	:	56
6	$hk1$	:	99
7	$hk2$	:	97
8	$hk3$	:	89

3.2 Data analysis

There are three stages in this process:

1. The production of an electron density map from the observed intensity data and calculated phases;

2. The interpretation of the map and derivation of a trial model for the structure;

3. The verification and refinement of the model.

An electron density map was derived using the following links of X-RAY 70 in turn, implemented on the CDC 6600 and 7600 computers at the University of London Computer Centre (see X-RAY 70

manual (Stewart, Kundell, Baldwin 1970)):

DATRDN: sets up a binary data file which is stored on tape (Warner, 1975).

DATFIX: sets scale factors for the data from each layer, to bring all the reflections on to the same scale

SIGMA2: finds statistical relationships between reflection intensities using the symbolic addition procedure of Karle and Karle (1963)

PHASE: derives phase information from the results of SIGMA2. The links SIGMA2 and PHASE had to be run a number of times altering the conditions of the relationships before sufficient phases were produced ($\sim$150) to provide an interpretable Fourier map

FOURR: prints out an electron density map of the asymmetric part of the unit cell, using F values from the observed intensities or E values (Stout & Jensen, 1968;p319) as coefficients in a Fourier series, together with the statistically derived phases.

The positions of the heavy atoms were found from a Fourier synthesis employing 163 phases. It was not immediately possible, however, to distinguish at which ends of the molecule the guanidino and carboxyl groups occurred,so two trial models were investigated, corresponding to the two possible dispositions of functional moieties. Using the program CRYLSQ three cycles of full-matrix least squares refinement, minimising the function $\Sigma(\omega(|Fo| - |Fc|)^2)$ with an overall temperature factor and unit weights for all reflections lowered the residual factors

$$R = \frac{\Sigma||Fo| - |Fc||}{\Sigma|Fo|}$$

for the two models from 0.428 to 0.244 and from 0.403 to 0.172 respectively. Since,in addition,the bond lengths and angles from the latter structure were in good agreement with expected values, this was adopted as the correct alternative.

Two further cycles of least squares refinement reduced R to 0.162 and a further three cycles, introducing anisotropic temperature factors and a weighting scheme then gave R = 0.126. Weights were $\omega = X.Y$ where:

if $\sin\theta > 0.45$, X = 1, else X = $\sin\theta$ / 0.45
if Fo < 6, Y = 1, else Y = 6/Fo

Using the program FOURR, a difference Fourier map was prepared, revealing the positions of eight of the nine hydrogen atoms. At this point, examination of the observed and calculated structure factors (computed using non-hydrogen atoms only) showed poor agreement for the hk3 layer (R = 0.362 for this layer). Examination of the original data tapes showed this to be due to an error in data collection, so this group of data was discarded (55 'observed' and 34 'unobserved' reflections). The overall R-factor was then 0.089, and a ΔF map clearly revealed the nine hydrogen atoms.

Eleven of the strongest reflections where then discarded as suffering from extinction, an overall temperature factor was assigned to the hydrogen atoms and all positional and thermal parameters further refined. The refinement converged after four cycles, the final R-factors being 0.061 for observed reflections and 0.064 for all measured reflections. The average shift/error of the parameters in the last cycle was 0.1.

4 Structural Results

4.1 Parameters and figures

Final fractional co-ordinates for the βGP molecule are given in Table A2.1, temperature factors in Table A2.2, bond lengths in Table A2.3 and bond angles for the heavy atoms in Table A2.4. Table A2.5 gives the main torsion angles and Table A2.6 the structure factors. The arrangement of the four molecules in the unit cell is shown in Fig. A2.2 and the yz plane

hydrogen bonding scheme in Fig. A2.3. Fig. A2.4 is a photograph of a crystal structure model of βGP constructed using a Beevers model kit.

4.2 Discussion

The molecule, in the crystal, is found to exist as a folded zwitterion, each terminal nitrogen atom being bonded to two hydrogen atoms. The five guanidyl hydrogen atoms are suitably placed for the formation of hydrogen bonds (Table A2.3). Three of these hold the molecules in sheets perpendicular to the c-direction (Fig. A2.2), the fourth provides a link between pairs of adjacent sheets forming bilayers which are connected to each other purely by non-bonded interactions (Fig. A2.3). The fifth is an intramolecular bond between N(3) and O(2) (Fig. A2.2). This heterodesmic bonding pattern may, in part, explain the range in melting point which is observed.

The bond lengths obtained (Table A2.3) are in good agreement with the usual values. The C(1)-O(1) and C(1)-O(2) bond lengths are effectively equal as are the C-N distances in the guanidyl group. This is as expected for the zwitterion. The bond angles about C(2) and C(3) (Table A2.4) deviate from the tetrahedral value by about 6^{o}, but the remaining angles are not remarkable.

Comparisons with the crystal structures of other GABA agonists including other α-ω guanidino acids may be found in 2.2.2.

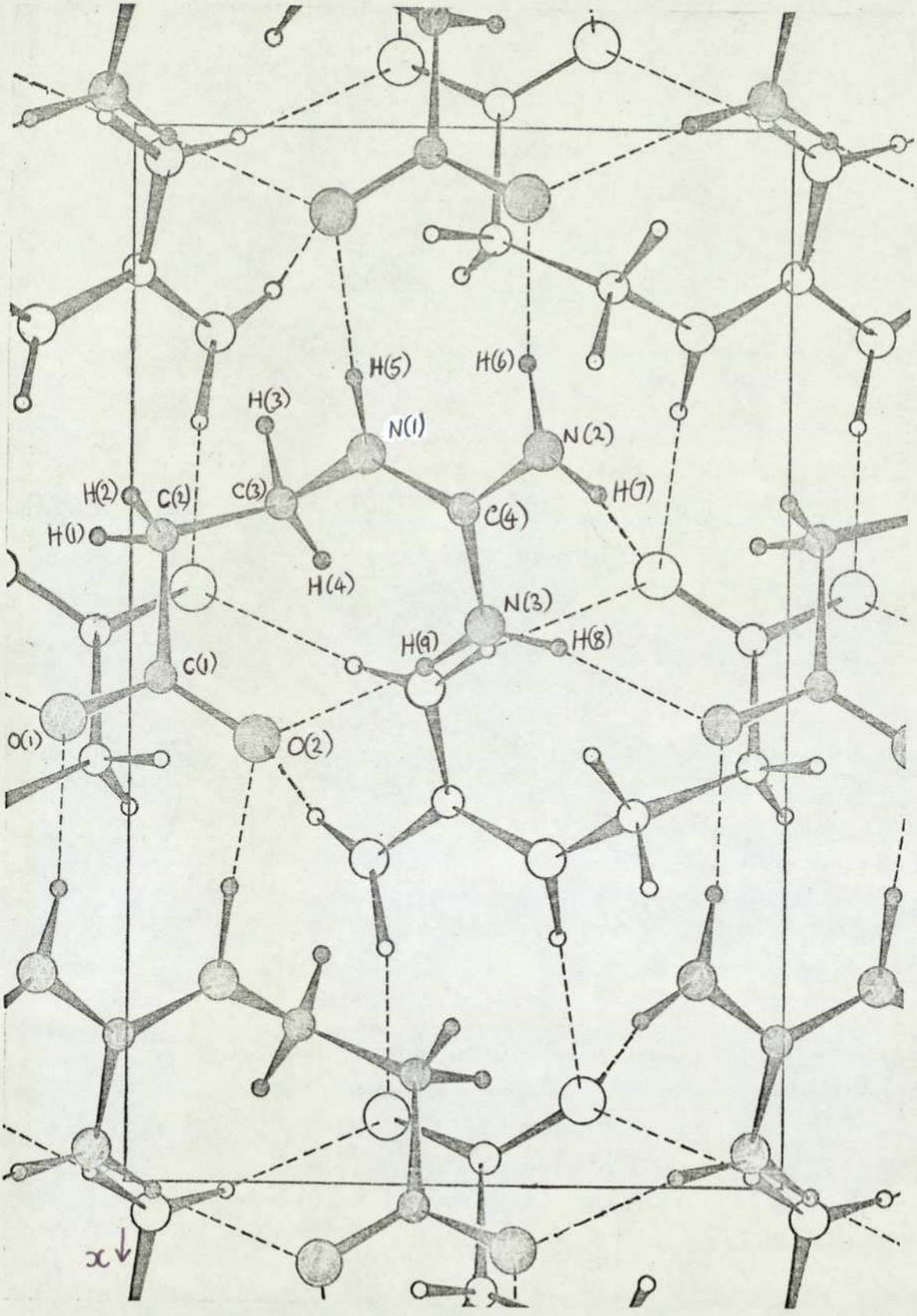

Fig. A2.2 z projection of unit cell of βGP

carbon

oxygen

nitrogen

hydrogen

Atoms on upper level are shaded

---------- hydrogen bonds

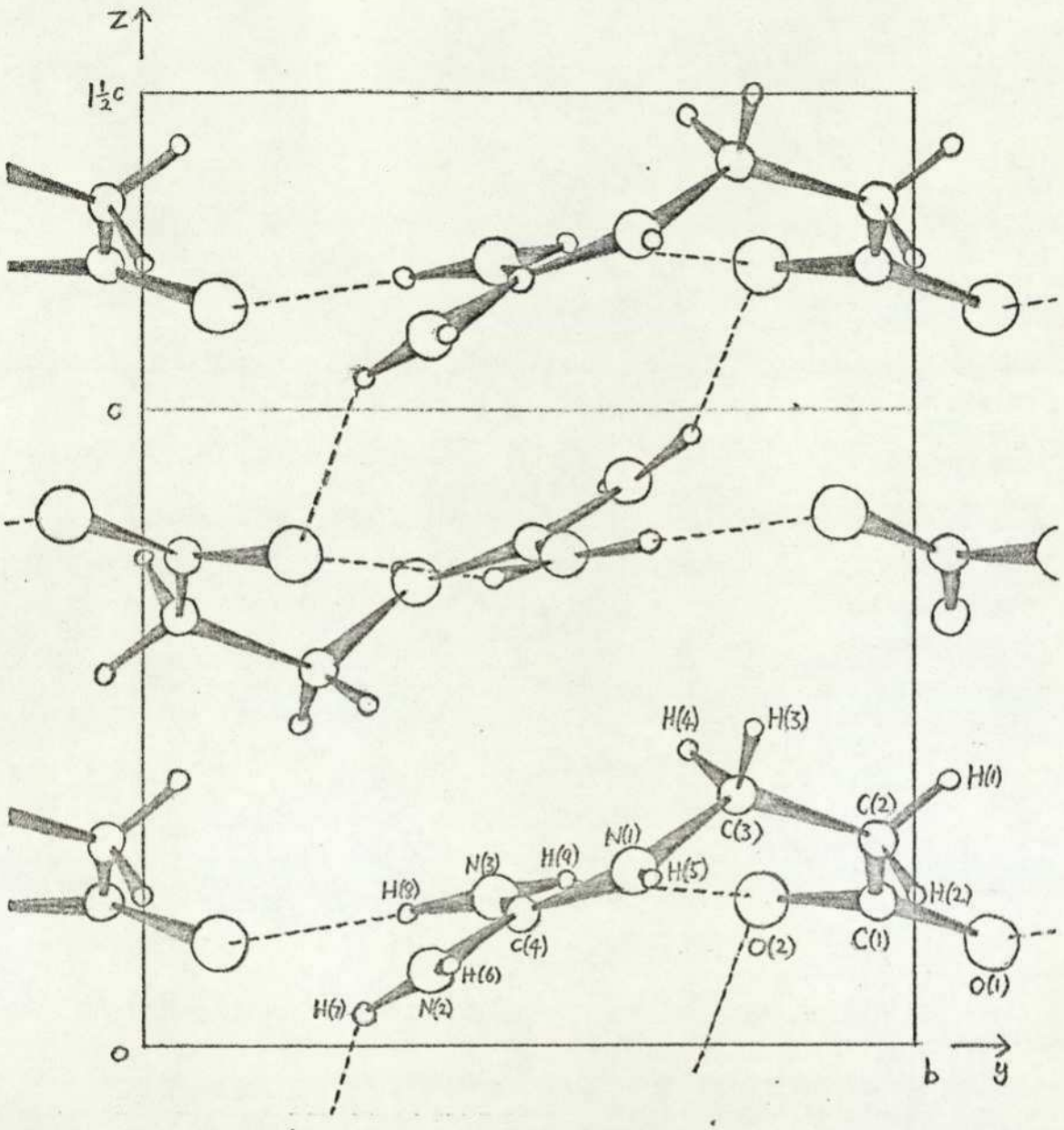

Fig. A2.3 x projection of part of unit cell of βGP showing hydrogen bonding scheme in the yz plane. For clarity, only half the contents of the unit cell in the x-direction is shown.

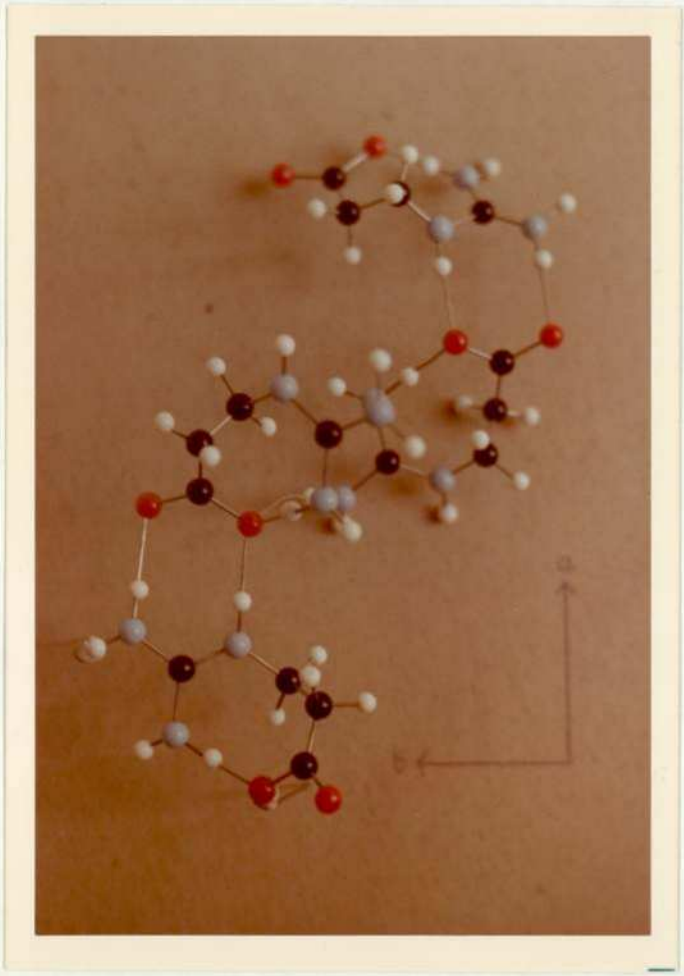

Fig. A2.4 Crystal structure model of β GP.
Viewed along $\sim[\bar{1}0\bar{1}]$

TABLE A2.1

βGP: Fractional Atomic Coordinates

ATOM	x	y	z	ATOM	x	y	z
C(1)	0.5226(2)	0.0511(5)	0.7714(4)	H(1)	0.390(3)	-0.049(7)	0.585(6)
C(2)	0.3982(2)	0.0492(5)	0.6783(5)	H(2)	0.352(4)	0.002(6)	0.755(5)
C(3)	0.3506(2)	0.2297(5)	0.5955(4)	H(3)	0.281(3)	0.202(6)	0.502(5)
C(4)	0.3626(2)	0.5083(5)	0.7935(4)	H(4)	0.411(3)	0.294(6)	0.534(5)
O(1)	0.5628(2)	-0.0982(4)	0.8367(4)	H(5)	0.235(3)	0.337(6)	0.748(5)
O(2)	0.5789(2)	0.1987(3)	0.7718(4)	H(6)	0.223(3)	0.604(6)	0.877(5)
N(1)	0.3100(2)	0.3563(4)	0.7267(4)	H(7)	0.346(3)	0.711(6)	0.953(6)
N(2)	0.3054(2)	0.6286(5)	0.8834(4)	H(8)	0.491(3)	0.656(7)	0.793(6)
N(3)	0.4696(2)	0.5431(5)	0.7711(5)	H(9)	0.510(4)	0.453(7)	0.740(6)

TABLE A2.2

FINAL THERMAL PARAMETERS x 100 $Å^2$

The temperature factor is of the form:

$$T = \exp\left\{-2\pi^2\left[(ha^*)^2U_{11} + (kb^*)U_{22} + (lc^*)^2U_{33} + 2hka^*b^*U_{12} + 2hla^*c^*U_{13} + 2klb^*c^*U_{23}\right)\right\}$$

ATOM	U_{11}	U_{22}	U_{33}	U_{12}	U_{13}	U_{23}
C(1)	2.4(4)	2.1(4)	3.6(4)	-0.1(1)	0.2(1)	-0.5(2)
C(2)	2.7(4)	2.6(4)	4.6(4)	-0.3(1)	-0.5(1)	-0.8(2)
C(3)	3.0(4)	3.3(4)	3.4(4)	-0.3(1)	-0.5(1)	-0.5(2)
C(4)	2.7(4)	2.3(4)	2.9(4)	+0.1(1)	-0.5(1)	+0.2(2)
O(1)	3.1(3)	2.6(4)	6.1(4)	+0.2(1)	-0.4(1)	+0.4(2)
O(2)	2.4(3)	2.5(4)	6.1(4)	-0.3(1)	-0.1(1)	-0.2(1)
N(1)	2.4(3)	2.5(4)	3.9(4)	-0.2(1)	+0.0(1)	-0.8(2)
N(2)	3.0(4)	3.2(4)	4.8(4)	+0.2(1)	-0.2(1)	-1.0(2)
N(3)	2.6(4)	2.5(4)	6.0(4)	-0.3(1)	+0.2(1)	-0.2(2)

The Overall Temperature Factor for the Hydrogens, U_{Hyd} = 1.5(3)

TABLE A2.3

βGP: Bond Lengths (Å)

C(1)	O(1) 1.249(4)	O(2) 1.259(4)	C(2) 1.529(3)	N(1)	H(5) 0.93(4)	
C(2)	C(3) 1.515(5)	H(3) 0.98(5)	H(2) 0.95(4)	N(2)	H(6) 0.98(4)	H(7) 0.88(4)
C(3)	N(1) 1.457(4)	H(3) 1.01(3)	H(4) 1.01(4)	N(3)	H(8) 0.87(5)	H(9) 0.86(5)
C(4)	N(1) 1.323(4)	N(2) 1.333(5)	N(3) 1.322(4)			

Hydrogen Bonds (Å)

N(1) - H(5) ----- O(2)		2.826(4)	H(5) ----- O(2)	1.89(4)
N(2) <	H(6) ----- O(1)	2.847(3)	H(6) ----- O(1)	1.88(4)
	H(7) ----- O(2)	2.967(4)	H(7) ----- O(2)	2.18(4)
N(3) <	H(8) ----- O(1)	2.837(5)	H(8) ----- O(1)	1.98(5)
	H(9) ----- O(2)	2.810(4)	H(9) ----- O(2)	2.02(5)

TABLE A2.4

βGP: Bond Angles

O(1) - C(1) - O(2)	124.3(2)°	N(1) - C(4) - N(2)	118.8(3)°
O(1) - C(1) - C(2)	116.8(3)°	N(1) - C(4) - N(3)	121.3(3)°
O(2) - C(1) - C(2)	118.8(3)°	N(2) - C(4) - N(3)	119.8(3)°
C(1) - C(2) - C(3)	116.6(3)°	C(3) - N(1) - C(4)	125.8(3)°
C(2) - C(3) - N(1)	114.8(3)°		

TABLE A2.5

βGP: Main Torsion Angles

O(2) -	C(1) -	C(2) -	C(3)	1°
C(1) -	C(2) -	C(3) -	N(1)	83°
C(2) -	C(3) -	N(1) -	C(4)	254°
C(3) -	N(1) -	C(4) -	N(3)	12°

TABLE A2.6 βGP Structure Factors

H	K	L	FO	FC	H	K	L	FO	FC
2	0	-9	1.02	.57	0	0	1	18.28	16.59
2	0	-8	0.00	.02	6	0	1	9.91	7.99
4	0	-8	2.32	1.93	8	0	1	21.50	21.28
6	0	-8	4.36	4.27	10	0	1	9.57	9.51
8	0	-8	2.39	2.03	12	0	1	12.53	12.88
2	0	-7	11.00	10.46	14	0	1	6.73	6.88
4	0	-7	6.57	5.97	2	0	2	14.04	13.82
6	0	-7	5.18	4.37	4	0	2	25.37	25.24
8	0	-7	9.77	8.63	6	0	2	1.02	.77
10	0	-7	4.27	4.07	8	0	2	4.62	5.75
2	0	-6	1.64	1.19	10	0	2	8.69	9.72
4	0	-6	2.92	1.81	12	0	2	3.60	4.14
6	0	-6	19.54	18.94	0	0	3	38.10	36.58
8	0	-6	8.64	7.76	2	0	3	28.92	28.46
10	0	-6	5.62	4.96	4	0	3	14.01	14.04
12	0	-6	7.50	6.66	6	0	3	2.31	2.58
2	0	-5	20.51	20.17	8	0	3	9.66	11.14
4	0	-5	7.92	7.82	10	0	3	12.58	12.81
6	0	-5	6.00	6.37	12	0	3	4.83	5.23
8	0	-5	13.86	13.25	0	0	4	19.90	17.73
10	0	-5	13.70	12.70	2	0	4	7.00	6.58
12	0	-5	2.13	2.09	4	0	4	4.16	4.32
2	0	-4	28.68	27.98	6	0	4	10.78	10.40
4	0	-4	23.30	22.29	8	0	4	13.73	14.57
6	0	-4	16.24	15.30	10	0	4	9.57	10.29
8	0	-4	9.06	10.13	12	0	4	6.04	6.31
10	0	-4	6.64	6.47	0	0	5	14.01	13.02
12	0	-4	7.13	6.17	2	0	5	12.67	14.21
2	0	-3	8.34	7.75	4	0	5	2.58	2.31
4	0	-3	2.81	1.95	6	0	5	1.09	1.31
6	0	-3	3.17	2.67	8	0	5	2.11	1.55
8	0	-3	3.15	3.56	10	0	5	11.37	12.14
10	0	-3	1.85	1.88	0	0	6	10.82	10.63
12	0	-3	1.30	.96	2	0	6	4.80	4.09
14	0	-3	.76	.26	4	0	6	4.48	4.69
4	0	-2	38.00	38.36	6	0	6	.75	.57
6	0	-2	5.43	5.82	8	0	6	6.41	6.79
8	0	-2	11.28	11.41	0	0	7	3.19	3.16
10	0	-2	2.14	2.02	2	0	7	5.73	5.47
12	0	-2	4.91	5.31	4	0	7	6.74	6.73
14	0	-2	2.15	1.92	6	0	7	5.59	5.60
4	0	-1	47.21	48.71	0	0	8	2.27	2.25
6	0	-1	12.51	12.76	2	0	8	1.86	1.46
8	0	-1	1.26	1.76	4	0	8	7.20	7.45
10	0	-1	10.39	12.02	1	2	-8	4.90	5.68
12	0	-1	8.83	7.77	2	2	-8	4.44	5.58
14	0	-1	4.50	4.97	3	2	-8	2.04	2.70
2	0	0	33.38	36.02	4	2	-8	3.74	4.89
4	0	0	15.00	14.90	5	2	-8	1.34	1.58
6	0	0	4.82	4.15	6	2	-8	3.16	3.91
8	0	0	19.02	19.73	7	2	-8	1.73	1.91
10	0	0	2.56	3.31	1	2	-7	3.24	3.58
12	0	0	1.10	1.48	2	2	-7	3.16	3.80
14	0	0	1.31	1.47	3	2	-7	4.51	5.22

H	K	L	FO	FC
4	2	-7	2.31	2.70
5	2	-7	4.28	4.96
6	2	-7	8.66	9.84
7	2	-7	1.95	2.30
8	2	-7	2.03	1.95
9	2	-7	1.55	1.37
10	2	-7	3.12	3.61
1	2	-6	.87	.98
2	2	-6	1.67	1.81
3	2	-6	2.91	3.78
4	2	-6	6.79	8.36
5	2	-6	3.09	3.42
6	2	-6	3.90	4.15
7	2	-6	.40	.34
8	2	-6	1.74	2.00
9	2	-6	2.00	2.20
10	2	-6	1.08	.96
11	2	-6	.67	.44
1	2	-5	8.56	10.15
2	2	-5	4.90	6.00
3	2	-5	11.01	13.78
4	2	-5	9.69	12.11
5	2	-5	2.72	3.98
6	2	-5	6.78	7.95
7	2	-5	3.69	3.86
8	2	-5	1.94	2.07
9	2	-5	5.06	5.46
10	2	-5	3.37	3.68
11	2	-5	1.40	1.66
12	2	-5	6.79	7.48
1	2	-4	26.86	23.44
2	2	-4	5.56	4.91
3	2	-4	3.49	3.94
4	2	-4	5.39	5.47
5	2	-4	5.35	5.97
6	2	-4	16.73	15.50
7	2	-4	2.75	2.87
8	2	-4	7.96	7.14
9	2	-4	12.59	11.13
10	2	-4	6.29	5.66
11	2	-4	.56	.27
12	2	-4	2.06	1.89
13	2	-4	0.00	.86
1	2	-3	0.00	.87
2	2	-3	29.07	30.57
3	2	-3	30.52	30.84
4	2	-3	10.09	10.32
5	2	-3	20.71	22.50
6	2	-3	4.80	4.84
7	2	-3	9.42	9.53
8	2	-3	4.59	4.90
9	2	-3	6.31	6.36
10	2	-3	9.32	8.88
11	2	-3	2.54	2.46
12	2	-3	9.71	9.78
13	2	-3	9.18	9.01
14	2	-3	3.83	3.28
1	2	-2	21.82	22.71
2	2	-2	9.96	8.55
3	2	-2	1.25	2.11
4	2	-2	13.98	13.44
5	2	-2	27.35	26.59
6	2	-2	24.04	22.50
7	2	-2	4.75	4.72
8	2	-2	4.60	4.79
9	2	-2	12.42	11.89
10	2	-2	6.59	6.73
11	2	-2	4.02	3.19
12	2	-2	1.54	1.33
13	2	-2	7.46	7.16
14	2	-2	3.40	3.36
1	2	-1	2.23	2.94
2	2	-1	27.75	26.29
3	2	-1	11.88	11.87
4	2	-1	20.15	18.09
5	2	-1	9.75	9.06
6	2	-1	1.79	.80
7	2	-1	2.60	2.79
8	2	-1	5.97	5.93
9	2	-1	15.87	15.08
10	2	-1	6.12	5.81
11	2	-1	.64	.51
12	2	-1	1.58	1.35
13	2	-1	3.23	3.09
14	2	-1	3.87	3.69
1	2	0	14.79	14.92
2	2	0	34.08	35.37
3	2	0	14.49	13.50
4	2	0	12.79	12.32
5	2	0	8.84	7.78
6	2	0	7.99	7.51
7	2	0	4.25	3.50
8	2	0	11.48	12.80
9	2	0	3.12	2.86
10	2	0	0.00	.03
11	2	0	.64	.66
12	2	0	9.15	8.83
13	2	0	5.60	5.20
14	2	0	6.11	5.99
0	2	1	18.87	17.93
1	2	1	37.12	37.90
3	2	1	8.46	7.21
5	2	1	2.69	2.78
6	2	1	17.03	16.57
7	2	1	14.40	16.17
8	2	1	7.73	8.35
9	2	1	2.14	2.29
10	2	1	7.89	7.82

H	K	L	FO	FC
11	2	1	2,06	1,89
12	2	1	,91	,66
13	2	1	2,24	2,25
0	2	2	31,77	35,04
1	2	2	11,64	11,46
2	2	2	24,40	23,85
3	2	2	25,94	23,98
4	2	2	9,24	8,12
5	2	2	15,73	15,65
6	2	2	9,12	9,87
7	2	2	5,56	5,74
8	2	2	20,91	21,52
9	2	2	5,24	4,78
10	2	2	3,99	3,78
11	2	2	6,06	6,34
12	2	2	11,69	11,98
13	2	2	2,67	2,28
0	2	3	8,16	8,74
1	2	3	28,24	24,76
2	2	3	25,46	23,11
3	2	3	24,76	23,65
4	2	3	3,56	3,19
5	2	3	6,07	7,72
6	2	3	14,30	16,87
7	2	3	12,27	14,04
8	2	3	1,30	1,13
9	2	3	2,88	2,54
10	2	3	7,84	6,90
11	2	3	5,65	5,16
12	2	3	3,04	2,90
0	2	4	7,06	7,28
1	2	4	21,03	20,66
2	2	4	4,16	4,15
3	2	4	,97	1,42
4	2	4	2,17	2,12
5	2	4	9,94	9,98
6	2	4	15,59	13,90
7	2	4	12,33	11,34
8	2	4	11,12	9,91
9	2	4	10,86	9,48
10	2	4	4,45	4,38
11	2	4	2,26	1,96
0	2	5	2,25	1,70
1	2	5	8,68	7,37
2	2	5	1,68	,17
3	2	5	14,35	12,64
4	2	5	1,26	1,04
5	2	5	7,12	6,17
6	2	5	4,91	2,98
7	2	5	2,46	1,83
8	2	5	2,32	2,66
9	2	5	0,00	,41
10	2	5	1,32	,35
0	2	6	7,60	6,36
1	2	6	12,99	10,53
2	2	6	8,90	7,42
3	2	6	9,33	8,36
4	2	6	11,00	9,65
5	2	6	4,81	4,57
6	2	6	2,76	2,47
7	2	6	,27	,96
8	2	6	1,67	1,63
9	2	6	4,67	4,90
0	2	7	7,64	7,17
1	2	7	4,79	4,71
2	2	7	5,47	5,08
3	2	7	2,31	1,53
4	2	7	4,16	4,07
5	2	7	,62	,70
6	2	7	3,20	2,83
7	2	7	,77	,79
0	2	8	3,40	3,26
1	2	8	6,48	5,95
2	2	8	10,50	8,64
3	2	8	2,48	2,35
4	2	8	3,53	3,17
1	3	-8	2,10	2,74
2	3	-8	,56	,30
3	3	-8	3,01	2,61
4	3	-8	2,40	1,93
5	3	-8	2,59	2,42
6	3	-8	,91	1,10
1	3	-7	2,06	1,69
2	3	-7	3,45	3,48
3	3	-7	2,58	2,77
4	3	-7	6,08	5,62
5	3	-7	1,44	1,83
6	3	-7	4,36	3,84
7	3	-7	2,44	2,21
8	3	-7	1,65	1,97
9	3	-7	3,12	2,86
1	3	-6	7,63	7,79
2	3	-6	8,62	8,50
3	3	-6	1,60	1,70
4	3	-6	0,00	,01
5	3	-6	,92	1,42
6	3	-6	,99	1,04
7	3	-6	4,98	4,96
8	3	-6	4,09	3,90
9	3	-6	2,32	1,95
10	3	-6	2,03	1,41
11	3	-6	5,34	5,02
1	3	-5	11,30	10,91
2	3	-5	5,74	5,09
3	3	-5	10,32	9,67
4	3	-5	4,11	3,47
5	3	-5	,79	1,08
6	3	-5	,82	,45

H	K	L	FO	FC
7	3	-5	0,00	,47
8	3	-5	2,67	2,72
9	3	-5	4,72	4,78
10	3	-5	4,58	4,34
11	3	-5	4,27	3,86
12	3	-5	1,04	1,09
1	3	-4	4,26	3,98
2	3	-4	2,11	1,64
3	3	-4	1,13	,26
4	3	-4	5,35	5,63
5	3	-4	2,63	2,34
6	3	-4	1,11	,48
7	3	-4	7,65	6,85
8	3	-4	2,03	1,93
9	3	-4	4,56	4,30
10	3	-4	5,37	4,82
11	3	-4	6,12	5,66
12	3	-4	3,11	3,00
13	3	-4	,09	,36
1	3	-3	7,68	9,06
2	3	-3	9,66	10,34
3	3	-3	5,27	5,54
4	3	-3	11,42	11,49
5	3	-3	7,98	8,06
6	3	-3	9,22	9,16
7	3	-3	2,86	3,41
8	3	-3	,46	,06
9	3	-3	12,12	12,02
10	3	-3	8,55	8,25
11	3	-3	6,10	5,71
12	3	-3	8,39	7,75
13	3	-3	,71	,44
1	3	-2	18,68	19,01
2	3	-2	11,79	11,12
3	3	-2	2,99	3,52
4	3	-2	3,18	3,30
5	3	-2	13,58	13,06
6	3	-2	7,74	7,37
7	3	-2	2,95	3,00
8	3	-2	2,64	2,16
9	3	-2	9,16	8,62
10	3	-2	18,73	17,90
11	3	-2	9,40	8,70
12	3	-2	3,08	3,06
13	3	-2	3,69	3,20
1	3	-1	17,95	17,83
2	3	-1	20,66	19,17
3	3	-1	5,98	5,50
4	3	-1	4,22	4,50
5	3	-1	15,50	15,92
6	3	-1	11,62	11,65
7	3	-1	1,90	1,97
8	3	-1	7,85	7,48
9	3	-1	28,29	28,06
10	3	-1	13,04	12,37
11	3	-1	3,03	3,03
12	3	-1	7,56	7,38
13	3	-1	1,04	,68
1	3	0	15,08	15,28
2	3	0	9,31	8,94
3	3	0	16,62	15,99
4	3	0	22,66	22,99
5	3	0	23,38	23,67
6	3	0	2,79	2,59
7	3	0	3,65	4,23
8	3	0	20,69	20,68
9	3	0	5,65	5,49
10	3	0	15,42	15,20
11	3	0	11,17	11,06
12	3	0	4,89	4,74
13	3	0	10,15	9,93
0	3	1	25,18	27,36
1	3	1	29,31	27,82
2	3	1	3,34	2,98
3	3	1	6,63	6,69
4	3	1	11,08	10,43
5	3	1	4,25	4,16
6	3	1	5,52	5,51
7	3	1	4,25	4,04
8	3	1	16,11	16,17
9	3	1	26,17	26,51
10	3	1	7,25	7,18
11	3	1	3,71	3,54
12	3	1	8,67	8,20
13	3	1	2,43	2,46
0	3	2	23,67	25,17
1	3	2	8,55	8,98
2	3	2	24,42	23,14
3	3	2	11,35	11,59
4	3	2	2,64	1,93
5	3	2	17,85	16,66
6	3	2	15,41	15,57
7	3	2	4,60	5,01
8	3	2	23,35	23,71
9	3	2	3,33	3,05
10	3	2	6,21	6,30
11	3	2	1,81	2,35
12	3	2	5,80	5,90
0	3	3	12,96	12,92
1	3	3	17,19	17,83
2	3	3	12,09	11,94
3	3	3	2,60	1,92
4	3	3	8,87	8,88
5	3	3	9,18	9,50
6	3	3	13,60	13,36
7	3	3	6,22	6,19
8	3	3	1,58	1,33
9	3	3	11,19	11,65

H	K	L	FO	FC
10	3	3	3,98	4,22
11	3	3	6,48	6,53
12	3	3	8,93	9,77
0	3	4	20,28	21,08
1	3	4	15,17	15,87
2	3	4	10,90	9,34
3	3	4	1,63	1,55
4	3	4	21,95	22,44
5	3	4	11,25	12,06
6	3	4	9,15	9,03
7	3	4	1,00	,87
8	3	4	7,11	7,32
9	3	4	6,33	6,26
10	3	4	8,22	7,95
11	3	4	4,40	4,59
0	3	5	3,41	3,12
1	3	5	13,65	13,28
2	3	5	5,15	5,20
3	3	5	13,25	13,74
4	3	5	6,24	6,07
5	3	5	3,69	3,26
6	3	5	6,92	6,43
7	3	5	2,96	2,33
8	3	5	8,64	9,23
9	3	5	5,56	6,30
10	3	5	4,99	5,46
0	3	6	2,78	2,82
1	3	6	11,74	11,17
2	3	6	7,91	7,96
3	3	6	1,52	1,56
4	3	6	7,35	7,56
5	3	6	9,08	10,06
6	3	6	2,69	2,49
7	3	6	5,23	5,17
8	3	6	3,37	3,17
0	3	7	4,35	4,02
1	3	7	7,19	6,73
2	3	7	2,11	2,18
3	3	7	8,75	8,99
4	3	7	2,00	2,09
5	3	7	1,36	1,58
6	3	7	4,42	4,53
0	3	8	2,31	2,36
1	3	8	1,33	1,67
2	3	8	4,22	4,34
3	3	8	2,61	2,75
2	1	-9	5,00	4,78
1	1	-8	0,00	,44
2	1	-8	3,19	3,09
3	1	-8	2,64	2,73
4	1	-8	,41	,39
5	1	-8	0,00	,41
6	1	-8	6,39	6,06
7	1	-8	4,94	4,62
8	1	-8	0,00	,74
1	1	-7	5,42	4,86
2	1	-7	7,81	7,20
3	1	-7	0,00	,58
4	1	-7	,71	,81
5	1	-7	2,26	2,48
6	1	-7	2,86	2,75
7	1	-7	4,31	4,51
8	1	-7	,41	,28
9	1	-7	2,42	2,19
10	1	-7	4,50	3,87
1	1	-6	5,48	5,44
2	1	-6	,39	,24
3	1	-6	11,61	11,53
4	1	-6	11,84	11,75
5	1	-6	2,56	2,49
6	1	-6	5,77	5,27
7	1	-6	3,66	3,52
8	1	-6	2,50	2,50
9	1	-6	9,52	9,70
10	1	-6	,33	,05
11	1	-6	,85	,58
12	1	-6	,49	,77
1	1	-5	3,84	4,18
2	1	-5	,22	,20
3	1	-5	3,28	3,64
4	1	-5	6,74	6,69
5	1	-5	7,41	8,04
6	1	-5	,76	,66
7	1	-5	9,77	9,94
8	1	-5	12,57	12,35
9	1	-5	7,75	7,38
10	1	-5	,79	1,19
11	1	-5	2,33	2,01
12	1	-5	5,23	4,88
13	1	-5	5,90	5,65
1	1	-4	,59	,72
2	1	-4	10,01	10,28
3	1	-4	25,10	24,46
4	1	-4	27,29	26,93
5	1	-4	11,26	11,24
6	1	-4	5,63	6,11
7	1	-4	2,94	2,76
8	1	-4	,54	,73
9	1	-4	9,04	9,17
10	1	-4	2,36	2,41
11	1	-4	4,72	4,69
12	1	-4	8,75	8,41
13	1	-4	1,73	1,73
1	1	-3	10,93	11,76
2	1	-3	5,13	5,45
3	1	-3	2,43	2,34
4	1	-3	4,41	4,73
5	1	-3	3,12	3,25

H	K	L	FO	FC
6	1	-3	7,60	7,37
7	1	-3	21,30	20,56
8	1	-3	13,92	15,85
9	1	-3	18,76	19,08
10	1	-3	10,04	10,38
11	1	-3	4,43	4,43
12	1	-3	7,03	6,82
13	1	-3	0,00	,34
14	1	-3	,73	,01
1	1	-2	37,29	39,07
2	1	-2	1,89	2,68
3	1	-2	39,22	41,04
4	1	-2	19,10	17,89
5	1	-2	8,24	7,34
6	1	-2	6,94	6,63
7	1	-2	7,74	7,32
8	1	-2	7,50	7,01
9	1	-2	,58	,52
10	1	-2	,83	,15
11	1	-2	6,93	7,29
12	1	-2	5,54	5,58
13	1	-2	2,86	2,98
14	1	-2	7,18	7,08
2	1	-1	23,19	25,12
3	1	-1	2,59	1,33
4	1	-1	36,48	36,64
5	1	-1	27,50	26,36
6	1	-1	5,66	5,25
7	1	-1	37,01	35,80
8	1	-1	,43	,53
9	1	-1	11,47	11,90
10	1	-1	3,82	4,54
11	1	-1	5,11	5,66
12	1	-1	8,18	7,84
13	1	-1	4,94	4,45
14	1	-1	1,95	1,98
1	1	0	18,00	17,62
2	1	0	9,61	9,88
3	1	0	28,36	29,00
4	1	0	19,65	18,95
5	1	0	39,46	38,23
6	1	0	8,12	8,03
7	1	0	14,51	13,63
8	1	0	6,80	7,14
9	1	0	1,12	,83
10	1	0	0,00	,26
11	1	0	2,74	3,88
12	1	0	4,20	4,15
13	1	0	7,26	7,61
14	1	0	4,27	3,23
2	1	1	29,42	31,21
3	1	1	36,72	37,91
4	1	1	3,68	3,36
5	1	1	19,55	18,89
6	1	1	3,48	3,00
7	1	1	25,10	24,63
8	1	1	4,00	4,05
9	1	1	1,70	1,54
10	1	1	4,66	4,92
11	1	1	3,17	2,63
12	1	1	4,53	5,02
13	1	1	1,48	,31
14	1	1	,69	,62
1	1	2	30,20	31,12
2	1	2	20,68	20,20
3	1	2	15,01	13,76
4	1	2	28,34	28,73
5	1	2	22,95	22,47
6	1	2	11,07	10,68
7	1	2	12,94	12,80
8	1	2	5,64	7,10
9	1	2	3,37	3,56
10	1	2	2,21	2,36
11	1	2	3,48	3,88
12	1	2	2,16	1,88
13	1	2	4,12	4,84
0	1	3	25,75	25,45
1	1	3	10,08	9,87
2	1	3	13,11	13,54
3	1	3	28,18	28,47
4	1	3	14,35	13,31
5	1	3	9,80	9,58
6	1	3	7,43	7,68
7	1	3	1,05	,15
8	1	3	11,18	11,19
9	1	3	2,49	2,51
10	1	3	10,50	10,96
11	1	3	3,85	4,10
12	1	3	3,24	3,23
0	1	4	1,32	,54
1	1	4	17,57	17,25
2	1	4	7,28	7,16
3	1	4	22,44	21,85
4	1	4	15,22	15,54
5	1	4	2,72	2,86
6	1	4	3,55	3,18
7	1	4	,54	1,16
8	1	4	6,05	6,06
9	1	4	3,32	2,77
10	1	4	2,45	2,08
11	1	4	2,37	2,62
12	1	4	3,46	4,01
0	1	5	17,63	17,25
1	1	5	3,08	3,43
2	1	5	,66	,94
3	1	5	4,10	4,55
4	1	5	6,53	6,79
5	1	5	9,54	9,65

H	K	L	FO	FC
6	1	5	4,64	3,95
7	1	5	5,78	5,28
8	1	5	2,71	3,16
9	1	5	,68	,46
10	1	5	1,88	1,98
0	1	6	4,95	4,86
1	1	6	6,16	5,90
2	1	6	2,34	2,13
3	1	6	8,19	7,62
4	1	6	8,38	8,50
5	1	6	,81	,64
6	1	6	2,55	2,40
7	1	6	6,82	6,99
8	1	6	4,97	4,99
9	1	6	6,94	7,70
0	1	7	4,90	5,35
1	1	7	1,83	1,72
2	1	7	5,01	4,51
3	1	7	1,34	1,40
4	1	7	3,75	3,49
5	1	7	6,12	6,08
6	1	7	,57	,54
7	1	7	1,47	1,53
0	1	8	2,02	2,01
1	1	8	2,09	1,90
2	1	8	6,77	6,24
3	1	8	,93	1,04
4	1	8	2,33	2,79
0	4	0	,60	,60
0	6	0	0,00	,39
0	8	0	,56	,76
1	4	0	17,22	18,19
1	5	0	3,05	2,56
1	6	0	1,58	1,45
1	7	0	15,87	16,83
1	8	0	2,45	2,48
2	4	0	15,76	15,44
2	5	0	3,69	3,13
2	6	0	9,05	8,90
2	7	0	8,91	8,47
2	8	0	11,83	12,30
3	4	0	23,92	27,24
3	5	0	8,15	7,99
3	6	0	2,77	2,52
3	7	0	11,01	11,35
3	8	0	2,67	2,35
4	4	0	13,71	13,99
4	5	0	4,80	4,75
4	6	0	3,31	3,25
4	7	0	11,62	11,53
4	8	0	3,41	3,46
5	4	0	17,55	15,75
5	5	0	3,59	2,43
5	6	0	10,25	10,44
5	7	0	,98	,96
5	8	0	1,10	,82
6	4	0	3,95	3,06
6	5	0	14,45	14,50
6	6	0	3,55	3,50
6	7	0	6,57	6,69
6	8	0	6,18	6,76
7	4	0	4,02	3,58
7	5	0	7,16	6,19
7	6	0	1,03	1,72
7	7	0	2,38	2,10
8	4	0	21,13	20,60
8	5	0	12,23	11,67
8	6	0	1,59	1,11
8	7	0	8,67	8,65
9	7	0	,87	1,05
9	6	0	7,29	6,91
9	5	0	1,54	1,71
9	4	0	12,66	12,06
10	4	0	10,48	9,41
10	5	0	7,34	6,61
10	6	0	3,79	3,84
11	4	0	2,66	2,59
11	5	0	8,72	7,92
12	4	0	1,80	1,52
12	5	0	5,41	5,01
-13	4	1	5,16	7,05
-12	4	1	8,97	9,06
-12	5	1	1,04	,83
-11	4	1	3,19	2,75
-11	5	1	4,06	4,04
-10	4	1	5,86	6,07
-10	5	1	5,43	4,91
-10	6	1	,55	,04
-9	4	1	6,00	6,05
-9	5	1	1,31	,52
-9	6	1	3,61	4,62
-9	7	1	1,12	1,56
-8	4	1	13,57	13,11
-8	5	1	9,63	8,82
-8	6	1	7,04	7,10
-8	7	1	5,21	5,89
-7	4	1	11,39	10,58
-7	5	1	5,12	4,31
-7	6	1	,33	,17
-7	7	1	2,91	2,75
-6	4	1	13,54	12,48
-6	5	1	7,46	7,75
-6	6	1	7,83	7,78
-6	7	1	7,06	7,01
-6	8	1	,88	1,07
-5	4	1	14,20	13,42
-5	5	1	6,51	5,81
-5	6	1	3,45	3,51

H	K	L	FO	FC
-5	7	1	11.96	11.58
-5	8	1	2.93	2.91
-4	4	1	19.86	19.01
-4	5	1	1.35	.76
-4	6	1	6.05	6.14
-4	7	1	5.77	5.52
-4	8	1	4.50	4.60
-3	4	1	2.18	2.09
-3	5	1	8.31	7.21
-3	6	1	6.51	7.64
-3	7	1	6.13	5.72
-3	8	1	8.60	8.86
-2	4	1	13.78	12.51
-2	5	1	7.72	7.11
-2	6	1	4.14	4.32
-2	7	1	5.95	5.63
-2	8	1	5.29	5.58
-1	4	1	1.46	1.75
-1	5	1	6.11	5.73
4	2	1	20.74	21.72
-1	7	1	9.83	9.55
-1	8	1	5.76	5.72
0	4	1	17.05	16.61
0	5	1	1.26	1.24
0	6	1	3.87	1.84
0	7	1	9.91	9.58
0	8	1	2.53	2.21
1	4	1	8.99	8.23
1	5	1	5.68	5.69
1	6	1	14.33	17.83
1	7	1	8.07	8.02
1	8	1	8.68	8.35
2	4	1	5.86	5.10
2	5	1	1.22	.08
2	6	1	9.39	10.03
2	7	1	2.69	2.89
2	8	1	7.86	8.42
3	4	1	8.71	8.68
3	5	1	8.26	7.05
3	6	1	3.92	3.54
3	7	1	7.87	7.57
3	8	1	5.08	5.31
4	4	1	15.00	14.54
4	5	1	7.22	7.80
4	6	1	2.57	2.31
4	7	1	8.78	8.60
4	8	1	3.54	3.35
5	4	1	16.71	17.25
5	5	1	1.09	.40
5	6	1	3.67	2.51
5	7	1	13.41	14.54
5	8	1	4.98	4.77
6	4	1	10.50	11.03
6	5	1	4.48	3.42
6	6	1	1.03	.84
6	7	1	8.85	8.52
6	8	1	2.21	2.44
7	4	1	12.66	14.79
7	5	1	9.24	9.02
7	6	1	5.04	4.24
7	7	1	2.55	2.79
8	4	1	2.69	2.40
8	5	1	2.54	2.30
8	6	1	0.00	.18
8	7	1	3.91	3.85
10	4	1	5.47	5.55
10	5	1	1.20	.02
10	6	1	1.23	1.07
11	4	1	4.35	4.49
11	5	1	3.35	3.20
12	4	1	8.87	8.79
-12	4	2	3.23	2.31
-11	4	2	8.13	7.12
-11	5	2	6.93	6.02
-10	4	2	2.73	2.30
-10	5	2	1.40	1.13
-10	6	2	0.00	.54
-9	4	2	8.11	7.12
-9	5	2	6.49	6.04
-9	6	2	1.63	1.81
-8	4	2	8.58	7.51
-8	5	2	17.64	17.39
-8	6	2	2.49	2.59
-8	7	2	9.52	9.36
-7	4	2	10.48	9.29
-7	5	2	11.73	11.34
-7	6	2	2.38	1.92
-7	7	2	3.19	2.88
-6	4	2	1.55	1.89
-6	5	2	9.74	9.53
-6	6	2	4.94	4.41
-6	7	2	8.02	7.05
-6	8	2	3.21	3.04
-5	4	2	13.14	14.48
-5	5	2	13.45	13.02
-5	6	2	8.21	7.97
-5	7	2	.40	1.51
-5	8	2	2.25	1.94
-4	4	2	13.58	14.94
-4	5	2	12.27	10.80
-4	6	2	9.32	8.47
-4	7	2	6.81	6.43
-4	8	2	2.48	2.69
-3	4	2	18.21	17.65
-3	5	2	2.17	2.07
-3	6	2	7.08	6.69
-3	7	2	1.34	1.41
-3	8	2	3.66	3.42

H	K	L	FO	FC
-2	4	2	12,88	12,42
-2	5	2	11,97	13,99
-2	6	2	15,53	16,18
-2	7	2	4,79	5,12
-2	8	2	12,36	11,73
-1	4	2	10,11	9,38
-1	5	2	1,63	1,42
-1	6	2	5,07	4,23
-1	7	2	11,40	10,99
-1	8	2	6,64	5,96
0	4	2	2,53	3,16
0	5	2	2,70	2,86
0	6	2	7,16	7,20
0	7	2	7,41	6,58
0	8	2	5,90	5,31
1	4	2	22,54	24,74
1	5	2	,65	,40
1	6	2	1,81	1,87
1	7	2	8,89	8,34
1	8	2	4,93	4,97
2	4	2	9,35	8,37
2	5	2	1,89	2,13
2	6	2	2,08	2,77
2	7	2	5,27	5,11
2	8	2	3,94	3,57
3	4	2	13,45	16,16
3	5	2	1,43	1,86
3	6	2	15,27	16,98
3	7	2	9,25	9,50
3	8	2	5,55	5,14
4	4	2	9,44	9,83
4	5	2	6,04	5,99
4	6	2	3,91	4,03
4	7	2	8,68	8,60
4	8	2	3,09	3,25
5	4	2	2,70	2,77
5	5	2	4,88	5,20
5	6	2	0,00	1,90
5	7	2	2,50	2,16
5	8	2	2,41	2,06
6	4	2	,87	,07
6	5	2	15,00	16,21
6	6	2	2,06	2,34
6	7	2	8,00	7,99
7	4	2	11,44	11,84
7	5	2	4,74	4,72
7	6	2	2,10	1,96
7	7	2	1,54	1,06
8	4	2	9,37	9,60
8	5	2	5,62	5,41
8	6	2	3,24	2,94
8	7	2	1,40	1,10
9	4	2	6,87	7,00
9	5	2	5,57	5,36
9	6	2	3,24	3,06
10	4	2	1,56	1,63
10	5	2	8,28	8,05
11	4	2	1,19	1,33
11	5	2	6,41	6,60
12	4	2	4,87	4,64

APPENDIX 3 DETERMINATION OF THE CRYSTAL AND MOLECULAR STRUCTURE OF DL HOMOCYSTEIC ACID

1. Preliminary work

1.1 Preparation of crystals

DL homocysteic acid (DLH) $C_3H_9NO_5S$, dissolves readily in water but the solubility is so great that it is difficult to produced well-formed cystals. DLH is only very sparingly soluble in organic solvents, so no useful crystals were forthcoming from such solutions. Usable, flat needle-like crystals were eventually obtained from an aqueous solution heated to 90°C for some hours. The crystal habit is illustrated in Fig. A3.1.

1.2 Physical properties of the crystals

After heating at 120°C for two hours the crystals showed no weight loss, indicating that they contained no water of crystallisation.

The density of DLH, measured by the flotation method, was 1.711 g/cc.

A melting point determination was carried out on a hot-stage microscope, giving a result of 274-6°C, a high value for an organic solid.

Optical investigation of the crystals revealed extinction parallel to prominent morphological axes, suggesting that DLH may crystallise in the orthorhombic system.

2. X-ray analysis

Ni filted Cu radition (Cu$k\alpha$, λ = 1.5418 Å) was used throughout.

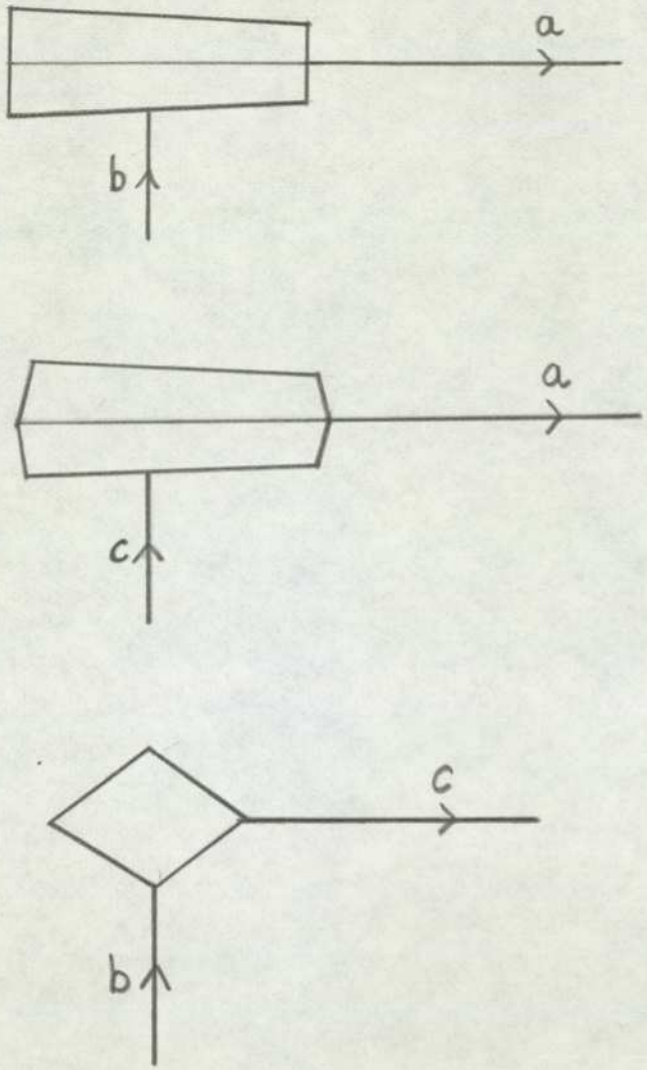

Fig. A3.1 Crystal habit diagrams for DLH crystals grown from aqueous solution

2.1 Preliminary photographs

A crystal was aligned along a needle axis (subsequently defined as a), on the goniometer of a Nonius Weissenberg camera, using double oscillation photographs. A rotation photograph was taken to determine the repeat distance along the needle axis and a zero layer Weissenberg photograph was taken.

The Weissenberg photograph revealed possible orthogonal axes, which together with the needle axis, could form the mutually perpendicular axes of an orthorhombic unit cell. Moreover, the two halves of each photograph were the same, and equivalent reflections on either side of the putative axes had the same intensity. Thus an orthorhombic cell was confirmed. It was only possible to index the reflections on the upper layers of the rotation photograph, however, if it was assumed that only every fourth reflection on the axes in the zero layer Weissenberg photograph appeared: that is, three out of four were systematically absent. This assumption provided a basis for the consistent indexing of the reflections observed on the rotation photograph, and showed that the reflections with mixed indices were systematically absent. Thus, the unit cell was F centred.

The other systematic absences were:

$0k0$, $k \neq 4n$
$00l$, $l \neq 4n$
$0kl$, k odd or l odd

A second crystal was aligned along one of the axes located in the Weissenberg photograph above. This axis was subsequently defined as b. A rotation photograph was taken and the axial spacing determined. This was the same as the spacing determined above on the assumption that three out of four axial reflections in the Weissenberg photograph were systematically absent. A Weissenberg photograph was taken, showing consistent axial lengths

and the following systematic absences:

hkl	mixed
$h00$	$h \neq 4n$
$00l$	$l \neq 4n$
$h0l$	$(h+l) \neq 4n$

The mean cell parameters from the two crystals were:

a = 6.10 Å
b = 20.38 Å
c = 23.41 Å

These approximate cell dimensions, with the measured density, show that there are sixteen molecules in the unit cell:

$Z = 16$

The International Tables for X-ray Crystallography Vol. 1 (Lonsdale, 1962) gave the space group unambiguously as F2dd. This is a non-centrosymmetric space group.

2.2 Data collection

The measurement of X-ray reflection intensities for DLH was carried out using Weissenberg film packs. The intensities were determined automatically by the SRC microdensitometer service at the Atlas Computer Laboratory. The film packs employed contained three films, with a thin sheet of aluminium foil between the second and third to ensure that intense reflected beams were recorded without saturating the emulsion of the last film. With an exposure of $\sim$ 26 hours, nearly all the reflections were recorded without saturation on at least one of the films, while even very weak reflections showed up clearly on the first film. Six layers of the a axis were investigated. One reflection of each pack was indexed, as required for the automatic microdensitomer scan, and the film packs were despatched together with cell parameters, X-ray wavelength and camera radius information.

The processing was completed in less than a fortnight making the entire data collection operation considerably quicker than the diffractometer method. The output from the Atlas microdensitometer scanning program contains a least squares refinement of the cell parameters as well as intensity measurements for each reflection. The precision of the cell parameters is, however, an order of magnitude poorer than those which can be obtained on the diffractometer. This is a result of the difficulty in measuring precise positions of diffraction spots on the film and the uncertainty inherent in film methods due to shrinkage in processing.

The final cell parameters were:

$a = 6.06 \pm .03$ Å
$b = 20.19 \pm .07$ Å
$c = 23.25 \pm .05$ Å
$\alpha = \beta = \gamma = 90^{o}$

giving a calculated density of 1.700 g/cc.

3. Data processing

3.1 Preparation of data

The intensity measurements were received on punched cards in the appropriate format for the X-RAY 72 suite of programs, (Stewart Kundell & Baldwin, 1972) which was to be used for data analysis. No Lorentz or Polarisation corrections had been applied. A unique set of data was prepared as described for βGP in Appendix 2.

The total number of unique reflections measured was 560, of which only 9, with intensities less than 50 above background, were designated as 'unobserved'. The remaining 551 reflections were regarded as 'observed'.

The reflections fell into six layer groups (including 'unobserved' reflections)

1	$0k\ell$:	80
2	$1k\ell$:	115
3	$2k\ell$:	110
4	$3k\ell$:	110
5	$4k\ell$:	82
6	$5k\ell$:	63

3.2 Data analysis

3.2.1 Location of sulphur atom

DLH contains one sulphur atom per molecule, the ratio of the squared atomic number of S to the sum of squared atomic numbers for the rest of the molecule being $\sim\frac{1}{2}$. Hence it was decided to solve the structure by the heavy atom method (see Stout & Jenson (1968); 270-299). The first step, therefore, was to determine the co-ordinates of the sulphur atom in the unit cell.

The sulphur atom was located by constructing two Harker sections ($0v\omega$ and $\frac{1}{4}v\omega$) using the X-Ray 72 links DATRDN (applying Lorentz and polarisation corrections and setting up a binary data file as for βGP, NORMSF (determing scale factors) and FOURR (calculating the sections of Patterson space using $|F|^2$ values as co-ordinates). The programs were implemented on the CDC 7600 computer at ULCC.

From the space group symmetry, two lines of the section at ($\frac{1}{4}v\omega$) should show a peak corresponding to the operation of the two d glide planes on the sulphur atom.

(1) d glide perpendicular to y:
Glide operation on xyz $\Rightarrow(\frac{1}{4} + x, \frac{1}{4} - y, \frac{1}{4} + z)$
Vector between the points is $(\frac{1}{4}, \frac{1}{4}-2y, \frac{1}{4})$
The Harker line $\frac{1}{4}v\frac{1}{4}$ shows at peak at $v = \frac{1}{4}$
Thus $\frac{1}{4}-2y = v = \frac{1}{4}$; so $y = 0$
(2) d glide perpendicular to z:
Similarly, vector is $(\frac{1}{4}, \frac{1}{4}, \frac{1}{4}-2z)$
The Harker line $\frac{1}{4}\ \frac{1}{4}\ \omega$ shows peaks at $\omega = \frac{1}{4}$ or 0;
so $z = 0$ or $-\frac{1}{8}$

The third symmetry element considered is the diad parallel to x. The operation of this diad should produce peaks on the $0v\omega$ section of Patterson space. On this Harker section peaks occur at:

i) $v = \frac{1}{4}$, $\omega = \frac{1}{4}$ $\quad y = 0, z = 0$

and ii) $v = \frac{1}{4}$, $\omega = 0$ $\quad y = 0, z = -\frac{1}{8}$

i) puts the sulphur atom on a diad, but diad symmetry is not present in an SO_3 group, so this can be discounted;

ii) is the larger peak and the remaining possibility, hence the sulphur atom is placed at:

$0, 0, \frac{1}{8}$

x being arbitrary in this space group.

$0, 0, \frac{1}{8}$ it should be noted, is not a special position, so that the sulphur atom is not constrained to these precise values. It was subsequently found to deviate slightly from $y = 0$ and $z = \frac{1}{8}$.

3.2.2 Location of further atoms by the heavy atom method and difference synthesis

The atomic co-ordinates of the sulphur atom were loaded into the X-RAY 72 binary data file (using the program LOADAT) and phases were generated (using program FC) for all the reflections, based on the sulphur atom position alone. These phases should approximate to the true ones since a considerable proportion of the scattering is due to the sulphur atom (the heavy atom method). The program FOURR was then employed to produce an electron density map of the asymmetric part of the unit cell using observed F values as co-ordinates. The relatively high symmetry of the cell caused the electron density map based on the presence of only one atom to develop false symmetry. Hence the map showed a pair of CSO_3 groups related by a diad parallel to Z. In order to proceed further, a single oxygen was chosen from each of the two alternatives and an F map produced using phases from the positions of S and O for each case, with scale factors and an overall temperature factor from the X-RAY 70 program DATFIX. Only one of the maps was

interpretable, and enabled the CSO_3 group to be located. The co-ordinates of this group were then subjected to three cycles of full-matrix least-squares refinement using the program CRYLSQ as described for βGP, which lowered the R-factor from 0.40 to 0.29. Isotropic temperature factors and unit weights were employed. Further progress was then possible by means of a difference map (FOURR using Fo-Fc as coefficients) restricting the reflections to those with Fc > Fo. This restriction improves the probability of obtaining approximately correct phases for most reflections (X-RAY 72 manual : Stewart, Kundell & Baldwin, 1972). Thus all but two of the non-hydrogen atoms were located. Repeating this process the remaining non-hydrogen atoms were found, and after three further cycles of refinement the R factor reached 0.130. At this point, the connectivity of the molecule was apparent, and some atom types had to be corrected. Further refinement then reduced the R factor to 0.081.

3.2.3 Further refinement using modified electronic populations

Attempts to refine the structure with anisotropic temperature factors consistently failed, resulting in negative determinants for the temperature factors of O1, O3 and O5. A negative temperature factor indicates that there is a deficiency of electron density on the atoms concerned. This may be a real physical effect or, more commonly perhaps, a result of the fact that in least squares refinements, the temperature factors amass the accumulated errors of data and model.

Noting that only the oxygens were affected and that, in molecular orbital calculations, oxygen atoms in ionised carboxyl groups (Borthwick & Steward, 1975[b]) and SO_3 groups (Richards, private communication) show considerable excess electron density, it was decided to test the effect of altering the electron population parameters of all the atoms in accordance with CNDO results. The population parameters which represent the number of electrons on the atom divided by the atomic number, were set at the values given in Table A3.1.

TABLE A3.1

DLH: CNDO fractional electronic populations

Atom	Fractional Populations
S1	0.93
C1	1.04
C2	0.98
C3	1.00
C4	0.94
N1	1.00
O1	1.07
O2	1.07
O3	1.07
O4	1.07
O5	1.07

A neutral atom has fractional population = 1.0. Population <1.0 indicates electron deficiency, hence +ive charge, and vice versa.

The experiment was a success, causing all temperature factors to become positive definite and lowering the R-factor to 0.069.

3.2.4 Positioning of hydrogens and final refinement

The hydrogen atoms were found by difference synthesis and successive least squares refinement. Fifteen reflections of low $2\theta/\lambda$ and/or high intensity were zero weighted due to extinction but no other weighting scheme was employed. Final least squares refinement with all hydrogen atoms present and an overall temperature factor for the hydrogens decreased the R-factor to 0.047. Isotropic temperature factors for the hydrogens would not refine, even with modified population parameters for the amino hydrogens (0.8) so it was presumed that the limit of the data had been reached.

4. Structural Results

4.1 Parameters and figures

Final fractional co-ordinates are given in Table A3.2 and thermal parameters in Table A3.3 Bond lengths and angles for the molecule are given in Table A3.4 and for the hydrogen-bonds in Table A3.5. Some torsion angles for the molecule may be found in Table A3.6 and structure factors in Table A3.7. The arrangement of molecules in $\frac{1}{4}$ of the unit cell is indicated in Fig. A3.2, where the hydrogen bonding scheme is also illustrated. The remainder of the cell contents may be generated by the F centering operation. Fig. A3.3 is a photograph of a Beevers model of the structure, illustrating the arrangement of molecules along the x axis.

4.2 Discussion

DL homocysteic acid, in common with the next lower homologue, cysteic acid (Ramanadham, Sikka & Chidambaram, 1973) shows a zwitterionic form in the solid state, the sulphonic acid and amino groups both being ionised. Molecules are bound together in an unusual and intricate hydrogen-bonding scheme which may account for the high melting point exhibited. Molecules of each enantiomorph

form hydrogen bonded double helices around the diad axes parallel to x, adjacent molecules being connected by the O_5-H_9---O_3 hydrogen bond (Figs. A3.2 & 3). This may explain the needle like habit of the material, since development along the helices would encourage the growth of a needle axis along x. This is the habit observed.

The helices are bound together by hydrogen bonding across the screw diads parallel to x, midway between neighbouring helices in the y and z directions (see Fig. A3.2). Four helices are linked together around each of the screw diads. As well as the bonds N_1-H_6---O_1 and N_1-H_7---O_2, a bifurcated hydrogen bond N_1-H_8----O_2 ---O_4 is involved in this process, and indeed, the distance H_8---O_1 (2.60) is only just beyond the range of possible involvement in bonding (Donohue, 1968, p.456). Two sets of this four-fold bonding arrangement are found around each of the screw diads.

The hydrogen-bond geometry is non-linear in all cases (Table A3.5) the deviation from linearity being ca.30^o in each of the single H-bonds. The H-bond lengths, however, are not remarkable. Since the hydrogen positions have large standard deviations, mainly because the scattering from hydrogens in a heavy atom structure is almost swamped by background, the distances and angles involving hydrogen atoms have high uncertainties. Hence the observed N-H and C-H distances and angles which are unusual (e.g. those involving H_3-H_8 in Table A3.4) may just reflect data insufficiency. The bond lengths and angles of the non-hydrogen atoms are close to usual values (Kennard et al, 1972) (Table A3.4).

In common with a number of other diacidic amino - acids, homocysteic acid exhibits an O_4-C_4-C_3N_1 torsion angle of less than 30^o (see Table A3.6), such that the carboxyl and amino groups lie close to a planar configuration. The atoms O_4-C_4-C_3-N_1-H_3 form a pseudo 5-ring, although the distance N_1-H_8 (2.94 Å) is too great to permit any intramolecular bonding. This quasi-planar configuration is also predicted in molecular orbital calculations on amino acids as different as glycine (Sabin & Oergirle, 1973) and ibotenic acid (Borthwick & Steward, 1975). It may be important in the pharmacological

activity of homocysteic acid, which is believed to mimic the natural excitatory transmitter, glutamic acid,at various mammalian synapses (Curtis & Watkins, 1963; Curtis, Duggan, Felix, Johnston, Tebēcis& Watkins, 1972).

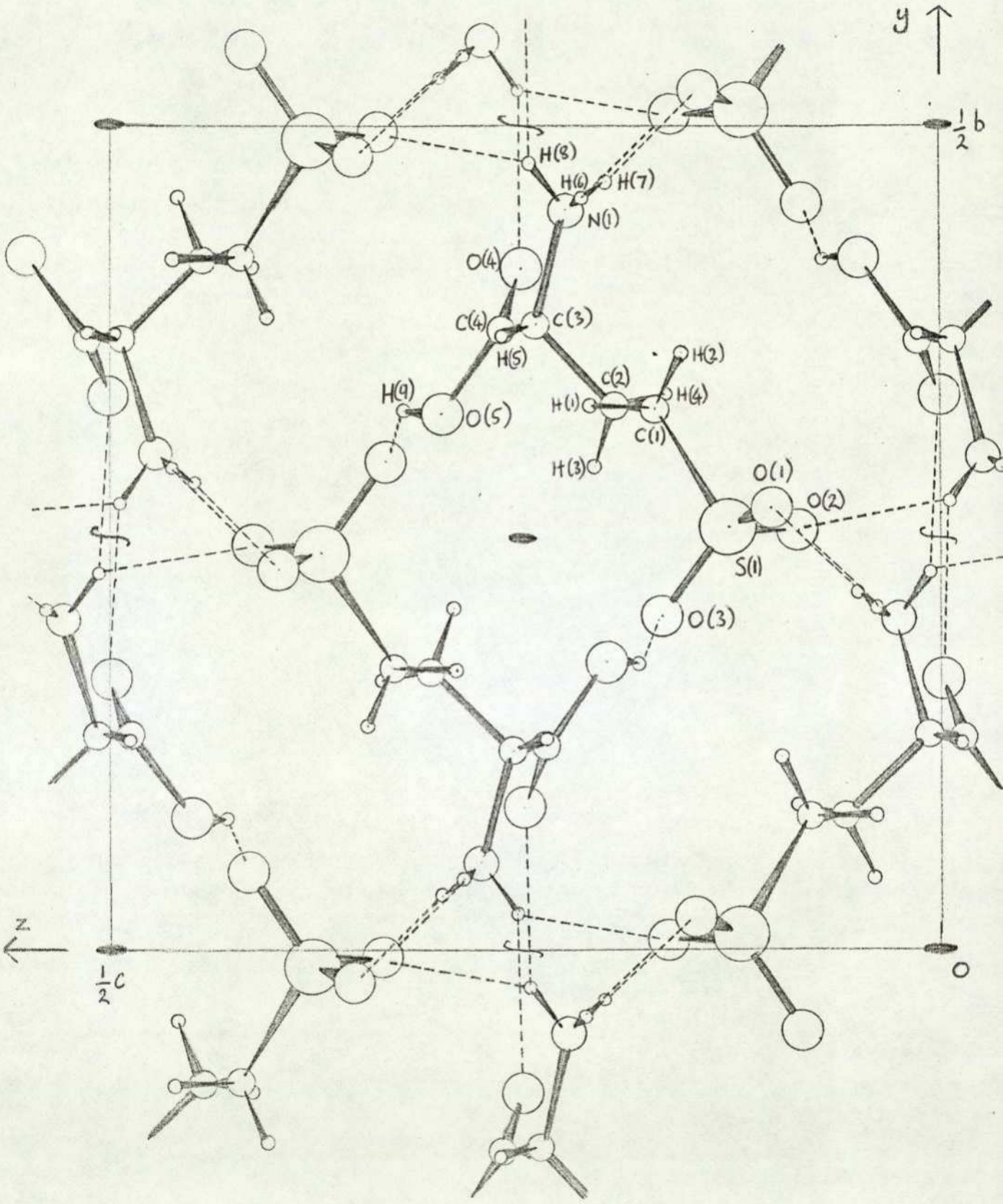

Fig. A3.2 DLH: arrangement of molecules in ¼ of the unit cell. x projection. The cell is idealised as a square.

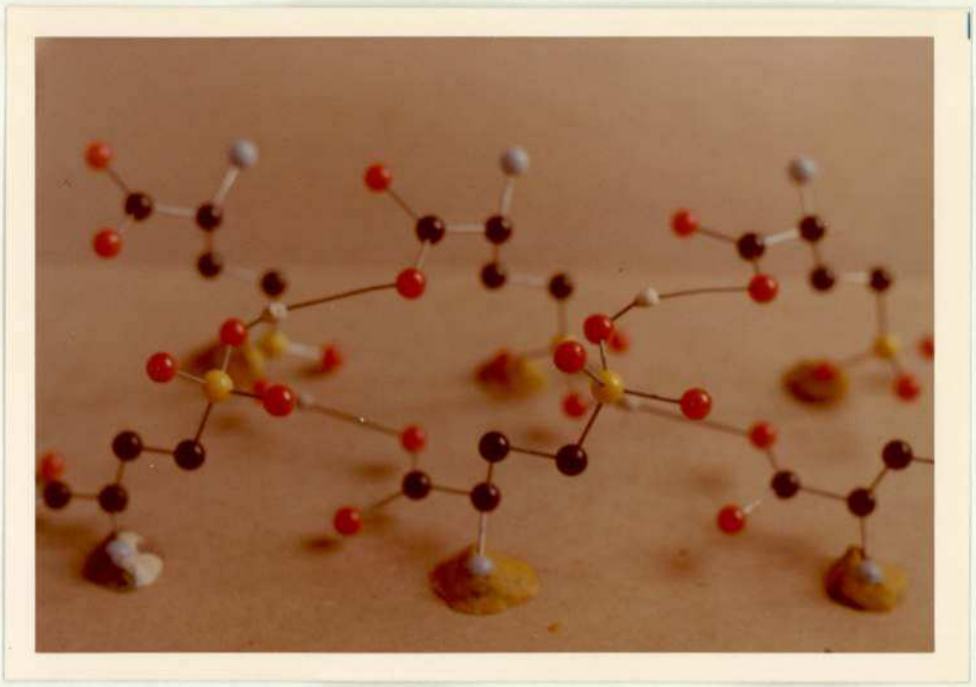

Fig. A3.3 Crystal structure model of DLH indicating the double helical arrangement of molecules along the x axis.

TABLE A3.2

Fractional atomic co-ordinates

Atom	x	y	z
S(1)	1.2500 *	.25850 (8)	.12865 (7)
C(1)	1.1976 (16)	.3292 (4)	.1714 (4)
C(2)	.9608 (16)	.3307 (4)	.1932 (3)
C(3)	.9286 (15)	.3800 (4)	.2426 (3)
C(4)	.6992 (14)	.3761 (4)	.2640 (3)
N(1)	.9745 (13)	.4482 (3)	.2237 (3)
O(1)	1.4640 (13)	.2704 (3)	.1018 (3)
O(2)	1.0741 (10)	.2536 (3)	.0875 (3)
O(3)	1.2583 (12)	.2016 (3)	.1675 (2)
O(4)	.5531 (11)	.4126 (3)	.2495 (3)
O(5)	.6688 (13)	.3259 (4)	.2991 (3)
H(1)	1.274 (16)	.331 (5)	.207 (5)
H(2)	1.215 (18)	.364 (5)	.155 (4)
H(3)	.919 (19)	.292 (6)	.207 (4)
H(4)	.812 (16)	.338 (5)	.163 (4)
H(5)	1.065 (16)	.374 (5)	.265 (4)
H(6)	1.105 (22)	.456 (6)	.213 (5)
H(7)	.840 (22)	.466 (7)	.200 (6)
H(8)	.987 (24)	.478 (7)	.246 (5)
H(9)	.527 (19)	.328 (5)	.321 (4)

+ Since space group F2dd has no fixed x origin, x for S(1) is set arbitrarily at $\frac{1}{4}$.

TABLE A3.3

Final thermal parameters x 100 Å^2

The temperature factor is of the form:

$$T = \exp\left[-2\pi^2\left[(ha^*)^2U_{11} + (kb^*)^2U_{22} + (lc^*)^2U_{33} + 2hka^*b^*U_{12} + 2hla^*c^*U_{13} + 2klb^*c^*U_{23}\right]\right]$$

Atom	U_{11}	U_{22}	U_{33}	U_{12}	U_{12}	U_{23}
S(1)	2.1 (7)	1.35 (7)	1.54 (7)	0.12 (7)	- 0.02 (7)	- 0.08 (6)
C(1)	4.9 *	3.0 (4)	3.2 (4)	- 0.4 (4)	0.2 (4)	- 0.8 (3)
C(2)	3.8 (1.0)	1.8 (4)	2.9 (4)	- 0.1 (3)	0.5 (4)	- 0.1 (3)
C(3)	4.2 (9)	1.5 (3)	2.1 (4)	- 0.1 (3)	- 0.2 (3)	0.1 (3)
C(4)	3.9 (9)	2.4 (4)	1.6 (4)	0.6 (4)	- 0.1 (3)	- 0.4 (3)
N(1)	4.0 (8)	1.5 (3)	2.5 (3)	0.3 (3)	0.2 (3)	- 0.1 (2)
O(1)	4.4 (8)	4.5 (3)	4.2 (3)	- 0.2 (3)	1.4 (3)	- 0.2 (3)
O(2)	5.1 (8)	3.4 (3)	3.9 (3)	0.2 (2)	- 1.3 (2)	- 0.6 (3)
O(3)	4.5 (8)	3.7 (3)	4.5 (3)	1.0 (3)	- 0.4 (3)	1.4 (2)
O(4)	4.8 (7)	3.1 (3)	3.9 (3)	0.3 (2)	0.3 (3)	0.4 (3)
O(5)	5.6 (8)	4.0 (4)	6.4 (4)	0.8 (3)	1.9 (3)	3.4 (4)

The overall temperature factor for the hydrogens, U_{Hyd} = 1.1 (8)

* Since x direction parameters have an arbitrary origin in the space group F2dd, one U_{11} has to be fixed during each cycle of refinement. U_{11} for C(1) was fixed during the final cycles, U_{11} for S(1) having been fixed earlier. Thus all U_{11}'s have been refined at some stage with respect to the other parameters.

	O(1)	O(2)	O(3)	C(1)		O(4)	O(5)
S(1)	1.457 (9)	1.435 (7)	1.461 (6)	1.767 (10)	C(4)	1.198 (11)	1.313 (11)
	C(2)	H(1)	H(2)		H(6)	H(7)	H(8)
C(1)	1.520 (15)	0.94 (10)	0.80 (11)	N(1)	0.84 (13)	1.05 (13)	0.81 (13)
	C(3)	H(3)	H(4)		H(9)		
C(2)	1.533 (11)	0.88 (11)	1.15 (10)	O(5)	1.00 (11)		
	C(4)	N(1)	H(5)				
C(3)	1.476 (14)	1.470 (10)	0.98 (10)				

O(1) - S(1) - O(2)	112.6 (5)	C(2) - C(3) - C(4)	109.7 (7)
O(1) - S(1) - O(3)	111.4 (4)	C(2) - C(3) - N(1)	111.1 (7)
O(1) - S(1) - C(1)	105.5 (4)	C(2) - C(3) - H(5)	102 (6)
O(2) - S(1) - O(3)	112.6 (4)	C(4) - C(3) - N(1)	109.2 (7)
O(2) - S(1) - C(1)	107.3 (4)	C(4) - C(3) - H(5)	127 (6)
O(3) - S(1) - C(1)	107.1 (4)	N(1) - C(3) - H(5)	97 (6)
S(1) - C(1) - C(2)	111.9 (6)	C(3) - N(1) - H(6)	115 (8)
S(1) - C(1) - H(1)	115 (6)	C(3) - N(1) - H(7)	110 (7)
S(1) - C(1) - H(2)	115 (7)	C(3) - N(1) - H(8)	121 (9)
C(2) - C(1) - H(1)	100 (6)	H(6) - N(1) - H(7)	121 (11)
C(2) - C(1) - H(2)	105 (8)	H(6) - N(1) - H(8)	88 (13)
H(1) - C(1) - H(2)	108 (9)	H(7) - N(1) - H(8)	99 (12)
C(1) - C(2) - C(3)	112.5 (7)	C(3) - C(4) - O(4)	124.4 (8)
C(1) - C(2) - H(3)	112 (7)	C(3) - C(4) - O(5)	112.5 (7)
C(1) - C(2) - H(4)	123 (5)	O(4) - C(4) - O(5)	123.0 (8)
C(3) - C(2) - H(3)	106 (7)		
C(3) - C(2) - H(4)	106 (5)	C(4) - O(5) - H(9)	114 (6)
H(3) - C(2) - H(4)	96 (8)		

TABLE A3.5

BOND LENGTHS AND ANGLES OF HYDROGEN BONDS

	H-acceptor (Å)	Donor-acceptor (Å)	Angle (donor-H-acceptor)^{o}
N(1)–H(6) --- O(2)	2.02 (12)	2.78 (2)	151 (10)
N(1)–H(7) --- O(1)	1.80 (11)	2.77 (2)	153 (11)
O(5)–H(9) --- O(3)	1.75 (11)	2.66 (2)	149 (8)
bifurcated bond			
N(1)–H(8) --- O(4)	2.24 (13)	2.92 (2)	141 (10)
N(1)–H(8) --- O(2)	2.36 (14)	2.96 (2)	132 (10)

TABLE A3.6

TORSION ANGLES(°)

O (4) - C (4) - C (3) - N (1)	25.2
O (4) - C (4) - C (3) - C (2)	-96.8
C (4) - C (3) - C (2) - C (1)	-176.6
C (3) - C (2) - C (1) - S (1)	164.5
C (2) - C (1) - S (1) - O (1)	168.9

Table A3.7 DLH structure factors

H	K	L	F OBS	F CALC	A	B
0	-18	18	28.78	26.72	26.72	.00
0	-22	8	33.95	31.64	31.64	.00
0	-16	4	35.89	40.81	-40.81	-.00
0	-14	-10	37.94	36.85	-36.85	-.00
0	-22	6	33.65	24.99	-24.99	-.00
0	12	22	43.01	43.52	43.52	.00
0	8	24	44.58	43.37	43.37	.00
0	-4	2	35.87	31.46	31.46	.00
0	2	26	46.48	51.64	51.64	.00
0	0	28	64.83	63.82	-63.82	-.00
0	22	12	26.87	32.74	-32.74	-.00
0	16	20	50.58	53.69	-53.69	-.00
0	-6	10	83.00	80.80	80.80	.00
0	-6	18	51.05	62.26	62.26	.00
0	4	28	46.67	43.62	-43.62	-.00
0	-4	24	60.98	56.68	-56.68	.00
0	-8	14	60.70	63.54	-63.54	-.00
0	-6	22	52.18	53.55	-53.55	-.00
0	-8	16	89.12	80.95	80.95	.00
0	-8	10	99.26	88.47	88.47	.00
0	-10	14	80.04	79.60	-79.60	-.00
0	-10	16	52.12	50.29	-50.29	-.00
0	-8	6	122.38	122.49	-122.49	-.00
0	-10	10	91.58	99.25	-99.25	-.00
0	-4	28	33.23	43.62	-43.62	-.00
0	-10	8	74.16	77.31	77.31	.00
0	-10	22	82.17	82.09	-82.09	-.00
0	-12	16	96.78	97.80	97.80	.00
0	-12	12	60.89	67.58	-67.58	-.00
0	-10	6	53.33	50.16	50.16	.00
0	-12	10	80.04	79.00	79.00	.00
0	-10	4	68.77	64.80	-64.80	-.00
0	-14	18	48.13	57.19	57.19	.00
0	-12	6	62.92	64.98	-64.98	-.00
0	-16	18	53.87	62.99	62.99	.00
0	-16	8	62.30	71.99	71.99	.00
0	-16	6	50.69	62.42	-62.42	-.00
0	-16	22	42.45	51.91	-51.91	-.00
0	-18	10	47.04	53.67	53.67	.00
0	-14	2	33.56	52.70	52.70	.00
0	-20	14	53.25	55.51	-55.51	-.00
0	-20	10	49.34	47.34	47.34	.00
0	-20	6	77.70	87.74	-87.74	-.00
0	-20	4	54.44	64.70	-64.70	-.00
0	-20	2	74.17	76.11	76.11	.00
0	-24	6	73.22	68.32	-68.32	-.00
0	-24	2	52.15	50.45	50.45	.00
0	-24	0	109.09	92.48	92.48	.00
0	-4	-8	62.53	63.60	63.60	.00
0	-16	-12	40.98	39.87	-39.87	-.00
0	-2	-6	97.87	111.00	-111.00	-.00
0	-4	-10	32.44	34.11	34.11	.00
0	-4	-12	139.39	130.60	-130.60	-.00
0	-4	-14	46.77	49.63	49.63	.00

H	K	L	F OBS	F CALC	A	B
0	-8	-20	38.07	38.96	-38.96	-.00
0	0	-12	68.01	80.88	80.88	.00
0	-4	-20	112.12	96.61	-96.61	-.00
0	-2	-18	50.04	42.69	42.69	.00
0	0	-16	99.30	82.20	82.20	.00
0	-12	-24	71.83	63.02	63.02	.00
0	-2	-22	45.34	43.59	-43.59	-.00
0	0	-20	56.85	42.09	-42.09	-.00
0	-6	-26	55.43	55.01	55.01	.00
0	0	-24	105.64	89.49	89.49	.00
1	3	19	58.87	62.85	-61.94	-10.63
1	17	21	34.90	34.38	-12.79	31.92
1	-1	13	38.47	34.77	-32.74	-11.70
1	1	17	23.80	25.66	-14.68	-21.05
1	5	21	56.68	57.56	3.20	57.47
1	11	23	34.91	33.08	32.17	7.68
1	9	23	27.44	31.52	30.00	-10.01
1	-1	15	34.00	36.51	36.50	.80
1	3	21	50.45	47.60	-39.07	-27.19
1	1	19	42.96	43.95	-35.72	-25.62
1	15	23	39.22	42.64	35.85	23.09
1	-3	9	80.63	75.22	75.05	-5.09
1	-3	11	98.39	97.78	93.88	-27.33
1	-3	7	119.51	114.23	110.62	28.50
1	-3	13	62.45	64.74	-61.67	-19.71
1	1	21	94.61	90.41	-42.17	79.97
1	9	25	33.22	34.07	-.16	-34.07
1	11	25	39.24	41.94	19.03	37.37
1	7	25	32.87	33.36	32.96	5.13
1	-3	15	73.15	72.52	36.83	62.47
1	-3	5	36.97	42.29	35.65	-22.75
1	5	25	36.91	35.11	25.77	-23.85
1	-3	17	84.19	83.99	4.29	-83.88
1	3	25	80.61	80.57	67.90	43.36
1	-5	11	86.39	85.30	-39.13	75.80
1	-5	13	105.11	100.73	-95.99	30.53
1	-5	9	78.05	73.07	60.21	41.40
1	1	25	67.64	66.87	41.15	-52.71
1	-5	17	101.70	103.86	43.71	94.21
1	5	27	34.93	33.14	-33.14	-.48
1	-5	7	120.06	115.50	100.49	-56.93
1	3	27	20.48	23.35	-19.51	12.82
1	-5	19	28.12	31.94	26.82	17.33
1	-7	13	87.33	87.84	-77.46	41.41
1	1	27	27.78	27.09	-17.64	20.65
1	-7	15	80.17	79.84	-48.92	63.10
1	-7	11	169.33	164.77	-77.59	-145.36
1	-5	5	126.36	122.96	-76.20	-96.51
1	-7	17	74.02	69.41	25.90	-64.39
1	-7	9	85.55	91.23	49.21	76.82
1	-7	19	34.35	35.58	31.30	-16.91
1	-7	21	68.58	68.73	-41.61	54.70
1	-7	7	47.35	50.27	14.59	48.10
1	-9	13	114.29	116.50	-51.28	-104.61

H	K	L	F OBS	F CALC	A	B	S
1	-9	17	68.07	68.14	64.74	21.25	
1	-9	11	48.03	49.33	-23.42	43.42	
1	-5	3	38.08	39.29	-27.68	27.88	
1	-9	19	28.12	30.54	26.19	-15.71	
1	-9	9	117.99	112.65	112.64	1.39	
1	-7	5	88.65	88.57	-79.55	-38.93	
1	-9	21	36.62	38.84	-17.97	-34.44	
1	-9	7	109.45	101.01	-36.51	-94.18	
1	-11	15	43.13	46.07	-30.48	34.54	
1	-11	17	66.10	71.55	67.51	-23.72	
1	-11	11	74.08	77.98	-29.53	-72.17	
1	-11	19	39.38	41.04	-.55	-41.04	
1	-11	9	105.76	105.99	105.99	-.84	
1	-7	3	147.39	149.99	149.19	15.48	
1	-11	21	63.67	60.58	-19.40	57.39	
1	-11	7	110.91	111.20	13.53	110.38	
1	-13	17	48.61	45.79	42.82	16.23	
1	-13	11	29.29	32.94	-3.57	32.74	
1	-13	9	110.47	115.04	37.36	108.81	
1	-9	3	176.20	179.33	168.54	61.27	
1	-13	21	52.67	53.80	-51.81	-14.49	
1	-11	5	58.88	61.48	-29.57	-53.90	
1	-13	7	50.57	53.09	13.67	-51.30	
1	-7	1	69.60	68.28	59.26	33.93	
1	-15	15	42.35	46.98	15.28	44.43	
1	-15	13	68.75	72.95	-71.91	-12.28	
1	-13	23	30.05	26.26	-24.11	-10.42	
1	-15	11	27.19	32.83	28.01	-17.13	
1	-15	19	40.38	39.69	10.96	-38.15	
1	-11	3	41.12	41.13	-41.08	1.94	
1	-13	5	83.33	83.09	-78.12	28.32	
1	-9	1	143.07	144.24	144.19	-3.96	
1	-15	21	40.79	41.40	-39.99	10.72	
1	-17	13	45.50	43.87	-28.41	-33.43	
1	-17	17	35.73	35.62	35.55	2.22	
1	-11	1	29.68	28.42	27.75	6.17	
1	-15	5	58.80	62.61	-54.24	-31.28	
1	-17	19	24.66	24.44	24.34	-2.20	
1	-15	3	131.64	134.43	19.52	-133.01	
1	-13	1	53.54	53.21	52.23	10.15	
1	-19	15	63.62	58.72	-27.68	51.78	
1	-17	5	86.02	85.72	-65.91	-54.80	
1	-19	9	65.76	61.94	47.82	39.37	
1	-19	17	47.02	48.03	46.27	12.86	
1	-17	3	123.36	121.42	72.81	97.17	
1	-19	7	30.21	32.05	1.24	32.03	
1	-21	11	37.30	36.08	31.00	18.45	
1	-21	13	27.45	32.13	-29.35	-13.08	
1	-21	9	30.52	29.68	26.63	-13.10	
1	-21	15	33.45	34.90	-20.20	-28.46	
1	-21	7	66.14	67.90	-35.38	-57.95	
1	-17	-1	56.23	56.53	-16.26	-54.15	
1	-19	1	75.53	77.59	76.59	12.44	
1	-21	3	29.81	28.64	2.49	28.53	

H	K	L	F OBS	F CALC	A	B
1	-23	9	40.07	36.88	24.22	27.81
1	-23	11	35.78	38.85	22.18	-31.89
1	-21	1	76.18	74.78	74.11	-10.00
1	-23	7	19.22	23.37	-12.64	19.66
1	-23	5	61.57	65.90	-65.90	-.23
1	-19	-5	24.03	26.42	-13.06	-22.97
1	-17	-7	67.16	66.37	65.97	-7.28
1	-25	1	38.57	42.10	27.92	-31.51
1	-25	-3	30.93	33.21	-32.29	7.74
1	-1	-7	118.43	112.33	12.34	111.65
1	-1	-9	27.24	27.69	26.13	9.16
1	-5	-15	21.88	24.10	-23.11	6.82
1	-1	-11	50.88	54.70	52.48	15.41
1	-17	-19	24.00	24.44	2.20	24.34
1	-19	-19	27.18	27.87	-20.79	-18.56
2	8	14	72.13	72.21	-67.14	26.58
2	18	14	51.39	52.40	-52.17	-4.88
2	4	12	96.29	98.48	-89.35	41.41
2	12	16	38.23	38.17	32.35	-20.27
2	14	16	57.07	59.44	54.51	23.71
2	6	14	63.86	64.05	57.53	28.14
2	10	16	121.04	125.51	124.91	12.23
2	2	10	64.90	64.69	32.56	-55.90
2	8	16	70.03	69.99	63.77	-28.85
2	6	16	112.30	113.66	112.88	-13.32
2	14	18	74.46	76.12	-72.29	23.84
2	2	12	87.34	86.81	-86.71	-4.23
2	10	18	30.98	31.03	-16.69	-26.16
2	16	18	23.44	21.26	21.05	2.95
2	8	18	35.40	32.57	32.55	-1.03
2	20	16	19.76	17.81	16.86	-5.72
2	4	16	39.86	40.64	-12.40	38.71
2	2	14	39.13	35.15	34.44	7.00
2	0	10	97.64	96.92	96.89	2.24
2	6	18	75.86	74.50	-64.06	38.03
2	18	18	49.85	48.81	-48.75	-2.53
2	14	20	40.01	38.98	-38.79	3.81
2	10	20	27.26	29.45	-29.13	4.33
2	8	20	34.64	34.16	-33.23	7.92
2	4	18	67.74	66.00	59.63	-28.29
2	2	16	109.07	106.48	103.83	23.59
2	6	20	79.48	79.32	-78.99	-7.26
2	0	14	60.07	60.17	-59.81	6.53
2	12	22	33.34	31.57	-29.24	-11.91
2	10	22	35.59	34.18	32.19	-11.48
2	8	22	61.13	57.83	-48.22	31.93
2	14	22	57.27	58.97	58.58	-6.78
2	-2	6	144.91	148.03	-110.61	98.38
2	2	20	118.02	119.80	-117.85	21.57
2	0	18	36.96	35.18	-17.22	-30.68
2	10	24	52.02	51.81	50.94	-9.50
2	6	24	31.74	32.44	31.12	-9.15
2	2	22	60.92	59.54	45.40	-38.52
2	4	24	33.31	32.83	30.45	-12.26

H	K	L	F OBS	F CALC	A	B
2	-4	10	117.87	121.31	120.63	12.79
2	-4	8	57.75	56.76	16.56	54.29
2	-4	14	33.89	32.98	-23.47	23.16
2	0	22	24.72	24.19	-24.12	-1.83
2	2	24	78.82	82.48	81.03	-15.41
2	8	26	21.31	22.80	.87	22.78
2	6	26	40.93	42.34	-37.34	19.94
2	-4	6	92.40	95.73	-89.53	-33.89
2	-4	18	66.37	66.00	59.63	-28.29
2	-6	10	65.66	60.78	60.71	2.98
2	-4	4	53.93	51.00	-31.64	40.00
2	-6	8	91.18	88.33	78.14	-41.20
2	0	26	36.24	34.04	33.60	-5.45
2	-6	6	49.69	44.12	-44.12	.24
2	-8	12	32.96	33.56	33.14	5.33
2	2	28	40.24	39.93	-39.06	8.32
2	-8	10	53.27	53.16	51.68	12.47
2	-8	8	24.52	23.24	20.85	-10.27
2	-6	4	116.93	119.04	118.44	-11.87
2	-10	14	127.03	124.83	113.28	52.44
2	-10	12	92.02	92.44	-88.39	-27.07
2	-8	6	37.88	35.04	17.27	-30.48
2	-10	10	54.67	50.28	47.46	16.61
2	-10	8	133.82	135.89	132.03	32.15
2	-8	4	49.52	50.95	25.20	-44.28
2	-12	14	60.06	59.30	-56.47	-18.12
2	-12	12	29.84	31.82	31.05	-6.95
2	-6	2	72.76	84.03	-82.26	17.16
2	-12	18	27.50	23.67	-3.07	-23.47
2	-10	6	38.70	42.88	-13.29	-40.77
2	-12	8	64.43	64.07	-63.81	-5.79
2	-10	4	75.96	72.68	-52.17	50.60
2	-14	14	42.93	40.16	6.68	-39.60
2	-8	2	70.54	74.24	47.47	57.08
2	-14	12	73.48	75.29	-75.15	-4.58
2	-12	6	48.94	50.85	-30.34	-40.81
2	-14	10	83.38	82.62	79.62	-22.07
2	-14	8	80.98	80.59	73.45	33.15
2	-12	4	39.39	43.29	40.74	-14.65
2	-10	2	18.12	15.58	14.19	-6.42
2	-14	22	60.95	58.97	-58.58	6.78
2	-14	6	31.22	31.87	-28.40	-14.46
2	-16	12	25.92	23.62	21.33	-10.14
2	-16	10	47.74	46.61	27.46	37.66
2	-16	8	93.97	94.05	-90.78	24.61
2	-12	2	44.66	47.13	-4.81	-46.88
2	-14	4	73.42	68.50	-63.24	26.33
2	-18	12	66.92	64.78	-61.18	-21.29
2	-18	10	46.64	45.10	38.86	22.88
2	-18	16	17.42	15.68	15.67	2.53
2	-14	2	68.45	71.38	71.03	7.06
2	-16	4	30.07	31.05	13.72	27.85
2	-18	8	45.70	45.59	38.36	-24.82
2	-18	6	69.76	65.40	-63.29	16.46

H	K	L	F OBS	F CALC	A	B
2	-16	2	30.09	31.19	21.59	22.51
2	-14	0	73.08	73.39	52.91	-50.85
2	-18	4	55.59	49.78	-47.63	-14.49
2	-20	14	20.77	16.99	13.24	-10.66
2	-18	2	56.28	64.08	63.39	9.37
2	-20	6	36.55	35.80	-27.40	-23.05
2	-20	4	29.19	27.74	27.73	-.83
2	-18	0	81.41	78.10	66.33	-41.25
2	-22	10	61.15	59.80	59.70	-3.47
2	-20	2	29.59	25.46	-11.70	22.61
2	-22	8	35.60	34.86	33.37	10.08
2	-22	6	49.03	48.53	-45.69	-16.35
2	-22	2	56.18	52.90	52.25	-8.27
2	-24	6	21.88	21.11	-17.69	-11.52
2	-22	-4	41.94	34.83	-21.20	27.64
2	-6	-12	184.49	187.66	-178.18	-58.91
3	9	19	40.70	38.74	-38.53	-4.03
3	1	13	68.12	69.45	-24.25	-65.08
3	-1	5	115.98	117.06	-33.33	112.21
3	-1	7	54.78	55.33	27.73	-47.88
3	15	19	42.10	43.79	-43.75	1.75
3	-1	9	100.44	98.44	71.30	-67.87
3	3	17	32.58	31.48	28.37	-13.63
3	1	15	68.30	66.66	30.10	-59.48
3	5	19	52.19	49.12	-45.80	-17.75
3	-1	11	52.54	51.52	46.99	-21.13
3	11	21	47.84	49.96	-24.24	43.68
3	13	21	22.72	21.08	-6.10	-20.18
3	3	19	81.16	79.79	-79.21	-9.56
3	1	17	78.67	75.06	20.99	72.07
3	5	21	67.95	68.38	-16.73	-66.30
3	1	19	42.63	38.77	-31.13	23.10
3	3	21	47.41	47.88	-39.33	27.31
3	-3	9	54.03	51.44	45.11	24.72
3	11	23	30.82	30.06	29.00	-7.92
3	7	23	30.43	34.44	34.24	3.72
3	-3	11	60.42	59.52	-5.34	59.28
3	-3	7	43.01	38.06	-36.86	9.48
3	-3	13	117.97	118.66	-96.65	-68.84
3	1	21	35.08	34.39	-31.10	-14.68
3	-3	15	59.99	57.15	27.12	-50.31
3	3	23	32.85	29.80	-15.44	25.49
3	7	25	41.69	40.86	37.07	-17.20
3	1	23	30.08	28.49	10.99	-26.29
3	5	25	22.63	23.19	13.26	19.02
3	-5	13	106.28	108.17	-100.82	39.20
3	-5	11	21.85	18.80	-18.61	2.68
3	-5	9	115.68	120.31	104.44	-59.73
3	-5	15	46.27	45.91	.44	45.91
3	3	25	28.84	29.07	23.30	-17.38
3	-5	7	34.05	29.69	21.49	20.49
3	-5	17	59.40	57.17	3.23	-57.08
3	-3	3	24.67	23.85	23.41	4.55
3	1	25	55.76	58.64	42.75	40.13

H	K	L	F OBS	F CALC	A	B
3	-7	13	63.68	65.70	-65.69	-1.03
3	-5	5	54.11	53.56	-50.53	17.76
3	-7	11	99.77	100.77	34.22	94.78
3	-7	15	74.12	69.22	4.94	-69.05
3	-7	17	87.05	85.28	61.64	58.94
3	-7	9	120.00	121.39	86.93	84.73
3	-7	7	56.01	58.53	13.93	-56.85
3	-9	13	83.82	83.06	-38.93	73.38
3	-9	15	42.42	40.11	-26.86	29.79
3	-9	11	83.89	84.83	-28.27	-79.98
3	-5	3	20.22	17.88	-17.51	-3.63
3	-9	17	65.67	64.41	60.53	-22.02
3	-9	9	113.20	117.80	112.75	-34.11
3	-3	1	38.50	39.56	-8.05	-38.73
3	-9	7	62.13	62.61	-43.34	45.18
3	-11	13	64.94	66.19	-23.40	-61.91
3	-11	15	47.58	44.73	6.05	-44.32
3	-11	11	72.51	72.38	-22.48	68.80
3	-11	17	44.24	41.84	37.13	19.29
3	-7	3	46.63	50.96	-36.59	-35.47
3	-7	25	39.82	40.86	17.20	37.07
3	-11	9	79.10	79.64	79.64	.21
3	-11	19	42.90	42.98	16.37	39.74
3	-9	5	72.78	76.99	-49.86	58.66
3	-11	7	47.80	48.48	-26.25	-40.75
3	-13	15	52.71	49.75	-9.93	48.75
3	-13	13	66.97	63.91	-63.89	-1.44
3	-13	11	64.02	62.87	31.50	-54.42
3	-13	17	59.41	57.91	54.77	-18.83
3	-9	3	54.15	52.62	-52.50	3.58
3	-13	9	78.64	78.88	7.56	-78.51
3	-7	1	33.60	33.88	20.67	-26.84
3	-13	7	45.11	45.48	-6.99	44.94
3	-15	13	48.25	43.94	-43.19	-8.11
3	-15	15	46.85	45.82	-13.76	-43.70
3	-15	11	46.77	43.63	-19.72	38.92
3	-11	3	33.43	32.43	2.98	32.29
3	-15	17	35.83	31.84	31.66	-3.39
3	-13	5	54.17	52.10	-48.27	19.60
3	-15	9	42.74	39.48	16.55	35.84
3	-15	7	27.64	24.92	-5.18	-24.37
3	-13	3	60.04	62.63	36.57	-50.84
3	-5	-1	58.89	72.18	71.75	7.83
3	-11	1	21.04	18.34	18.14	2.74
3	-17	13	34.57	32.26	-19.39	25.78
3	-15	5	47.83	48.44	-48.13	-5.47
3	-17	11	29.59	29.94	21.39	-20.95
3	-17	15	22.98	22.43	.15	22.43
3	-17	9	51.08	50.54	48.35	-14.73
3	-17	17	32.82	31.79	31.42	4.89
3	-17	7	50.73	47.68	-20.65	42.98
3	-13	1	44.68	47.67	37.51	-29.42
3	-15	3	85.84	90.23	60.79	66.68
3	-17	5	40.02	40.34	-22.32	33.61

H	K	L	F OBS	F CALC	A	B
3	-19	11	38.01	38.24	32.39	20.33
3	-19	13	38.21	37.86	-37.85	.78
3	-17	3	73.06	73.63	31.27	-66.66
3	-19	15	42.17	42.26	-16.32	-38.98
3	-19	7	59.76	58.34	-5.60	-58.07
3	-19	5	36.98	36.25	-27.95	-23.09
3	-17	1	41.96	39.30	39.00	4.82
3	-21	9	30.86	29.46	28.72	6.53
3	-21	11	30.66	30.69	16.66	-25.77
3	-21	7	47.82	47.17	-28.95	37.24
3	-19	1	48.55	44.22	38.67	-21.45
3	-21	5	52.47	49.21	-48.86	5.80
3	-21	3	29.84	26.27	15.73	-21.04
3	-21	1	24.88	24.04	-22.54	8.38
3	-23	5	27.77	32.58	-30.05	12.58
3	-23	1	23.37	23.62	23.10	4.95
3	-1	-3	56.45	63.07	62.40	9.23
4	4	10	44.31	46.95	-26.45	-38.79
4	16	12	42.70	42.91	-42.30	-7.18
4	2	8	35.87	38.55	-36.16	-13.36
4	10	14	37.70	37.08	-34.86	-12.63
4	8	14	30.08	34.67	34.66	-.76
4	4	12	86.78	90.91	-86.05	29.30
4	0	4	133.51	119.67	-117.58	-22.28
4	16	14	34.84	39.89	38.28	11.22
4	2	10	21.11	19.57	12.94	14.68
4	6	14	26.61	30.47	-21.26	21.83
4	12	16	70.60	69.17	68.97	-5.26
4	8	16	67.20	69.64	65.60	-23.36
4	4	14	56.74	56.07	55.48	8.14
4	18	14	18.38	22.25	-3.95	21.89
4	0	8	112.51	105.49	102.26	25.89
4	16	16	36.86	33.58	27.11	-19.81
4	12	18	34.19	35.94	-31.56	-17.20
4	4	16	56.96	59.94	59.55	6.82
4	2	14	36.81	37.78	16.42	-34.02
4	14	18	16.22	17.75	17.71	-1.18
4	6	18	44.53	43.29	14.69	40.72
4	0	12	67.82	66.33	-56.21	35.20
4	2	16	24.92	26.57	18.09	19.46
4	8	20	35.15	34.95	-31.35	-15.44
4	12	20	17.15	21.88	-20.76	6.91
4	-2	6	68.07	64.28	-61.83	17.58
4	0	16	60.49	61.48	61.24	-5.41
4	4	20	50.46	53.01	-52.44	-7.79
4	-2	4	17.99	17.98	12.47	-12.96
4	8	22	17.45	17.25	10.47	13.70
4	10	22	32.23	33.54	-33.01	-5.94
4	0	20	66.74	67.57	-67.56	-.95
4	-4	8	106.01	104.93	102.14	-24.01
4	2	22	26.82	26.17	-18.58	-18.43
4	-4	6	35.95	34.15	-20.36	27.41
4	6	24	12.33	12.33	8.84	-8.60
4	-4	4	130.24	115.44	114.86	11.50

H	K	L	F OBS	F CALC	A	B
4	-6	8	58.02	56.33	53.31	-18.21
4	-6	16	22.60	24.21	-3.19	-24.00
4	0	24	40.43	43.93	32.93	29.08
4	-6	6	24.91	19.37	19.21	2.47
4	-8	12	98.80	99.91	-96.98	-24.02
4	-8	10	46.24	47.83	47.38	-6.51
4	-8	8	120.05	121.78	97.85	-72.50
4	-4	2	24.07	27.62	13.59	-24.05
4	-6	22	21.21	24.74	-23.95	6.22
4	-4	24	36.49	39.91	39.24	7.27
4	-8	6	68.52	73.74	-72.85	11.41
4	-10	8	24.75	25.46	-14.33	-21.04
4	-8	4	92.01	92.31	-35.78	-34.10
4	-6	2	60.21	61.70	12.44	60.44
4	-12	12	79.06	77.30	-64.42	42.73
4	-12	10	53.54	54.07	51.41	-16.75
4	-12	8	100.31	101.62	69.10	74.51
4	-10	4	37.26	35.10	-31.46	15.56
4	-8	2	20.31	22.55	20.07	-10.28
4	-4	0	124.20	130.24	116.60	58.04
4	-12	6	54.64	58.03	-57.84	-4.72
4	-10	2	44.10	44.02	9.44	-42.99
4	-12	4	77.30	79.11	-62.37	48.66
4	-8	0	50.26	50.19	45.99	20.10
4	-14	6	30.78	31.00	-10.71	29.09
4	-12	2	66.10	71.78	70.53	-13.32
4	-16	10	45.73	45.83	45.83	-.75
4	-16	8	62.89	57.99	44.01	-37.76
4	-14	2	46.75	46.19	4.83	-45.93
4	-12	0	52.49	54.52	42.70	33.89
4	-16	4	72.90	71.46	-45.42	-55.16
4	-18	10	29.09	27.26	25.56	-9.49
4	-18	12	18.04	13.70	-5.45	12.57
4	-18	8	20.27	17.51	-15.72	7.72
4	-16	2	89.21	89.71	88.83	-12.56
4	-18	6	29.27	31.08	-20.37	23.47
4	-18	4	20.64	17.88	17.07	5.30
4	-16	0	46.39	48.96	41.62	-25.78
4	-18	2	43.94	40.54	-3.63	40.38
4	-20	8	25.36	28.73	28.09	-6.02
4	-20	6	54.15	55.66	-54.54	11.14
4	-20	4	15.56	18.02	-17.91	1.97
4	-20	2	51.90	54.37	52.98	12.19
4	-20	0	66.92	65.47	40.27	51.63
4	-16	-6	32.11	35.70	35.44	4.23
5	15	7	50.04	48.24	45.48	16.09
5	1	3	76.00	68.61	-28.58	-62.37
5	9	9	48.43	52.46	5.62	-52.15
5	11	9	37.90	41.35	31.92	26.29
5	7	9	28.67	28.65	-11.24	26.36
5	13	9	47.20	48.68	-1.64	-48.65
5	3	7	83.27	73.54	62.30	-39.07
5	17	7	41.22	37.88	35.99	-11.81
5	5	9	62.01	61.85	-5.72	-61.59

H	K	L	F OBS	F CALC	A	B
5	15	9	23.61	24.52	-7.53	23.33
5	11	11	43.05	43.67	-39.59	18.44
5	7	11	45.35	49.29	-28.98	39.87
5	13	11	35.97	36.81	-33.14	-16.01
5	1	5	105.80	98.42	-31.82	93.14
5	3	9	33.00	30.76	21.98	21.52
5	5	11	41.79	43.52	-41.41	-13.39
5	9	13	38.63	46.53	3.16	46.43
5	11	13	33.55	34.80	12.69	-32.40
5	1	7	46.03	43.17	25.66	34.71
5	7	13	30.60	34.63	-24.19	-24.78
5	13	13	40.53	37.60	-32.14	19.50
5	3	11	26.93	25.34	-16.90	-18.89
5	9	15	30.25	28.16	28.15	-.37
5	1	11	31.95	33.18	-18.82	-27.32
5	9	17	47.71	46.22	39.20	-24.48
5	3	15	23.32	24.72	5.11	-24.19
5	1	13	41.35	42.54	-16.47	39.22
5	7	17	20.60	22.36	18.35	12.78
5	5	17	37.89	43.57	21.48	-37.90
5	3	17	36.11	39.54	33.43	21.11
5	7	19	29.69	24.25	-22.36	-9.40
5	5	19	19.50	14.86	-10.71	10.31
5	-3	5	51.73	44.74	-30.83	-32.42
5	-1	19	16.98	15.42	-2.75	15.17
5	-3	3	56.25	56.17	-39.87	-39.57
5	-5	7	40.11	40.81	12.11	-38.97
5	-5	15	17.73	22.81	11.88	-19.47
5	-5	5	74.25	69.03	-58.37	-36.86
5	-7	7	44.12	44.09	7.00	43.53
5	-5	3	79.03	77.11	-76.90	5.77
5	-7	5	44.94	44.83	-40.16	19.92
5	-9	7	47.45	49.06	44.94	-19.68
5	-7	3	58.56	60.05	-39.50	-45.24
5	-9	5	23.69	23.79	-20.59	11.91
5	-5	1	41.37	43.29	39.09	18.61
5	-11	15	16.21	16.55	-9.21	13.75
5	-11	7	44.70	45.20	17.61	41.63
5	-9	3	65.39	68.04	-18.79	65.40
5	-7	1	53.91	56.45	52.72	20.17
5	-11	5	29.21	28.64	-27.15	-9.11
5	-13	7	21.77	26.86	8.57	-25.45
5	-11	3	61.22	65.48	20.03	-62.34
5	-9	1	54.17	56.53	51.91	22.36
5	-13	5	36.83	40.55	-40.18	5.52
5	-13	3	37.48	42.03	-4.78	41.75
5	-15	5	23.81	20.60	-19.57	-6.43
5	-13	1	47.74	50.65	49.93	-8.48
5	-15	3	37.44	40.17	-5.50	-39.80
5	-15	1	40.83	40.61	39.28	10.32
5	-17	5	61.88	60.19	-59.90	5.90
5	-17	3	29.32	27.21	14.77	22.85
5	-17	1	33.56	35.29	33.57	10.88

APPENDIX 4 DOCUMENTATION FOR PROGRAM SOLVEFF

1. Philosophy of the program

SOLVEFF is a FORTRAN program designed to calculate solvent effect energies for solute molecules of up to 30 atoms exhibiting any conformation in a 2 dimensional array of conformation space. A continuum approximation is used for the solvent which can be any liquid for which data is available. For each conformation the energies calculated are:

1) The cavity energy (required to produce a cavity in the solvent to accommodate the solute molecule);

2) The electrostatic interaction energy between solute and solvent;

and 3) The dispersion interaction energy between solute and solvent.

The algorithms used for these terms are described in section 2.3.2.

Each of these terms requires an approximation to the molecular shape of the solute molecule. The model for molecular shape in 2) is taken to be a spheroid for the bulk of the calculations performed in the present work (2.3.3). The axis of the spheroid is the best least squares straight line through the molecule; the axial length is the distance between the feet of the perpendiculars of the extreme atoms to the least squares line (+ 2 Å to allow for Van der Waal's radius); and the radius is the distance from the line to the furthest atom (+ 1 Å). The program can also calculate quantity 2) on a spherical approximation.

The spherical cavity (also employed for ease of calculation in the relatively insignificant terms 1) and 3)) is that sphere which has the same volume as the spheroid described above.

2. Program Description

A heirarchy diagram for the program is given in Fig. A4.1 and a logic flow chart in Fig. A4.2. On entry into the program all

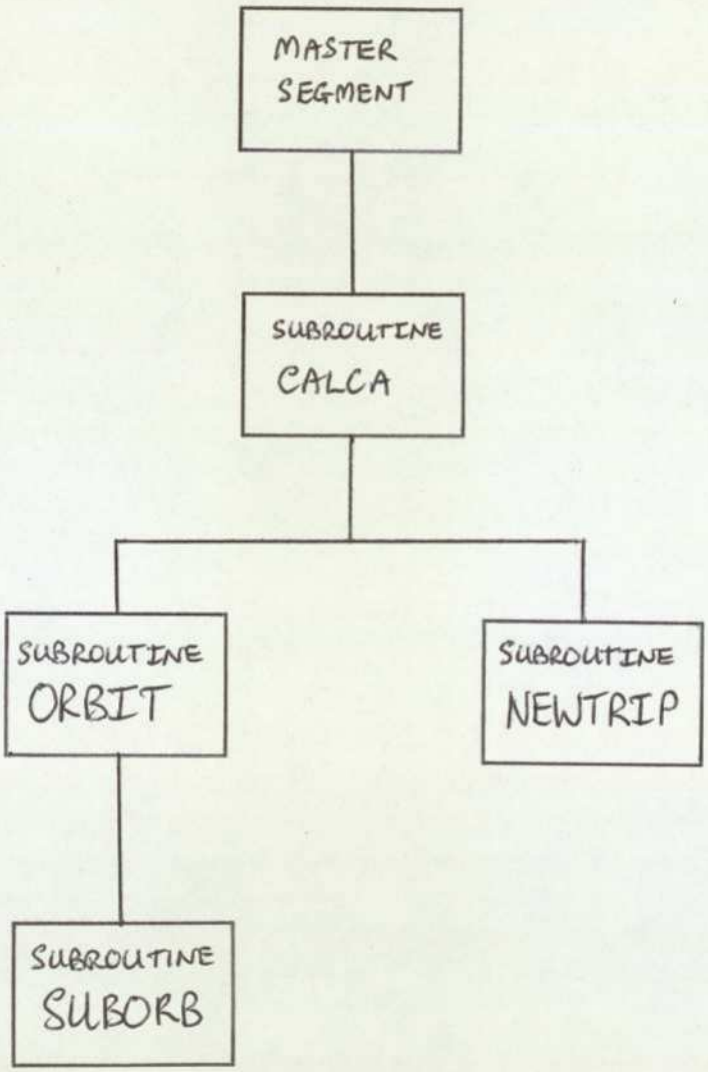

Fig. A4.1 Heirarchy diagram for program SOLVEFF, illustrating subroutine calling structure

molecular data for solvent and solute is input (as described in next section). For each conformation, torsion angles, isolated molecule energy and dipole moment components from MO calculations are then input and processed.

The processing proceeds as follows:

1) Total dipole moment (M) is calculated from the components. Values of component/total dipole are calculated to be used in the subroutine NEWTRIP (see section 4).

2) The subroutine CALCA is called, which operates rotations on the molecule using the dependent subroutines ORBIT and SUBORB. These rotation subroutines are identical to those used in the molecular geometry package MOGEO (Borthwick & Warner, 1973.) The subroutine NEWTRIP is then called which calculates the dimensions of the solute cavity as follows. The least squares line though the molecule is found by a Newton-Raphson iterative procedure (Walsh, 1966) the starting vector being the line parallel to the total dipole moment vector passing through the molecular midpoint (see section 4 below). The length of the molecule (DISMAX) is found by sorting the distances between the feet of perpendiculars from atoms to the line, and the radius (RADMAX) is found by sorting the distances of atoms from the line. The radius (Å) of the sphere having the same volume as the spheroid is then calculated in CALCA.

3) The distance between mean charge centres in the molecule (XT) is calculated for the conformation under calculation.

4) The angle between the least squares line and the total dipole moment vector is calculated (ANG).

5) The internal field factors (AIF), necessary for calculating electrostatic interaction energy in the spheroidal approximation, are calculated from the axial ratio of the spheroid.

6) Dipole moment components parallel and perpendicular to the least squares line are calculated (MU).

7) Electrostatic interaction energy values (WES) for the dipole, parallel and perpendicular to the least squares line, are calculated in the spheroidal approximation, and total electrostatic energy (EES) put equal to their sum.

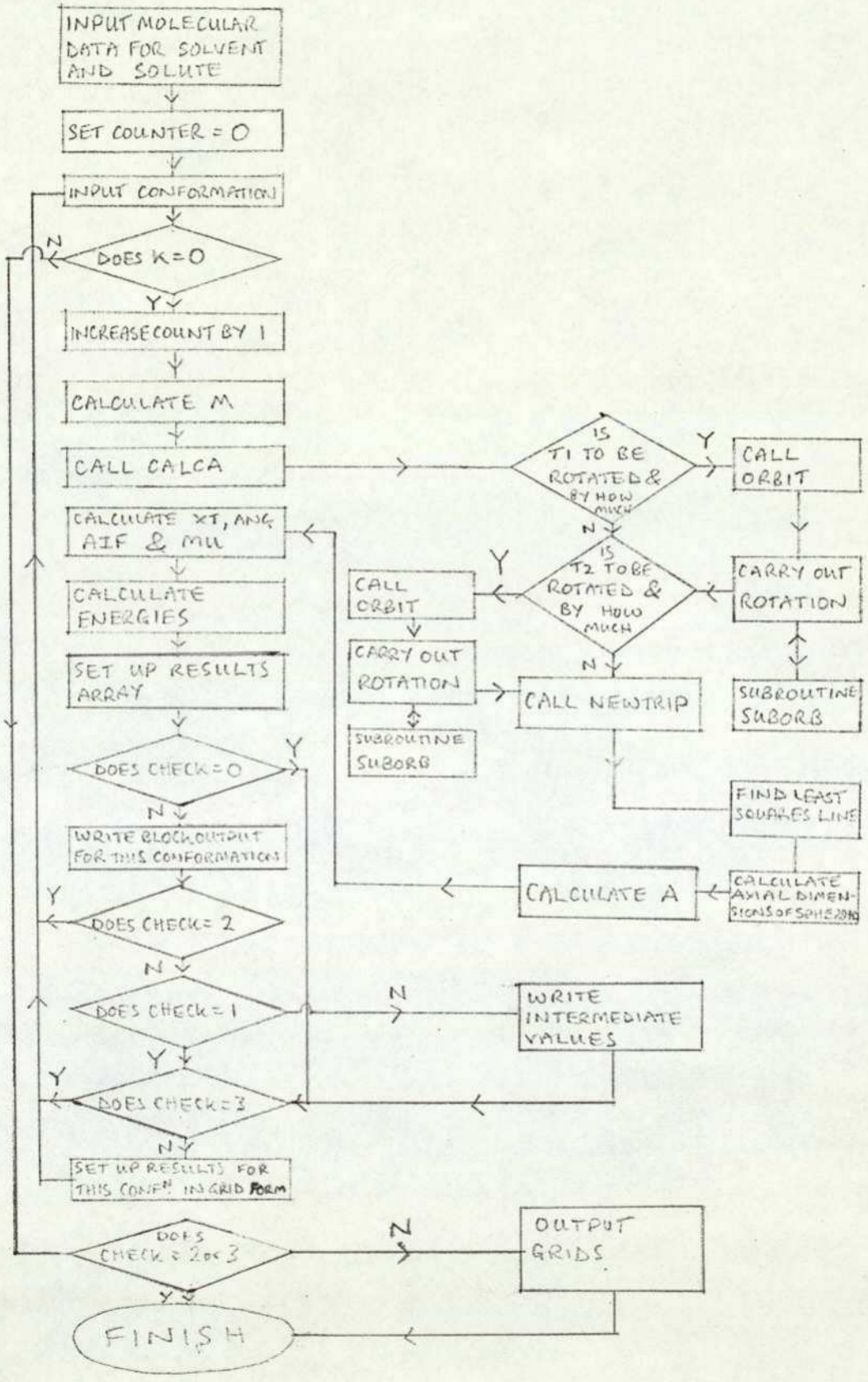

Fig. A4.2 The SOLVEFF Program; Flow Chart

8) Electrostatic energy in the spherical approximation (OES) is calculated.

9) Dispersion interaction energy (EDIS) is calculated.

10) Cavity energy (ECAV) is calculated.

11) Total energy for the spheroidal approximation (ETOT) and the spherical approximation (OTOT) are calculated.

12) Torsion angles, spheroid dimensions, XT, energies and convergence parameters from NEWTRIP are set up in the array RESULTS and printed out.

13) If in testing mode (see next section) co-ordinates and certain intermediate values are printed out for each conformation investigated.

14) Energies for each conformation are assembled in the array EGRID, to be printed in grid form later.

15) Program returns to read in the next conformation.

When all conformations have been processed, a grid printing routine comes into operation and outputs the isolated molecule energy (E) and all the calculated energies: EES, OES, EDIS, ECAV, ETOT, OTOT in grid form.

3. Data input

A data deck for SOLVEFF consists of the following parts:

1) Title in 60A1 format.

2) Mode in F2.0 format. Variable name for this item is CHECK. The value of CHECK governs the type of output produced.

CHECK = 0 Output of energy grids only

CHECK = 1 Block printout: torsion angles (T_1, T_2), sphere radius (A), intercharge distance (XT), energies (E, EES, EDIS, ECAV, ETOT, OES, OTOT), spheroid dimensions (DISMAX, RADMAX), convergence parameters (ICY, DFX) and the angle between least squares line and dipole moment vector in degrees (ANG); and grid printout of energy grids.

CHECK = 2: Block printout only

CHECK = 3: (Test mode) Block printout and values used during calculations: co-ordinates (variable name: COORD (I,J)), extreme atoms along least squares line (LINE (1) and LINE (2)), atom furthest from line (FARATOM), dipole components parallel and perpendicular to line (MU (1) and MU(2)) and internal field factors (AIF (1) and AIF (2)).

3) Solvent information, on two separate cards:

i) Name of solvent, Format: (20A1)

ii) Solvent data (F8.6, 2F6.4, 3F6.2, 2F6.3) in order: Density (DENSOL), acentric factor (WB), reduced refractive index $\frac{n^2-1}{n^2+2}$ (DB), ionisation potential (IB), static dielectric constant (EPS), surface tension (GAMMA), microscopic cavity factor (KB), function of surface tension and expansion (FUNGE). The definitions of these parameters can be found in 2.3.2 and their values for the solvents used are given in Table A4.1 below.

4) Solute parameters

This information is on n+7 cards, where n is the number of atoms.

i) Number of atoms (NATOM) (I2).

ii) Numbers of the atoms defining negative and positive charge centres (NO1, NO2, NH1, NH2, NH3) (5I3).

iii) Acentric factor (W), reduced refractive index (DA), ionisation potential (IA) (3F8.4).

iv)-(n+iii) Atomic co-ordinates, x y z (COORD (I,J)). One atom per line (3F8.4). These must be the co-ordinates for a molecule with the torsion angles to be varied set out 0^o, 0^o, otherwise the torsion angles printed by the program will not correspond to the normal convention used.

n+ iv) Number of atoms in first rotated group (NGP1) (I2).

n + v) Numbers of the atoms in first rotated group (ORB(I)) (30I3).

TABLE A4.1 SOLVEFF PARAMETERS FOR VARIOUS SOLVENTS

Parameter	Symbol in (2.3.2) calcs.	Variable name in SOLVEFF	Solvent		
			Water	Octanol	Octane
Number density	d_b	DENSOL	0.0333	0.003835	0.003715
Acentric factor	w_b	WB	0.023	0.400	0.400
$\frac{n_b^2 - 1}{n_b^2 + 2}$	D_b	DB	0.206	0.258	0.241
Ionisation potential	I_b	IB	12.6	9.7	9.8
Dielectric constant (@ 37°C: physiol. temp.)	ε	EPS	74.51	10.3	2.07
Surface tension (@ 37°C)	γ	GAMMA	70.1	25.9	21.8
Cavity factor	K_b	KB	1.277	0.6	0.6
Function of γ and expansion	$F(\gamma,A)$	FUNGE	1.571	1.950	1.756

n + vi) Number of atoms in second rotated group (NGP2) (I2).

n + vii) Numbers of the atoms in second rotated group (ORB2(I)) (30I3).

5) Grid setup card (EBASE, IGRID1, IGRID2) (F8.3, 2I3)

EBASE is the invariant part of the isolated molecule input energy, e.g. for GABA, nearly all the isolated molecule energies start with -83.4, as in -83.422191 for instance. Hence EBASE is taken to be -83.4. The use of EBASE saves repetitive punching of the first three digits. IGRID1 and IGRID2 specify the size of the 20^{o} array of conformations considered, e.g. if 10 values of T_1 occur in the input data, then IGRID1 = 10.

6) Conformational data

Up to 400 conformations can be input in one run. If grid printout is desired, the conformations must fall on a 20^{o} grid of conformation space, i.e. $T_1 = 20n$ and $T_2 = 20n$ where n is an integer. In this way, an entire 360 x 360, 20^{o} energy surface can be processed in a single run (361 conformations). If grid printout is not required, there is no restriction on the torsion angles which may be input.

The data for two conformations is input on each card (I1, 2(2F4.0, F8.2, 3F6.2)) as follows:

Execution parameter (k) = 0 on all but the last card (see below), then two sets of conformational data: torsion angles (T_1, T_2) isolated molecular energy (E) and dipole moment components (MX, MY, MZ) for this conformation. The last card must be a solitary 1 (I1) (i.e. k= 1).

4. The least squares procedure

Subroutine NEWTRIP, which is used to find the best least-squares line through the molecule contains a number of parameters which may be adjusted to change the convergence characteristics of the iterative procedure. The logic of the subroutine is shown in

in Fig A4.3. Essentially, the program optimises the six element vector $\underline{X}$ (which defines the least squares line) in order to minimise the value of the sum of the squared distances from each atom to the line. A Newton-Raphson iterative procedure (Walsh, 1966) is employed and the algorithms are developed as follows.

The distance from the point $k\ (x_k y_k z_k)$ to the line $\frac{x-a}{l} = \frac{y-b}{m} = \frac{z-c}{n}$ is

$$D_k = \left\{(l\lambda + (a-x_k))^2 + (m\lambda + (b-y_k))^2 + (n\lambda + (c-z_k))^2\right\}^{\frac{1}{2}} \quad \text{where}$$

$$\lambda = -\left\{\frac{l(a-x_k) + m(b-y_k) + n(c-z_k)}{l^2 + m^2 + n^2}\right\}$$

The function $\sum_{k=1}^{m}(D_k^2)$, where m is the number of atoms is to be minimised. Each $D_k = f_k(a,b,c,l,m,n)$, i.e. $f_k(x_1 \ldots x_6) = f_k(\underline{X})$.

At the beginning of the procedure, the variables x_i have the following values: x_1, x_2, x_3 = co-ordinates of the mean point of the molecule; x_4, x_5, x_6 = dipole moment direction cosines MX/M MY/M, MZ/M. The required minimum is at $x_1 + \delta_1$, $x_2 + \delta_2 \ldots x_6 + \delta_6$.

The Newton-Raphson iterative procedure for the minimisation of a sum of squares gives a definition for δ_j (the adjustment to x_j):

$$\sum_{k=1}^{m} \frac{\partial f_k(\underline{X})}{\partial x_i} f_k(\underline{X}) + \sum_{j=1}^{6}\left[\sum_{k=1}^{m} \frac{\partial f_k(\underline{X})}{\partial x_i}\frac{\partial f_k(\underline{X})}{\partial x_j} + f_k(\underline{X})\frac{\partial^2 f_k(\underline{X})}{\partial x_i \partial x_j}\right]\delta_j = 0$$

As an approximation for ease of handling, $f_k(\underline{X})\frac{\partial^2 f_k(\underline{X})}{\partial x_i \partial x_j}$ is neglected. This is correct if $f_k(\underline{X}+\underline{\partial}) = 0$. If $f_k(\underline{X}+\underline{\partial}) \neq 0$, the convergence will be slowed down, but a substantial gain in computing time will be made by having no explicit second derivatives to calculate. The final result should not be affected. Hence the

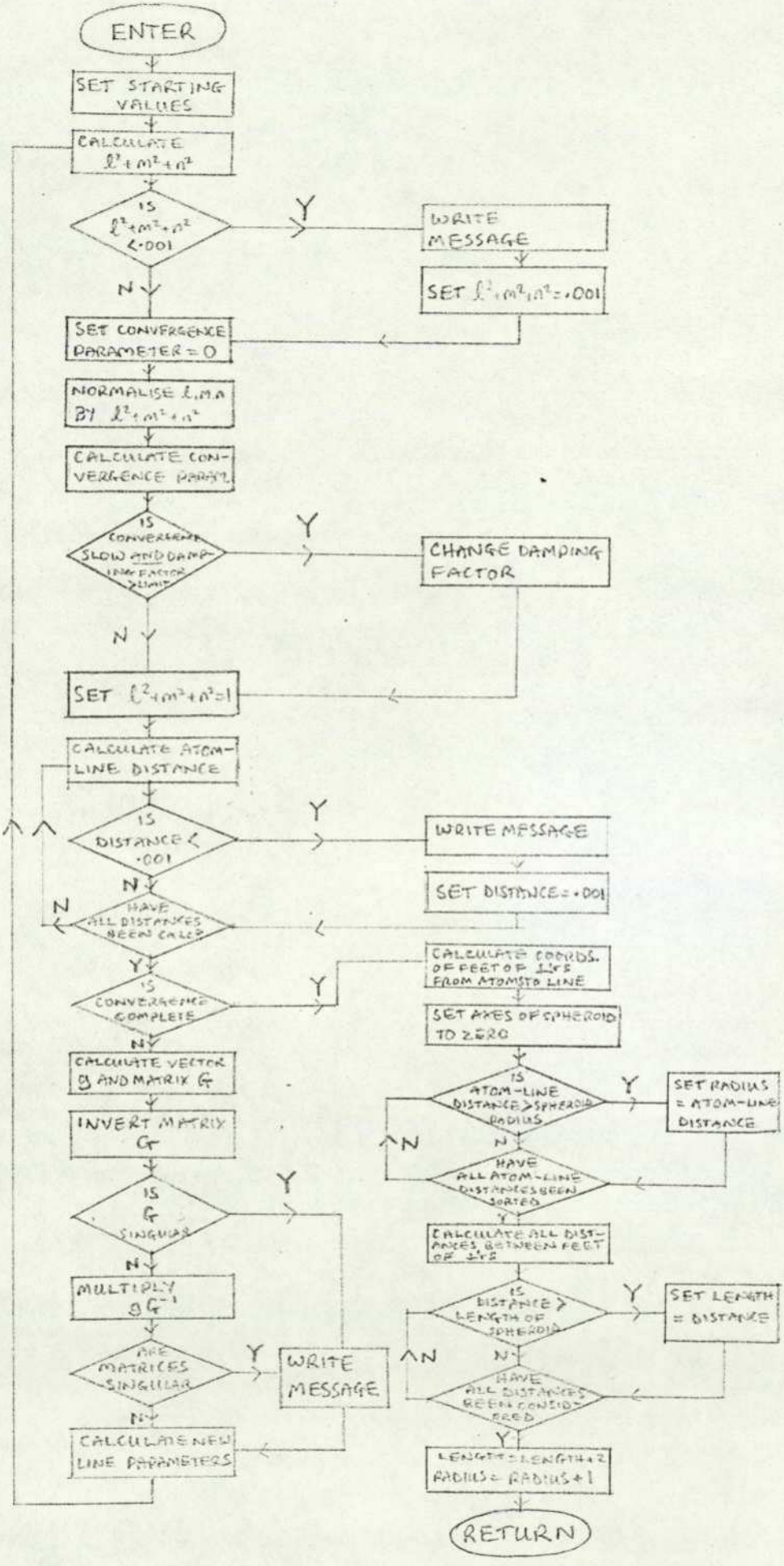

Fig. A4.3 Subroutine NEWTRIP Flow Chart

's are defined by:

$$\sum_{k=1}^{m} \frac{\partial f_k(\underline{X})}{\partial x_i} f_k(\underline{X}) + \sum_{j=1}^{6} \left[\sum_{k=1}^{m} \frac{\partial f_k(\underline{X})}{\partial x_i} \frac{\partial f_k(\underline{X})}{\partial x_j} \right] \delta_j = 0$$

Thus, defining vector $\underline{g}$ and matrix $\underline{\underline{G}}$ to accord with the equation above, $\underline{\delta} = -\underline{\underline{G}}^{-1} \underline{g}$ and the iteration is $\underline{X}_{n+1} = \underline{X}_n - \underline{\underline{G}}^{-1} \underline{g}_n$ n being the cycle of iteration. A damping factor C may be necessary to avoid oscillation in successive cycles in some cases, so the formula becomes:

$$\underline{X}_{n+1} = \underline{X}_n - C\underline{\underline{G}}^{-1} \underline{g}_n$$

To prevent the matrix $\underline{\underline{G}}$ being singular and thus uninvertable, a constant is added to each of the diagonal terms. Optimisation for fast convergence suggests this constant should be ~ 2.

The variable names used in the program for the items above are:

X(I)	$\equiv x_i$
D(k)	$\equiv D_k$
DD(k,I)	$\equiv \frac{\partial D_k}{\partial x_i}$
P(J)	$\equiv \delta_j$
BG(I,J)	$\equiv G_{ij}$
SG(I)	$\equiv g_i$
BGINV(I,J)	$\equiv G_{ij}^{-1}$
CLAM	$\equiv C$

The parameter indicating the degree of convergence between successive cycles is $DFX = \sum_{j=1}^{6} (\delta_j^2)$. Convergence is considered complete when DFX $<$ .0001 since differences in ETOT values are $< \frac{1}{2}$kCal/mole between cycles at this stage. The variable ODF is set equal to $\frac{1}{2}$DFX at the end of each cycle so that, when the new DFX is found, ODF-DFX positive indicates a satisfactory rate of convergence. If ODF-DFX is ≤ 0, the variable CLAM is multiplied by 0.75, thus introducing a damping factor in the convergence.

There are two ways in which the convergence routine can fail:

i) An oscillation can be set up (i.e. calculated δ_j's are too large). In extreme cases, this can become an actual divergence.

ii) The convergence becomes very slow (i.e. δ_j's are far too small).

The first problem is very much more common and more serious, hence a slow rate of convergence is usually corrected by the introduction of a damping factor. The variable CLAM is multiplied by 0.75 in every cycle that ODF$\leqslant$DFX, but a lower limit of CLAM = 0.2 is set which prevents a conformation with a slow rate of convergence as in case ii) failing to converge appreciably in the 20 cycles maximum. Compounds which show convergence problems can often be treated by adjusting the starting value and limit value of CLAM, the relationship between ODF and DFX, and the total number of iterations allowed.

5. Notes on program execution

The SOLVEFF program has been implemented on the ICL 1905E computer at the City University via the MAXIMOP on-line system and on the CDC 7600 computer at ULCC. In the former cases, about six seconds of mill time is required for each conformation, but in the latter, execution time is reduced more than one hundred fold to about .05 seconds. The storage required is ~18k words.

APPENDIX 5 P.A.R. FOR AMINO-ACID TRANSMITTERS

1. Parameters employed

The recent reviews by Hansch (1973) and Goodford (1973) have described in detail modern methods in PAR studies, and give numerous examples of their use. The parameters which are considered fall into three categories:

(i) Hydrophobic parameters

A measure of molecular hydrophobicity is given by the partition coefficient (P) of a substance between octanol and water. This is expressed in free energy terms as log P, which is additive for molecular fragments (Leo, Hansch, Elkins, 1971). Hence the log P value for a wide range of molecules can be calculated from existing data for particular moieties much of which is tabulated by Leo et al (1971) who also provide detailed rules for carrying out such calculations. The discrepancies between different measurements of log P for individual substances are sometimes very large. This is reflected in large log P uncertainties for some moieties and hence in large uncertainties in calculated log P's for molecules containing them.

(ii) Electronic parameters

In aromatic compounds, the Hammett constant, σ, provides a measure of the electronic nature of particular sites on a ring, and hence the likelihood of dissociation or reaction occurring at the site. The equivalent parameters for aliphatic compounds, which have been used with success in PAR studies, are the dissocation constants, pK, for various functional groups in a molecule. These are generally measured by titration.

(iii) Steric parameters

The Taft Steric parameter (Taft, 1956) is a measure of the effect on molecular reactivity of the presence of a

substituent in a molecule. Again, this has been found to provide correlations with biological activity in certain types of compound (Hansch, 1973). The parameter (Es) is measured directly via the equilibrium constant of the dissociation reaction of molecules containing the substituent group under consideration. Es has units of energy and is additive for molecular fragments.

2. Results for amino-acid transmitters

The values of log P and Es for a number of GABA agonists were calculated using the data from Leo et al (1971) and Hansch (1973) and the additivity method from Leo et al (1971). The results are listed in Table A5.1. The values of pK were obtained from Conway (1952) and other sources as shown.

The major variable among these compounds is log P. pK and Es do not alter markedly, and hence are not calculated for all the compounds. No clear relationship exists between values of log P and potency (cf. Table 1.1). Note particularly the extremely low log P values of taurine and homotaurine. The values of log P would not be expected to change significantly with small changes in conformation (Nys & Rekker, 1973).

Results for glutamate agonists are not listed separately as log P for a glutamate agonist may be obtained from the log P of the corresponding GABA agonist + (-0.85 ± 0.05) for the extra carboxyl group. Again, no relationship between log P and potency is forthcoming.

TABLE A5.1

Physicochemical parameters for GABA agonists

Molecules are considered as fully extended. In most cases several routes of calculation are used and the mean found

Substance	log P	Uncertainty	No. of calcs.	pk		ref	Es (calculated as subsituents on a carboxyl group from Hansch (1973, 109))
				-	+		
Glycine	-1.31	0.09	3	2.34	9.70	(a)	- 0.61
β alanine	-0.83	0.10	3	3.60	10.19	(a)	- 0.68
GABA	-0.37	0.10	4	4.04	10.71	(b)	- 0.97
δ AVA	0.17	0.10	4	4.27	10.77	(a)	- 1.00
ε ACA	0.72	0.10	4	4.43	10.75	(a)	- 1.01
7 ACA	1.27	0.10	1				
α-γdiaminobutyrate	-1.71	0.25	2				
γamino n valerate	-0.05	0.10	1	4.02	10.40	(a)	
αGA	-0.9	0.3	3				
βGP	-0.4	0.3	4				
δGB	0.1	0.3	4				
βGB	-0.1	0.3	2				
δGP	0.6	0.3	1		~12 (a) (by comparison with arginine)		
taurine	-5.1	0.5	3	1.5	8.75	(a)	
homotaurine	-4.6	0.5	3				
ImAc	-0.86	0.20	2		~6 (a) (histidine)		
MeImAc	-0.23	0.20	1				
ImPr	-0.33	0.20	2				
ImLa	-1.4	0.2	2				
ATA	-0.91	0.15	1	1.80	8.34	(c)	
trans ACA	-0.67	0.15	1	3.55	9.46	(c)	
cis ACA	-0.67	0.15	1				
muscimol	-1.2	0.2	1				

a Conway 1952 b King 1954 c Beart et al 1972

APPENDIX 6 DERIVATION OF $P(x_R)$ CURVE IN EARLIER CONFORMATIONAL SAR WORK

The publication Steward and Clarke (1975) is the original version of the conformational SAR method described in section 3.2. A slightly different technique was employed in this paper for the derivation of the $P(x_R)$ curve than that described above, so for completeness, the method used is described here.

The curve was based on the potencies of glycine, GABA, muscimol, ATA and imidazole acrylic acid. Representing the value of $P(x_R)$ at the various points considered by k_1 ---- k_5, the following equations can be established assuming the log(potency) $\propto$ log(interaction probability):

$$k_1 = P(x_R = 3.25) = 1/C_{\text{glycine}} \simeq 1/1300$$
$$k_2 = P(x_R = 5.0) = 1/C_{\text{muscimol}} \simeq 1$$
$$k_3 = P(x_R = 5.8) = 1/C_{\text{ATA}} \simeq 1/3$$
$$k_4 = P(x_R = 7.0) = 1/C_{\text{Imid Acr.}} \simeq 0$$

The estimates of x_T for ATA and muscimol are slightly different from those in section 3.2. The x_T's here were measured from models, whereas the more recent work employed the molecular geometry package MOGEO (Borthwick & Warner, 1973) to calculate x_T values for these molecules.

GABA has three x_T peaks in the range 3 - 7 Å, one of which (4.1 Å) is of very low probability (.028) and is hence ignored. The two remaining peaks are at 5.0 and 5.65 Å with probabilities (.420) and (.325) respectively. The potency of GABA can then be represented by:

$$.420\ k_2 + .325\ k_5 = 1 \quad \text{where } k_5 = P(x_R = 5.65)$$

The equation for k_5 can be solved as follows to give a total of five points on the $P(x_R)$ curve

$$k_5 = \frac{1 - .420\ k_2}{.325}$$

$$= \frac{.580}{.325} \simeq 1.8$$

The $P(x_R)$ curve was then constructed by hand from these five fixed points. It is illustrated in Fig. A6.1 where the k values are scaled so as to make the peak probability 1.0.

The results from this probability curve were moderately successful in correlating potency and interaction probability, but the resultant slope of the log(potency) vs log(total interaction probability) was $\sim$ 1.8, whereas the initial assumption had been a slope of 1.0. Clearly, a more realistic result should be found for a self-consistent regression line. Hence the study reported in section 3.2 was carried out, in order to develop a self-consistent scheme. The improved x_T values for ATA and muscimol obtained in the more recent work precluded the use of the method above for the development of the x_R curve. An analytical curve was therefore developed, which may not be physically meaningful, but does provide a more precise method of calculating $P(x_R)$ values than the hand-interpolated curve.

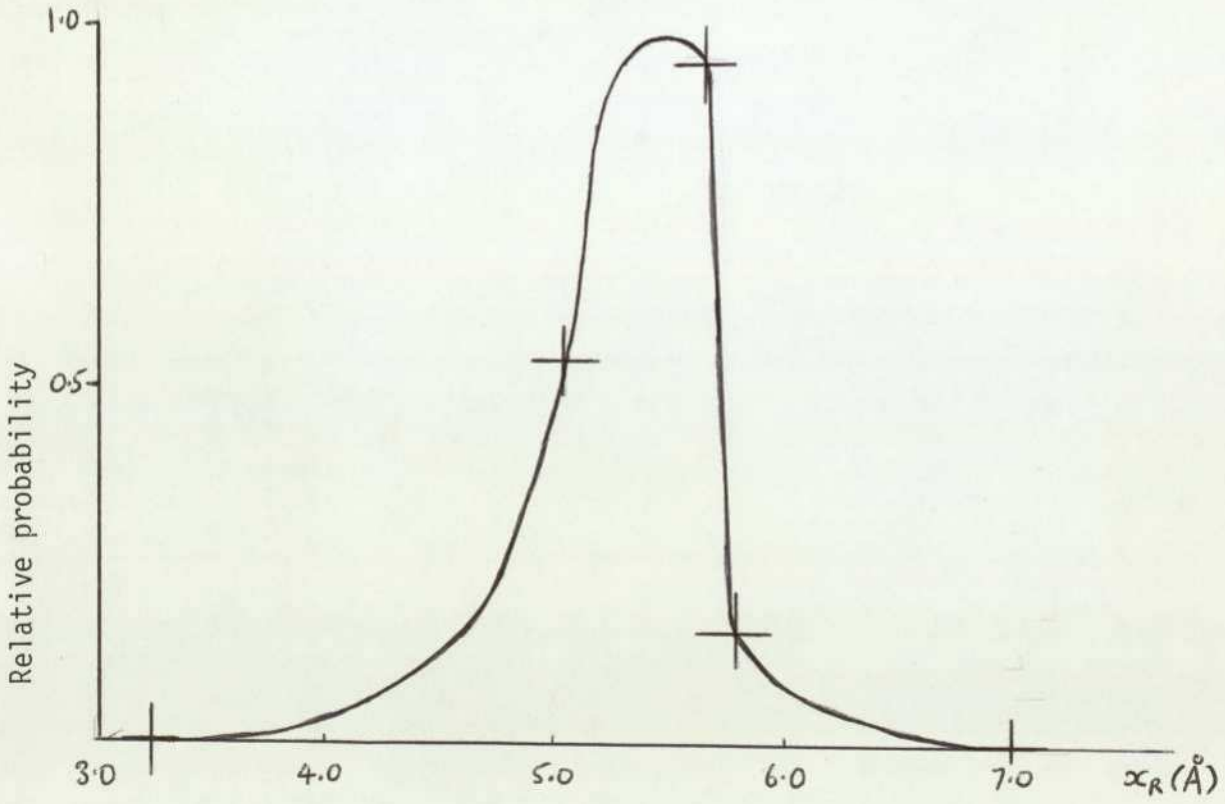

Fig. A6.1 Original $P(x_R)$ distribution from Steward & Clarke (1975)

REFERENCES

Abe A., Jernigan R.L. and Flory P.J (1966) J.Am.Chem.Soc. 88 631

Allison A.C. (1972) in "Cell Interactions" L.G. Silvestri (Ed.) North Holland Publishing Co. p. 156

Andrews P.O. and Johnston G.A.R. (1973) Nature New Biol. 243 29

Aprison M.H., Davidoff, R.A. and Werman R. (1970) In "Handbook of Neurochemistry" vol. 3 A. Lajtha (Ed) Plenum Press N.Y.

Ariëns E.J. (1954) Arch. Intern. Pharmacodyn 99 32

Arunlakshana O. and Schild H.O. (1959) Br. J. Pharmacol. Chemother. 14 48

Bangham A.D., Standish M.M. and Watkins J.C. (1972) see Fox C.F. Scientific American Feb. 1972, p. 34

Bastiansen O. Seip H.M. and Boggs J.E. (1971)

Beart P.M., Curtis D.R. and Johnston G.A.R. (1971) Nature New Biol. 234 80

Beart P.M., Johnston G.A.R. and Uhr M.L. (1972) J. Neurochem 19 1855

Beddell C.R. Moult J. and Phillips D.C. (1970) in "Molecular properties of drug receptors" R. Porter and M. O'Connor (Eds) Churchill

Beers W.H. and Reich E. (1970) Nature 228 917

Bennett J.P, Mulder, A.H. and Snyder S.H. (1975) Life. Sci. 15 1045

Bennett J.P., Logan W.J. and Snyder S.H. (1973) J. Neurochem 21 1533

Beveridge D.L. (1973) in Pullman and Courriere (1973)

Beveridge D.L., Radna R.J. and Kelly M.M. (1974[a]) J. Am. Chem. Soc.

Beveridge D.L., Radna R.J., Schnuelle G.W. and Kelly M.M. (1974[b]) in "Proceedings of the 7th Jerusalem Symposium on Molecular and Quantum Pharmacology" B. Pullman and E.D. Bergmann (Eds) Reidel, Boston

Beveridge D.L. and Schnuelle G.W. (1974) J. Phys. Chem. 78 2064

Biscoe T.J., Evans R.H., Headley P.M., Martin M. and Watkins J.C. (1975) Nature 255 166

Blake C.C.F., Johnson L.N., Mair G.A., North A.C.T., Phillips D.C. and Sarma V.R. (1967) Proc. Roy. Soc. B167 378

Blaisie J.K., Goldman D.E., Chacko G. and Dewey M. (1972) Biophys. J. 12 253a

Boakes R.S., Bradley P.B., Briggs I, and Dray A. (1970) Br. J. Pharmac 40 202

Bodor G., Bednowitz A.L., and Post B. (1967) Acta Cryst. 23 482

Borthwick P.W. and Steward E.G. (1975[a]) J. Mol. Struct. in press

" " (1975[b]) in preparation

" " (1975[c]) unpublished M/S

Borthwick P.W., Livingstone D.I. and Steward E.G. (1975) J. Mol. Struct. in press

Borthwick P.W. and Warner D. (1973) "The MOGEO system" unpublished

Bowery N.G. and Brown D.A. (1974) Br. J. Pharmac. 50 205

Bowman W.C., Rand M.J. and West G.B. (1968) "Textbook of Pharmacology" Blackwell, Oxford & Edinburgh)

Bradford H. and McIlwain H. (1966) J. Neurochem 13 1163

Brehm L., Hjeds H. and Korgsgaard-Larsen P. (1972) Acta Chem. Scand. 26 1298

Buckingham A.D. (1953[a]) Aust. J. Chem 6 93

Buckingham A.D. (1953[b]) Aust. J. Chem 6 324

Burgen A.S.V. (1970) in "Molecular properties of drug receptors" R. Porter and M. O'Connor (Eds.) Churchill

Burgen A.S.V. (1966) J. Pharm. Pharmac. 18 137

Burger A. (1970) in "Fundamental concepts in drug-receptor interactions" J.F. Danielli, J.F. Moran and D.J. Triggle (Eds.) Acad. Press N.Y. & London

Catalan J. and Fernandez-Alonso J.I (1975) J. Mol. Struct. 27 59

Changeux J.P., Blumenthal R., Kasai M. and Podleski T. (1970) in "Molecular properties of drug receptors" R. Porter and M. O'Connor (Eds.) Churchill

Changeux J.P., Thiery J., Tung Y., and Kittel C. (1967) Proc. Nat. Acad. Sci. USA 57 335

Chothia C.H. (1970) Nature 225 36

Chothia C.H. and Pauling P. (1969) Nature 223 919

Clark A.J. (1937) "Heffters Handbuch der experimentallen Pharmackologie" vol. 4 General Pharmacology. Springer-Verlag, Berlin

Clarke G.R. and Steward E.G. (1975[a]) J. Physiol. 249 22P

Clarke G.R. and Steward E.G. (1975[b]) in preparation see appendix 3

Collins J.F. and Hill R.G. (1974) Nature 249 845

Constanti A. and Quilliam J.P. (1974) J. Physiol. 241 1P

Conti F., Damiani A., Pietronero C. and Russo N. (1971) Nature New Biol. 233 232

Conway B.E. (1952) "Electrochemical Data" Elsevier, Amsterdam

Crossman A.R., Walker R.J. and Woodruff G.N. (1974) Br. J. Pharm. 51 137P

Crow T.J. (1974) Nature 252 634

Curtis D.R., Hösli L., Johnston G.A.R. and Johnston I.H. (1968) Exp. Brain Res. 5 235

Curtis D.R., Duggan A.W., Felix D. and Johnston G.A.R. (1970[a]) Nature 226 1222

Curtis D.R., Duggan A.W., Felix D. and Johnston G.A.R. (1970[b]) Nature 228 676

Curtis D.R. and Johnston G.A.R. (1970) in "Handbook of Neurochemistry Vol. 4" A. Lajtha (Ed.) Plenum Press N.Y. and London

Curtis D.R., Duggan A.W., Felix D., Johnston G.A.R. and McLennan H. (1971) Brain Res. 33 57

Curtis D.R., Duggan A.W., Felix D., Johnston G.A.R., Tebecis A.K. and Watkins J.C. (1972a) Brain Res. 41 283

Curtis D.R., Game C.J.A., Johnston, G.A.R., McCullogh R.M. and MacLachlan R.M. (1972b) Brain Res. 43 242

Curtis D.R. and Johnston G.A.R. (1974) Ergebnisse Der Physiologie 69 97

Curtis D.R., Johnston G.A.R., Game C.J. and McCulloch R.M. (1974) J. Neurochem 23 605

Curtis D.R. and Watkins J.C. (1960) J. Neurochem 6 117

Curtis D.R. and Watkins J.C. (1963) J. Physiol 166 1

" " (1965) Pharmacol Rev. 17 347

Dale H.H. (1914) J. Pharmacol 6 147

Danon F. and Pitzer K.S. (1962) J. Chem. Phys. 36 425

Davidson N. and Southwick C.A.P. (1971) J. Physiol. 219 689

Davies J. and Watkins J.C. (1973a) Nature New Biol. 238 63

Davies J and Watkins J.C. (1973b) Brain Res. 59 311

Davson H. and Danielli J.F. (1935) J. Cell Comp Physiol 5 495

Denburg J.L., Eldefrawi M.E. and O'Brien R.D. (1972) Proc.Nat.Acad. Sci. USA 69 177

de Plazas S.F. and de Robertis E. (1974) J. Neurochem. 23 1115

de Robertis E. and de Plazas S.F. (1974) J. Neurochem. 23 1121

Derissen J.L. Endeman H.J. and Peerdeman A.F. (1968) Acta. Cryst.(B) 24 1349

Dewar M.J.S. (1969) "The Molecular Orbital Theory of Organic Chemistry" McGraw-Hill, N.Y.

Diamond J. (1968) J. Physiol 194 669

Diebel R.N.and Swinehart D.F. (1957) J. Phys. Chem. 61 333

Dixon W.E. (1906) Brit. Med. J. 2 1807

Dixon W.E. (1907) Med. Magazine 16 454

Dray A. and Straughan D.W. (1974) Br. J. Pharm. 51 133P

Dudel J. (1965a) Pflügers Archiv. 283 104

Dudel J. (1965b) Pflügers Archiv. 284 81

Duggan A.W. (1974) Exp. Brain. Res. 19 522

Edward J.T., Farrell P.G. and Job J.L. (1973) J. Phys. Chem. 77 2191

" " " (1974) J. Am. Chem. Soc. 96 902

Edwards C. and Kuffler S.W. (1959) J. Neurochem. 4 19

Elliott T.R. (1905) J. Physiol. 32 401

Engelhart E and Loewi O. (1930) Arch. Exp. Path. Pharmakol. 150 1

Elliott A. (1965) J. Sci. Instrum. 42 312

Engstrom L.H. (1972) see Fox C.F. Scientific American Feb. 1972 p. 31

Farnell L., Richards W.G. and Gannelin C.R. (1974) J. Theor. Biol. 43 389

Feltz A. (1971) J. Physiol. 216 391

Feltz A. and Rasminsky M. (1974) Neuropharmacology 13 553

Finean J.B. (1972) Sub-cellular Biochem. 1 363

Florey E. and Murdock L.L. (1974) Comp. Gen. Pharmacol. 5 91

Fonnum F. and Storm-Mathisen J. (1971) J. Neurochem. 18 1105

Franks A. (1958) Br. J. Appl. Phys. 9 349

Gaddum J.H. (1937) J. Physiol. 89 7P

Gaddum J.H. (1957) Pharmacol. Rev. 9 211

Gilardi R. (1973) Nature New Biol. 245 86

Gill E.W. (1959) Proc. Roy. Soc. B 150 381

Gill E.W. (1965) in "Progress in Medicinal Chemistry" Vol. 4
G.P. Ellis and G.B. West (Ed) Butterworths

Gingell D. (1973) J. Theor. Biol. 38 677

Godfraind J.M., Krnjevic K. and Pumain R. (1970) Nature 228 675

Golebiewski A. and Parczewski A. (1974) Chem. Rev. 74 519

Goodford P.J. (1973) in "Advances in Pharmacology and Chemotherapy"
vol. II S. Garattini, A. Goldin, F. Hawking, I.J. Kopin
and R.J. Schitzer (Ed) Acad. Press. N.Y.

Gorinsky C. and Moss D.S. (1973) J. Cryst. Mol. Struct. 3 299

Gray G. (1975) Proc. Roy. Soc. B. 190 369

Haldeman S., Huffman, R.D., Marshall K.C. and McLennan H. (1972)
Brain Res. 39 419

Haldeman S. and McLennan H. (1973) Brain Research 63 123

Ham N.S. (1974) in "Proceedings of the 7th Jerusalem Symposium on
Quantum and Molecular Pharmacology" B. Pullman and E.D.
Bermann (Eds) Reidel, Boston USA

Hansch C. (1973) in "International Encyclopaedia of Pharmacology
and Therapeutics" Section 5: Structure-Activity Relationships
Vol. 1. C.J. Cavallito (Ed) Pergamon Press N.Y. and London

Hill A.V. (1909) J. Physiol 39 361

Hill R.G., Simmons M.A., and Straughan D.W. (1974) J. Physiol
239 122P

Hinazumi H. and Mitsui T. (1971) Acta Cryst. AC(b) 27 2152

Hirokawa S. (1955) Acta Cryst. 8 637

Hoyes J. (1971) M. Phil. Thesis, The City University, London

Hutchison H.T., Werrbach K., Vance C., and Haber B. (1974) Brain Res. 66 265

Halicioglu T. and Sinanoglu O. (1969) Ann. N.Y. Acad. Sci. 158 308

Iitaka Y. (1960) Acta Cryst. 13 35

Iitaka Y. (1961) Acta Cryst. 14 1

Iversen L.L. (1972) in "Perspectives in Neuropharmacology" S.H. Snyder (Ed) Oxford Univ. Pres N.Y., London & Toronto

Iversen L.L. and Johnston G.A.R. (1971) J. Neurochem. 18 1939

Jain M.K. (1974) Arch. Biochem. Biophys. 164 20

Jasper H.H., Khan B.T. and Elliott K.A.C. (1965) Science 147 1448

Jasper H.H. and Koyama I. (1967) Fed. Proc. 26 373

Jensen L.H. (1955) Acta Cryst. 8 237

Johnson J.L. (1972) Brain Research 37 1

Johnston G.A.R., Beart P.M., Curtis D.R., Game C.J.A., McCulloch R.M. and MacLachlan R.M. (1972) Nature New Biol. 240 219

Johnston G.A.R., Curtis D.R., Beart P.M., Game C.J.A., McCulloch R.M. and Twitchin P. (1975) J. Neurochem. 24 157

Johnston G.A.R., Curtis D.R., Davies J. and McCulloch (1974) Nature 248 804

Johnston G.A.R., Curtis D.R. de Groat W.C. and Duggan A.W. (1968) Biochem. Pharmacol. 17 2488

Jönsson P.G. and Kvick A. (1972) Acta Cryst. B28 1827

Jose P. and Pant L.M. (1965) Acta Cryst. 18 806

Katz B. (1966) "Nerve, muscle and synapse" McGraw-Hill, N.Y.

Kanters J.A., Kroon J., Beurskens P.T. and Vliegenthart J.A. (1966) Acta Cryst. 21 990

Karle I.L. and Karle J. (1963) Acta Cryst. 16 969

Karlin A. (1967) J. Theor. Biol. 16 306

Kaye G.W.C., Laby T.H. (1966) "Tables of Physical and Chemical constants" 13th Ed. Longmans

Kennard O., Watson D.G., Allen F.H., Isaacs N.W., Motherwell W.D.S., Pettersen R.C. and Town W.G. (1972) "Molecular Structures and Dimensions Vol. A1" Int. Union of Cryst. N.V.A. Oosthoek's Uitgevers Mij. Utrecht

Kerkut G.A., Nicolaidis S., Piggott S.M., Rasool C.G. and Walker R.J. (1974) Br. J. Pharm. 51 134P

Keynes R.D. (1972) Nature 239 29

Kier L.B. (1970) in "Fundamental concepts in drug-receptor interactions" J.F. Danielli, J.F. Moran and D.J. Triggle (Eds.) Acad Press N.Y.

Kier L.B. (1971) "Molecular Orbital Theory in Drug Research" Acad Press N.Y.

Kier L.B. and Truitt E.B. (1970) Experientia 26 988

Kier L.B., George J.M. and Höltje H.D. (1974) J. Pharmaceut Sci. 63 1435

Kier L.B. and Höltje H.D. (1975) J. Theor. Biol. 49 401

Kihara T. (1953) Rev. Mod. Phys. 25 831

King E.J. (1954) J. Am. Chem. Soc. 76 1006

Konishi H., Ashida T. and Kakudo M. (1968) Bull. Chem. Soc. Jap. 41 2305

Krnjevic K. (1970) Nature 228 119

Krnjevic K. and Phillis J.W. (1963) J. Physiol. 165 274

Krnjevic K. and Schwartz S. (1967) Exp. Brain Res. 3 320

Kuriyama K., Sisken B., Haber B., and Roberts E. (1968) Brain Res. 9 165

Kutsnetsov S.G. and Ghokov S.N. (1962) "Synthetic Atropine-like Substances" State Publicity House of Medical Literature Leningrad, English Translation: US Dept. Comm J.P.R.S. 1975

Katz B. (1966) "Nerve, muscle and synapse" McGraw-Hill, N.Y.

Kanters J.A., Kroon J., Beurskens P.T. and Vliegenthart J.A. (1966) Acta Cryst. 21 990

Karle I.L. and Karle J. (1963) Acta Cryst. 16 969

Karlin A. (1967) J. Theor. Biol. 16 306

Kaye G.W.C., Laby T.H. (1966) "Tables of Physical and Chemical constants" 13th Ed. Longmans

Kennard O., Watson D.G., Allen F.H., Isaacs N.W., Motherwell W.D.S., Pettersen R.C. and Town W.G. (1972) "Molecular Structures and Dimensions Vol. A1" Int. Union of Cryst. N.V.A. Oosthoek's Uitgevers Mij. Utrecht

Kerkut G.A., Nicolaidis S., Piggott S.M., Rasool C.G. and Walker R.J. (1974) Br. J. Pharm. 51 134P

Keynes R.D. (1972) Nature 239 29

Kier L.B. (1970) in "Fundamental concepts in drug-receptor interactions" J.F. Danielli, J.F. Moran and D.J. Triggle (Eds.) Acad Press N.Y.

Kier L.B. (1971) "Molecular Orbital Theory in Drug Research" Acad Press N.Y.

Kier L.B. and Truitt E.B. (1970) Experientia 26 988

Kier L.B., George J.M. and Höltje H.D. (1974) J. Pharmaceut Sci. 63 1435

Kier L.B. and Höltje H.D. (1975) J. Theor. Biol. 49 401

Kihara T. (1953) Rev. Mod. Phys. 25 831

King E.J. (1954) J. Am. Chem. Soc. 76 1006

Konishi H., Ashida T. and Kakudo M. (1968) Bull. Chem. Soc. Jap. 41 2305

Krnjevic K. (1970) Nature 228 119

Krnjevic K. and Phillis J.W. (1963) J. Physiol. 165 274

Krnjevic K. and Schwartz S. (1967) Exp. Brain Res. 3 320

Kuriyama K., Sisken B., Haber B., and Roberts E. (1968) Brain Res. 9 165

Kutsnetsov S.G. and Ghokov S.N. (1962) "Synthetic Atropine-like Substances" State Publicity House of Medical Literature Leningrad, English Translation: US Dept. Comm J.P.R.S. 1975

Lambrecht G. and Mutschler E. (1974) in "Proceedings of the 7th Jerusalem Symposium on Quantum and Molecular Pharmacology" B. Pullman and E.D. Bergmann (Eds) Reidal, Boston USA

Langley J.N. (1905) J. Physiol 33 374

Lea T.J. and Usherwood P.N.R. (1973) Comp. Gen. Pharmacol 4 333

Leo A., Hansch C. and Elkins D. (1971) Chem. Rev. 71 525

Levine Y.K. and Wilkins M.H.F. (1971) Nature New Biol. 230 69

Loewi O. (1922) Pflüger's Archiv 193 201

Lonsdale K. (Ed) (1962) "International Tables for X-ray Crystallography Vol. 3 Kynoch Press, Birmingham.

Lowagie C. and Gerschenfeld H.M. (1974) Nature 248 533

Lucy J.A. (1964) J. Theor. Biol. 7 360

Maeda T. Fujiwara T. and Tomita K. (1972) Bull. Chem. Soc. Jap. 45 3628

McBride W.J. and Van Tassel J. (1972) Brain Res. 44 177

McDonald T.J. and O'Brien R.D. (1972) J. Neurobiol. 7 277

McGeer E.G., McGeer P.L. and McLennan H. (1961) J. Neurochem 8 36

McLennan H. (1970a) "Synaptic Transmission" Saunders, Philadelphia

McLennan H. (1970b) Nature 228 674

McLennan H. (1973) Cand. J. Physiol. Pharmacol. 51 774

McLennan H. (1974) Neuropharmacology 13 449

Mittag A.W. (1970) in "Fundamentals of Cell Pharmacology" S.Dikstein (Ed) Chas. C. Thomas, Springhill, USA

Moran J.F. and Triggle D.J. (1970) in "Fundamental concepts in drug-receptor Interactions" J.F. Danielli, J.F. Moran and D.J. Triggle (Ed) Acad. Press N.Y.

Morgan I.G., Zanetta J.P., Breckenridge W.C., Vincendon G. and Gombos G. (1973) Brain Res. 62 405

Nicoll R.A. (1975) Proc. Nat. Acad. Sci USA 72 1460

Nys G.G. and Rekker R. F. (1973) Chimie Therapeutique 5 521

Obata K., Ito M. Ochi R., and Sato N. (1967) Exp. Brain Res. 4 43

Obata K. Takeda K. and Shinozaki H. (1970) Exp. Brain Res. 11 327

Oegerle W.R. and Sabin J.R. (1973) J. Mol. Struct. 15 131

Okaya Y. (1966) Acta Cryst. 21 726

Onsager L. (1936) J. Am. Chem. Soc. 58 1486

Osborn J.A. (1945) Phys. Rev. 62 351

Parisi M., Rivas E. and de Robertis E. (1971) Science 172 56

Parry-Jones G., Roberts R.T. and Ahmed A.J. (1971) Molecular Physics 22 547

Parsons D.F. (1970) in Johnson symposium on probes of biological membranes

Partington P., Feeney J. and Burgen A.S.V. (1971) Mol. Pharmacol. 8 269

Paton W.D.M. (1961) Proc. Roy. Soc. B. 154 21

Paton W.D.M. and Rang H.P. (1965) Proc. Roy. Soc. B. 163 1

Paton W.D.M. (1970) in "Molecular properties of drug receptors" R. Porter and M. O'Connor (Eds) Churchill

Pauling P. and Petcher T.J. (1972) Nature New Biol. 236 112

Pfeiffer C. (1956) Science 124 29

Pitzer K.S. (1955) J. Am. Chem. Soc. 77 3427

Pople J.A. and Beveridge D.L. (1970) "Approximate Molecular Orbital Theory" McGraw-Hill, N.Y.

Pople J.A., Santry D.P. and Segal G.A. (1965) J. Chem. Phys. 43 5129

Pullman B., Courrière P. and Berthod H.(1974) J. Med. Chem. 17 439

Pullman B. and Berthod H. (1974) J. Med. Chem. 17 439

Pullman B. and Berthod H. (1974) C.R. Acad. Sci. Paris 278 series D 1433

Pullman B. and Berthod H. (1975) Theor. Chim. Acta 36 317

Pullman B. and Courriere P. (1973) in "Conformation of biological molecules and polymers" Jerusalem Symposium V, Israel Acad. Sci. and Hum. Jerusalem

Pullman A. and Pullman B. (1975) Quart. Rev. Biophys. 7 505

Pullman B. (1974) in "Proceedings of the 7th Jerusalem Symposium on Molecular and Quantum Pharmacology" B. Pullman and E.D. Bergmann (Eds) Reidel, Boston

Purpura D.P., Girado M., Smith T.G., Callan D.A. and Grundfest H. (1959) J. Neurochem. 3 238

Ramanadham M., Sikka S.K. and Chidambaram R. (1973) Acta Crys. B29 1167

Rang H.P. (1971) Nature 231 91

Rang H.P. and Ritter J.M. (1969) Mol. Pharmacol. 5 394

Richards W.G. (1974) Proc. Roy. Soc. 14 Nov.

Richards W.G., Aschman D.H. and Hammond J. (1975) J. Theor. Biol 52 223

Roberts E. (1975) Biochem. Pharmacol. 23 2637

Robbins J. (1959) J. Physiol. 148 39

Roy P.N., Majumdar S.K. and Saha N.N. (1967) Ind. J. Phys 41 771

Schueler see Gill(1959)
Schmitt F.O., Bear R.S. and Clark G.L. (1935) Radiology 25 131
Scholte T.G. (1949) Physica 15 437, 450
Sequeira A., Rajagapal H. and Chidambaram R. (1972) Acta Cryst. B28 2514

Segal M., Sims K., Maggiora L. and Smissman E. (1973) Nature New Biol. 245 88

Shinozaki H. and Konishi S. (1970) Brain Res. 24 368

Shinozaki H. and Shibuya I (1974) Neuropharacol 13 665

Sinanoglu O (1967) Advan. Chem. Phys 12 283

Sinanoglu O (1968) in "Proc. Int. Conference on Molecular Associations in Biology" B. Pullman (Ed) Acad. Press N.Y.

Sinanoglu O. (1974) Theor. Chim. Acta 33 279

Sinanoglu O. (1969) see Halicioglu

Singer S.J. and Nicolson G.L. (1972) Science 175 720

Smythies J.R. (1974) Ann. Rev. Pharmacol 14 9, (1974[b]) J. Theor. Biol.

Stephenson R.P. (1956) Br. J. Pharmacol. Chemother 11 379

Steward E.G., Borthwick P.W., Clarke G.R. and Warner D. (1975) Nature 256 600

Steward E.G. and Clarke G.R. (1975) J. Theor. Biol. 52 493

Steward E.G., Player R.B., Quilliam J.P., Brown D.A. and Pringle M.J. (1971) Nature New Biol 233 87

Steward E.G., Player R.B. and Warner D. (1973a) Nature New Biol. 245 88

" " " (1973b) Acta Cryst. B29 2038

" " " (1973c) Acta Cryst. B29 2825

Steward E.G. Warner D. and Clarke G.R. (1974) Acta Cryst. B30 813

Stewart J.M., Kundell F.A. and Baldwin J.C. (1970,72) X-ray 70, 72 Computer Science Centre, Univ. of Maryland, USA

Stout G.H. and Jensen L.H. (1968) "X-ray Structure Determination" Macmillan, N.Y.

Straughan D.W. (1974) Neuropharmacology 13 495

Svenneby G. and Roberts E. (1973) J. Neurochem. 21 1025

Swagel M.W., Ikeda K. and Roberts E. (1973) Nature New Biol. 246 91

Symons M.C.R. (1974) Proc. Roy. Soc. 14 Nov.

Szasz G.J., Sheppard N. and Rank D.H. (1948) J. Chem. Phys. 16 704

Taft R.W. (1956) in "Steric effects in organic chemistry" Newman M.S. (Ed) Wiley, N.Y.

Takeuchi A. and Onodera (1973) Nature New Biol. 236 55

Takeuchi A. and Takeuchi N. (1964) J. Physiol 170 296

Takeuchi A. and Takeuchi N. (1965) J. Physiol. 177 225

Takeuchi A. and Takeuchi N. (1967) J. Physiol. 191 575

Takeuchi A. and Takeuchi N. (1969) J. Physiol 205 377

Taylor (1948) J. Chem. Phys. 16 257

Tomita K., Harada M. and Fujiwara T. (1973) Bull. Chem. Soc. Jap. 46 2854

Tomita K. Higashi H. and Fujiwara T. (1973) Bull. Chem. Soc. Jap 46 2199

Tredgold R.H. (1973) Nature New Biol. 242 209

Tredgold R.H. and Sproule R.C. (1973) Biochim Biophys. Acta 317 569

Thyagaraja Rao S., Srinivasan R. and Valambal V. (1968) Ind. J. Pure Appl. Phys. 6 523

Ueoka S., Fujiwara T. and Tomita K. (1972) Bull. Chem. Soc. Jap. 45 3634

Urry D.W. (1972) Proc. Nat. Acad. Sci U.S.A. 69 1610

Usherwood P.N.R. (1972) Neurosci. Res. Prog. Bull. 10 136

Usherwood P.N.R. and Grundfest H. (1965) J. Neurophysiol. 28 479

Van Gelder N.M. (1971) Can. J. Physiol. Pharmacol. 49 513

Vasquez C., Parisi M. and de Robertis E. (1971) J. Mem. Biol. 6 353

Walsh J. (1966) "Numerical analysis - an introduction" Acad. Press N.Y.

Warner D. (1975) Ph.D. Thesis. The City University, London

Warner D., Borthwick P.W. and Steward E.G. (1975) J. Mol. Struct. 25 397

Warner D., Player R.B. and Steward E.G. (1973) International Union of Crystallography. 1st European meeting. B.4 Chester, England

Warner D. and Steward E.G. (1975) J. Mol. Struct. 25 403

Watase H. (1958) Bull. Chem. Soc. Jap 31 932

Watase H., Tomiie Y. and Nitta I (1958) Bull. Chem. Soc. Jap 31 714

Waud D.R. (1968) Pharmacol Rev. 20 49

Wertz D.H. and Allinger N.L. (1974) Tetrahedron 30 1579

Wilkins M.H.F. Blaurock A.E. and Engelman D.M. (1971) Nature New Biol. 230 72

Wold S. (1974) Chemica Scripta 5 97

Worthington C.R. (1970) in Johnson symposium on probes of biological membranes

Worthington C.R. (1971) in "Biophysics and Physiology of Excitable Membranes" W.J. Adelman (Ed) Van Nostrand

Worthington C.R. and Liu (1973) Arch. Biochem. Biophys. 157 573

Young A. and Snyder S.H. (1974) Proc. Nat. Acad. Sci. USA 71 4002

Zukin S.R., Young A.B. and Snyder S.H. (1974) Proc. Nat. Acad. Sci. USA 71 4802